Investigating relationships between hydrocarbonoclastic bacteria and micro-algae

Haydn Frank Thompson

Submitted for the degree of Doctor of Philosophy

Heriot-Watt University
School of Engineering & Physical Sciences
June 2017

ABSTRACT

Crude oil spills damage marine ecosystems due to the potentially toxic nature of the petrochemical hydrocarbon constituents and their recalcitrance to degradation. Polycyclic aromatic hydrocarbon components (PAHs) are one group of hydrocarbons in crude oil that are of particular concern due to their genotoxicity and potential to bioaccumulate. Their potential to cause damage in marine environments can be mitigated by the presence and activities of hydrocarbonoclastic bacteria. The phycosphere of marine eukaryotic phytoplankton (micro-algae) has recently been shown as an important biotope where hydrocarbonoclastic bacteria can be found, and the association between these organisms is largely unexplored. This thesis presents new insight into the relationship between these organisms by performing enrichment experiments with crude oil and individual hydrocarbon substrates, as well as whole-genome analysis of an algal-associated hydrocarbon-degrader, and using molecular probes for the *in situ* visualization (by CARD-FISH) and whole-community analysis (by Flow-FISH) of hydrocarbonoclastic bacteria associated with laboratory cultures and field samples of micro-algae. Results demonstrated variations in the tolerance of different diatom species to PAHs, and that intermediate metabolites formed from the partial biodegradation of PAHs can be more harmful to diatoms compared to that of their parent PAH compounds. *Thalassiosira pseudonana* presence enhanced phenanthrene dissolution and PAH-degrading bacteria formed cell clusters in EPS aggregates. The genome of an obligate hydrocarbonoclastic bacterial species (*Polycyclovorans algicola*) found associated with marine micro-algae possessed genes involved in cell communication, horizontal gene transfer and nutrient sharing that may play an important role in the organism's association with its eukaryotic host cells. Indeed, these interactions are likely to allow these hydrocarbonoclastic bacteria to be supported on the phycosphere of micro-algae in the absence of petrochemical exposure. Microcosm experiments with field samples of micro-algae and bacterial consortia showed that crude oil biodegradation, in particular the PAH fraction, was enhanced compared to that by the free-living bacterial community, and revealed certain groups (e.g. members of the order BD7-3) that had not previously been reported to become enriched in the presence of crude oil. Using Flow-FISH, epibiotic members of the genus *Marinobacter* were found associated with micro-algae in sea surface field samples, and CARD-FISH was used to show this same group associated with the soft tissues of the coral *Lophelia pertusa* from polyp samples collected from different coral mounds in the deep North Atlantic.

ACKNOWLEDGEMENTS

Firstly I would like to thank my supervisors Dr. Tony Gutierrez and Dr. Alexander Loy for their support and for always being available for critical feedback and assisting me in structuring my research. Also thanks to my reviewers Dr. Derek Jamieson and Dr. Mark Hartl for support throughout. My sincerest gratitude goes to Margaret Stobie, Dr. David Brown, Dr. David Berry, Dr. Sandra Brooke, Dr. Peter Morris and Dr John Kinross for their guidance in techniques when I first started. Many thanks also to NERC and those involved in the James Cook Changing Oceans Expedition for providing me with coral samples, SEPA for micro-algal identification and Dr. Colin Moore for captaining the RV *Serpula* on Loch Creran.

I would like to give a special thank you to Angelina Angelova for assisting with genetic data collection and analysis, Dr. Martin Jones and Dr. James MacKinlay for assistance with hydrocarbon analysis and Dr. Márton Palatinszky for collecting Raman cell spectra. Thanks also go to the Iain Fraser Cytometry Centre, in particular Dr. Raif Yuecel for his invaluable assistance in cytometric analysis and figure preparation. Once again, special thanks goes to Dr. Tony Gutierrez for helping me with phylogenetic tree analysis and figure preparation, and guidance during this course of study.

Thanks to the James Watt Scholarship for funding my research, and to Brenda Thake and The Haptonema Charitable Trust for additional financial support.

DEDICATION

I would like to dedicate this thesis to my parents Wiebke and Dominic Thompson. Thank you both. I would also like to dedicate this thesis to Brenda Thake, Bobby Norman and Opa (Jüne Jans) who have been my inspiration.

DECLARATION STATEMENT

ACADEMIC REGISTRY
Research Thesis Submission

Name*:*	Haydn Frank Thompson		
School:	School of Engineering & Physical Sciences		
Version: *(i.e. First, Resubmission, Final)*	Final	Degree Sought:	Doctor of Philosophy

Declaration

In accordance with the appropriate regulations I hereby submit my thesis and I declare that:

1) the thesis embodies the results of my own work and has been composed by myself
2) where appropriate, I have made acknowledgement of the work of others and have made reference to work carried out in collaboration with other persons
3) the thesis is the correct version of the thesis for submission and is the same version as any electronic versions submitted*.
4) my thesis for the award referred to, deposited in the Heriot-Watt University Library, should be made available for loan or photocopying and be available via the Institutional Repository, subject to such conditions as the Librarian may require
5) I understand that as a student of the University I am required to abide by the Regulations of the University and to conform to its discipline.
6) I confirm that the thesis has been verified against plagiarism via an approved plagiarism detection application e.g. Turnitin.

* *Please note that it is the responsibility of the candidate to ensure that the correct version of the thesis is submitted.*

Signature of Candidate*:*	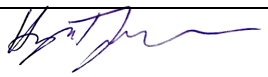	Date:	14/06/2017

Submission

Submitted By *(name in capitals):*	
Signature of Individual Submitting:	
Date Submitted:	

For Completion in the Student Service Centre (SSC)

Received in the SSC by *(name in capitals):*			
Method of Submission *(Handed in to SSC; posted through internal/external mail):*			
E-thesis Submitted (**mandatory for final theses**)			
Signature:		Date:	

TABLE OF CONTENTS

CHAPTER 1: INTRODUCTION **1**

1.1 A historical perspective of hydrocarbons, carbon-based life forms and the evolution of marine microbes **1**

1.2 Crude oil **3**

1.2.1 The origin of fossil fuels 3

1.2.2 Composition, uses and properties of petroleum hydrocarbons 5

1.3 Fate of petroleum hydrocarbons in marine environment **10**

1.3.1 Nutrient cycling 10

1.3.2 Marine hydrocarbonoclastic bacteria 11

1.3.3 Hydrocarbon degradation pathways 12

1.4 The relationship between hydrocarbonoclastic bacteria and marine micro-algae **14**

1.4.1 Symbiosis 14

1.4.2 Extracellular polymeric substances (EPS) and marine snow aggregates 17

1.4.3 Micro-algal and bacterial community response to crude oil 21

1.5 Thesis outline **24**

CHAPTER 2: INTERACTIONS BETWEEN MARINE HYDROCARBONOCLASTIC BACTERIA AND THEIR MICRO-ALGAL HOSTS **27**

2.1 Introduction **27**

2.2 Materials and Methods **33**

2.2.1 PAH metabolite-driven interactions between *Polycyclovorans algicola* strain TG408 and micro-algae 33

2.2.1.1 Assessing the effect of phenanthrene and naphthalene on *Thalassiosira pseudonana* and *Chaetoceros calcitrans* 33

2.2.1.2 Determining the effect of known intermediate breakdown products of PAH biodegradation on *T. pseudonana* 35

2.2.1.3 Determining the effect of breakdown products produced during phenanthrene degradation by *P. algicola* strain TG408 on the growth of *T. pseudonana* 36

2.2.1.4 Determining whether *T. pseudonana* has the ability to degrade phenanthrene 37

2.2.1.5 Determining whether carbon released from the bacterial degradation of phenanthrene can be incorporated into micro-algal biomass 39

2.2.2 Determining what mechanism(s) underpin a symbiotic relationship between hydrocarbonoclastic bacteria and micro-algae 41

2.2.2.1 Enrichment of *Skeletonema costatum* and *Lingulodinium polyedrum* with phenanthrene and probing for hydrocarbonoclastic bacteria using Catalyzed Reporter Deposition Fluorescence *In Situ* Hybridisation (CARD-FISH) 41
2.2.2.2 Determining the effect of micro-algal cells and their produced extracellular substances on the dissolution of phenanthrene 42
2.2.2.3 Determining whether *P. algicola* (TG408) and three other hydrocarbon-degraders grow on selected diatom-derived organic nutrients. 43
2.2.2.4 Testing *P. algicola* for growth on intermediate breakdown products from microbial degradation of phenanthrene 45
2.3 Results 46
2.3.1 PAH metabolite-driven interactions between *P. algicola* strain TG408 and micro-algae 46
2.3.1.1 Assessing the effect of phenanthrene and naphthalene on *T. pseudonana* and *C. calcitrans* 46
2.3.1.2 Determining the effect of known intermediate breakdown products of PAH biodegradation on *T. pseudonana* 49
2.3.1.3 Determining the effect of breakdown products produced during phenanthrene degradation by *P. algicola* strain TG408 on the growth of *T. pseudonana* 51
2.3.1.4 Potential of *T. pseudonana* to degrade phenanthrene 53
2.3.1.5 Determining whether carbon released from the bacterial degradation of phenanthrene can be incorporated into micro-algal biomass 54
2.3.2 Determining what mechanism(s) underpin a symbiotic relationship between hydrocarbonoclastic bacteria and micro-algae 56
2.3.2.1 Enrichment of *S. costatum* and *L. polyedrum* cultures with phenanthrene and probing for hydrocarbonoclastic bacteria using Catalyzed Reporter Deposition Fluorescence *In Situ* Hybridisation (CARD-FISH) 56
2.3.2.2 Determining the effect of micro-algal cells and their produced extracellular substances on the dissolution of phenanthrene 58
2.3.2.3 Determining whether *P. algicola* (TG408) and three other hydrocarbon-degraders grow on selected diatom-derived organic nutrients. 60
2.3.2.4 A screening for *P. algicola* growth on intermediate breakdown products from microbial degradation of phenanthrene 61
2.4 Discussion 62
2.4.1 PAH metabolite-driven interactions between *Polycyclovorans algicola* strain TG408 and micro-algae 62
2.4.2 Determining what mechanism(s) underpin a symbiotic relationship between hydrocarbonoclastic bacteria and micro-algae 66
CHAPTER 3: SEARCHING THE *POLYCYCLOVORANS ALGICOLA* GENOME FOR HYDROCARBON DEGRADATION GENETIC POTENTIAL 70
3.1 Introduction 70

3.2 Materials and Methods **71**
3.3 Results and Discussion **73**
CHAPTER 4: ENHANCED CRUDE OIL BIODEGRADATIVE POTENTIAL OF HYDROCARBONOCLASTIC BACTERIA ASSOCIATED WITH NATURAL POPULATIONS OF PHYTOPLANKTON **84**
4.1 Introduction **84**
4.2 Materials and Methods **87**
4.2.1 Field sample collection and crude oil enrichment setup 87
4.2.2 Hydrocarbon analysis 88
4.2.3 Nucleic acid extraction 90
4.2.4 Quantification of phytoplankton using chlorophyll-*a* measurements and the bacterial population using real-time PCR 91
4.2.5 Barcoded amplicon metagenomic sequencing and analysis 92
4.2.6 Phylogenetic tree 93
4.3 Results **94**
4.3.1 Degradation of Heidrun crude oil 94
4.3.2 Phytoplankton and bacterial community dynamics 97
4.3.3 Bacterial community analysis 101
4.4 Discussion **106**
CHAPTER 5: PROBING THE NORTH EAST ATLANTIC FOR EPIBIOTIC *MARINOBACTER* **114**
5.1 Introduction **114**
5.1.1 *Marinobacter* associations in the photic zone 115
5.1.2 *Marinobacter* associations with deep-sea corals 116
5.2 Materials and Methods **120**
5.2.1 Phytoplankton field sampling and analysis 120
5.2.1.1 Field sample collection and fixation 120
5.2.1.2 FISH procedure 121
5.2.1.3 Laser/Channel selection and flow-cytometric analysis 123
5.2.1.4 Flow-FISH data analysis 123
5.2.1.5 Statistical analysis: 125
5.2.2 *Lophelia pertusa* field sampling and analysis 125
5.2.2.1 Sample collection and fixation 125
5.2.2.2 Polyp storage solution analysis 126
5.2.2.3 Decalcification and sectioning 126
5.2.2.4 CARD-FISH analysis 127
5.2.2.5 Autofluorescence detection using confocal laser scanning microscopy 128
5.3 Results **128**

5.3.1 Detection of *Marinobacter* associated with phytoplankton 128
5.3.1.1 Strategy 1 128
5.3.1.2 Strategy 2 132
5.3.2 Detection of *Marinobacter* associated with *Lophelia pertusa* 134
5.3.2.1 Analysis of the *L. pertusa* polyp storage solution 134
5.3.2.2 Autofluorescence detection using confocal laser scanning microscopy 135
5.3.2.3 Identification of *Marinobacter* cells associated with *L. pertusa* 136
5.4 Discussion 140
5.4.1 *Marinobacter* associated with phytoplankton in northeastern Atlantic waters 140
5.4.2 *Marinobacter* associated with the cold-water coral *Lophelia pertusa* in northeastern Atlantic waters 142
5.4.3 Conclusions 145
CHAPTER 6: CONCLUSION 146
APPENDICES 154
Appendix A: The effect of 1-hydroxy,2-naphthoic acid on *T. pseudonana* 154
Appendix B: Preparations for Section 2.2.1.3 156
Appendix B.1: Incubating *P. algicola* with phenanthrene and pyruvate to extract fractions while monitoring growth 156
Appendix B.2: Selecting ONR7a:F/2+Si ratio 157
Appendix C: Raman spectra for *T. pseudonana* and *P. algicola* comparison 158
Appendix D: CARD-FISH probe optimization 160
Appendix E: Details of micro-algal and bacterial growth media 164
Appendix F: Heidrun crude oil 165
References 166

CHAPTER 1: INTRODUCTION

1.1 A historical perspective of hydrocarbons, carbon-based life forms and the evolution of marine microbes

Recent research has shown that various aromatic and aliphatic hydrocarbons are ubiquitous in the universe (Allamandola *et al.*, 1989; Kwok and Zhang, 2011; Tielens, 2008). These hydrocarbons are created by interstellar radiation and are present in cosmic dust, which falls to earth at an estimated 40,000 tons per year (Galliano *et al.*, 2008; Zook, 2001). The earth formed roughly 4.5 billion years (Ga) ago as a hot, volcanic rocky planet, composed mostly of iron and nickel metallosilicates (Dalrymple, 2001; Wood *et al.*, 2006). A primordial atmosphere on earth, rich in the hydrocarbon methane (CH_4) and also ammonia (NH_3), was short-lived due to photolysis and loss of H_2 by thermal escape leaving predominantly N_2, CO_2 and H_2O (Brimblecombe, 1986; Cnossen *et al.*, 2007; Kuhn and Atreya, 1979). During the famous meteorite cascade (~3.8 Ga) carbonaceous chrondites and comets collided with the earth's crust, bringing with them huge quantities of organic carbon and nitrogen incorporated into a variety of molecular families as well as water (Gomes *et al.*, 2005; Kvenvolden *et al.*, 1970). Some notable compounds found within these meteorites include organic molecules (amino acids, ketoacids, nucleobases, alcohols, aromatic and aliphatic hydrocarbons (Gargaud *et al.*, 2010; Martins *et al.*, 2008). Kerogen, as will be explained in the next section, is an intermediate hydrocarbon molecule in crude oil formation. The Murchison meteorite, for example, contained a kerogen-like insoluble organic material ($C_{100}H_{20}N_3O_{12}S_2$) that is amphiphilic (like cell membrane phospholipids) and is thought to have been important in the formation of phospholipid bilayers essential to life that appeared during the cooler early Archaean (Gargaud *et al.*, 2010). This combination of organic molecules is hypothesized to have created oil slicks in the prebiotic oceans (Hadean – Archaean eon), with photochemical alkylation of polycyclic aromatic hydrocarbons (PAHs) by UV radiation forming primitive pigments that were active in photochemical reactions (Mahajan *et al.*, 2003).

The earliest sedimentary rocks left today date back to roughly 3.8 Ga (Brimblecombe, 1986). Samples of rock from Australia show that early mat-forming prokaryote species were found in complex microbial communities as early as 3.48 Ga with anoxygenic photosynthetic mats appearing from 3.4 Ga and the entire range of marine habitats being filled by prokaryotes by 3 Ga (Gargaud *et al.*, 2010; Noffke *et al.*, 2013). The

membranes of prokaryotes contain a diversity of hydrocarbons, including among many others phospholipids and hopanoids, which have aliphatic tails or side chains (Schoell *et al.*, 1992; Sohlenkamp and Geiger, 2016). The atmosphere of the earth during early prokaryotic evolution was a reducing one where organisms would have used hydrogen as an electron donor for energy production. For example, methanogenic anaerobic prokaryotes were likely to be abundant during this time and contributed to earth's atmosphere formation by fermenting CO_2 and H_2 into the hydrocarbon methane (CH_4) (Grenfell *et al.*, 2010). Any oxygen produced by photosynthetic autotrophs (i.e. cyanobacteria) that had evolved light harvesting centers would have reacted with reduced minerals (e.g. pyrite, FeS_2) to make hydroxides (e.g. limonite, $2Fe_2O_3.3H_2O$) in 'the great rusting' (Brimblecombe, 1986). Gradually between 2.8 and 2 Ga, overcoming oxygen toxicity and using H_2O as a hydrogen donor, oxygenic microbes altered the atmosphere on a planetary scale to produce the oxidizing atmosphere we have today (Archer and Barber, 2004; Brimblecombe, 1986; Gargaud *et al.*, 2010). This drastically lowered the concentration of CO_2 in the atmosphere and began the biogeochemical carbon delivery of organic carbon and $CaCO_3$ to the earth's crust (Hayes and Waldbauer, 2006). The biologically fixed carbon would also have drastically increased the concentrations of hydrocarbons in the oceans (Goutx and Saliot, 1980; Saliot, 1981).

The next stage in the evolution of primary producers was the formation of the eukaryotic cell. Although the root of life is ambiguous, the evidence from the reduced genomes of endosymbiotic mitochondria and chloroplasts shows us that cells engulfing prokaryotic cells and the subsequent transfer of nuclear material to the host is a likely method of eukaryotic cell formation (Keeling and Archibald, 2008; Martin, 1999; Nowitzki *et al.*, 1998). There is debate whether chloroplasts and mitochondria should be classed as endosymbionts or organelles (Gargaud *et al.*, 2010). The earliest eukaryotic-resembling life forms appear in the fossil record in the Mesoproterozoic era (~1.8 Ga). Multiple endosymbiotic events are thought to have occurred to create the diverse microalgae with the range of photosynthetic potential we see today (Raven and Allen, 2003). A certain group of cyanobacteria evolved the light harvesting antenna pigment chlorophyll-*a*, an aromatic porphyrin ring with a magnesium (Mg) atom in the centre of the pigment and a phytol (diterpene hydrocarbon) side chain (chemical formula: $C_{55}H_{72}O_5N_4Mg$). Chlorophyll and other light harvesting pigments combined with two (Types I and II) reaction centers proved to be an evolutionarily successful

organization for capturing sunlight energy and a system that has radiated (via adaptive radiation or progressive occupation) throughout both prokaryotic and eukaryotic organisms (Archer and Barber, 2004; Croce and van Amerongen, 2014; Ruban *et al.*, 2011). The presence of chlorophyll in the sea is significantly correlated with hydrocarbon content and organic carbon in the water, with some bacteria able to feed directly on the isoprenoid hydrocarbon side chains of the photosynthetic pigments (Rontani *et al.*, 1999; Zsolnay, 1973).

In summary, since before the Archaean meteors fell, hydrocarbons including petroleum-like hydrocarbons (PAHs, aliphatics and high molecular weight compounds) would have been present on earth and in the marine environment. Since the Archaean eon biogenic hydrocarbons (made by life processes e.g. membrane lipids) would also have been present. These hydrocarbons were present not only as a carbon source for carbon-based life forms but also may have played a vital role in the formation of living cells. Also, as we shall see in forthcoming sections, hydrocarbons would have been involved in genetic mutagenicity, evolution and cell signalling interactions (Arber, 2000; La Rocca *et al.*, 1996; Singer *et al.*, 2003). This means that organic hydrocarbon compounds were available for interactions with biota before carbon fixation had evolved in cyanobacteria and hence long before the formation of crude oil in underground reservoirs (see Section 1.2.1). It also means that relationships between hydrocarbonoclastic bacteria (bacteria that degrade hydrocarbons, which will be addressed in the forthcoming sections) and eukaryotic micro-algae may have developed during the evolution of marine eukaryotic micro-algae and may have since developed into more complex interactions over billions of years.

1.2 Crude oil

1.2.1 The origin of fossil fuels

Fossil fuels (e.g. crude oil/petroleum, coal, oil shales, tar sands, natural gas) are produced naturally by the fossilization of the remains of living organisms (Alhassan and Andersson, 2013; Brown *et al.*, 2000; Solash *et al.*, 1978). The connection between biogenic molecules and fossil fuels has been apparent for almost a century. In 1936 Alfred E. Treibs noticed that derivatives of heme and chlorophyll pigments were found in organic mineral substances (fossil fuels) as porphyrins (metallo/petro-porphyrins) (Treibs, 1936). These ‘chemofossils’ are molecules that retained the shape of their

parent biogenic structures and which can be used as biological markers to determine the source organisms of the oil (Petrov, 1987). This finding gave rise to the term 'fossil fuel' - a broad term for a range of organic chemicals that humans have become reliant on for the majority of their energy needs (Kvenvolden, 2006; Thomas et al., 2016).

Fossil fuels are formed when organic matter (e.g. bacteria, marine micro-algae, zooplankton or terrestrial plants) is partially degraded to produce humic substances, which are buried in sediments and become porous source rocks (Whiticar, 1996; Zelibor *et al.*, 1988). Here the pressure and heat gradually build up to transform the organic matter into kerogen (waxy high molecular weight compound). Oil shales and tar sands can be high in kerogen if they have not reached high enough temperatures for conversion to petroleum and gas. At high temperatures kerogen undergoes catagenesis, but as the earth's crust (and mantle) are saturated to various degrees with water the process is termed hydrous pyrolysis, where at high temperature and pressure water dissociates into H^+ and OH^- ions, which act as a strong acid and strong base, causing a range of chemical reactions leading to the complex multitude of hydrocarbons that humans utilize in industry (Bell and Rossman, 1992; Holzapfel, 1969; Hyndman and Hyndman, 1968; Schimmelmann *et al.*, 2001; Yang *et al.*, 2013).

The precursory relationship of kerogen to petroleum is similar to that of lignite to coal in that lignite is a derivative of lignin, just as petro-porphyrins are derivatives of biological pigments; lignin being a structural hydrocarbon (with aromatic rings) produced by plants (Hatcher, 1988; Stefanova *et al.*, 2004). Within some kinds of kerogen we can still find structures like lignin, humic substances, polyester fibres (e.g. cutin containing waxy C_{16}-C_{18} acids) (Becker, 1997). The presence or absence of water, variations in pressure and temperature, the quality of kerogen (type of decayed organism) and time are variables that contribute to the properties of fossil fuels (Petrov, 1987). Only under certain conditions known as the 'petroleum window' does petroleum (crude oil) form. Petroleum formation is influenced largely by the distance from the magmatic body and the stage of metamorphosis (time), and can be characterized by several factors including a high isoprenoid:*n*-alkane ratio (Petrov, 1987). Crude oil varieties from around the world represent different stages in the 'petroleum window', or stages of fossilization of biogenic material. Therefore they contain varying concentrations of biological markers, or 'chemofossils', which can be found up to a

total concentration in crude oil of up to 35 - 40% of the total volume of crude oil (Petrov, 1987).

Petroleum hydrocarbons contain alkanes with a range of isoprenoid side chains (up to C_{45} isoprenoids). These isoprenoids could be relics of biogenic molecules (e.g. plastoquinone isoprenoid side chains, phytol/chlorophyll, vitamin A or vitamin E side chains) (Dawson *et al.*, 2013; Petrov, 1987; Powell and McKirdy, 1973). Hopanoids (pentacyclic compounds e.g. hopane with a variety of side chains), which are present in bacterial cell membranes and estimated to be some of the most abundant classes of chemicals on earth, are examples of biological markers/chemofossils and sources of crude oil hydrocarbons (Schoell *et al.*, 1992). Similarly steroids/steranes and terpenoids/terpanes could be biological markers in crude oil that betray eukaryotic organism-origin (Oudot and Chaillan, 2010; Schoell *et al.*, 1992). Other hydrocarbons are transformed to greater or lesser degree by catagenesis and/or hydrous pyrolysis, for example lipids (e.g. C_{12}-C_{26} fatty acids) are the biogenic source of alkanes (Petrov, 1987). In fact, studying the chemical constituents of fossil fuels gives geologists valuable information about paleo-environments and biological origin (Schoell *et al.*, 1992; Zhao *et al.*, 2014). Marine micro-organisms in the ancient Tethys Sea region are thought to have contributed as much as 68% of modern oil and gas reserves, 90% of which were formed since or during the Jurassic (~200 Ma) (Zou *et al.*, 2015).

1.2.2 Composition, uses and properties of petroleum hydrocarbons

Petroleum hydrocarbons eventually reach the surface of the earth's crust after a period of time that can range from as little as 5000 years to the over a billion years (Didyk and Simoneit, 1989 & 1990; Ghori *et al.*, 2009). They are transported to the surface either by natural seeps (e.g. volcanic activity and tectonic movement) or by anthropogenic activity (e.g. drilling and spillage). Crude oil spills have occurred almost every year since records began in the 1970s and at the start of the century it was estimated that anthropogenic activity accounted for 53% of crude oil entering the marine environment while natural seeps accounted for the other 47% (Kvenvolden and Cooper, 2003; ITOPF, 2010). Humans are interested in crude oil largely due to the useful fuel fractions (e.g. petrol and diesel) for energy production and petrochemicals (e.g. benzene and ethylene), which are produced by fractional distillation or by steam cracking (e.g. production of alkenes for the polymer and plastic industries) (Copeland *et al.*, 1996;

Guo and Li, 2012; Olahová *et al.*, 2014). Petroleum fractions are treated in a variety of ways (e.g. desulphurized) and mixed to form desired consumer products, for example hydro-desulphurized kerosene or catalytic-cracked gas oil, which are both complex mixtures of straight and branched *n*-/iso/cyclo-alkanes, aromatics and alkenes and used a fuels (Swigert *et al.*, 2014). Uses for petroleum fractions include various solvents, fuels, lubricants and paint/varnish additives, whereas byproducts from petroleum refining can be used as raw materials in petrochemical industries and have a range of applications including polymerization (plastics), chemical and pharmaceutical synthesis and many more (da Silva *et al.*, 2015; Eneh, 2011; Suh *et al.*, 2010).

Crude oil contains a range of non-hydrocarbon constituents including water, fine solids (e.g. sand/clay/colloids), salts (mainly sodium/calcium/magnesium chloride), sulphur (e.g. sulphate, sulphur dioxide), nitrogen (nitrate, ammonium) and a range of trace metals (mainly vanadium and nickel), all of which vary in quality and quantity depending on the reservoir and which are present in the form of crude oil emulsions (Doyle *et al.*, 2011; Eneh, 2011; Huang *et al.*, 2016; Guéguen *et al.*, 2011; Proemse *et al.*, 2012a,b; Redman *et al.*, 2012). Also crude oil contains a diversity of heteroatomic hydrocarbons including carbazole, thiols/thiophenes as well as the biomarkers mentioned above (Eneh, 2011). Petroleum hydrocarbons range from simple pure straight-chain hydrocarbons at one extreme, to branched heteroatomic polycyclics at the other (Becker, 1997).

Resins (mixture of waxes and asphaltenes) are high-molecular weight crude oil constituents. These act as dispersants in crude oil and contain a complex mixture of oily molecules like terpenes (e.g. squalene) and other complex structures (Becker, 1997). Waxes can be summarized as esters, alcohols, and fatty acids with 16 or more carbon atoms (i.e. aliphatic in nature), whereas asphaltenes can be summarized as reduced products of complex aromatic macrocyclic structures polymerized through sulphide links (Becker, 1997). Petroleum hydrocarbons are usually extracted first from the crude oil reservoir and heavier molecules (waxes/asphaltenes/kerogen) are extracted last. These heavy molecules are still useful as flash pyrolysis of resins and kerogen leads to decarboxylation (CO_2 release) and/or methane (CH_3) production and makes shorter chain petroleum compounds, like jet fuel (del Río *et al.*, 1993).

The properties that petroleum hydrocarbons have in common are that they are generally hydrophobic and lipophilic due to all or most of the molecule being non-polar and therefore they accumulate in cell membrane phospholipid bilayers, which enhances their cellular availability (Sikkema *et al.*, 1995). Like trace metals, hydrocarbons conform with the Langmuir and Freundlich models of adsorption to plastics, and can behave in the marine environment in a similar way to other non-polar molecules like insecticides (e.g. dichlorodiphenyltrichloroethane 'DDT' and the organochloride dieldrin) and industrial conservative pollutants (e.g. polychlorinated biphenyls 'PCBs' and halocarbons) (Clark *et al.*, 2001; El-Dib *et al.*, 1978; Radi *et al.*, 2015; Schmidt *et al.*, 2004). They therefore have the potential to bioaccumulate and may also interact with these other toxic pollutants in an antagonistic synergistic way; sublethal effects are likely to be extremely diverse (Clark *et al.*, 2001; Xiu *et al.*, 2014). The toxicity of aromatic compounds is generally greater than aliphatic compounds, and the middle molecular weight (MMW) compounds are generally more toxic than high molecular weight (HMW) (Clark *et al.*, 2001). The low molecular weight (LMW) compounds are also toxic although they are volatile and are lost to the environment or weathered fastest (Clark *et al.*, 2001; Yamada *et al.*, 2003).

The LMW (*n*-/iso-/cyclo-) alkane pollutants are central nervous system (CNS) depressants and general irritants, which can solubilize fats, membranes, mucous and enter the myelin sheath of nerve fibers (Galvin and Marashi, 1999; Raines *et al.*, 2001; Ritchie *et al.*, 2001). In humans they can also cause asphyxiation and respiratory problems (Galvin and Marashi, 1999). Reported dangers of recalcitrant HMW alkanes are less due to chemical toxicity and more to the danger of physical smothering of organisms, with sessile organisms unable to escape oil spillage and, for example, sea birds' feathers becoming smothered with HMW hydrocarbons and losing their thermal insulation and buoyancy (Erlacher *et al.*, 2013; Hartung, 1995; Suchanek, 1993; Yang *et al.*, 2014). Although alkanes and alkenes are widely used in emollients and pharmaceuticals, the biological effects of these exogenic aliphatic hydrocarbons can range from therapeutic to pathogenic (Williams *et al.*, 1992). Cycloalkanes display higher toxicity to marine bacteria than *n*-alkanes, while alkenes (present in crude oil in variable quantities) can form genotoxic epoxides (e.g. styrene epoxides) (Fabiani *et al.*, 2012; Grigson *et al.*, 2006). Other chemicals present in crude oil (e.g. heavy metals) can also be released to the environment causing additional toxicity to organisms, whereas some other compounds are intentionally added to petroleum products (e.g. the

anti-knock agents methyl *tert*-butyl ether and methylcyclopentadiene), which can have a range of toxic impacts on organisms (Borghoff *et al.*, 2010; Daughtrey *et al.*, 1997; Li *et al.*, 2008; Puttaswamy and Liber, 2012).

Aromatic compounds (e.g. benzene, toluene, ethylbenzene, phenanthrene) are the most notable petroleum hydrocarbon compounds in terms of their toxic effects on metazoans and they are therefore of particular interest to humans (Swigert *et al.*, 2014; Sverdrup *et al.*, 2002). There are many possible routes of aromatic hydrocarbon toxicity, with various enzymes able to act upon them (as shall be described in Section 1.3.3). Taking the simplest aromatic molecule benzene, for example, it has been found that some molecules can be expelled by animals unchanged through breath, excreted in urine as phenol, catechol or hydroquinol/one or be subjected to sulfation (Laskin and Goldstein, 1977). Pigs, for example, convert the benzene to phenylsulphate then to glucuronide in a process linked with chronic benzene toxicity (Laskin and Goldstein, 1977). The central nervous system, cardiovascular and gastrointestinal systems are badly affected by benzene (Laskin and Goldstein, 1977).

The complexity of biological effects of hydrocarbons increases when considering polycyclic aromatic hydrocarbons (PAHs). Around 25 – 35% of total hydrocarbons in crude oil are PAHs depending on the oil type (Head *et al.*, 2006). PAHs are recognized as highly toxic, persistent in the environment and have the potential to bioaccumulate (Rios *et al.*, 2007). The United States Environmental Protection Agency, for example, has designated 16 PAHs as priority pollutants due to their carcinogenicity and their risk in terms of exposure to humans (Bojes and Pope, 2007). PAHs act either due to their lipophilic qualities by arranging themselves in the cell membrane and interrupting cellular processes (e.g. by altering permeability or light dependent photosynthetic reactions) or otherwise by undergoing change and then covalently binding to important structures (e.g. forming DNA and protein adducts) (Aksmann and Tukaj, 2008; Pohjola *et al.*, 2003; Santella *et al.*, 1995; Sikkema *et al.*, 1995). Generally speaking, LMW (e.g. naphthalene) aromatics display acute toxicity while HMW aromatics (e.g. benzo[a]pyrene) exhibit chronic toxicity (Yamada *et al.*, 2003). PAHs accumulate by binding to colloidal materials or biota and plastics (Andelman and Suess, 1970; Frias *et al.*, 2010; Kalmykova *et al.*, 2013; Liang *et al.*, 2007; Mato and Isobe, 2001).

In the marine environment, for example, PAHs cause toxic effects in a range of organisms from the sea surface to the sea floor (Couillard and Lee, 2005; Louvado *et al.*, 2015; Özhan and Bargu, 2014a; Pérez *et al.*, 2010). The responses of phytoplankton to PAH contamination are diverse with toxic effects detectable at concentration as low as 1 μg L^{-1} and with some species able to metabolize PAHs (e.g. naphthalene and benzo[*a*]pyrene) (Bopp and Lettieri, 2007; Fan and Reinfelder, 2003; Haritash and Kaushik, 2009; Özhan *et al.*, 2014). Crude oil in general can stimulate phytoplankton growth at low concentrations (≤1 mg L^{-1}) (Özhan *et al.*, 2014, and references therein) and conversely higher concentrations can be lethal, however the aromatic molecules in particular can cause micro-algal mortality (Adekunle *et al.*, 2010; D'souza *et al.*, 2016; Gilde and Pinckney, 2012; Johansson *et al.*, 1980; Özhan and Bargu, 2014a,b,c; Prouse *et al.*, 1976). The adsorption of PAHs to micro-algae can result in biomagnification and accumulation of PAHs further up the food chain in zooplankton and fish, however these effects are also accompanied by passive diffusion of dissolved PAHs onto the cell membranes and into the cells (Berrojalbiz *et al.*, 2009; Binark *et al.*, 2000; Sikkema *et al.*, 1995; Wang and Wang, 2006). PAHs (and petroleum hydrocarbons more generally) are toxic to zooplankton while fish eggs and larval development are also disrupted (Carls *et al.*, 2008; Johansson *et al.*, 1980).

PAH accumulation in marine animals has an impact not just on the health of the ecosystem but also has a negative economic effect on fisheries, with valuable target species becoming tainted with both LMW and HMW PAHs (Berntssen *et al.*, 2010; Goodlad, 1996; Haruhiko Nakata *et al.*, 2003; Xiu *et al.*, 2014). Also toxicity and damage to apex predator populations like whales and dolphins has a negative impact on tourism due to the amenity value these species have, which can also be interpreted as an economic impact (Formigaro *et al.*, 2014; Hughes, 2001). Many human communities worldwide rely heavily on marine ecosystems for sustenance, which can be damaged by crude oil spills (Adger, 2000; Brookfield *et al.*, 2005; Daly *et al.*, 2016; Graham *et al.*, 2010; White *et al.*, 2012). The way most governments and organizations have dealt with toxic hydrocarbons in crude oil and elsewhere is to suggest safety limits, i.e. the concentration of exposure over time. The detoxification of PAHs is of great significance to human health, and information obtained by investigating the organisms responsible for oil degradation could be vital in dealing with the future oil pollution.

1.3 Fate of petroleum hydrocarbons in marine environment

1.3.1 Nutrient cycling

The organisms in the environment can be generally divided into primary producers (cyanobacteria, eukaryotic micro-algae and macro-algae/higher plants), consumers (protozoa, invertebrates, vertebrates), and decomposers/detritivores (heterotrophic bacteria, archaea and fungi) (Hagen *et al.*, 2012; Sherr and Sherr, 1988). Marine primary producers produce roughly half of global fixed carbon through oxygenic photosynthesis, with marine phytoplankton making a significant contribution, and this organic carbon supports the marine food web (Ducklow *et al.*, 2001; Field *et al.*, 1998; Sherr and Sherr, 1988). Diatoms are a group or eukaryotic micro-algae that are estimated to be responsible for 20 and 25% of global primary production (Armbrust *et al.*, 2004; Falciatore and Bowler, 2002). Bacteria and phytoplankton are important in the delivery of nutrients (e.g. carbon, nitrogen, phosphorus, sulphur) in aggregates or marine snow to the deep sea (termed the 'biological pump'), with some nutrients bound in recalcitrant forms (e.g. pristane, phytane and hopanoids) or inorganic forms (e.g.$CaCO_3$) and, as has been discussed in Section 1.2.1, buried in sediments (Broecker and Clark, 2009; Buchan *et al.*, 2014; Ducklow *et al.*, 2001; Summons *et al.*, 1999).

Prokaryotes (in particularly heterotrophic bacteria) are responsible for recycling nutrients in the marine environment and the interactions of these organisms with phytoplankton are biogeochemically significant (Buchan *et al.*, 2014). For example some members of the bacterial genus *Marinobacter* are phytoplankton-associated and are thought to be important in global cycling of carbon, manganese, nitrogen, phosphorus and iron (Handley and Lloyd, 2013; Singer *et al.*, 2011). One well defined symbiotic association between phytoplankton and bacteria that is of particular relevance to the sulphur cycle is the algal production of DMS-P (dimethylsulfoniopropionate) and subsequent conversion to DMS (dimethyl sulfide) largely by bacteria (Howard *et al.*, 2008; Kiene, 1990; Stefels and Boekel, 1993). In the atmosphere above the ocean DMS is oxidized to form various sulphur-containing compounds which form cloud condensation nuclei that reflect the sun's radiation (Aumont *et al.*, 2002; Howard *et al.*, 2008). Organisms that significantly influence populations of bacteria (e.g. viruses and zooplankton) are therefore also important to nutrient cycling (Miki and Jacquet, 2008). Carbon nutrients are commonly shared between bacteria actively (e.g. release of molecules that cannot be degraded further) or passively (e.g. bacterial cell lysis due to

viral activity and leakage of bacterial cell contents) in a complex process that involved many groups of organisms (Amin *et al.*, 2009; Jermy, 2009; Miki and Jacquet, 2008; Pelz *et al.*, 1999; Webb *et al.*, 2003). As we shall see in the coming sections bacteria also play a fundamental role in cycling petroleum hydrocarbons.

1.3.2 Marine hydrocarbonoclastic bacteria

The sum of biological and physical processes that modify crude oil in the environment is called weathering. The fate of each fraction of crude oil is different in the marine environment: lower molecular weight oils form slicks on the surface (that are subject to spreading/drift, wave mixing and volatilization/evaporation), heavier resins form tar balls (with low surface area that are persistent), while emulsions are more easily degradable (Atlas and Hazen, 2011; Harayama *et al.*, 1999; Xue *et al.*, 2015; Yamada *et al.*, 2003). Sunlight (UV) radiation causes photo-oxidation of floating petroleum hydrocarbon molecules (Aksmann and Tukaj, 2008; Huang *et al.*, 2014). Micro-algae and zooplankton (and to some extent metazoans) have been reported to exhibit limited capabilities in metabolism of petroleum hydrocarbons (via cytochrome P450 and other enzyme systems) (Akcha *et al.*, 2000; Arias *et al.*, 2016; Berrojalbiz *et al.*, 2009; Kirso and Irha, 1998; Snyder, 2000). Hydrocarbon-degrading (hydrocarbonoclastic) bacteria, however, are seen as the most effective group of micro-organisms involved in remediating crude oil in the marine environment, due to their detected enrichment after oil spills (Head *et al.*, 2006; McGenity *et al.*, 2012; Tadros and Hughes, 1997; Xue *et al.*, 2015). Past research by various researchers demonstrated that all natural ecosystems are more than 99% dominated by yet uncultured microorganisms (Ravin *et al.*, 2015). The marine environment is unique in that it is the only ecosystem to harbor obligate hydrocarbonoclastic bacteria (Mishamandani *et al.*, 2014; Yakimov *et al.*, 2007). In 2010 there were over 175 known bacterial genera that demonstrated an ability to utilize hydrocarbons as sole carbon sources (Prince *et al.*, 2010) although more have been discovered since then (Gutierrez *et al.*, 2012b,c,2013b). Investigating the function of these underexplored prokaryotes is central to our understanding of remediation of toxic hydrocarbon pollutants in the marine environment and also more generally in understanding microbial ecology and nutrient cycling.

Various factors affect the speed of bacterial crude oil degradation. Aerobic degradation of hydrocarbons occurs at a higher rate than anaerobic degradation, and oil slicks

hamper aerobic degradation not only by limiting gas exchange between the ocean and the atmosphere but also attenuating sunlight (resulting in less algal O_2 production) (Hambrick *et al.*, 1980; Meckenstock *et al.*, 2004; Xue *et al.*, 2015). Also low concentrations of nutrients (e.g nitrogen and phosphorus) limit hydrocarbon degradation (Leahy and Colwell, 1990). Factors affecting the physico-chemical properties of hydrocarbons have resulting impacts on microbial degradation. Variations in salinity and pressure may impact microbial degradation, however environments exhibiting low salinity (e.g. estuaries) or high pressure (e.g. the deep sea) are likely to have pre-adapted bacteria that can utilize petroleum hydrocarbon substrates (Atlas, 1981; Bælum *et al.*, 2012; Leahy and Colwell, 1990; Tam *et al.*, 2002). As salinity decreases hydrocarbon solubility increases (Gold and Rodriguez, 1989) and hydrocarbon aqueous concentrations increase, possibly increasing hydrocarbon toxicity. Deeper in the water column salinity generally decreases, however temperature decreases and pressure increases (Ingleby and Huddleston, 2007). Lower temperatures and higher pressures result in lower hydrocarbon solubility, increasing the partioning of crude oil into the non-aqueous phase and lowering their bioavailability to hydrocarbonoclastic bacteria (Sawamura *et al.*, 1993; Wilkes and Schwarzbauer 2010). Furthermore low temperatures can slow down biological degradation of hydrocarbons due to retardation of metabolic processes (e.g. enzyme activity, translation, cell replication), although in cold environments like the Arctic there are pre-adapted bacterial species that can degrade hydrocarbons effectively (Atlas, 1981; Atlas and Hazen, 2011; Daly *et al.*, 2016; Hazen *et al.*, 2010). Biosurfactants (e.g. emulsifiers and dispersants) have been used to increase rates of weathering and bioremediation: these compounds reduce the surface tension of immiscible petroleum hydrocarbons and increase the surface area and therefore bioavailability of the compounds to bacteria (Bælum *et al.*, 2012; Haritash and Kaushik, 2009; Henry *et al.*, 2011).

1.3.3 Hydrocarbon degradation pathways

According to McGenity *et al.* (2012) specific mechanisms are required to degrade the variety of hydrocarbons that are present in crude oil. Degradation pathways for various compounds give details of the specific enzyme catalyzed reactions that alter the chemical composition of substrates in steps. Each step or sequence of steps might be performed by a single bacterium (intracellularly or extracellularly), or degradation may be halted at a certain step due to a lack of substrate-specific enzymes/genes and the

intermediate metabolite may be released to the environment, making it available for enzymatic degradation by other organisms/microbial communities (McGenity *et al.*, 2012; Pelz *et al.*, 1999). The pathways used by hydrocarbonoclastic bacteria are likely to vary for different species and with the various environmental conditions mentioned in the previous section (e.g. oxygen availability) (Harayama *et al.*, 2004; Wentzel *et al.*, 2007). During aerobic alkane degradation, for example, *n*-alkanes can undergo β-oxidation (sub-terminal oxidation) by alkane hydroxylases and be subsequently converted to the corresponding carboxylic acids, which can then be degraded in the same way as fatty acids (i.e. acyl-CoA formation and entry into the Krebs cycle) (Wentzel *et al.*, 2007). This is, however, just one degradation pathway of many that might take place in aerobic habitats. In anaerobic conditions denitrifying bacteria and sulphate reducing bacteria have been shown to use fumarate to rearrange the *n*-alkane carbon skeleton to produce (1-methylalkyl)-succinyl-CoA (Harayama *et al.*, 2004; Rabus *et al.*, 2011). Cycloalkanes also undergo β-oxidation to fatty acids (Xue *et al.*, 2015). During aerobic aromatic hydrocarbon degradation a common pathway is conversion to a dihydrodiol (via oxidase enzymes) followed by *ortho*- or *meta*-cleavage and insertion into the Krebs cycle as acetyl-CoA (Haritash and Kaushik, 2009; Kanaly and Harayama, 2000; Xue *et al.*, 2015). PAH degradation pathways can also include conversion by dioxygenases to epoxides (and many other intermediates) (Xue *et al.*, 2015). In a similar way to *n*-alkanes, the anaerobic degradation of aromatic molecules is aided by organic acids (e.g. 4C-dicarboxylic acids) with benzoyl-CoA reported as a major intermediate (Haritash and Kaushik, 2009; Jaekel *et al.*, 2015; Rabus *et al.*, 2014).

Aromatic hydrocarbon substrates that are not completely mineralized by weathering processes are of particular ecological relevance due to their toxicity. These intermediate metabolites (termed reactive oxygen species) are more attractive to nucleophiles or electrophiles (possibly increasing their reactivity) than the parent hydrocarbons due to increased polarity or unbalanced charges in the hydrocarbon molecule, increasing their solubility and bioavailability in the aqueous phase. Intermediates can take a variety of forms (quinones, epoxides, aldehydes, alcohols, etc.) and may have multiple functional groups (Rabus *et al.*, 2014). The toxicity of the monoaromatic hydrocarbons has already been mentioned briefly in Section 1.2.2 and the monoaromatic intermediate metabolites can be toxic to eukaryotes and prokaryotes alike (Schweigert *et al.*, 2001). The HMW intermediates are likely to be more persistent in the environment and both

HMW and LMW aromatic intermediates can form free radicals (McGenity *et al.*, 2012). Free radicals cause oxidative stress and alter cellular molecules, causing a range of diseases, and may be more toxic than their parent hydrocarbons (Lobo *et al.*, 2010; Zielinska-Park *et al.*, 2004). Some intermediate metabolites formed during PAH degradation are examined in Chapter 2. Interestingly hydrocarbon compounds produced by the petrochemical and/or pharmaceutical industries may exhibit extremely similar or identical chemical structures to the intermediates from hydrocarbon degradation and also contaminate the marine environment (Crane *et al.*, 2006; Zuccato *et al.*, 2006).

1.4 The relationship between hydrocarbonoclastic bacteria and marine micro-algae

1.4.1 Symbiosis

The phycosphere is a zone where bacterial growth is stimulated by algal presence (Bell and Mitchell, 1972). Carbon fixation by marine eukaryotic micro-algae provides an environment rich in dissolved organic carbon (DOC) that is hugely important for bacterial production and has resulted in the evolution of species-specific relationships (symbioses) (Goecke *et al.*, 2013). Although there are many other influences on bacterial populations (e.g. zooplankton grazing), bacterial population growth has been shown to follow phytoplankton growth tightly (Riemann *et al.*, 2000). In exchange for organic carbon nutrients micro-algae receive other nutrients in mutualistic relationships that can be obligate or facultative and direct or indirect. For example, it has been estimated that half micro-algal species are cobalamin (vitamin B_{12}) auxotrophs, a nutrient which they obtain through bacterial production (Croft *et al.*, 2005). The background concentrations of cobalamin produced by bacteria in the oceans might be high enough to support cobalamin auxotrophs, and non-auxotrophic micro-algae may also acquire cobalamin from the environment (Droop, 2007; Kazamia *et al.*, 2012). Iron is an example of a growth-limiting nutrient in the marine environment (Landry *et al.*, 2000a,b). A genus of well-studied hydrocarbonoclastic bacteria (*Marinobacter*) that are closely associated with micro-algae (dinoflagellates and coccolithophores) have been shown to produce vibrioferrin siderophores that release iron in the presence of sunlight and increase micro-algal iron uptake more than twenty-fold (Amin *et al.*, 2009). Extracellular polymeric substances (EPS) produced by another algal-associated oil-degrading bacterium (*Halomonas*) exhibit trace metal binding capacities (Ca, Fe, Mn, Mg, Al) and may be involved in nutrient sharing between bacteria and micro-algae

(Gutierrez *et al.*, 2012a). Symbiotic relationships between phytoplankton and bacteria in the marine environment can involve vitamins, metals, DOC and nitrogen in a variety of ways (mutualism, commensalism or parasitism, etc.) (Amin *et al.*, 2012).

The *Roseobacter* clade (*Alphaproteobacteria*) is a notable group of bacteria that are particularly common in surface waters due to their intimate relationships with micro-algae (Geng and Belas, 2010; Moran *et al.*, 2007; Pinhassi *et al.*, 2004). Members of this clade produce acyl homoserine lactones (bacterial signalling molecules that control cell density in a process called 'quorum sensing') and may communicate with micro-algae via these molecules, although they also produce other molecules thought to be important in symbiosis, for example tropodithietic acid (TDA), an antibiotic inhibiting algicidal bacteria, and iron binding siderophores (Geng and Belas, 2010). *Phaeobacter inhibens* (*Roseobacter* clade) produces TDA, which helps both bacterium and the symbiotic *Emiliania huxleyi* algal host survive, although the same bacterium (once it detects algal senescence) can release an algicidal substance (coordinated using acyl homoserine lactones) (Wang *et al.*, 2016b). An obligate symbiotic relationship exists between the dinoflagellate *Pfiesteria piscicida* and bacterium *Silicibacter* sp. TM1040 (*Roseobacter* clade) in which both organisms cannot be cultured without the other. Geng and Belas (2010) suggest that eukaryotic phytoplankton can sometimes mimic quorum sensing by interacting with organisms living on their extracellular bacterial biofilm. Amin *et al.* (2015) found that intricate relationships exist between *Sulfitobacter* (*Roseobacter* clade) and *Pseudo-nitzschia multiseries* (a coastal marine diatom) where indole-3-acetic acid (IAA) and nitrate are passed from the bacterium to the diatom, and tryptophan, DMS-P, ammonium and taurine are transferred from the diatom to the bacteria cells. Sometimes physical associations between micro-algae and bacteria can be extremely close: endobacteria have been found within the endoplasmic reticulum membrane surrounding the chloroplast of *Pinnularia nobilis* (Schmid, 2003a,b). Similarly Villareal (1990) found an N_2-fixing cyanobacterial symbiont located between the frustule and the micro-algal cell membrane of a marine diatom. Other authors have found N_2-fixing bacteria supplying nitrogen to micro-algae (Kneip *et al.*, 2007; Moisander *et al.*, 2008). Thompson *et al.* (2012) performed an experiment that uncovered major nutrient (N and C) exchange between a cyanobacterium and a prymnesiophyte.

In recent years novel hydrocarbonoclastic bacteria have been isolated from laboratory cultures of marine micro-algae (Green *et al.*, 2006; Gutierrez *et al.*, 2012b,c,2013b, 2014). Close associations between hydrocarbonoclastic bacteria might be partially explained by the examples of nutrient sharing that have been outlined above, with the hydrocarbonoclastic bacteria receiving organic carbon (hydrocarbons) in return for metals or vitamins (Amin *et al.*, 2009; Gutierrez *et al.*, 2012a). Micro-algae can potentially produce a range of hydrocarbons. In previous sections the relationship between lipids and petroleum hydrocarbons has been described, including the similarities between fatty acid and *n*-alkane degradation. Micro-algae are certainly effective in producing triglycerides, and it may be feasible in a nutrient-sharing environment (like the phycosphere) for alkane degrading bacterial populations to be maintained via fatty acid degradation (see Section 1.4.2) (Chisti, 2006). Interestingly, Schirmer *et al.* (2010) uncovered an alkane biosynthesis pathway in a cyanobacterium, and Lea-Smith *et al.*, (2015) found that the marine cyanobacteria *Prochlorococcus* and *Synechococcus* produce alkanes (an estimated 308 – 771 million tons annually), which could possibly sustain hydrocarbonoclastic bacteria. Recalcitrant biomarkers (e.g. chlorophyll side chain phytol and phytol derivatives pristane and phytane) found in crude oil can even be degraded by some hydrocarbonoclastic bacterial taxa (e.g. pseudomonads) (Dawson *et al.*, 2013; Rontani *et al.*, 1999). Isoprenoid quinones are a group of compounds with a hydrocarbon skeleton that are ubiquitous in living cells and are important in photosynthesis and respiration (e.g. benzoquinones and naphthoquinones (Nowicka and Kruk, 2010). Although not a marine example, *Shewanella* species release isoprenoid quinones during degradation of humic acids and these free molecules can function as electron acceptors (Newman and Kolter, 2000).

One widespread phenomenon in nature is the production of the volatile compound isoprene (C_5H_8), common in terrestrial plants, marine algae, bacteria and even human breath (Fall and Copley, 2000; Hryniuk and Ross, 2009; Kuzma *et al.*, 1995; Shaw *et al.*, 2010). Isoprene production in the Colne estuary, UK, was found to be lower at night and at low tide, and its role is suggested to maintain an organism's cell membrane structure at times of stress (Exton *et al.*, 2012). Acuña Alvarez *et al.*, (2009) demonstrate that microbial degradation of isoprene in Colne estuary, UK, is significant, and McGenity *et al.* (2012) posited that this isoprene could sustain hydrocarbonoclastic microbial communities during periods between oil spills. Four noteworthy micro-algal genera that produce isoprene are *Thalassiosira*, *Skeletonema*, *Chaetoceros*, and

Emiliania (Exton *et al.*, 2013). PAH-degrading bacteria that are associated with micro-algae might benefit from micro-algal production of aromatic hydrocarbons (Binark *et al.*, 2000; Borneff *et al.*, 1968). *Botryococcus braunii* produces a range of hydrocarbons including straight-chain (dienes), isoprenoid hydrocarbons and ether lipids with different functional groups (e.g phosphate, hydroxyl and methyl groups) (Metzger Largeau, 2005). More benefits to hydrocarbonoclastic bacteria of micro-algal associations are discussed in the next section and pertain to the attractiveness of micro-algae to hydrocarbonoclastic bacteria due to sorption of hydrocarbons not just onto the algal cells (e.g. cell membranes and diatom frustules) but into the EPS produced by micro-algae (Andelman and Suess, 1970; Schmidt *et al.*, 2004; Sikkema *et al.*, 1995; Yamada *et al.*, 2003).

1.4.2 Extracellular polymeric substances (EPS) and marine snow aggregates

EPS are ubiquitous in the environment and are produced by both single-celled and multicellular organisms (Wotton, 2005). According to Aslam *et al.* (2012) EPS contributes as much as 60% and 99% of particulate organic carbon (POC) and dissolved organic carbon (DOC) respectively. The structure and size of EPS can range from larger particulate organic matter (POM) and transparent exopolymer particles (TEP) to much smaller colloidal (cEPS) and dissolved (dEPS) molecules (Aslam *et al.*, 2012; Freiwald and Roberts, 2005; Gärdes *et al.*, 2011; Hoffman *et al.*, 2009). EPS are primarily composed of carbohydrates, proteins, lipids and nucleic acids (Abed, 2010; Iwabuchi *et al.*, 2002). A simplistic illustration of bacterial loosely-bound and tightly-bound EPS (LB-EPS and TB-EPS respectively) was outlined by Zhao *et al.* (2015) (with TB-EPS closer to the cells), and this illustration is included in Figure 1. The resulting organization is that the volume of EPS surrounding a microbial cell (both prokaryotic and eukaryotic) can be many multiples of the actual cell volume. Some functions of EPS include biomineralization, solution complexation, metal ligand formation, redox cycling, biosorption, mineral dissolution, oil emulsification and aggregate formation (Iwabuchi *et al.*, 2002; Tourney *et al.*, 2009; Tourney and Ngwenya, 2014). EPS can protect micro-organisms from harsh environments and pathogens/predators by providing a barrier and can also facilitate the communication of marine microbes (Wotton, 2005).

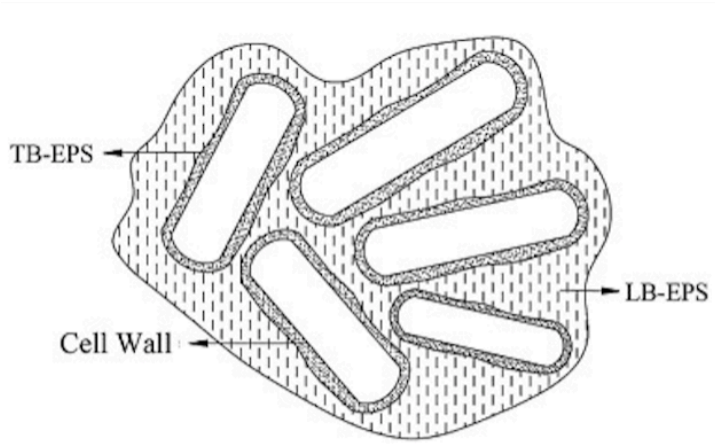

Figure 1. Showing five bacterial cells and the distribution of loosely-bound (LB) and tightly-bound (TB) EPS (Zhao *et al.*, 2015).

Diatoms and dinoflagellates produce a gelatinous EPS rich in proteoglycans and/or polysaccharides whereas diatoms in particular have been shown to produce sticky transparent exopolymers towards the end of blooms that bind planktonic cells and result in sinking organic matter (Myklestad, 1995; Passow *et al.*, 1994). Rates of photosynthesis have been shown to increase in micro-algal EPS aggregates (Alldredge and Silver, 1988). Within the EPS aggregates (or marine snow) bacterial communities are distinct from free-living communities (Delong *et al.*, 1993). Likewise those communities attached to microalgae are often different from the free-living communities (Crump *et al.*, 1999). Micro-algae provide surfaces for bacterial attachment and also provide carbon in the form of EPS, which are remineralized by bacteria (Delong *et al.*, 1993; Grossart, 1999; Simon *et al.*, 2002a). Bruckner *et al.* (2008) showed that a benthic diatom (*Cymbella microcephala*) changed its EPS composition in response to being incubated with different bacteria: *Proteobacteria* caused an increase in diatom polysaccharide secretion whereas *Bacteroidetes* increased the quantity of soluble EPS compounds excreted by the diatom. Also Bruckner *et al.* (2011) found that both diatoms' and various bacterial groups' EPS quality was affected by community composition and that extracellular proteins (and many other chemical groups) may be involved in cell-signalling.

During infamous oil spills including the Deepwater Horizon (DH), Ixtoc 1 and Tsetis oil spills, large quantities of mucus rich marine snow were detected, which became coagulated with crude oil (Passow *et al.*, 2012; Patton *et al.*, 1981). While this 'flocculent material' formation was inhibited by dispersants (Corexit EC9500A and

EC9527A) during the DH oil spill, researchers detected increased sorption of crude oil to the remaining EPS aggregates after dispersant application (Fu *et al.*, 2014; Passow, 2016). Corexit EC9500A application alone can result in EPS production by phytoplankton-associated bacteria that has a higher protein content than algal-derived EPS, highlighting the range of factors at play during marine oil spill EPS production (van Eenennaam *et al.*, 2016). Hydrocarbonoclastic bacteria and exopolysaccharide-producing bacteria dominated the bacterial community in marine snow during the DH oil spill, with subsequent enrichment of secondary metabolite degrading bacteria (Arnosti *et al.*, 2015). Various other organisms (including zooplankton) were also incorporated into the rapidly sinking marine oil snow (Daly *et al.*, 2016; Passow, 2016). Marine oil snow (MOS) formation has been detected in laboratory microcosm experiments studying crude oil enrichment of non-axenic diatom (*Skeletonema costatum*) and bacteria cultures (Mishamandani *et al.*, 2016). Although bacteria are capable of producing MOS without micro-algae, bacteria have been shown to enhance micro-algal MOS formation with the latter producing the majority of EPS (Passow and Alldredge, 1994; Passow *et al.*, 1994,2012; Ziervogel *et al.*, 2012). Indeed, MOS may provide an ecological niche where intricate relationships between microorganisms occur. Interestingly aggregate-associated bacteria grow faster than the free-living community (Riemann *et al.*, 2000). Halomonads are a group of bacteria that have been shown to produce high molecular weight, heterogeneous EPS with lipophilic qualities that effectively emulsifies crude oil (Gutiérrez *et al.*, 2007). Arnosti (2011) identified a possible mutualistic relationship where a halomonad produced emulsifying EPS while hydrocarbonoclastic bacteria (e.g. *Cycloclasticus*) directly target the hydrocarbons in MOS. *Pseudomonas* strains can produce EPS in large quantities and at the same time use crude oil as a sole carbon source (Hino *et al.*, 1997). Iwabuchi *et al.* (2002) identified a *Rhodococcus* sp. that produced EPS that increased its aromatic hydrocarbon tolerance, and the EPS it produced also enhanced *Cycloclasticus* PAH degradation, notably ethyl fluorene, phenanthrenes, and dibenzothiophenes.

Different enzyme groups within marine snow have variable activities. Mucilaginous aggregates exhibit highest protease and high lipase activity (Zoppini *et al.*, 2005). Polysaccharide-hydrolyzing enzyme activity was detected within the MOS formed during the DH oil spill, however generally in marine snow polysaccharide degradation is never complete and these molecules form a recalcitrant web-like matrix available for the attachment of bacteria (Arnosti *et al.*, 2015; Zoppini *et al.*, 2005). Extracellular

enzymes are important factors influencing global nutrient cycles (Arnosti, 2011). Lipases, the most active extracellular enzyme group, show highest activity in aggregates (Zoppini *et al.*, 2005). The lipid content of mucilaginous aggregates in the Adriatic Sea is 17 – 25% (dry weight) and fatty acids are released extracellularly that can support a range of bacteria (Pistocchi *et al.*, 2005). Similarly, other authors have found lipase activity to be prominent in particle-associated bacteria with oils, fats and triglycerides metabolized (with aminopeptidase and β-glucosidase exhibiting lower activity) (Martinez *et al.*, 1996; Riemann *et al.*, 2000; Ziervogel *et al.*, 2012). Nutrient degradation products that result from the organic substrate degradation in MOS by extracellular enzymes may be attracted by, or withheld for a period of time inside, the recalcitrant polysaccharide-rich EPS mucilage (Amin *et al.*, 2012; Gutiérrez *et al.*, 2007; Vetter *et al.*, 1997). This might explain why some bacteria have been shown to increase their extracellular enzyme production when nutrients are limited (Hoppe, 1983). Diatoms have been shown to increase levels of EPS production when nutrients are limited and Vetter *et al.* (1997) argue that a net gain in carbon could be achieved by EPS-associated bacteria in the marine aggregates even with dissolution of DOM/DOC into the free-living environment occurring (Thornton, 2002; Ziervogel *et al.*, 2012; Zoppini *et al.*, 2005).

The range of chemicals released in marine EPS aggregates and on the surface of micro-algal cells by bacteria and algae is more diverse than simply proteases, lipases and glucosidases, and the interactions taking place here are not subject to advective mixing, allowing complex interactions between microbes to occur (Amin *et al.*, 2012). Other enzymes released may be algicidal, antibacterial or bacteriolytic and their release may be coordinated via quorum sensing (Gram *et al.*, 2002; Holmström and Kjelleberg, 1999; Wang *et al.*, 2016b). The enrichment of hydrocarbonoclastic bacteria in MOS is a good indicator that hydrocarbon degradation is taking place (Arnosti *et al.*, 2015). It is possible that hydrophobic hydrocarbons (possibly resembling petroleum hydrocarbons or actual degradation products of petroleum hydrocarbons themselves) are used as signalling molecules during microbial interactions. Amin *et al.* (2012), for example, highlighted many hydrophobic hydrocarbon signalling molecules that may be released by diatoms including fucoserratene and ectocarpene, while *Pseudomonas aeruginosa* (a versatile hydrocarbon degrader) produces the quorum-sensing autoinducer 3-oxo-C12-HSL (Amin *et al.*, 2012; Zhang *et al.*, 2011a). The *Pseudomonas* genus is associated with diatoms in sea mucilage (Pistocchi *et al.*, 2005).

Also according to Singer *et al.* (2003) limonene, cumene, phenol and farnesol are secondary plant metabolites that may stimulate bacteria in a variety of ways (e.g. in PCB degradation). Salicylate, a well documented intermediate degradation product of PAHs (e.g. naphthalene and phenanthrene), may regulate or alter gene expression (of gene *bphA* for example) in *Pseudomonas* and *Burkholderia* strains (Master and Mohn, 2001; Phale *et al.*, 2007; Pinyakong *et al.*, 2003). Isoprene may also be involved in cell signalling and isoprenoid quinones' putative role in extracellular electron transfer has been described in the previous section (Fall and Copley, 2000; Newman and Kolter, 2000).

1.4.3 Micro-algal and bacterial community response to crude oil

Generally petroleum hydrocarbons are considered potentially toxic to phytoplankton (Sargian *et al.*, 2005). Diatoms and dinoflagellates have previously exhibited higher mortality in response to higher concentrations of oil (Adekunle *et al.*, 2010). Similarly Gilde and Pinckney (2012) found an inverse relationship between phytoplankton biomass and crude oil concentration, however in this study community structure was altered, with chlorophytes and diatoms (and cyanobacteria) exhibiting relatively higher abundance compared to dinoflagellates. Dinoflagellates display varying responses when incubated with individual hydrocarbons (e.g. naphthalene and benzo[*a*]pyrene) and complex mixtures of hydrocarbons (e.g. crude oil), and the application of nutrients or dispersants further confounds phytoplankton community responses, with dinoflagellates more resistant than diatoms at low nutrient concentrations (opposite results were collected when nutrient concentrations were high) (Özhan and Bargu, 2014a,b,c). These results show that community response varies with hydrocarbon quality. Crude oil can disrupt photosystem II light absorption (Chronopoulou *et al.*, 2013) and the spreading of oil layers on the ocean surface affects sunlight penetration in the photic zone by blocking especially the blue and UV wavelengths (Evdokimov *et al.*, 2003). D'souza *et al.* (2016) observed, however, that in an area where there are natural hydrocarbon seeps the phytoplankton community (measured by chlorophyll-*a* concentration) was enriched. This may be due to cyanobacterial chlorophyll-*a* rather than eukaryotic micro-algal pigments, and the authors state that the results are not controlled for influences of nutrient concentration and protistan grazing pressure. Chronopoulou *et al.*, (2013) also argue that grazing pressure may be reduced in presence of crude oil, and the possible resultant phototrophic and also

hydrocarbonoclastic organism enrichment can result in depleting nutrient concentrations and subsequent selection of diazotrophic organisms like cyanobacteria. Small diatoms (<20 μm) have previously been stimulated by crude oil enrichment, a finding not reflected by the larger diatoms (González *et al.*, 2009). Özhan *et al.* (2014) showed that overall phytoplankton were stimulated by the DH crude oil spill, but this was likely due to only certain species benefitting rather than all. Some authors argue that phytoplankton community structure can be used to detect crude oil pollution events by being distinguishable from other influences on community (Parsons *et al.*, 2014; Parsons *et al.*, 2015). According to Paul *et al.* (2013b) the DH oil-contaminated seawater was toxic to not only phytoplankton but also bacteria, and the mutagenic impacts were still detectable over a year after the spill and may have contributed to hereditary DNA alterations. Prophage-induction at times of crude oil-induced stress may also be important factors affecting the both phytoplankton and bacterial communities during oil spills (McGenity *et al.*, 2012).

Many studies have shown sequential blooms of different groups of bacteria after crude oil enrichment of marine seawater in the field and in mesocosm experiments in the laboratory (Yakimov *et al.*, 2007). After the DH oil spill in the Gulf of Mexico the Macondo crude oil caused blooms of *Cycloclasticus* and to a lesser extent *Colwellia* (*Gammaproteobacteria*) in the surface water and blooms of other *Gammaproteobacteria* members in deep water (*Oceanospirillales*) (Wang *et al.*, 2016a; Yang *et al.*, 2016). *Cycloclasticus* are known degraders of PAHs (acenaphthene, anthracene, biphenyl, fluoranthene, fluorene, naphthalenes, phenanthrene and pyrene) whereas *Colwellia* are commonly enriched by crude oil and their role in degradation has not been fully elucidated (Geiselbrecht *et al.*, 1998; Yakimov *et al.*, 2004a; Yang *et al.*, 2016). Brakstad *et al.* (2015) incubated the Macondo (DH) oil at low temperatures with seawater samples from the Norwegian coastline and found that indigenous hydrocarbonoclastic bacterial groups were enriched. Specifically the *Gammaproteobacteria Marinobacter, Cycloclasticus* and *Colwellia* increased in abundance, with a late bloom of *Pelagibacter* (*Alphaproteobacteria*, *Roseobacter* clade) after 64 days possibly inferring a return to pre-oil conditions. *Marinobacter* is a versatile bacterial genus with many members able to degrade a range of petroleum hydrocarbons including PAHs and aliphatic hydrocarbons (Melcher *et al.*, 2002; Mounier *et al.*, 2014). Oil enrichment of Arctic ice cores once again showed increased abundance in the *Gammaproteobacteria* community but the species identified were

psychrotolerant (*Colwellia*, *Marinomonas* and *Glaciecola*). *Glaciecola* are putative hydrocarbon degraders whereas *Marinomonas* strains are capable of degrading chrysene and phenanthrene (Brakstad *et al.*, 2008; Melcher *et al.*, 2002). According to Yakimov *et al.* (2007) *Alcanivorax*, *Thallassolituus* and *Oleispira* are commonly enriched hydrocarbonoclastic species (all three are *Gammaproteobacteria* of the *Oceanospirillales* order). *Thallassolituus* strains can degrade a range of aliphatic hydrocarbons while *Oleispira* strains are obligate *n*-alkane degraders (Yakimov *et al.*, 2003,2004b). *Alcanivorax* (branched- and *n*-alkane degraders) were the first obligate hydrocarbonoclastic bacteria isolated from the marine environment (Yakimov *et al.*, 1998). Mishamandani *et al.* (2016) added crude oil to a laboratory culture of the marine diatom *Skeletonema costatum* and discovered that a variety of hydrocarbon-degrading bacterial genera were enriched, starting with *Methylophaga* and followed by *Polycyclovorans*, *Arenibacter*, *Parvibaculum* and members of the *Roseobacter* clade. *Polycyclovorans*, *Arenibacter* and members of the *Roseobacter* clade (*Sulfitobacter*) can consume a range of PAHs (Gutierrez *et al.*, 2013b,2014; Mas-Lladó *et al.*, 2014). *Parvibaculum* degrade linear hydrocarbons while *Methylophaga* was considered until recently to be a 1C-compound degrader but can degrade hexadecane (Janvier and Grimont, 1995; Mishamandani *et al.*, 2014; Schleheck *et al.*, 2004).

In some cases, when incubated together, primary producers and heterotrophic (hydrocarbonoclastic) bacteria have been shown to degrade petroleum hydrocarbons more effectively than hydrocarbonoclastic bacterial cultures alone. Although not a marine example, synergistic effects on hydrocarbon degradation were detected when the green alga *Chlorella sorokiniana* was incubated with various hydrocarbon degraders: over 85% of hydrocarbon substrates (salicylate, phenol and phenanthrene) were removed (Borde *et al.*, 2003). All three compounds inhibited *Chlorella* growth. In bioreactors the same algal species released biosurfactants and oxygen that increased phenanthrene degradation by *Pseudomonas migulae* (Muñoz *et al.*, 2003). Safonova *et al.* (1999) collected resistant algae (green algae and cyanobacteria) and found that mixed cultures were able to degrade black oil better than individual cultures, with the cyanobacteria aiding green-algal survival. Warshawsky *et al.* (2007) found that the freshwater alga *Selenastrum capricornutum* enhanced benzo[*a*]pyrene degradation by a *Mycobacterium* species. And finally, although not a eukaryotic micro-algal example, Abed, (2010) studied remediation with mixed cultures of cyanobacteria and heterotrophic (hydrocarbonoclastic) bacteria and concluded that exudates produced by

the phototrophs aided petroleum hydrocarbon degradation. Examples of positive marine eukaryotic micro-algal influence on hydrocarbon degradation are absent in the literature.

1.5 Thesis outline

Relationships between marine micro-algae and hydrocarbonoclastic bacteria are likely to play a central role in decontamination of petroleum hydrocarbons in the marine environment. Not only do micro-algae adsorb hydrophobic molecules onto their cell surfaces but they also produce hydrocarbons and lipids in much higher quantities than are input into the marine environment by natural hydrocarbon seeps, anthropogenic spillage and atmospheric fallout combined (Clark *et al.*, 2001). The sheer number of marine hydrocarbonoclastic bacterial and micro-algal species and also the array of hydrocarbon molecules makes it difficult for researchers to investigate all of the species, niches, functions, interactions, relationships, and the significance thereof, although this too allows the researcher scope to discuss this subject area from various different perspectives. An individual microorganism may have the capacity to be a consumer, producer, decomposer, scavenger, symbiont, pathogen, sessile, planktonic or any number of combinations of the above. Likewise an individual hydrocarbon or its intermediate metabolites may be classed as a fuel, carbon nutrient substrate, signalling molecule, toxin or mutagen. The exact details of the vast majority of microbial relationships during hydrocarbon degradation and their implications for the environment are still to be elucidated. In order to achieve a better understanding of these relationships and to add to the information in the literature a variety of approaches need to be adopted. Therefore this thesis has been divided in to four chapters that represent four different approaches: **Chapter 2)** living cultures of micro-algae and bacteria from algal and bacterial culture collections were subjected to artificial laboratory conditions, **Chapter 3)** the genome of a hydrocarbonoclastic bacterium was sequenced and annotated, **Chapter 4)** marine seawater containing living micro-organisms were collected from the environment subsequently subjected to artificial conditions in the laboratory, and **Chapter 5)** environmental samples were preserved in the field and subsequently brought back to the laboratory for analysis. In terms of methodology, as will become apparent, a range of cultivation techniques, analytical chemical methods, genetic based analyses and microscopic methods were used to answer a range of research questions.

Chapter 2 was split into two parts:

1. PAH metabolite-driven interactions between the PAH-degrading bacterium *Polycyclovorans algicola* strain TG408 and micro-algae

The following hypotheses were tested: a) Growth of selected common diatoms (specifically *Thalassiosira pseudonana* and *Chaetoceros calcitrans*) is inhibited by LMW PAHs (namely phenanthrene and naphthalene), b) *T. pseudonana* growth is inhibited by phenanthrene degradation products, c) *T. pseudonana* cannot degrade phenanthrene, and d) Phenanthrene degraded by *P. algicola* and intermediate metabolites are incorporated into the micro-algal cell biomass. To test these hypotheses I used a combination of cell culturing and haemocytometer counting, fluorometric chlorophyll-*a* concentration analysis, gas chromatography-mass spectrometry (GC-MS), light microscopy, and Raman spectroscopy.

2. Determining what mechanism(s) underpin a symbiotic relationship between hydrocarbonoclastic bacteria and micro-algae

The following hypotheses were tested: a) Hydrocarbonoclastic bacteria found within micro-algal culture collections are attached to the algal cells (or the tightly bound EPS surrounding the cell) and dissociate during phenanthrene enrichment, b) Diatom cell presence and diatom-derived extracellular substances enhance the dissolution of phenanthrene in artificial seawater media (ASW), c) Selected marine hydrocarbonoclastic bacteria can produce colonies on agar using only micro-algal derived nutrients, and d) *P. algicola* can grow on phenanthrene degradation products. To test these hypotheses I used a combination of catalyzed reporter deposition fluorescence *in situ* hybridization (CARD-FISH) fluorescence microscopy, GC-MS, bacterial plating and out-growing. Due to the lack of environmental samples used in this chapter it was difficult to forecast the impact of the results in the environment, where multispecies interactions may overshadow any of the observed effects of PAH enrichment/contamination. This led to the manipulation of environmental samples in microcosm experiments used in Chapter 4.

Chapter 3 involved sequencing the genome of *P. algicola* in order to determine whether or not it consists of previously discovered PAH catabolic genes. To do this a combination of DNA extraction, sequencing, gene annotation and a range of online genetic databases were used.

Chapter 4 investigated the response of a planktonic assemblage of microorganisms from Loch Creran on the west coast of Scotland to crude oil enrichment. The following hypotheses were tested: a) Bacteria associated with eukaryotic micro-algae make a significant contribution to the degradation of crude oil, and b) Micro-algal associated bacteria play an important role in shaping microbial community dynamics in response to crude oil enrichment. To test these hypotheses I used a combination of nested PCR, qPCR, MiSeq 16S rRNA sequencing GC-MS and GC-FID.

Chapter 5 involved probing environmental samples in search of hydrocarbonoclastic bacteria (with a focus on the *Marinobacter* genus) in order to assess whether populations exist and where they are located in the phycosphere and deep sea. The benefit of fixing samples immediately after removal from the environment is that cell growth and/or community changes cease to occur, so the data produced is a representation of the state of the environment in question. Chapter 5 was split into two parts:

1. Assessing the population of *Marinobacter* in a phytoplankton trawl of the North East Atlantic.

The following hypothesis was tested: *Marinobacter* are closely associated with oceanic phytoplankton. To test this hypothesis fluorescence *in situ* hybridization methods were combined with flow-cytometric methods (Flow-FISH).

2. Assessing the population of *Marinobacter* associated with deep-sea cold-water coral (specifically *Lophelia pertusa*).

Originally this section was intended to follow up metagenomic analyses performed by a research group at a different institution with an aim to probe for specific bacterial taxa, however this work was postponed. Therefore the following hypothesis was tested: *Marinobacter* are closely associated with *L. pertusa*. To test this hypothesis a range of histological methods were used in combination with CARD-FISH to produce qualitative data. This final subsection was included to address the possibility of interactions of hydrocarbonoclastic bacteria with other marine eukaryotes. The production of EPS by eukaryotes and the knowledge of hydrocarbon-transfer to sediments via marine snow make deep-sea fauna (e.g. *Cnidaria* and *Porifera*) and reef habitats likely places to find hydrocarbonoclastic bacteria.

CHAPTER 2: INTERACTIONS BETWEEN MARINE HYDROCARBONOCLASTIC BACTERIA AND THEIR MICRO-ALGAL HOSTS

2.1 Introduction

In the first half of the chapter the focus was on the PAH metabolite-driven interactions between *Polycyclovorans algicola* strain TG408 and micro-algae. PAHs and PAH-degrading bacteria (e.g. *P. algicola*) were chosen as the major focus of this chapter because of the toxic effects of PAHs on primary producers (e.g. eukaryotic micro-algae) and consumers (e.g. fish and humans), their ability to bioaccumulate through food webs and their genotoxic (e.g. mutagenic and/or carcinogenic) effects (Couillard and Lee, 2005; Kanaly and Harayama, 2000; Louvado *et al.*, 2015; Pérez *et al.*, 2010). LMW-PAHs were used (specifically naphthalene and phenanthrene) because they exhibit acute toxicity and would be more suitable for shorter length experiments than HMW hydrocarbons (Yamada *et al.*, 2003). PAHs can be toxic to phytoplankton at concentrations as low as 1 μg L^{-1} (Özhan *et al.*, 2014). Diatoms were selected as the focal eukaryotic micro-algal group for experimentation in this chapter due to the recent findings of hydrocarbonoclastic bacteria closely associated with diatom cultures (Gutierrez *et al.*, 2013b; Gutierrez *et al.*, 2016). Diatoms share complex mutualistic nutrient sharing relationships with bacteria (described in Chapter 1) (Amin *et al.*, 2015; Villareal, 1990). They are also prominent producers of extracellular polymeric substances (EPS), specifically transparent exopolyers (TEP) (Myklestad, 1995; Passow *et al.*, 1994; Thornton, 2002). Diatoms may absorb petroleum hydrocarbons in their porous silica frustules (Özhan *et al.*, 2014), and small diatoms (<20 μm) can increase biomass in response to crude oil (González *et al.*, 2009). Diatoms have been linked with the formation of MOS aggregates during crude oil enrichment (Mishamandani *et al.*, 2016).

The *Thalassiosira* and *Chaetoceros* genera are important in terms of percentage contribution to total diatom biomass and are therefore important genera in terms of marine oxygen production and carbon fixation (Leblanc *et al.*, 2012). They may be important in the transfer of toxic PAHs along the food chain (Wang and Wang, 2006). The species *Thalassiosira pseudonana* and *Chaetoceros calcitrans* specifically are widely used in mariculture (Baker and Herson, 1978; Napolitano *et al.*, 1990). They were also readily obtainable axenic strains from the culture collection of algae and

protozoa (CCAP) after some attempts to treat the non-axenic diatom *Skeletonema costatum* with antibiotics proved unfruitful. Both *Thalassiosira* and *Chaetoceros* are likely to display interesting interactions with bacteria: *C. calcitrans* has exhibited enhanced production when incubated with a pseudomonad bacterium (Sureshkumar *et al.*, 2014), while amino acid production by *T. pseudonana* can be enhanced in when incubated with bacteria (Paul *et al.*, 2013a). There is a lack of information in the literature regarding hydrocarbonoclastic bacterial interactions with these important diatom species. The first aim in this chapter was to determine whether naphthalene and phenanthrene enrichment inhibited or stimulated growth of two axenic cultures of diatoms (*T. pseudonana* strain 1085/12 and *C. calcitrans* strain 1010/11). Although the toxicological effects of PAHs have been assessed for certain diatom species (including depuration rates for *T. pseudonana*) (Bopp and Lettieri, 2007; Fan and Reinfelder, 2003), the effects of phenanthrene and naphthalene have not been compared for *T. pseudonana* and *C. calcitrans*. The two diatom strains were individually incubated with either naphthalene or phenanthrene and populations were monitored using cell counts and chlorophyll-*a* extractions in acetone (Arar and Collins, 1997).

PAHs are degraded and/or metabolized by bacteria in numerous stages (catalyzed by different enzymes) in which aromatic rings are successively cleaved resulting in eventual conversion to pyruvate and insertion into the Krebs cycle (Habe and Omori, 2003; Kim *et al.*, 2008; Lyu *et al.*, 2014; Peng *et al.*, 2008; Pinyakong *et al.*, 2003). Partial or incomplete breakdown (both intra- or extra-cellular) of PAHs either within a species or community of bacteria has the potential to result in various oxidized aromatic forms containing singular or combinations of oxidized regions or subunits (e.g. hydroxyl/alcohol, carboxyl/acidic, epoxide, ester, ketone/quinone groups) (Bolton *et al.*, 2000; Kazunga and Aitken, 2000). As oxygen is more electronegative (3.44 on the Pauling scale) than carbon (2.55) and hydrogen (2.2) these intermediate metabolites have dipole moments (i.e. non-uniform distribution of charges) and therefore have increased solubility and bioavailability in the aqueous phase compared to their parent compounds. Therefore an investigation into the effects of aromatic intermediate metabolites as well as the parent LMW PAHs on micro-algal cell growth and photosynthesis was considered in this chapter.

In order to determine whether intermediate phenanthrene metabolites inhibit or stimulate *T. pseudonana* growth and light absorption the diatom was incubated in

separate treatments containing one of six known chemical intermediates of microbial phenanthrene degradation (as identified by Arias *et al.*, 2008; Gao *et al.*, 2013 and Hadibarata *et al.*, 2011). The intermediates were 1,2-dihydroxynaphthalene, 1-hydroxy,2-naphthoic acid, phthalic acid, salicylic acid, diphenic acid, and 9,10-phenanthrenequinone. The 9,10-phenanthrenequinone can also be formed from phenanthrene photo-oxidation, biotransformation, or chemical oxidation, whereas the one-ring compounds (salicylic acid or phthalic acid) are also representative intermediates of bacterial naphthalene degradation (Annweiler *et al.*, 2000; Huang *et al.*, 2014; Martonová *et al.*, 1972;). These intermediate metabolites were predicted to have varying biological effects upon marine micro-algae because of their similarity (molecular weight/shape/elemental composition) and possibly also therefore biological effect to signalling molecules, hormones or pharmaceuticals. For example, salicylic acid is a signalling molecule in plants that can reduce abiotic stress (Horváth *et al.*, 2007; Kazemi *et al.*, 2010;). Salicylic acid is also the active metabolite of aspirin that can also contaminate aquatic environments (Hignite and Azarnoff, 1977) and is added to cosmetic products (e.g. Vosene anti-dandruff shampoo). Other intermediate metabolites, such as 9,10-phenanthrenequinone, may exhibit higher toxicity to aquatic organisms than their parent compounds due to the production of intracellular reactive oxygen species (Wang *et al.*, 2009; Xie *et al.*, 2006). Also in this chapter the effects of fractions (containing unknown chemical intermediates) extracted from different stages of phenanthrene degradation by the PAH-degrading bacterium *P. algicola* strain TG408 (Gutierrez *et al.*, 2013b) on the growth and light absorption of *T. pseudonana* were investigated. To identify for effects of intermediate metabolites of PAH degradation upon micro-algae, the growth of the algae was monitored by cell count measurements during exposure experiments. Secondly, a Pulse Amplitude Modulated fluorometer (PhytoPAM, Walz) was used to provide rapid *in vivo* measurements of maximal photosystem II photochemical efficiency (or maximum quantum yield, Y, which is equal to variable fluorescence divided by maximal fluorescence, F_v/F_m) for dark-adapted micro-algal cells using saturating multiple turnover flashes (Genty *et al.*, 1989; Schreiber *et al.*, 1995, 2011; Suggett *et al.*, 2003). This is a measure of maximal photochemical efficiency, which is responsive to nutrient and/or toxin metabolism in micro-algae, and is used generally as a parameter for 'algal health' (Berges *et al.*, 1996; Kromkamp and Forster, 2003).

T. pseudonana has previously been shown to respond to benzo[*a*]pyrene (BaP) by up-regulating enzymes known to be involved in inactivation of intermediate metabolites (glutathione S-transferase targeting BaP-7,8-diol and dihydrodiol dehydrogenase targeting *trans*-dihydrodiol compounds) and reactive oxygen species (ascorbate peroxidase) (Carvalho *et al.*, 2011). However, PAH-degradation by this diatom has not been measured directly. Furthermore the incorporation of carbon derived from the degradation of PAHs into diatom biomass has not been investigated. Incorporation of petroleum hydrocarbons into diatoms could either be done directly by the micro-alga or otherwise via primary degradation by hydrocarbonoclastic bacteria and subsequent transfer of some secondary carbon-based metabolite. Detection of the latter would be of great significance to hydrocarbonoclastic bacterial interactions. The phenanthrene degradation capability of *T. pseudonana* (without assistance from hydrocarbonoclastic bacteria) was assessed in this chapter by using gas chromatography/mass spectrometry (GC-MS) to measure phenanthrene concentrations in diatom cultures after 2-week incubations.

Following this, a stable isotope tracing experiment was carried out to detect whether carbon metabolites produced during the degradation of phenanthrene by *P. algicola* are incorporated into the biomass of the axenic diatom *T. pseudonana*. Uniformly ^{13}C-labelled phenanthrene was introduced to the artificial algal/bacterial cultures in two ways: firstly with *Polycyclovorans algicola* (strain TG408) and *T. pseudonana* incubated together with ^{13}C-labelled phenanthrene, and secondly with the bacterial species removed before micro-algal incubation (sequential culture), leaving the degraded ^{13}C-intermediate metabolites diluted to a concentration where optimum diatom growth was measured. Raman spectroscopy was used to identify ^{13}C-incorporation in algal and bacterial cells. Raman spectrometers detect Stokes-scattered photons. Stokes scattering is the more frequent type of inelastic scattering, where photons are re-emitted at a lower energy and longer wavelength (λ) than the incident photons (λ_0) (i.e. 'red-shifted') (Wagner, 2009). The wavenumber (reported in cm^{-1}) of scattered photons is calculated using formula:

$$\text{Raman wavenumber} = (\lambda_0^{-1} - \lambda^{-1}) \times 10^7 \text{ (Wagner, 2009)}$$

Heavier atoms (e.g. ^{13}C-labelled) emit photons at higher energy and therefore Raman wavenumber is decreased. Raman fluorescent peaks (e.g. phenylalanine) can therefore be used to detect incorporation of stable isotopes (Huang *et al.*, 2007b; Wagner, 2009).

In the second half of the chapter the focus was on determining what mechanism(s) underpin a symbiotic relationship between hydrocarbonoclastic bacteria and micro-algae. The hydrocarbonoclastic bacterium *P. algicola* strain TG408, which was used in the first half of the chapter, exhibits a narrow nutritional spectrum consisting of hydrocarbons (aliphatic and aromatic) and small organic acids. Another bacterium (*Algiphilus aromaticivorans* strain DG1253) is capable of degrading two- and three-ring PAHs and a narrow range of alkanes and organic compounds. These two PAH degraders were isolated from laboratory cultures of the diatom *Skeletonema costatum* (CCAP1077/1C) and the dinoflagellate *Lingulodinium polyedrum* (CCAP 1121/2) respectively (Gutierrez *et al.*, 2012b; Gutierrez *et al.*, 2013b). To determine what mechanism(s) underpin these symbiotic relationships the PAH-degrading bacteria were visualized *in situ* under normal laboratory conditions and after phenanthrene enrichment. Catalyzed reporter deposition fluorescence *in situ* hybridization (CARD-FISH) is a method of amplifying weak fluorescence signals due to low ribosome number and can allow signals to be visible clearly on an autofluorescent background (e.g. pigment-containing phytoplankton) (Pernthaler *et al.*, 2002; Schönhuber *et al.*, 1999). Previously, CARD-FISH has been used to detect epiphytic bacteria on algae (Mayali *et al.*, 2011; Simon *et al.*, 2002b; Tujula *et al.*, 2005), although hydrocarbonoclastic bacteria have not previously been shown associated with their micro-algal hosts using microscopy. The aim here was firstly to determine whether these PAH-degrading bacterial species become enriched when exposed to phenanthrene, and secondly to visualize, for the first time, the presence of these bacteria on the surface (phycosphere) of micro-algae. The locality of the hydrocarbonoclastic bacterial in relation to their micro-algal hosts and changes in locality during petroleum hydrocarbon enrichment may be important factors in the relationship of these organisms.

Marine micro-algal EPS can contain many complex non-polar molecules (e.g. poly-unsaturated fatty acids) (Dewapriya and Kim, 2014) incorporated into macromolecular protein/lipid/polyssacharide matrices (as outlined in Chapter 1). Potential complexation of petroleum hydrocarbons to EPS molecules would influence distribution/partitioning and therefore the fate of hydrocarbons (Kalmykova *et al.*, 2013; Sikkema *et al.*, 1995). In this chapter the effects of extracellular substances produced by two axenic diatom species (*T. pseudonana* and *C. calcitrans*) on phenanthrene dissolution was investigated. Axenic diatom strains were used in order to guarantee that the extracellular substances were algal-derived. The concentration of phenanthrene in

diatom cultures was determined after removal of diatom cells and compared with diatom-free controls by performing extractions with ethyl acetate (as per Palackal *et al.*, 2002). GC-MS was then used to quantify the phenanthrene (a common method for PAH quantification) (Coelho *et al.*, 2011; Diercks *et al.*, 2010; Yamada *et al.*, 2003). An increase in phenanthrene concentration in the micro-algal cultures would highlight the attractiveness of the phycosphere biotope to hydrocarbonoclastic bacteria, and the production of extracellular substances (like EPS) may also influence the degradation rate of PAHs due to surfactant qualities.

EPS-production was investigated further as a mechanism in the relationship between hydrocarbonoclastic bacteria and micro-algae: an experiment was designed to determine which bacteria (from 4 different genera) can grow directly on nutrients derived from diatom cultures without the need for nutrient sharing with a microbial community. The four PAH-degrading species tested included *P. algicola* strain TG408 and *A. aromaticivorans* strain DG1253 (mentioned above) and additionally *Arenibacter algicola* strain TG409 and *Marinobacter* sp. strain MCTG268 (both originally isolated from *Skeletonema costatum* culture CCAP1077/1C). *A. algicola* strain TG409 can consume a wide range of organic substrates including naphthalene and phenanthrene (Gutierrez *et al.*, 2014). *Marinobacter* sp. strain MCTG268 was isolated by enrichment with naphthalene as sole carbon source (Gutierrez *et al.*, 2016). Members of the genus *Marinobacter* are well-known for their ability to degrade a range of hydrocarbons (Yakimov *et al.*, 2007), and the closest relative of strain MCTG268 is *Marinobacter algicola*, which can grow on *n*-hexadecane and *n*-tetradecane (Green *et al.*, 2006). The bacteria were inoculated independently from one another on agar plates containing various algal nutrient fractions extracted from two axenic micro-algal cultures (*T. pseudonana* strain 1085/12 and *C. calcitrans* strain 1010/11). Fractions included not only extracellular nutrients but also lysed micro algal cell contents, in an attempt to tease apart nutrient preference in the 4-hydrocarbonoclastic bacterial species. The agar plates produced by *T. pseudonana* and *C. calcitrans* were prepared separately to detect algal-species-specific differences in nutrient quality.

At the end of Chapter 2 the focus of study was specifically on *P. algicola* strain TG408. This strain was of particular interest because of its inability to form colonies on the micro-algal derived nutrients in the previous section, a finding that raised questions about the relationship this organism has with the 'host' diatom from which it was

isolated (i.e. *S. costatum*). This organism can form clearing zones on phenanthrene crystal coated agar plates (Gutierrez *et al.*, 2013b), however it does not form visible colonies as it does on pyruvate-agar. Growth of *P. algicola* was therefore assessed on agar plates containing six known chemical intermediates resulting from microbial phenanthrene degradation (1,2-dihydroxynaphthalene, 1-hydroxy,2-naphthoic acid, phthalic acid, salicylic acid, diphenic acid, 9,10-phenanthrenequinone) to determine whether these are converted into colonies/biomass more effectively than phenanthrene.

2.2 Materials and Methods

2.2.1 PAH metabolite-driven interactions between Polycyclovorans algicola strain TG408 and micro-algae

2.2.1.1 Assessing the effect of phenanthrene and naphthalene on Thalassiosira pseudonana and Chaetoceros calcitrans

The diatoms *T. pseudonana* strain 1085/12 and *C. calcitrans* strain 1010/11 were purchased from the Culture Collection of Algae and Protozoa (CCAP) in an axenic state. Axenic cultures were maintained using sterile artificial seawater medium (ASW) F/2+Si (Appendix E) and bacterial presence was monitored weekly by DAPI staining on filter sections and spread-plating using ZM/10 agar (Appendix E). If bacterial presence was detected approximately 1 ml of vegetative diatom culture was incubated with F/2+Si medium amended with antibiotics (270 μg ml^{-1} penicillin, 135 μg ml^{-1} streptomycin and 27 μg ml^{-1} chloramphenicol) (Guillard, 1973) and carbendazim (1 μg ml^{-1}) (Mahan *et al.*, 2005) overnight and subsequently maintained in exponential-phase for three subcultures in sterile F/2+Si medium. Both species were grown to exponential-phase on a 12-h light/dark cycle (with light provided by fluorescent white bulb producing a photon flux density of 150 μmol m^{-2} s^{-1}) at 16°C on an orbital shaker (100 rpm). Throughout this chapter all glassware used had been previously acid-washed (0.1M HCl), rinsed three times with distilled water and autoclaved (at 121°C for 15 min) prior to use. In order to assess the tolerance of the two diatoms species to phenanthrene and naphthalene *Thalassiosira pseudonana* and *Chaetoceros calcitrans* were individually incubated with either naphthalene (Fisher, 99%) or phenanthrene, (Aldrich, ≥99.5%) and growth was monitored using either direct cell counts or chlorophyll-*a* extraction.

The five PAH-enrichment experiments were set up in triplicate in 100 ml conical flasks containing 50 ml (final volume) of F/2+Si media:

- 1) *C. calcitrans* and 2) *T. pseudonana* incubated with naphthalene (at saturation concentration).
- 3) *C. calcitrans* and 4) *T. pseudonana* incubated with 80 mg L^{-1} of phenanthrene.
- 5) *T. pseudonana* incubated with 4 mg $L^{-1}$of phenanthrene.

For the naphthalene incubations saturation concentration was achieved by placing (in a laminar flow cabinet) ~0.17 g of naphthalene crystals into test tubes, which were then placed into the conical flasks containing sterile F/2+Si medium and hermetically sealed with the screw caps. The naphthalene was allowed to volatilize and equilibrate between the headspace and the medium for 3 days at 16°C. For both phenanthrene incubations the phenanthrene (final concentration of either 80 mg L^{-1} or 4 mg L^{-1} in F/2+Si medium) was added to the conical flasks dissolved in acetone and the acetone was allowed to evaporate in a laminar flow cabinet. Sterile F/2+Si medium was then added to the conical flasks and the phenanthrene was allowed to equilibrate for 3 days at 16°C. For phenanthrene incubations conical flasks were topped with sterile cotton bungs instead of screw caps. Inoculation with either *T. pseudonana* or *C. calcitrans* occurred at the 3-day time-point for all three experiments: a volume of 0.5 ml of exponential-phase diatoms was added to the appropriate conical flasks. The conical flasks were incubated with shaking (100 rpm; 16°C) with a 12-h light/dark cycle (photon flux density = 150 µmol m^{-2} s^{-1}). Triplicate no-PAH control incubations were included for all of the above treatments (PAHs were not added to the controls). For chlorophyll-*a* measurements 0.5 ml was extracted from each flask and passed through grade GF/C glass microfiber filters (Whatman) to collect the micro-algal biomass. Filters where then placed in individual Falcon tubes containing 5 ml of 90% acetone, incubated at -20°C for 24 h before being analysed using a fluorometer (HORIBA Scientific Fluoromax-4) at an excitation of 485 nm and emission of 685 nm. For diatom cell counts 25-30 µl was extracted from each flask and placed into a haemocytometer for microscopic analysis. Sampling occurred immediately after inoculation and at three-day intervals.

2.2.1.2 Determining the effect of known intermediate breakdown products of PAH biodegradation on T. pseudonana

T. pseudonana was incubated in separate quadruplicate F/2+Si medium treatments containing one of six intermediate breakdown products, and growth was monitored using direct cell counts. The maximal photosystem II photochemical efficiency (or maximum quantum yield, 'Y') was measured using a PhytoPAM (Walz) fluorometer. Individual stock solutions of six chemical intermediates of phenanthrene degradation dissolved in acetone were prepared: phthalic acid (Sigma-Aldrich ≥99.5%), salicylic acid (Sigma 99%), diphenic acid (Aldrich ≥96.5%), 1-hydroxy,2-naphthoic acid (Aldrich ≥97.0%), 1,2-dihydroxynaphthalene (Aldrich technical grade) and 9,10-phenanthrenequinone (Aldrich 95%). In a laminar flow cabinet 32 µg of each of the six dissolved chemical intermediates was added separately to four test tubes and the acetone was allowed to evaporate. F/2+Si medium (13 ml) was added to each test tube and the chemical intermediates were allowed to equilibrate into the medium overnight at 16°C. This created a total of six quadruplicate treatments (24 test tubes). An additional four control tubes were included containing only F/2+Si medium (without chemical intermediate supplement). Each test tube was inoculated with 3.5 ml of exponential-phase *T. pseudonana* culture. The final concentration of each chemical intermediate in each flask after diatom inoculation was 1.93 µg ml^{-1}. The seven quadruplicate incubations were placed on a 12-h light/dark cycle (photon flux density = 350 µmol m^{-2} s^{-1}) and inverted daily. Samples were taken from each tube periodically for cell counts (0.5 ml) and PhytoPAM measurements (2 ml). The reported aqueous solubilities of the intermediates are as follows: phthalic acid 7 mg ml^{-1} (at 25°C), salicylic acid 2.24 mg ml^{-1} (at 25°C), diphenic acid 100 µg ml^{-1} (at 20°C), 9,10-phenanthrenequinone 7.5 µg ml^{-1} (no data was available for aqueous solubilities of 1-hydroxy,2-naphthoic acid or diphenic acid). The above intermediate compounds were used well below their aqueous solubilities. They were used at equal aqueous concentrations (1.93 µg ml^{-1}) to provide comparative toxicity information based on compound type rather than concentration.

Subsequently this experiment was repeated for just one of the chemical intermediates (1-hydroxy,2-naphthoic acid) that displayed interesting results (possible stimulation of light absorbance) (see Appendix A). This time, however, the experiment was performed in conical flasks containing 46 ml F/2+Si medium to which 4 ml of exponential-phase *T. pseudonana* exponential-phase inoculum was added. These flasks were then placed on an orbital shaker (100 rpm; 16°C) with a 12-h light/dark cycle

(photon flux density = 150 μmol m^{-2} s^{-1}). Flasks were set up in quadruplicate treatments containing 0 (control), 0.5, 1 and 2 μg ml^{-1} of 1-hydroxy,2-naphthoic acid dissolved in F/2+Si medium. Once again samples were taken from each tube periodically for cell counts (0.5 ml) and PhytoPAM (2 ml). Upon termination the chlorophyll-*a* concentration of each treatment was measured by passing 5 ml from each conical flask through a GF/C filter and adding this to 90% acetone and measuring with a fluorometer (Fluoromax 4) as described in the previous section (results of this experiment are found in Appendix A).

2.2.1.3 Determining the effect of breakdown products produced during phenanthrene degradation by P. algicola strain TG408 on the growth of T. pseudonana

The aim in this section was firstly to determine whether fractions extracted from different stages of phenanthrene degradation by the PAH-degrading bacterium *P. algicola* strain TG408 (Gutierrez *et al.*, 2013b) inhibit the growth and light absorption of *T. pseudonana*. The second aim was to choose a fraction (extracted on either day 2, 4 or 6) that inhibited the diatom growth least (as a preliminary study for a ^{13}C-tracing experiment in Section 2.2.1.5). In order to address these aims, a culture of *P. algicola* was introduced to a phenanthrene-containing growth medium (ONR7a, for recipe see Appendix E) and fractions of this were extracted and stored for subsequent incubation with *T. pseudonana*. In a laminar flow cabinet, 60 mg of phenanthrene (dissolved in acetone) was added to three conical flasks (500 ml) and the acetone allowed to volatilize. ONR7a (495 ml) medium was then added to each conical flask and the phenanthrene was allowed to equilibrate into the medium for 2 days (at 25°C) in preparation for *P. algicola* inoculation (final concentration of phenanthrene in flasks was 120 μg ml^{-1}). A culture of *P. algicola* was prepared in ONR7a amended with 0.1% sodium-pyruvate to an optical density at 600 nm (OD600) of 0.29 ± 0.011. A volume of 10 ml of this culture (OD600 ~0.29 ± 0.011) was used to inoculate three conical flasks containing 490 ml fresh ONR7a amended with sodium-pyruvate (0.1% final concentration). At the same time, another 3 × 10 ml volumes of the *P. algicola* culture (OD600 ~0.29 ± 0.011) was washed (×3) with sterile ONR7a (3,000 *g*; 10 min) and the cells re-suspended in 5 ml of ONR7a. The 5 ml washed *P. algicola* samples were used to inoculate the conical flasks containing 495 ml of phenanthrene-equilibrated ONR7a medium. The phenanthrene- and pyruvate-amended cultures were incubated at 25°C on a shaker (100 rpm). Growth was monitored in both the phenanthrene- and pyruvate-amended cultures using OD600 measurements (results in Appendix B.1).

After days 2, 4 and 6, a volume of 120 ml was taken from the phenanthrene cultures and, in sterile conditions in a laminar flow cabinet, passed through a GF/C filter (×2 layers thick) and stored at 4°C. Filtrate from the ONR7a (0.1% pyruvate) *P. algicola* incubations were also prepared in this way on day 9. These phenanthrene (or pyruvate) metabolite-containing fractions were used for challenging the diatom *T. pseudonana* in the following way. Firstly an experiment (outlined in Appendix B.2) was performed in order to determine the maximum ratio of ONR7a/F/2+Si to use that would (in the absence of phenanthrene) not be extremely detrimental to *T. pseudonana* growth, and the ratio chosen was 3:1 (i.e. 75% ONR7a and 25% F/2+Si). Conical flasks containing five different treatments were set up in triplicate. The treatments contained 75% of either: 2, 4 or 6-day phenanthrene degradation ONR7a fractions, pyruvate ONR7a fractions or sterile ONR7a (control). The treatments were topped up with 25% of exponential-phase *T. pseudonana*. The total volume on each conical flask was 50 ml. The conical flasks were incubated with shaking (100 rpm; 16°C) with a 12-h light/dark cycle (photon flux density = 150 μmol m^{-2} s^{-1}). Every other day (from day 1 – 9), each conical flask was sampled (1-ml volumes) for cell counts, and 2 ml was sampled for photosynthetic efficiency measurements using PhytoPAM (an additional PhytoPAM measurement was also taken 4 h after incubation.

2.2.1.4 Determining whether T. pseudonana has the ability to degrade phenanthrene

In triplicate *T. pseudonana* cultures were prepared in F/2+Si medium and allowed to reach exponential-phase. In a laminar flow cabinet 0.74 ± 0.01 mg of phenanthrene (dissolved in acetone) was pipetted into clean and sterilized test tubes fitted with PTFE-lined screw tops and the acetone was allowed to evaporate. A volume of 3 ml F/2+Si medium was added to each tube and the phenanthrene was allowed to equilibrate into the medium for 3 days at 16°C to make a final concentration of 246.7 ± 3.3 mg L^{-1} phenanthrene in F/2+Si. The following three treatments were set up in two batches, one in triplicate and the other in quadruplicate:

1. *T. pseudonana* in F/2+Si medium incubated with phenanthrene.
2. *T. pseudonana* in F/2+Si medium incubated with phenanthrene and 3% (v/v) phosphoric acid (biological matrix surrogate for phenanthrene recovery)
3. Sterile F/2+Si medium incubated with phenanthrene.

At the start of the experiment a volume of 100 µl of exponentially growing inoculum *T. pseudonana* cells was added to the treatments 1 and 2 above. Tubes were incubated on a 12-h light/dark cycle at 16°C (photon flux density = 150 µmol m^{-2} s^{-1}) and mixed by gentle inversions once daily. The triplicate incubations were used for measuring algal growth by taking direct cell counts with a haemocytometer as previously described. The quadruplicate incubations were used for GC-MS analysis to determine whether *T. pseudonana* degrades phenanthrene when incubated in F/2+Si medium. For phenanthrene quantification (GC-MS) 3 ml of HPLC-grade ethyl acetate was added to the quadruplicate incubations after a 2-week long incubation and shaken vigorously by hand for 10 seconds before vortexing for 30 seconds. Aliquots of the non-aqueous top layer were stored in hermetically sealed vials at 4°C.

All GC-MS analyses were carried out on a Shimadzu QP2010 Ultra GC-MS with split/splitless injector. The column was a HP5 MS (length: 360 m, diameter: 0.25mm, film thickness: 0.25 µm). Heptanone was used as an internal standard. A stock solution of heptanone dissolved in ethanol was diluted with ethyl acetate to give 20 mg L^{-1}, which was added to the experimental ethyl acetate extractions at a ratio of 9:1 (to give a concentration in the sample of 2 mg L^{-1} heptanone). Phenanthrene in ethyl acetate was used as the calibration standard. Dilutions were made from a stock solution in order to create a calibration range of 0.1 – 4 mg L^{-1}. The calibration levels were then treated as outlined above to produce a calibration curve. A volume of 1 µl of sample was injected into the GC-MS using an AOC 5000 auto-sampler. The injector temperature was set to 250°C. The selected ion monitoring (SIM) method was used. The GC conditions were as follows: pressure = 53.5 kPa / total flow = 4 ml min^{-1} / column flow = 1 ml min^{-1} / linear velocity 36.3 cm s^{-1} / purge flow = 1 ml min^{-1} / sampling time = 1 min. The oven temperature was initially 50°C for 2 min followed by an increase to 80°C (at 4°C min^{-1}), an increase to 240°C (at 10°C min^{-1}) and finally a hold of 4.5 min (total 30 min). The MS conditions were as follows: start time = 2.4 min / end time = 29 min / ion source =200°C / interface = 250°C / solvent cut = 2.3 min. The mass to charge ratio (*m*/*z*) for heptanone was 57. The *m*/*z* for phenanthrene was 178. To ascertain accuracy, three trials on a standard, diluted to contain 5 mg L^{-1} of phenanthrene, gave 5.05, 5.14 and 5.17 mg L^{-1}. The retention time for heptanone was 3.32 min, whereas that for phenanthrene was 19.43 min.

2.2.1.5 Determining whether carbon released from the bacterial degradation of phenanthrene can be incorporated into micro-algal biomass

Uniformly ^{13}C-labelled phenanthrene was synthesized by methods described in Zhang *et al.*, (2011b). In light of the results of intermediate metabolite algal incubations and the possible toxicity of the phenanthrene and intermediate metabolites to *T. pseudonana* found in previous sections, ^{13}C-phenanthrene was introduced to a culture of *T. pseudonana* in two ways:

1. 'Co-culture' treatments in which *P. algicola* and *T. pseudonana* were incubated together with ^{13}C-phenanthrene.
2. 'Sequential culture' treatments in which various fractions of ^{13}C-phenanthrene degradation by *P. algicola* were extracted and subsequently incubated with *T. pseudonana*.

Stock solutions of ^{13}C and ^{12}C phenanthrene dissolved in acetone (5 mg ml^{-1}) were prepared. Also exponential-phase *T. pseudonana* and *P. algicola* were prepared, the former grown in in Berges artificial seawater medium (ASW) (Berges *et al.*, 2001) (Appendix E), which contained no carbon source, and the latter grown in ONR7a amended with 0.1% Na-pyruvate. For the 'co-culture' treatments a volume of 4 µl of ^{13}C-phenanthrene stock (containing 20 µg of phenanthrene) was placed in triplicate 20 ml glass test tubes with aluminum foil-lined screw tops and acetone was allowed to evaporate (this produced a final phenanthrene concenatration in Berges ASW of 1 µg ml^{-1}). Berges ASW (11 ml) without vitamins was added to the tubes and phenanthrene was allowed to enter solution for 3 days in the dark at 16°C. Late exponential-phase *T. pseudonana* (1 ml) was added in triplicate. Also in triplicate, an exponential-phase *P. algicola* culture (1 ml) was washed (×3) with 1 ml of Berges ASW by centrifuging at 8,000 *g* for 5 min and re-suspending in fresh medium. The bacterial pellets were re-suspended in 1 ml of fresh medium and this was added to their respective *T. pseudonana*-containing test tubes. Berges ASW vitamins were added and tubes were incubated at 16°C on a 12-h light/dark cycle (photon flux density = 150 µmol m^{-2} s^{-1}). Growth of *T. pseudonana* was monitored by extracting 30 µl of sample daily and performing haemocytometer counts. Samples (1 ml) of each treatment were taken after day 3, 8, 15 and 30 and placed in 1 ml microfuge tubes. Control samples were incubated with ^{12}C-phenanthrene and treated in exactly the same way.

For the 'sequential-culture' treatments a volume of 200 µl of ^{13}C-phenanthrene stock (containing 1 mg of phenanthrene, equal to 25 µg ml^{-1} in 40 ml of Berges ASW) was placed into triplicate acid-washed and sterilized 50 ml conical flasks with foil-lined screw top lids and the acetone was allowed to evaporate in the dark. Berges ASW (40 ml) was added (without vitamins) and phenanthrene was allowed to enter solution for 3 days at 25°C in the dark. Late exponential-phase *P. algicola* (3 × 7.5 ml) ONR7a-pyruvate culture and washed (3 times) with fresh Berges ASW with no organic carbon source. The bacterial pellets were re-suspended to a final volume of 10 ml and then transferred into the conical flasks containing phenanthrene and Berges ASW, topped up with 40 µl (1000× Berges vitamin solution) and incubated at 25°C on 12-h light/dark cycle (photon flux density = 150 µmol m^{-2} s^{-1}). After 2 and 4 days, a 20 ml samples were taken from the conical flasks and passed through a 0.22 µm Isopore filter to remove bacteria. These 20 ml filtrates were frozen awaiting the results of an identical experiment using ^{12}C-phenanthrene to determine the appropriate ratio of Berges ASW/phenanthrene-fraction that would not inhibit *T. pseudonana* growth. The ratios used were 3:2 (Berges ASW/day 2 fraction), 9:1 (Berges ASW/day 4 fraction) and 4:1 (Berges ASW/day 4 fraction), and the final volumes were 10 ml of each treatment in test tubes topped up with 5 µl of vitamins (1000 ×) and late exponential-phase *T. pseudonana* (1 ml). *T. pseudonana* growth was measured using a haemocytometer and experiments were terminated when stationary phase (~2 weeks) was reached. Samples (1 ml) from each treatment were taken on day 5 and 10 and placed in 1 ml microfuge tubes.

Samples from both co- and sequential-culture treatments were fixed for 3 h in 3% PFA before washing (×3) with PBS (pH 7.3) and were stored in 1:1 (v/v) solution of PBS (1x) and ethanol at -20 °C. Raman cell spectra were collected by Dr. Márton Palatinszky at the University of Vienna, Division of Microbial Ecology. Preserved cells were spotted (0.5 – 1 µl) onto aluminum-coated slides (EMF). A Labram HR Evolution (Horiba Scientific) Raman microscope equipped with two measuring lasers (532 nm/500 mW and 785 nm/100 mW with wavelength optimized back illuminated and front illuminated CCD detectors, respectively) was used to collect Raman emission spectra. Each scan was performed over a wavenumber range of 400 – 3100 cm^{-1} with a spectral resolution of 1 cm^{-1}. Spectra were acquired using single scans of 20 seconds duration with the 523 nm laser and the 100× objective lens (grating = 300 gr mm^{-1}, ND filter = 2.5%, slit size = 100 µm, hole size = 300 µm). Spectra were viewed using

LabSpec 6 HORIBA Scientific software. Five to ten bacterial and/or diatom cells from each sample were measured. When measuring *T. pseudonana*, the cells were photo-bleached with both lasers for 1 minute to quench algal autofluorescence. The phenylalanine peak was used for detection of ^{13}C incorporation, which is revealed by a lower wavenumber relative to ^{12}C cells, due to the heavier mass of phenylalanine conferred by the stable isotope (as explained in Section 2.1). The *T. pseudonana* culture (unlabelled) and ^{12}C control treatments were used for Raman peak comparison.

2.2.2 Determining what mechanism(s) underpin a symbiotic relationship between hydrocarbonoclastic bacteria and micro-algae

2.2.2.1 Enrichment of Skeletonema costatum and Lingulodinium polyedrum with phenanthrene and probing for hydrocarbonoclastic bacteria using Catalyzed Reporter Deposition Fluorescence In Situ Hybridisation (CARD-FISH)

As has been mentioned in the introduction, *Polycyclovorans algicola* strain TG408 and *Algiphilus aromaticivorans* strain DG1253 are hydrocarbonoclastic bacteria that display versatility in degrading PAHs. These strains were originally isolated from laboratory cultures of *Skeletonema costatum* (CCAP1077/1C) and *Lingulodinium polyedrum* (CCAP 1121/2) respectively (Gutierrez *et al.*, 2012b,2013b). In order to visualise the PAH-degrading bacteria horseradish peroxidase (HRP)-labelled oligonucleotide probes that target *P. algicola* and *A. aromaticivorans* (PCY223 and ALGAR209 respectively) were optimized for use with CARD-FISH using the method outlined in detail in Appendix D, in which multiple formamide concentrations were compared for probe intensity and non-specific binding in the target organisms. The optimum formamide concentrations for highest fluorescent signal intensity of the target probes and minimum levels of non-specific binding (using the NON338 probe) were 55% for PCY223 and 40% ALGAR209 (see Appendix D).

The non-axenic diatoms *Skeletonema costatum* (1077/1C) and *Lingulodinium polyedrum* (1121/2) were purchased from the Culture Collection of Algae and Protozoa (CCAP). In a laminar flow cabinet, 200 μg of phenanthrene dissolved in acetone was added to six (out of a total of twelve) conical flasks (100 ml) and the acetone allowed to evaporate. F/2+Si medium (49 ml) was added to all twelve conical flasks (making a phenanthrene concentration of 4 μg ml^{-1}), which were plugged with sterile cotton bungs topped with foil. At 16°C the phenanthrene was allowed to equilibrate with the

seawater medium in the flasks for 3 days prior to onset of the experiment. Exponential-phase *S. costatum* or *L. polyedrum* culture (1 ml) was added to the conical flasks to create the following four triplicate treatments: 1) *S. costatum* with F/2+Si (control); 2) *S. costatum* with F/2+Si and phenanthrene; 3) *L. polyedrum* with F/2+Se (control); and 4) *L. polyedrum* with F/2+Se and phenanthrene (see Appendix E for F/2+Se recipe). The conical flasks were placed on an orbital shaker as previously described with a 12-h light/dark cycle (photon flux density = 150 μmol m^{-2} s^{-1}). On sampling days (0, 3, 5 and 8) a volume of 0.5 ml from each treatment was passed through an Isopore polycarbonate membrane (0.22 μm) gently and fixed with 3% (v/v) PFA for 3 h at 4°C before being washed 3 times with sterile PBS (1x) and air-dried. Small areas (4 mm^2) of the filters were cut out using flame-sterilized scissors. To avoid loss of loosely associated bacterial cells the filter sections were dipped into 0.2% (wt/vol) agarose solution before being mounted onto glass slides and air dried (Pernthaler *et al.*, 2002). The CARD-FISH protocol used was the same as described in Appendix D. Formamide concentrations used were 55% for the PCY223 probe on *S. costatum* and 40% for ALGAR209 probe on *L. polyedrum* and Cy3-labelled tyramides were used for signal amplification. The unlabelled competitor probe (c1ALGAR209) was always used with ALGAR209. Samples were covered in mountant (80% [v/v] Citifluor, 14% [v/v] Vectashield, 1 μg ml^{-1} DAPI in 100% PBS [pH 9]) before microscopic observation. Samples were visualized using a Zeiss (Axio Scope.A1) epifluorescence microscope fitted with Carl Zeiss Filter Sets 01, 09 and 15 (for use with DAPI, Fluorescein and Cy3 respectively) and a Zeiss digital fluorescence imaging camera (AxioCam MRm). Epifluorescence micrographs were overlaid using Zeiss Zen-Blue (2012) image processing module.

2.2.2.2 Determining the effect of micro-algal cells and their produced extracellular substances on the dissolution of phenanthrene

Complexation or immobilisation of phenanthrene with algal-derived EPS may explain locations of PAH-degrading bacteria noticed in the previous section. The aim here was determine if micro-algal presence and micro-algal derived extracellular products increase the concentration of phenanthrene in the F/2+Si medium inoculated with micro-algae by increasing the dissolution of crystallised phenanthrene attached to the sides of conical flasks compared to non-biological controls. It was necessary to use axenic micro-algal strains in order to guarantee that the extracellular pruducts were not of bacterial (or fungal or archaeal) origin. To address these aims two axenic diatom

strains (*T. pseudonana* strain 1085/12 and *C. calcitrans* strain 1010/11) were incubated in media containing phenanthrene crystals and after subsequent removal of the diatom cells the remaining growth medium (F/2+Si) was measured for phenanthrene concentration using GC-MS. In a laminar flow cabinet 2 mg of phenanthrene (dissolved in acetone) was added to 9 conical flasks (100 ml) and the acetone allowed to evaporate overnight in the dark to create a thin film of phenanthrene crystals around the conical flasks. F/2+Si medium (49.5 ml) was then added to all 9 conical flasks, which then were plugged with sterile cotton bungs topped with foil. All flasks were incubated at 16°C for 3 days to allow the phenanthrene to equilibrate with the seawater medium prior to inoculation and commencement of the experiment. After this initial 3 days, late-exponential-phase diatom cultures (0.5 ml) (either *T. pseudonana* or *C. calcitrans*) were added to the conical flasks to create the following triplicate incubations at a concentration of 40 mg L^{-1} phenanthrene:

1) *C. calcitrans* with F/2+Si and phenanthrene
2) *T. pseudonana* with F/2+Si and phenanthrene
3) F/2+Si with phenanthrene (uninoculated control)

The conical flasks were placed on a shaker at 100 rpm at 16°C with a 12-h light/dark cycle (photon flux density = 150 µmol m^{-2} s^{-1}). After inoculation, chlorophyll-*a* readings were taken on sampling days 0, 2, and 8 using the same method described in Section 2.2.1.1. Upon termination of the experiment (at day 8), 5 ml of medium from each conical flask was taken using a glass syringe and passed through a Whatman GF/C filter (1.2 µm pore size) to filter the diatom cells (controls were treated identically). Of the resultant filtrate volumes, 2 ml of each was added to 2 ml ethyl acetate in Polytetrafluoroethylene (PTFE)-lined screw top glass test tubes and analysed by gas chromatography/mass spectrometry (GC-MS) in order to quantify phenanthrene concentrations. The GC-MS analysis was performed in the same way as was previously described in Section 2.2.1.4.

2.2.2.3 Determining whether P. algicola (TG408) and three other hydrocarbon-degraders grow on selected diatom-derived organic nutrients.

The same axenic diatom cultures were used as in Section 2.2.2.2 (*T. pseudonana* strain 1085/12 and *C. calcitrans* strain 1010/11) in order to confirm that bacterial growth was supported directly by algal derived carbon substrates and not by other bacteria (or fungal or archaeal community members). The PAH-degrading bacteria selected were

from four different genera. *P. algicola* and *A. aromaticivorans* (strains PCY223 and DG1253 respectively) (both of order *Xanthomonadales* of the class *Gammaproteobacteria*) have been introduced in Section 2.2.2.1. The other two PAH-degraders used were *Marinobacter* sp. strain MCTG268 (from a well-known hydrocarbon degrading genus) and *Arenibacter algicola* strain TG409 (family Flavobacteriaceae of the phylum *Bacteroidetes*). The two separate diatom cultures (*C. calcitrans* and *T. pseudonana*) were grown in F/2+Si medium on a 12-h light/dark cycle at 16°C (photon flux density = 150 µmol m^{-2} s^{-1}) and allowed to grow into stationary phase (4 weeks). The bacterial strains were grown on ZM/10 (*A. algicola*), ONR7a amended with filter-sterile (0.2 µm) 0.1% Na-pyruvate (*P. algicola* and *Marinobacter* sp. MCTG268), or ZM/10 amended with filter-sterile (0.2 µm) 0.1% Na-pyruvate (*A. aromaticivorans*) and placed on a shaker (80 rpm) in the dark at 24°C until cloudy (4 -7 days). The cultures were introduced to four agar-treatments in order to determine whether the 4 selected hydrocarbonoclastic bacteria could utilize organic nutrients derived from diatom cultures to produce colonies (biomass) on agar. The four treatments (outlined in Table 1) were designed to alter the exact source and quality of nutrients with a variety of filtration and/or autoclaving procedures – treatment 2, for example, produced extracellular diatom derived nutrients (e.g. soluble EPS).

Table 1. Descriptions of the diatom culture treatments (1-4) and rationales. Each treatment was preformed on *C. calcitrans* and *T. pseudonana* cultures alike.

Treatment Number	Treatment Description	Rationale
1	Sterile filtered (0.2 µm) culture autoclaved (121°C, 15 minutes)	A test for growth on extracellular diatom-derived soluble nutrients subjected to heat and pressure
2	Sterile filtered (0.2 µm) culture added to autoclaved F2+Si agar (1:1) after cooling to below 55 °C	A test for growth on extracellular diatom-derived nutrients (e.g. soluble EPS)
3	Autoclaved culture (unfiltered)	A test for growth on extracellular and intracellular diatom-derived nutrients subjected to heat and pressure
4	Autoclaved culture diluted 1:1 with filtered seawater	A dilution of treatment 3

Agar plates were adjusted to the same concentrations of trace metals and vitamins. A sterile loop was dipped into bacterial cultures and streaked onto agar plates containing

the four treatments. To confirm viability, each bacterium was also streaked onto agar plates containing ONR7a amended with filter-sterile (0.2 μm) 0.1% Na-pyruvate (*P. algicola* and *Marinobacter* sp. MCTG268), ZM/10 amended with filter-sterile (0.2 μm) 0.1% Na-pyruvate (*A. aromaticivorans*) or ZM/10 (*A. algicola*). Additionally agar plates containing treatments 1 – 4 (Table 1) were left without bacterial inoculation (negative control). Plates were incubated at 24°C and results were taken after one week. Bacterial cells that produced colonies comparable to controls were marked with a '+' for positive growth. Weak growth where bacterial biomass was just visible by eye but wasn't comparable to viable controls was marked in brackets, '(+)'. Plates that had no growth by eye were marked with a '-'.

2.2.2.4 Testing P. algicola for growth on intermediate breakdown products from microbial degradation of phenanthrene

In this section the aim was to determine whether *Polycyclovorans algicola* strain TG408 could form colonies on agar plates containing intermediate breakdown products from microbial phenanthrene degradation. This was done because it was the only PAH-degrading strain that did not form colonies in the previous section, it forms clearing zones on phenanthrene enriched agar without any visible colony formation (Gutierrez *et al.*, 2013b), and it displayed limited growth in liquid culture (Appendix B.1) and undetectable incorporation of phenanthrene-derived carbon in the stable isotope probing experiment (Section 2.3.1.5). To address this aim *P. algicola* was inoculated onto agar plates containing minimal media (ONR7a) enriched with six different chemical intermediates. Firstly *P. algicola* was inoculated in 3 ml of ONR7a medium amended with 0.1% Na-pyruvate and placed on a shaker (80 rpm) in the dark at 24°C until cloudy (~7 days). Stock solutions of phthalic acid (Sigma-Aldrich ≥99.5%), salicylic acid (Sigma 99%), diphenic acid (Aldrich ≥96.5%), 1-hydroxy,2-naphthoic acid (Aldrich ≥97.0%), 1,2-dihydroxynaphthalene (Aldrich technical grade) and 9,10-phenanthrenequinone (Aldrich 95%) dissolved in acetone were prepared. Agar plates containing ONR7a with no carbon source were also prepared. In a laminar flow cabinet spots of acetone containing the six reagent-stock solutions were dripped on to individual agar plates (in triplicate) and the acetone allowed to evaporate leaving the sterile reagent patches. A sterile loop was dipped into the *P. algicola* culture and streaked through dried areas of reagent on agar plates containing the six treatments. To confirm viability a loop of *P. algicola* culture was also streaked onto an agar plate containing ONR7a amended with filter-sterile (0.2 μm) 0.1% Na-pyruvate. Additionally agar plates

enriched with the 6 chemical intermediates were left without bacterial inoculation (negative control). Plates were incubated at 24°C and results for growth were observed after 3 weeks. The aim here was to determine whether *P. algicola* could grow on any of these six intermediate metabolites by forming colonies on the agar. Previously published data show a limited selection of carbon sources that result in growth of *P. algicola*, although these six molecules were not previously investigated for growth with this strain (Gutierrez *et al.*, 2013b). This may also provide information on the specificity of enzymes involved in degradation of PAHs by *P. algicola*.

2.3 Results

2.3.1 PAH metabolite-driven interactions between P. algicola strain TG408 and micro-algae

2.3.1.1 Assessing the effect of phenanthrene and naphthalene on T. pseudonana and C. calcitrans

Growth-inhibition experiments were performed using naphthalene and phenanthrene individually in culture enrichments. The aqueous solubility of naphthalene at 25°C is 31 mg L^{-1} (Pearlman *et al.*, 1984) and the aqueous solubility of phenanthrene at 21°C is 0.82 mg L^{-1} (Verschueren, 2001). Naphthalene is extremely volatile with a vapour pressure of 0.085 mm Hg at 25°C and was used at saturation concentration in a stoppered vessel. Phenanthrene is much less volatile than naphthalene with a vapour pressure of 1.21×10^{-4} mm Hg at 25°C and was added directly to the seawater medium. Phenanthrene was used in a non-stoppered vessel and therefore a very high concentration of 80 mg L^{-1} was used to maintain the diatom cultures at saturation concentration during the course of the experiment, as phenanthrene is volatile in aqueous solution (Guha and Jaffé, 1996). In the second phenanthrene incubation a lower concentration (4 mg L^{-1}) was used in order to investigate whether diatom tolerance to phenanthrene is increased by volatilization of phenanthrene to below saturation concentration in the seawater medium. *T. pseudonana* and *C. calcitrans* were individually incubated with either naphthalene or phenanthrene and growth was monitored using either direct cell counts or chlorophyll-*a* extraction and concentration measurement. The 5 PAH-enrichment experiments were:

- 1) *C. calcitrans* (Figure 2A and B) and 2) *T. pseudonana* (Figure 2C and D) incubated with naphthalene (at saturation concentration).

- 3) *C. calcitrans* (Figure 2E) and 4) *T. pseudonana* incubated (Figure 2F) with 80 mg L^{-1} of phenanthrene.
- 5) *T. pseudonana* incubated with 4 mg L^{-1} of phenanthrene (Figure 2G and H)

In the naphthalene growth-inhibition experiments results of Student's *t* tests on each day showed that by day 3 both of the control incubations had increased cell numbers compared with their relative controls (*C. calcitrans* $p < 0.01$; *T. pseudonana* $p < 0.01$), and these differences increased by day 6 (*C. calcitrans* $p < 0.001$; *T. pseudonana* $p < 0.001$) (Figure 2A and C). Mann-Whitney U tests confirmed that *C. calcitrans* and *T. pseudonana* chlorophyll-*a* concentrations were higher relative to their naphthalene-free controls at day 3 ($p = 0.05$) and day 6 (*C. calcitrans* $p = 0.05$, *T. pseudonana* $p < 0.05$) (Figure 2B and D). These significant differences show that naphthalene has an inhibitory effect on both species of micro-algae.

Cell count results for *T. pseudonana* and *C. calcitrans* cultures subjected to 80 mg L^{-1} phenanthrene were not collected but instead chlorophyll-*a* readings were taken as a surrogate for diatom production. Chlorophyll-*a* readings at 80 mg L^{-1} phenanthrene showed no growth of *C. calcitrans* after 9 days with decreasing chlorophyll-*a* levels from incubation (Figure 2E), whereas *T. pseudonana* chlorophyll-*a* readings at 80 mg L^{-1} phenanthrene show limited growth (i.e. low tolerance) after 9 days with chlorophyll-*a* concentrations reaching an average of 50 μg ml^{-1} (Figure 2F). In the phenanthrene (80 mg L^{-1}) growth-inhibition experiments *C. calcitrans* control incubations displayed significantly higher chlorophyll-*a* concentrations than phenanthrene treatments on day 3 ($p < 0.05$) and day 9 ($p < 0.01$) (Figure 2E). Similarly, *T. pseudonana* control incubations were significantly different from phenanthrene treatments on day 3 ($p < 0.01$) and day 9 ($p < 0.01$) (Student's *t* test) (Figure 2F). One replicate in the *T. pseudonana* incubation on day 9 displayed a much lower chlorophyll-*a* concentration (0.3 μg L^{-1}) than the two other incubations (58.9 and 89.3 μg L^{-1}). For this reason there were no significant differences found between *T. pseudonana* and *C. calcitrans* treatments (Mann Whitney-U Tests) on day 9, although this was evidence that *T. pseudonana* may be the more resistant strain to phenanthrene. High chlorophyll-*a* concentrations in control incubations demonstrate the inhibitory effect of phenanthrene on micro-algal growth.

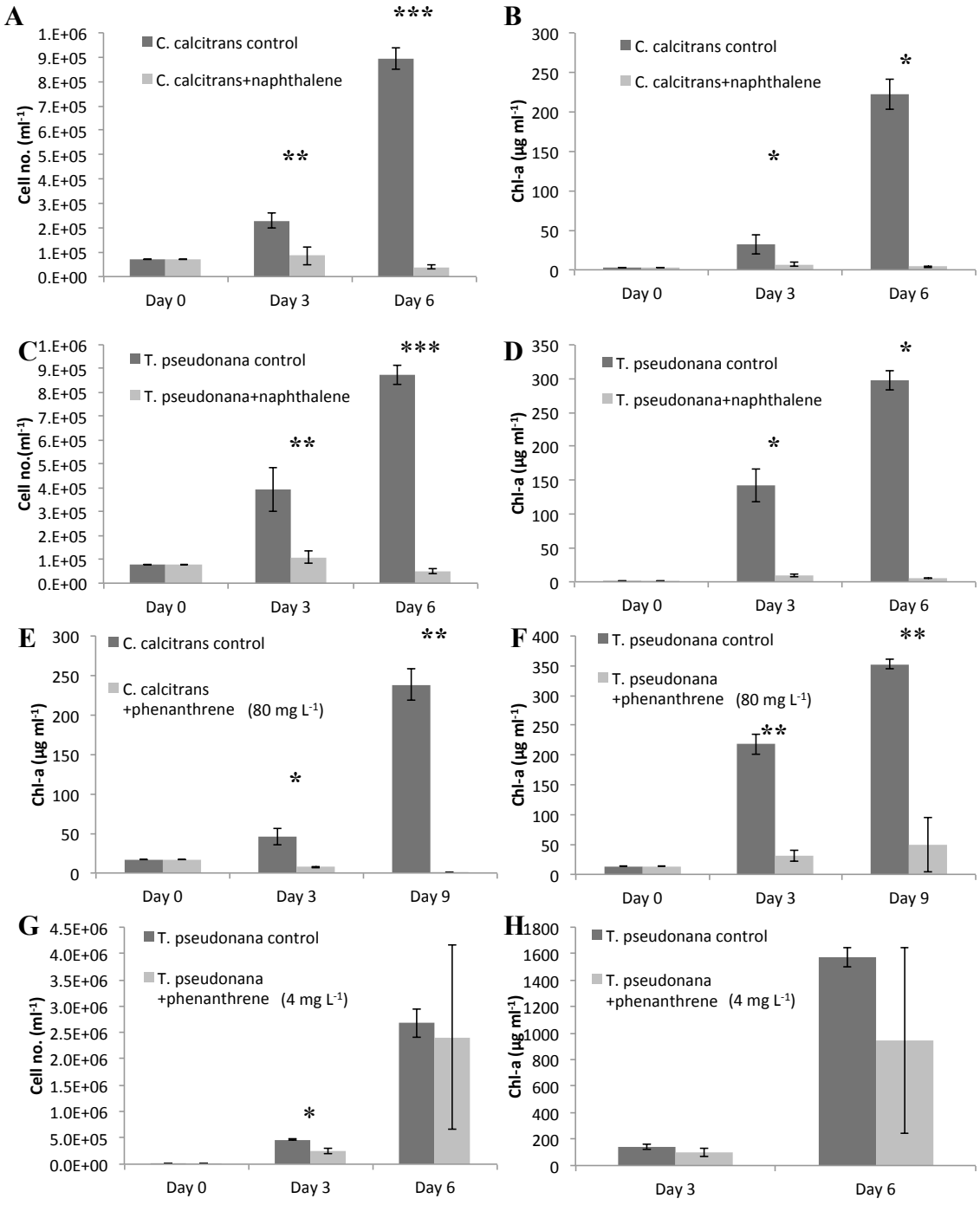

Figure 2. Variations in cell growth (cell number ml^{-1}) or chlorophyll-*a* (Chl-*a*) concentration (µg ml^{-1}): *C. calcitrans* in response to naphthalene enrichment (A and B), *T. pseudonana* in response to naphthalene enrichment (B and C), *C. calcitrans* response to phenanthrene (80 mg L^{-1}) enrichment (E), *T. pseudonana* response to phenanthrene (80 mg L^{-1}) enrichment (F), and *T. pseudonana* in response to phenanthrene (4 mg L^{-1}) enrichment (G and H). Means and standard deviation are shown for three replicates. Significant differences between PAH-enriched and control incubations are shown by asterisks (*,**,*** denotes 95%, 99%, 99.9% significance levels).

Experiments assessing the tolerance of *C. calcitrans* to 4 mg L^{-1} of phenanthrene were not undertaken due to the higher tolerance of *T. pseudonana* to higher phenanthrene concentrations (80 mg L^{-1}) in the previous experiment. In the phenanthrene (4 mg L^{-1}) growth-inhibition experiment with *T. pseudonana* the control incubations on day 3 had grown to ~200,000 cells ml^{-1} more than phenanthrene incubations ($p = 0.011$, Student's *t* test) (Figure 2G). Interestingly on day 6 two of the phenanthrene replicates displayed higher cell numbers than control. There was no significant difference in cell numbers between phenanthrene and control incubations on day 6 (Mann-Whitney *U*, $p = 0.513$). On day 3 there was no significant difference in chlorophyll-*a* concentrations between *T. pseudonana* incubations ($p = 0.148$, Student's *t* test), and neither was there on day 6 ($p = 0.26$, Student's *t* test) (Figure 2H).

The results in this section show that naphthalene inhibits the growth of both diatom strains at saturation. The results also suggest that *T. pseudonana* is more resistant to higher (saturation) levels phenanthrene enrichment than *C. calcitrans,* and that lower levels of phenanthrene enrichment are not as toxic to *T. pseudonana* as higher levels of enrichment, with volatilization of phenanthrene a possible reason for increased tolerance of *T. pseudonana* at lower saturation concentrations. The slight differences in trends of the cell number and chlorophyll-*a* data in the phenanthrene (4 mg L^{-1}) enrichment infer that there may be differences in the photosynthetic responses of diatoms, which may be interesting to measure in future.

2.3.1.2 Determining the effect of known intermediate breakdown products of PAH biodegradation on T. pseudonana

After incubation of *T. pseudonana* with six intermediate metabolites of phenanthrene degradation (at concentrations of 1.93 μg ml^{-1}) cell growth and maximal photosystem II (PSII) photochemical efficiency (or or quantum yield, $Y = F_v/F_m$) were measured. Analysis of day 2 cell numbers showed that control, phthalic acid, salicylic acid and diphenic treatments had highest cell numbers, followed by 1-hydroxy,2-naphthoic acid and finally 1,2-dihydroxynaphthalene and 9,10-phenanthrenquinone had lowest cell numbers ($p < 0.05$) (Figure 3A). Day 2 results included 1,2-dihydroxynaphthalene and 9,10-phenanthrenequinone, but due significant differences in variance on day 4 and day 7 these two chemical intermediates were left out of the statistical model (1-way ANOVA with Tukey's *post hoc* test), which is shown by and absence of lower case letters in Figure 3A days 4 and 7.

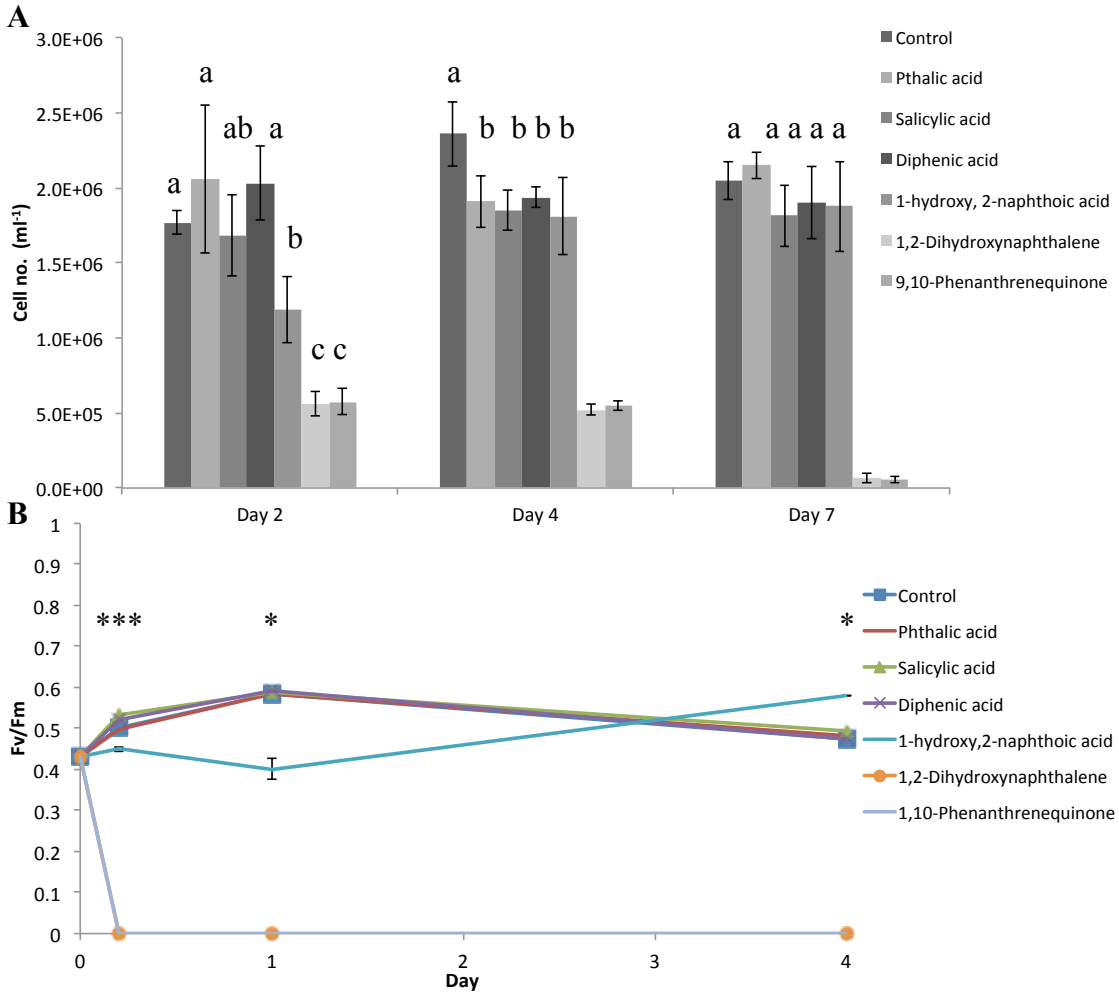

Figure 3. Variation in cell growth (A) and maximal quantum yield of PSII (F_v/F_m) (B) in *T. pseudonana* in response to enrichment with six chemical intermediates of phenanthrene biodegradation (at 1.93 µg ml^{-1}). Means and standard deviation are shown for four replicates. Lower case letters show the results of Tukey's *post hoc* test: a treatment sharing the same letter with another treatment at the same time-point denotes the treatments were not significantly different from each another (A). Significant differences between PAH-enriched and control incubations are shown by asterisks (*,**,*** denotes 95%, 99%, 99.9% significance levels) (B).

PhytoPAM results showed that the 1,2-dihydroxynaphthalene and 9,10-phenanthrenquinone had zero photochemical efficiency after just 4 h (Figure 3B), and was subsequently not included in the statistical model for days 4 and 7 cell numbers. On day 4 the control incubation exhibited highest cell numbers. However by day 7 the other 4 incubations had caught up with the control, including notably 1-hydroxy,2-naphthoic acid. Significant differences in photosystem II quantum yields were detected at each time point with Kruskall-Wallace tests, even when 1,2-dihydroxynaphthalene and 9,10-phenanthrenquinone were not included in the statistical model. Specific

differences between groups could not be elucidated by post hoc Mann-Whitney U tests with Bonferroni correction, but the 1-hydroxy,2-naphthoic acid treatment median quantum yield was most different from the other groups on day 1 (lower) and 4 (higher) and is the likely reason for the Kruskall Wallace test results.

These results show that 1,2-dihydroxynaphthalene and 9,10-phenanthrenquinone are more toxic than the other chemical intermediates when incubated at the same concentration (1.93 μg ml^{-1}). Also 1-hydroxy,2-naphthoic acid enrichment initially slows the growth rate of *T. pseudonana* cell, however growth rate then increases, with Photosystem II health possibly higher than the control on day 4. To investigate this effect further this experiment was repeated with *T. pseudonana* using 1-hydroxy,2-naphthoic acid at a range of concentrations: flasks were set up in four quadruplicate treatments containing 0 (control), 0.5, 1 and 2 μg ml^{-1} of 1-hydroxy,2-naphthoic acid dissolved in F/2+Si medium. The results of this experiment were not significant: there was no effect of 1-hydroxy,2-naphthoic acid on cell growth, maximal quantum yield of PSII (F_v/F_m) of chlorophyll-*a* concentration over 14 days. The results to this experiment are outlined in detail in Appendix A, Figure 28.

2.3.1.3 Determining the effect of breakdown products produced during phenanthrene degradation by P. algicola strain TG408 on the growth of T. pseudonana

T. pseudonana was introduced to growth medium (ONR7a) fractions extracted from *P. algicola* phenanthrene-degradation medium on days 2, 4 and 6. *T. pseudonana* was also introduced to fractions extracted from pyruvate-enriched *P. algicola* cultures and ONR7a sterile medium for comparison. The results for the incubation of *T. pseudonana* with *P. algicola*-fractions are shown in Figure 4. At each time point individual 1-way ANOVAs (with Tukey's *post hoc* tests) were performed with log_{10} cell numbers (Figure 4A). From 27 to 217 h the 5 treatments showed significant differences. The control ('ONR') and day 2 phenanthrene fraction ('PHE 2') incubations displayed the most cell growth after 217 h, displaying significantly higher cell numbers than the other phenanthrene fraction treatments ('PHE 4' and 'PHE 6'). The day 2 phenanthrene fraction treatment also displayed higher cell numbers than the pyruvate fraction treatment ('PYR') from 123 – 217 h. The control incubation had significantly higher numbers than the pyruvate incubation from 168 – 217 h only. Day 4 and 6 phenanthrene degradation fractions ('PHE 4' and 'PHE 6') proved to be toxic to the microalgae, shown by a lack of cell growth.

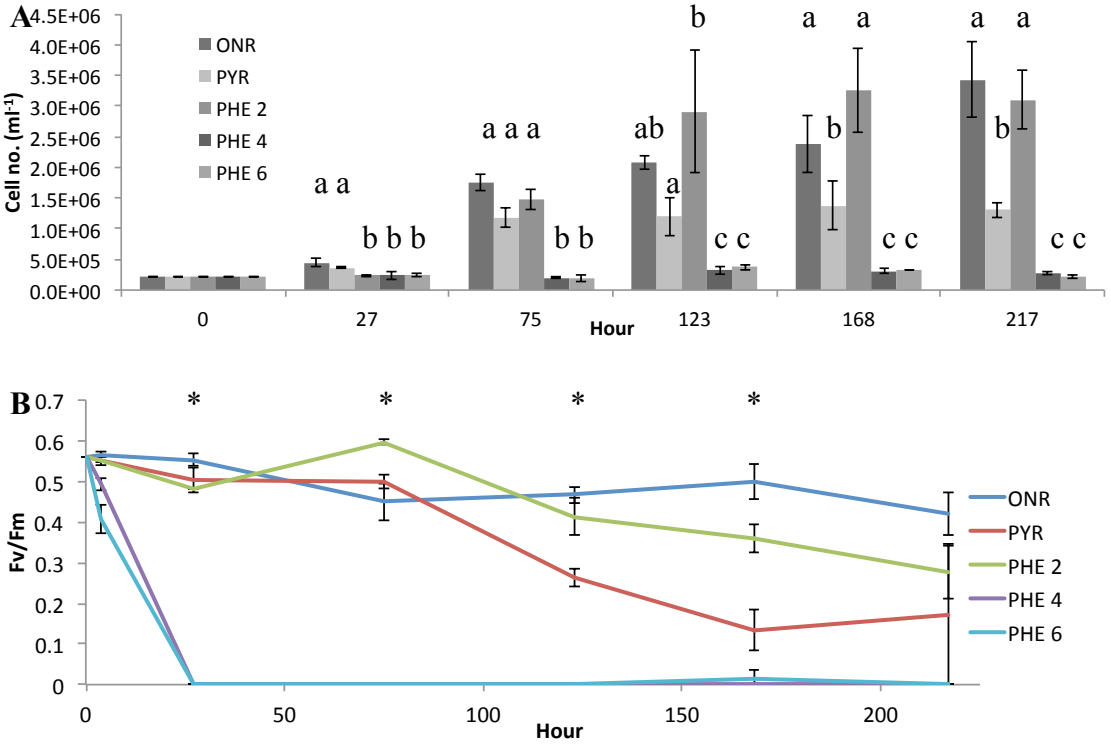

Figure 4. Variation in cell growth (A) and maximal quantum yield of PSII (F_v/F_m) (B) in *T. pseudonana* in response to incubation with fractions from different stages of phenanthrene degradation by *P. algicola*. Means and standard deviation are shown for three replicates. *T. pseudonana* was introduced to five treatments amended with either ONR7a (ONR), pyruvate (PYR), day 2, day 4, or day 6 *P. algicola* phenanthrene degradation products (PHE 2, PHE 4 and PHE 6 respectively). For cell counts (A) lower case letters show the results of Tukey's *post hoc* test: a treatment sharing the same letter with another treatment at the same time-point denotes the treatments were not significantly different from each another. For maximal quantum yield of PSII (B) significant differences (Kruskall Wallace tests) between PAH-enriched and control incubations are shown by asterisks point (not including PHE 4 and PHE 6) (*,**,*** denotes 95%, 99%, 99.9% significance levels).

The samples from the incubation of *T. pseudonana* with *P. algicola*-filtrates were also put through the PhytoPAM machine to monitor the light absorbance efficiency of photosystem II (Figure 4B). PhytoPAM results showed significant ($p < 0.05$) differences in groups at every sampling point from 4 – 217 h (Kruskall Wallace test). Day 4 and 6 phenanthrene degradation fractions ('PHE 4' and 'PHE 6') showed zero photosystem II activity at 27 h and were therefore not included in the pairwise Mann-Whitney U tests. After Bonferroni correction was applied, no significant differences were found between photosystem II quantum yields in each treatment. The significant

differences found in the 5-group Kruskall Wallace were not simply due to 4- and 6-day fraction amended treatments (PHE 4 and PHE 6) being outliers because the test was repeated without these groups and there were differences ($p < 0.05$) between three remaining groups (ONR, PYR and PHE 2) from 27 – 168 h (possibly due to lower PSII quantum yield in the pyruvate filtrate incubation). Upon termination of the experiment there was no significant difference detected between the three groups (ONR, PYR and PHE 2) (Figure 4B). From these results we can determine that day 2 phenanthrene-degradation filtrate did not significantly inhibit *T. pseudonana* light harvesting function or cell division, and also that filtrates from day 4 and 6 arrested photosynthesis within a day of incubation of *T. pseudonana*.

2.3.1.4 Potential of T. pseudonana to degrade phenanthrene

In order to determine whether *T. pseudonana* could degrade phenanthrene the following three treatments were set up in quadruplicate:

1. *T. pseudonana* in F/2+Si medium incubated with phenanthrene.
2. *T. pseudonana* in F/2+Si medium incubated with phenanthrene and 3% (v/v) phosphoric acid.
3. Sterile F/2+Si medium incubated with phenanthrene.

At the start of the experiment each of the tubes contained 0.74 ± 0.01 mg of phenanthrene (238.7 ± 3.2 mg L^{-1} in treatments 1 and 2, 246.7 ± 3.3 mg L^{-1} in treatment 3). After 2-week long incubations GC-MS analysis was performed to measure the mass of phenanthrene left in the tubes. GC-MS analysis detected a significant difference in the phenanthrene concentrations between the three treatments (1-way ANOVA, $p = 0.02$). Tukey's *post hoc* test, however, identified that the difference was between acid inhibited control (Treatment 2 above) and the F/2+Si control (Treatment 3 above) ($p = 0.023$) (Figure 5); Tukey's *post hoc* test showed that the phenanthrene concentration in the *T. pseudonana* incubation with phenanthrene (Treatment 1 above) was not significantly different from either of the control incubations ($p > 0.05$). The very slight degradation reported in the acid-inhibited control might be explained by differences in % recovery of analyte (phenanthrene) from the sample matrix (biological matric vs. solvent) (Andreasson *et al.*, 2015). Treatment 3 was not a realistic surrogate with regards to biological sample matrix (i.e. contains no cells) and concentration (246 vs. 238 mg L^{-1}) and therefore these results although statistically different should be interpreted as not being due to biological degradation by *T. pseudonana*.

Spike/recovery data for this analyte and biological matrix were not calculated. Results show no significant phenanthrene degradation by *T. pseudonana* in comparison to acid-inhibited controls. Incubations were started at *T. pseudonana* cell concentrations of ~100,000 cells ml^{-1}. In the phenanthrene incubation numbers reached 300,000 cells per ml^{-1} (3-fold increase), whereas in the control incubation without phenanthrene they reached 600,000 after 2 weeks (~ 6-fold increase).

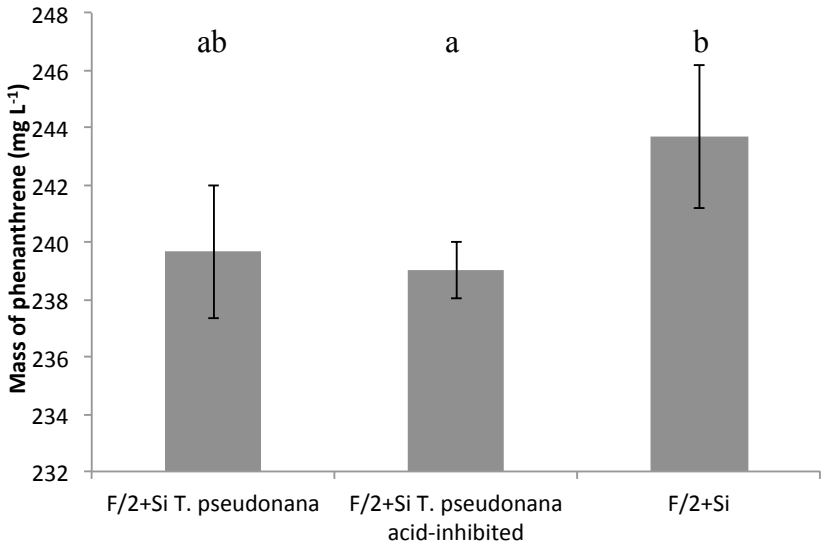

Figure 5. Concentration of phenanthrene (mg L^{-1}) (means ± standard deviation) in the three triplicate treatments after 2 weeks: live *T. pseudonana* (left hand column), acid inhibited *T. pseudonana* (middle column) and F/2+Si medium without *T. pseudonana*. Lower case letters show the results of Tukey's *post hoc* test: a treatment sharing the same letter with another treatment denotes the treatments were not significantly different from each another.

2.3.1.5 Determining whether carbon released from the bacterial degradation of phenanthrene can be incorporated into micro-algal biomass

The unlabelled *T. pseudonana* culture was used for Raman peak comparison. Phenylalanine aromatic rings exhibit a stretching vibration (ring breathing) producing sharp peaks at roughly the 1001 – 1004 wavenumber cm^{-1} position in unlabelled cells and at the 967 cm^{-1} position in strongly ^{13}C-labelled cells (explained in Section 2.1), whilst many smaller peaks can be formed between these wavenumbers in partially labelled cells (in conjunction with reduction in the peak height at the ~1000 cm^{-1} position) (Huang, *et al.*, 2007b; Matthäus *et al.*, 2008; Wagner, 2009; Wu *et al.*, 2011). In all spectra obtained in this study (both *T. pseudonana* and *P. algicola*) phenylalanine peaks were detectable around wavenumber 1000 cm^{-1} and none was reduced in size or

replaced by peaks at lower wavenumbers (Figure 6). Examples of *T. pseudonana* phenylalanine spectral regions from the sequential-culture (^{13}C and ^{12}C) treatments (after 10 days of incubation) are shown overlaid on the same plot in Figure 6A. Both *T. pseudonana* and *P. algicola* phenylalanine spectral regions obtained from cells extracted from the co-culture treatments on days 3 and 15 are shown in Figure 6B. The grey circles in both the figures highlight the spectral regions where ^{13}C-phenylalanine peaks were expected. These results indicate that there was no detectable incorporation of the ^{13}C-signal in either the *P. algicola* or the *T. pseudonana* cells. Examples of full spectra from *P. algicola* or the *T. pseudonana* cells across wavenumbers 400 – 2000 cm^{-1} can be found in Appendix C. It was surprising not to detect ^{13}C incorporation in *P. algicola* cells, however this set of experiments were intended as pilot experiments to determine a ^{13}C incorporation timeline in the bacterium. An experiment performed over a longer time period may have resulted in detectable ^{13}C incorporation into *P. algicola*.

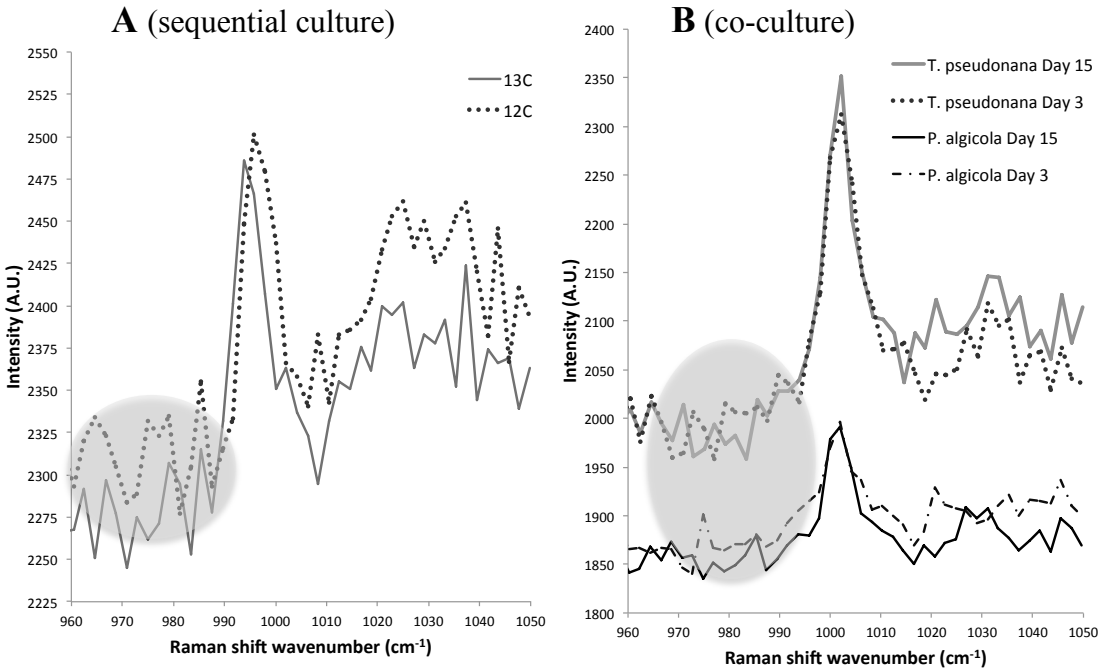

Figure 6. Raman spectra showing phenylalanine peaks for *T. pseudonana* cells from the sequential-culture (^{13}C and ^{12}C) treatments (A) and *T. pseudonana* and *P. algicola* cells extracted from the (^{13}C) co-culture treatment on days 3 and 15 (B). The grey circles highlight the lack of detectable ^{13}C-phenylalanine peaks at lower wavenumbers. Spectra are overlaid on the same y-axis showing intensity in arbitrary units (A.U.) and intensity values are only proportional to the individual spectrum and not across other cell spectra. Spectra collected by Dr. Márton Palatinszky.

2.3.2 Determining what mechanism(s) underpin a symbiotic relationship between hydrocarbonoclastic bacteria and micro-algae

2.3.2.1 Enrichment of S. costatum and L. polyedrum cultures with phenanthrene and probing for hydrocarbonoclastic bacteria using Catalyzed Reporter Deposition Fluorescence In Situ Hybridisation (CARD-FISH)

CARD-FISH was carried out on filter-concentrated samples from both micro-algal cultures using Cy3-labelled tyramides for signal-amplification/reporter-deposition, which resulted in orange signals from the target bacteria in both phenanthrene enrichments. The following Figures (7 - 8) show epifluorescence micrographs of phenanthrene-enriched micro-algal cultures that have were concentrated onto 0.22 μm filters and probed using CARD-FISH. All figures are at the same magnification using a ×100 objective lens and show three-channel (blue, green, orange) emission overlays. In some cases due to confounding autofluorescence issues, the green channel is turned down or absent. Channels represent different dichroic filter sets with the green channel showing diatom autofluorescence, the orange channel (Cy3) showing target hydrocarbonoclastic (either *P. algicola* or *A. aromaticivorans*) probed cells and also diatom autofluorescence, and the blue (DAPI) channel showing bacterial and diatom cells/nuclei.

For *S. costatum* cultures day 0 filters were mostly devoid of *P. algicola*. Nevertheless positive signals were found eventually, with Figure 7A showing two *P. algicola* cells (orange/yellow): one appears associated with *S.costatum* (right center of image) and the other appears unattached to the diatom (left centre). It is impossible to tell in Figure 7A whether the *P. algicola* cell is attached to diatom cell because the three-dimensional structure of the algal culture is disrupted by filtration. By day 5 there were many more signals, most of which were unattached to *S. costatum* (Figure 7C) but again some appeared to be very close to the diatom cells (Figure 7B and D). In Figure 7A green diatom autofluorescence is stronger than images B through D. In image D some of the diatom cells are autofluorescent in the orange channel, which is overlaid on the blue channel. Samples from day 8 were not noticeably different from day 5 in terms of *P. algicola*/PCY223 positive signal number or distribution (photos not included).

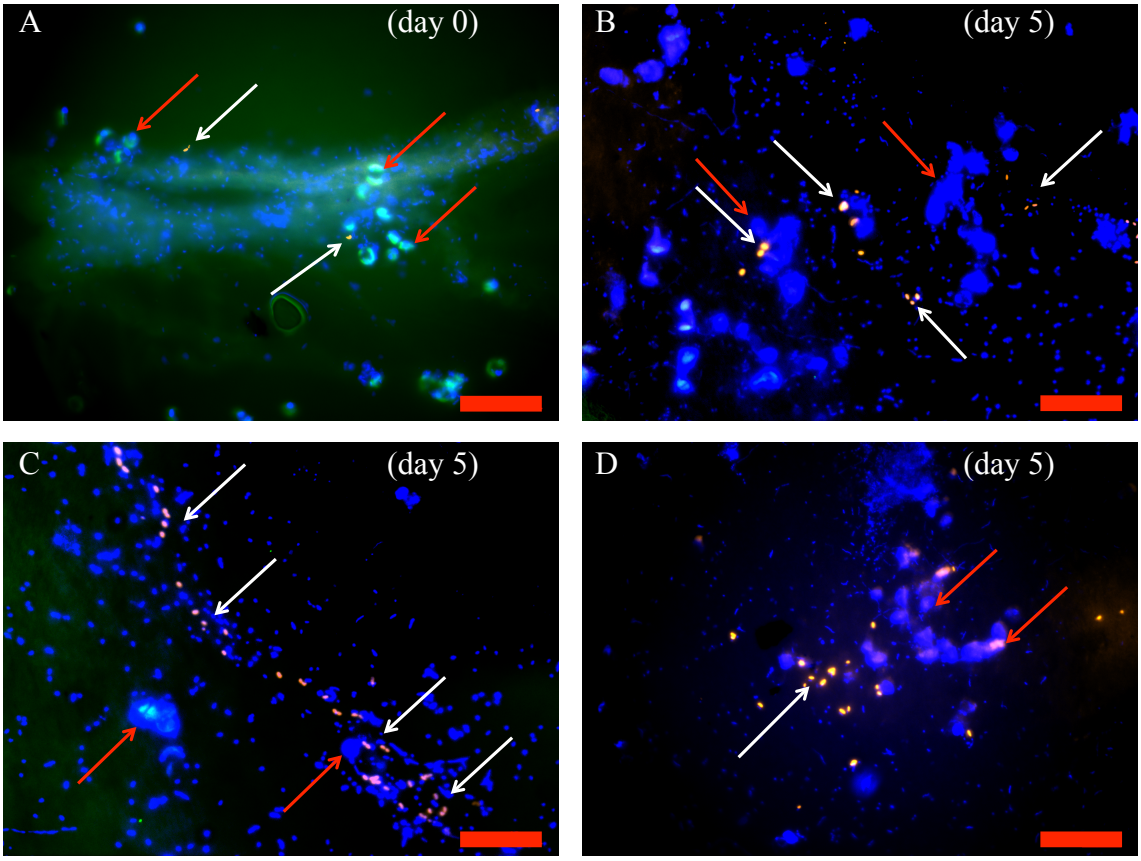

Figure 7. Epifluorescence micrographs of the *S. costatum* culture (CCAP1077/1C) enriched with phenanthrene and hybridized with probe PCY223 on day 0 (A) and day 5 (B – D). *P. algicola* cells are shown in orange (Cy3-PCY223 probe) and pointed out with white arrows while *S. costatum* cells are pointed out with red arrows. Other bacterial (small, ca. 1 µm) and *S. costatum* (big, ca. 10 µm) cells are blue (DAPI) and the green channel displays autofluorescence. Scale bar (red) in bottom right of each image is 20 µm in length.

For *A. aromaticivorans* the cells were in very low numbers as single cells on day 0 and not attached to *L. polyedrum* (Figure 8A and B). On day 3 only very slightly more cells were found (images not shown) but by day 8 phenanthrene enrichments showed noticeably more *A. aromaticivorans* cells (orange) (Figure 8C and D). In image C orange cells are shown apparently attached to the *L. polyedrum* cell (blue) whereas in image D *A. aromaticivorans* cells are associated with other densely clustered bacteria (blue). *A. aromaticivorans* cells did appear to be more localized and in clusters (possibly bound to EPS) compared to *P. algicola*. Like the *S. costatum* culture most of the area of the filter sections did not have any positive signals and were dominated by other bacteria.

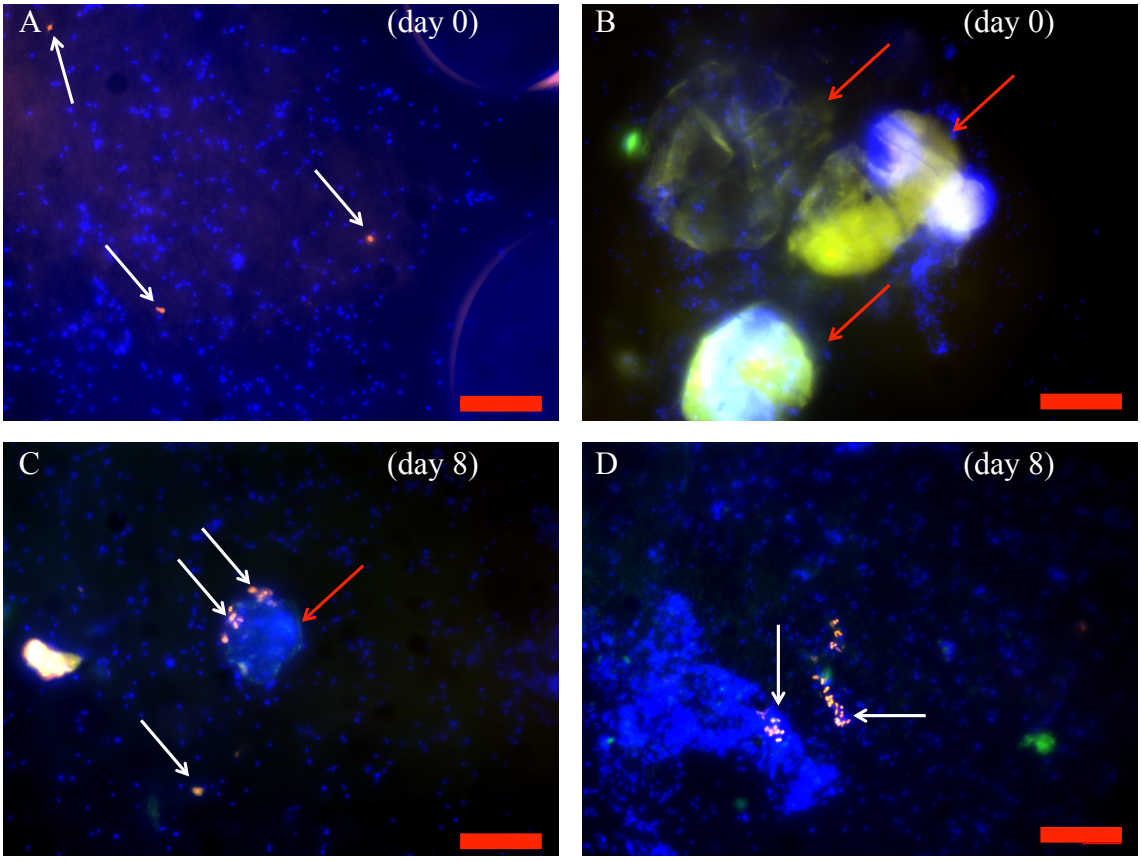

Figure 8. Epifluorescence micrographs of the *L. polyedrum* culture (CCAP 1121/2) enriched with phenanthrene and hybridized with probe ALGAR209 (and competitor probe cALGAR209) on day 0 (A– B) and day 8 (C – D). *A. aromaticivorans* cells are shown in orange (Cy3- ALGAR209 probe) and pointed out with white arrows while dinoflagellate cells are pointed out with red arrows. Other bacterial (small, ca. 1 µm) and *L. polyedrum* (big, ca. 30 µm) cells are blue (DAPI) and the green channel displays autofluorescence. Scale bar (red) in bottom right of each image is 20 µm in length.

2.3.2.2 Determining the effect of micro-algal cells and their produced extracellular substances on the dissolution of phenanthrene

In order to determine whether the presence of micro-algae and their derived extracellular substances increased the dissolution of crystallised phenanthrene two diatom species (*T. pseudonana* strain 1085/12 and *C. calcitrans* strain 1010/11) were incubated with phenanthrene and allowed to grow for two weeks. Presence of crystallised phenanthrene persisted on the glass conical flasks throughout the duration of the experiment and was therefore available for dissolution. Diatom growth was confirmed in the presence of phenanthrene (at 40 mg L^{-1}) in both diatom cultures (Figure 9B), with *T. pseudonana* exhibiting significantly higher chlorophyll-*a*

concentrations (87.33 ± 6.72 mg L^{-1}) than *C. calcitrans* (53.17 ± 6.20 mg L^{-1}) on day 2 (Student's *t* test, $p < 0.01$). On day 8 no significant difference was found between micro-algal chlorophyll-*a* concentrations of *T. pseudonana* (346 ± 13 mg L^{-1}) and *C. calcitrans* (310 ± 57 mg L^{-1}) on day 8.

At this point (day 8), after passing all treatments though GF/C filters (thus removing diatom cells from two treatments), the remaining media were measured for phenanthrene concentration using GC-MS. In order to conform to parametric assumptions phenanthrene concentration data was $\log_{10}$ transformed before 1-way ANOVA was used performed. Concentrations of phenanthrene in algal media were not significantly different. *T. pseudonana* exhibited higher phenanthrene concentration (0.291 ± 0.006 mg L^{-1}) than the control incubation (0.250 ± 0.017 mg L^{-1}) ($p < 0.05$) but *C. calcitrans* incubations did not (0.277 ± 0.003 mg L^{-1}) ($p = 0.06$) (Figure 9A) (1-way ANOVA with Tukey's *post hoc* test).

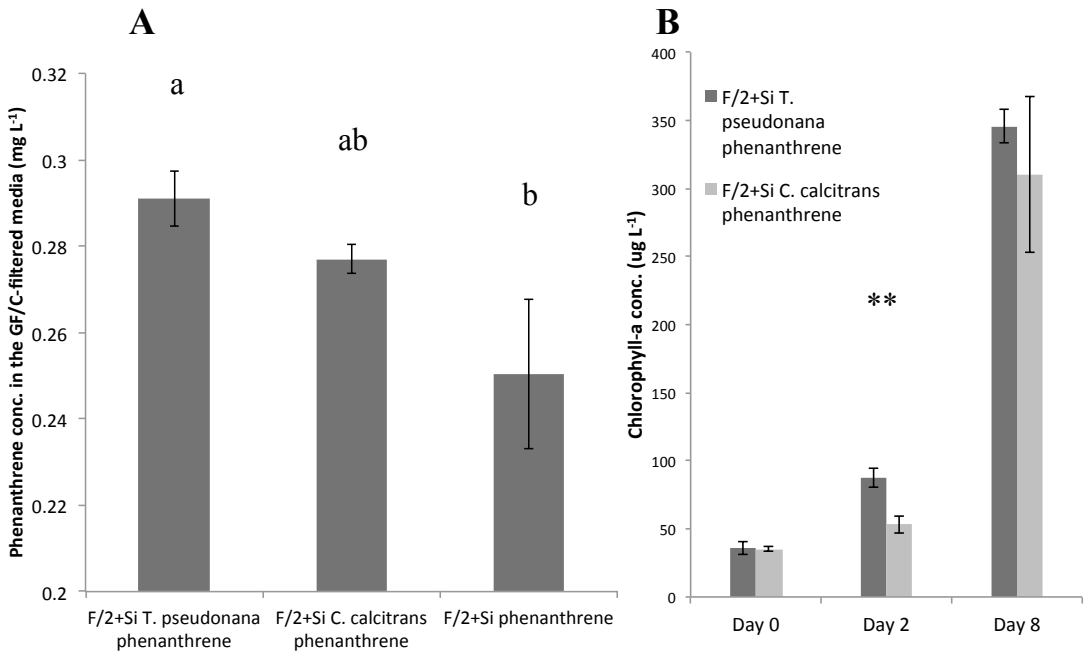

Figure 9. (A) Concentration of phenanthrene (mg L^{-1}) (means ± standard deviation) in three treatments: *T. pseudonana* in F/2+Si medium (left hand column), *C. calcitrans* in F/2+Si medium (middle column) and sterile F/2+Si medium (right hand column). Lower case letters show the results of Tukey's *post hoc* test: a treatment sharing the same letter with another treatment denotes the treatments were not significantly different from each another. (B) Chlorophyll-*a* concentrations (μg L^{-1}) in *T. pseudonana* and *C. calcitrans* treatments from days 0, 2 and 8. Significant differences between diatom treatments are shown by asterisks (*,**,*** denotes 95%, 99%, 99.9% significance levels).

These results show that the presence of *T. pseudonana* and its derived extracellular products increases the concentration of phenanthrene in F/2+Si medium, possibly by increasing the dissolution of crystallised phenanthrene from the surface of the conical flasks. As algal cells were removed before phenanthrene quantification, these results do not take into account any phenanthrene that may also be adsorbed to the micro-algal cells themselves.

2.3.2.3 Determining whether P. algicola (TG408) and three other hydrocarbon-degraders grow on selected diatom-derived organic nutrients.

After one week *P. algicola* formed no colonies on any of the treatment agar plates apart from the positive control (Table 2). *Marinobacter* sp. MCTG268 on the other hand grew on all diatom-derived treatments. For both *A. algicola* (TG409) and *A. aromaticivorans* (DG1253) growth was variable with strongest growth on autoclaved soluble extracellular diatom-derived nutrients (treatment 1). For *T. pseudonana*-derived agar plates both *A. algicola* and *A. aromaticivorans* preferred undiluted nutrient agar treatments (1 and 3). *A. aromaticivorans* did not grow on treatment 2 (extracellular soluble diatom-derived nutrients) or treatment 4 (autoclaved diatom cells). *A. algicola* also showed no growth on treatment 4 after 1 week. Both *A. algicola* and *A. aromaticivorans* showed strong or weak growth on all *C. calcitrans*-derived agar treatments. All bacteria formed colonies on the positive control agar plates (Table 2), while no colonies were formed on negative control (un-inoculated) agar treatments. These results show that *P. algicola* alone could not convert nutrients derived from diatom cultures into biomass on agar plates in one week and therefore may rely on nutrient-sharing with other micro-algal-associated heterotrophic bacteria. The other three hydrocarbonoclastic bacteria appear to have a broader nutritional range, with *Marinobacter* sp. strain MCTG268 exhibiting strong growth on all 8 diatom-agar treatments. Some weaker growth was noticed on *T. pseudonana* culture-derived agar plates.

Table 2. Colony formation by four hydrocarbonoclastic bacteria on agar plates containing diatom-derived organic nutrients. *C. calcitrans* and *T. pseudonana* treatments are labelled 1 – 4 with the numbers corresponding to treatments in Table 1 (Section 2.2.2.3) (see footnote). The first column lists the bacterial species inoculated. + / **(+)** / – indicates bacterial growth / weak growth / no growth respectively.

	Diatom culture treatment								
	T. pseudonana				*C. calcitrans*				
Bacterium	**1**	**2**	**3**	**4**	**1**	**2**	**3**	**4**	**Control**
P. algicola	-	-	-	-	-	-	-	-	+
A. algicola	+	(+)	(+)	-	+	+	+	+	+
A. aromaticivorans	(+)	-	(+)	-	+	(+)	(+)	(+)	+
Marinobacter sp. MCTG268	+	+	+	+	+	+	+	+	+

Treatment index: 1 – filtered (f) and autoclaved (ac), 2 – f, 3 – ac, 4 – ac (½ dilution) Control – ONR7a amended with filter-sterile (0.2 μm) 0.1% Na-pyruvate (*P. algicola* and *Marinobacter* sp. MCTG268), ZM/10 amended with filter-sterile (0.2 μm) 0.1% Na-pyruvate (*A. aromaticivorans*) or ZM/10 (*A. algicola*).

2.3.2.4 A screening for P. algicola growth on intermediate breakdown products from microbial degradation of phenanthrene

P. algicola was inoculated onto agar plates containing minimal media (ONR7a) enriched with six different chemical intermediates (phthalic acid, salicylic acid, diphenic acid, 1-hydroxy,2-naphthoic acid, 1,2-dihydroxynaphthalene and 9,10-phenanthrenequinone). *P. algicola* did not produce visible colonies on salicylic acid, 1-hydroxy,2-naphthoic acid or 9,10-phenanthrenequinone. Growth was visible on agar plated spotted with phthalic acid, 1,2-dihydroxynaphthalene and diphenic acid (as well as the ONR7a control containing pyruvate) (Figure 10). *P. algicola* colonies exhibit a slightly umbonate off-white morphology when grown with pyruvate; pyruvate agar plates were used as a positive control to demonstrate colony formation (Figure 10A). Growth on the other three substrates resulted in a more transparent outer region of growth (Figures 10A-C). Phthalic acid (Figure 10C) exhibited the weakest growth, as represented by translucent colony morphology. No bacterial growth was detected un-inoculated plates (negative controls) that were enriched with the six intermediate metabolites.

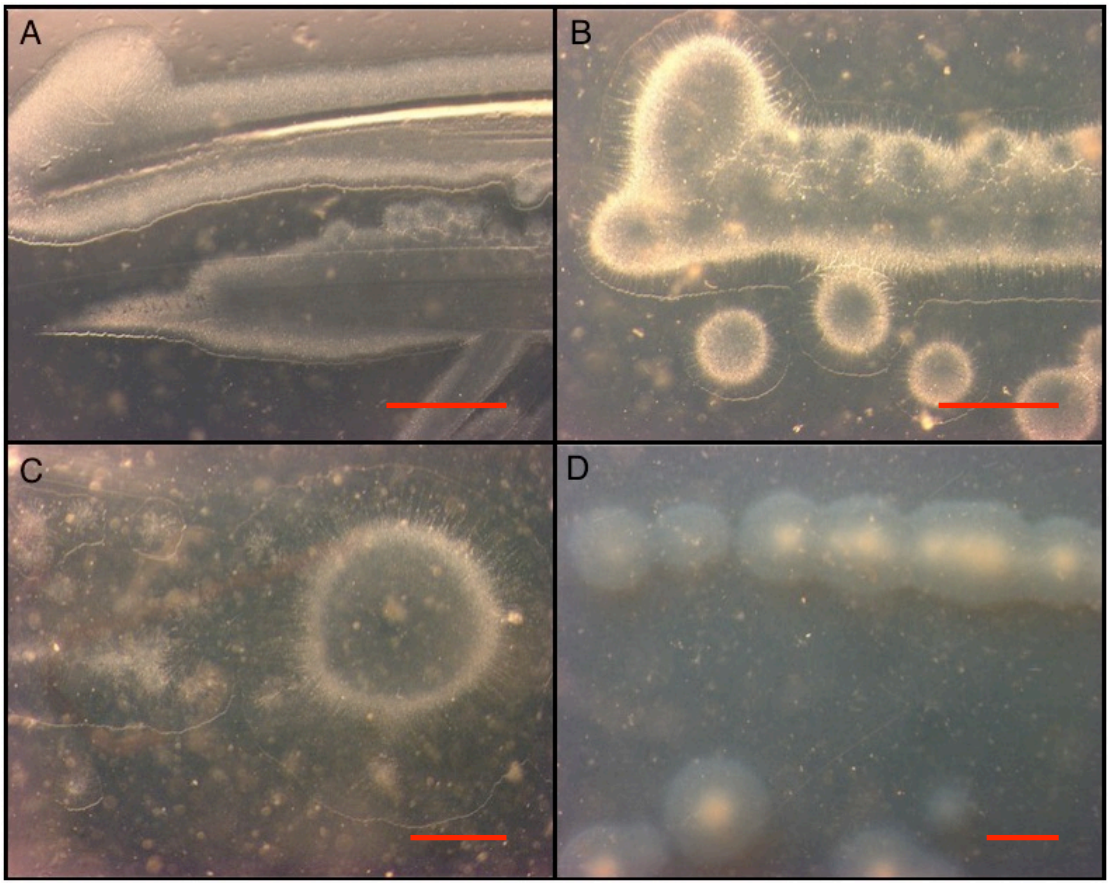

Figure 10. Micrographs of *P. algicola* colonies grown on ONR7a agar plates enriched with 1,2-dihydroxynaphthalene (A) diphenic acid (B) phthalic acid (C) and pyruvate (positive control) (D). Scale bar (red) in bottom right of each image is 1 mm in length.

2.4 Discussion

2.4.1 PAH metabolite-driven interactions between Polycyclovorans algicola strain TG408 and micro-algae

In Section 2.3.1.1 *C. calcitrans* was more sensitive to LMW PAH exposure than *T. pseudonana*. Growth of both diatom species was halted by naphthalene, whereas inoculation with 80 mg L^{-1} of phenanthrene resulted in limited growth of *T. pseudonana* only. After incubation with 4 mg L^{-1} of phenanthrene there was a clear tolerance of *T. pseudonana* to phenanthrene after six days (likely due to phenanthrene volatilization), with one of the triplicate incubations exhibiting higher cell numbers than the control incubation without phenanthrene. *T. pseudonana* (4 – 9 µm long) cells are slightly larger than those of *C. calcitrans* (2.5 – 5 µm long), and the results are substantiated by the finding of Echeveste *et al.* (2010) that larger phytoplankton cells are more tolerant than small cells to organic pollutants, most likely due in part to their smaller surface area to volume ratio (Del Vento and Dachs, 2002). Naphthalene displayed high toxicity

possibly due to its higher volatility and solubility (Turner *et al.*, 2014). Based on these results phenanthrene was chosen as the LMW-PAH and *T. pseudonana* was chosen as the axenic diatom strain with which to explore PAH metabolite-driven interactions further.

Inoculation of *T. pseudonana* with the six known intermediate metabolites of LMW PAH degradation demonstrated the toxicity of 1,2-dihydroxynaphthalene and 9,10-phenanthrenequinone to the diatom at a concentration of 1.93 μg ml^{-1} (Section 2.3.1.2). The other four intermediate metabolites had no effect on the diatom as no difference in cell numbers were observed after 7 days at the same concentration (although on day 4 the control incubation had significantly higher cell numbers). The 1-hydroxy,2-naphthoic acid and salicylic acid incubations exhibited slightly slower growth rates eventually catching up with the other incubations. The 1-hydroxy,2-naphthoic acid incubation also had a different pattern of Photosystem II light harvesting efficiency (measured with PhytoPAM) to the other incubations, increasing beyond the control after four days. This warranted further investigation (Appendix A), where no significant differences between control and 1-hydroxy,2-naphthoic acid treatments were determined in either cell number or Photosystem II quantum yield. The results show that PAH-derived intermediates of degradation, such as alcohol/diol or dione/quinone are likely to be more toxic to micro-algae than their corresponding aromatic organic acids. The comparatively high toxicity of the two metabolites 9,10-phenanthrenequinone and 1,2-dihydroxynaphthalene to *T. pseudonana* was possibly due to the formation of free-radicals inside the diatom cells, which could form covalent bonds disrupting multiple processes (e.g. DNA damage) (Gilde and Pinckney, 2012; Zielinska-Park *et al.*, 2004). They were particularly disruptive to the Photosystem II light harvesting efficiency, and possibly caused algal-mortality due to interference in photosynthetic processes (e.g. electron transfer) (Aksmann and Tukaj, 2008). Conversely, the organic acids 1-hydroxy,2-naphthoic acid, salicylic acid and phthalic acid had no measured effect on *T. pseudonana* cell division and photosynthesis when incubated at the same concentration. Whilst the intracellular action of these metabolites on the diatoms was not investigated, it might be similar to protocatechuic or ascorbic acid by way of neutralizing free radicals by donating H^+ ions (Bendich *et al.*, 1986; Huang *et al.*, 2003). A hydrocarbonoclastic bacterium (associated with micro-algae) that produced diols and quinones is a potential danger to the survival of the microalgae, but this would depend on their concentration within the immediate vicinity of the micro-

algal cells. The intermediates also have solubility several orders of magnitude greater than the parent hydrocarbons and are therefore more bioavailable to algal cells. An aldo-keto reductase (dihydrodiol dehydrogenase) has been found in *T. pseudonana*, a representative of a class of enzymes that can (also in humans) convert aromatic dihydrodiols into quinones, although it is unknown whether such enzymes are effective on diols like 1,2-dihydroxynaphthalene/naphthalene-1,2-diol (Carvalho *et al.*, 2011; Zhang *et al.*, 2012). It is possible that aromatic diols act as or are converted to reactive oxygen species like aldehydes or quinones in *T. pseudonana*. Aromatic aldehydes for example can be converted into quinones by ciliates (Netzeva and Schultz, 2005).

Incubation of *T. pseudonana* with intermediate metabolites of phenanthrene degradation by *P. algicola* (Section 2.3.1.3) revealed significant and drastic differences in the level of toxicity to *T. pseudonana* between PAH-metabolites extracted on different days. The 'day 2' *P. algicola* fraction was tolerated by *T. pseudonana* whereas 'day 4' and 'day 6' fractions were highly toxic to the diatom, completely disrupting photosynthesis after one day of incubation (*P. algicola* pyruvate metabolites were also harmful to the diatom). The differences may have been due to the quantity of phenanthrene metabolites in the filtrates (not measured) or variations in the quality of metabolites (e.g. diol or quinone presence). Degradation of phenanthrene by *P. algicola* created an orange colouration of the ONR7a growth medium. Previous experiments by other authors on phenanthrene degradation by *Pseudomonas* sp. strain PPD also detected orange coloured metabolites, and formation of 1-hydroxy,2-naphthoic acid was detected (with an absorbance maximum at 300 nm) during the early exponential growth phase (Deveryshetty and Phale, 2009). Unlike *Pseudomonas* sp. strain PPD, *P. algicola* didn't have an exponential-phase or indeed hardly any measurable growth by optical density (Appendix B Figure 29), perhaps inferring limited carbon uptake from phenanthrene, but mineralization of the phenanthrene by *P.algicola* has been reported nevertheless (Gutierrez et al. 2013b). The orange metabolites in the *P. algicola*-phenanthrene culture also displayed a broad absorbance peak from 320 – 360 nm (UV-A photon range) (Appendix B Figure 30). This suggests that there were a range of chemical intermediates produced by *P. algicola* (Law, 1981; Zhang *et al.*, 2015), and that 3-ring PAHs (i.e. un-cleaved phenanthrene metabolites) were prominent in the solution (Yu, 2002).

To investigate the intracellular uptake of intermediate phenanthrene metabolites by *T. pseudonana* stable isotope tracing experiments were performed. The 'day 2' phenanthrene degradation filtrate was used (along with more dilute day 4 fractions) in the 'sequential culture' stable isotope tracing experiment (Section 2.3.1.5). Before the stable isotope tracing experiment could proceed it first had to be established whether or not *T. pseudonana* degraded phenanthrene (Section 2.3.1.4). This was necessary to ensure that any ^{13}C-incorporation was not due to direct micro-algal phenanthrene degradation but due to hydrocarbonoclastic bacterial degradation. While *T. pseudonana* growth was confirmed in phenanthrene incubations there was no significant reduction in the concentration of phenanthrene by live diatom cells compared with acid-inhibited controls. The results of stable isotope probing using Raman spectroscopy showed no evidence of carbon-transfer to the diatom as detected by phenylalanine peak shifts, both in sequential and co-cultures. Interestingly there was no detectable ^{13}C-incorporation in *P. algicola* either, which was unexpected having been found in previous PAH-degradation experiments with other hydrocarbonoclastic bacteria (Annweiler *et al.*, 2000; Kästner *et al.*, 1999). This does not necessarily mean there was no incorporation into the bacteria, just that it may have been beyond detectable limits using Raman, a result that is supported by the lack of bacterial cell growth in phenanthrene amended ONR7a medium and the fact that the clearing zones produced by this bacterium on phenanthrene sprayed agar plates are not filled with visible bacterial colonies. Previous authors have applied Raman spectroscopy to study the ecophysiology and metabolic history of cells as it provides biochemical information inferring cellular status (e.g. live or dead cells can be differentiated, and cells' growth on different nutrients can be detected) (Chrimes *et al.*, 2013; Huang *et al.*, 2007a; Notingher *et al.*, 2002; Wagner, 2009). Both the bacterial and diatom cells from the stable isotope incubations in this chapter were well preserved and exhibited easily detectable phenylalanine peaks. However, in the phenanthrene co-culture treatments, the spectra from *P. algicola* cells on day 15 were different from those extracted on day 3: day 15 cells displayed complete absence of fluorescent bands in nucleic acid regions (wavenumber ~800 cm^{-1}) and reductions in possible lipid or protein bands (1200 – 1400 cm^{-1}) (Appendix C, Figure 32B). These results may indicate a lack of DNA replication and/or DNA repair interference (i.e. genotoxicity) due to phenanthrene or metabolite-linked DNA adduct formation (Hu *et al.*, 2012; Yu, 2002). Both phenanthrene-treated diatom and bacterial cell spectra exhibited two distinct peaks at wavenumbers ~1450 cm^{-1} and ~1650 cm^{-1}, which may be lipid spectral regions (Huang, *et al.*, 2007b; Wu *et al.*, 2011) (Appendix

C, Figures 32 and 33). Lipid modification and increases in cell membrane surface area in response to non-polar contaminants has been identified previously (Sikkema *et al.*, 1995), although the reasons for the high intensity lipid Raman peaks in the present study are unknown.

According to Gutierrez *et al.* (2014) the ability to partially degrade hydrocarbon substrates coupled with the apparent inability to grow on the same substrates is not uncommon in bacteria. Limited ^{13}C-incorporation into the bacterium may infer that enzymatic action by *P. algicola* is extracellular or that some other biologically active or harmful metabolite is being transferred without incorporation into the algal biomass. Extracellular enzymatic release in bacteria has been well documented as an initial re-mineralization stage in the marine environment (and specifically in marine snow and marine aggregates) and is viewed as having central importance in the marine carbon cycle and bacterial interactions (Arnosti, 2010; Gram *et al.*, 2002; Kamer and Rassoulzadegan, 1995; Karner and Herndl, 1992; Vetter *et al.*, 1997). The results above may suggest evidence against carbon transfer from this particular hydrocarbonoclastic bacterium (*P. algicola*) to *T. pseudonana*, however the experiment performed with different algal species (e.g. *S. costatum*) may produce different results. A community of bacteria and algae, rather than isolated axenic strains, is likely to exhibit different and more complex interactions (see Chapter 4). *P. algicola* was investigated further in the next section, including its relationship with *Skeletonema costatum* and its ability to grow on algal-derived nutrients and intermediate metabolites of PAH degradation.

2.4.2 Determining what mechanism(s) underpin a symbiotic relationship between hydrocarbonoclastic bacteria and micro-algae

CARD-FISH analysis of phenanthrene enriched non-axenic *S. costatum* and *L. polyedrum* micro-algal cultures (Section 2.3.2.1) suggested that the previously low-abundance hydrocarbonoclastic bacteria (*P. algicola* and *A. aromaticivorans*) started to become more numerous after 5 – 8 days (respectively). This implies that the response of *P. algicola* to phenanthrene is not immediate and the lag phase may be due to the bacteria detecting the release of EPS produced by the micro-algae. Although the PAH-degraders increased in abundance they clearly did not dominate the bacterial community (shown by the DAPI staining), which fits in with the limited growth of *P. algicola* on phenanthrene carbon substrate mentioned in the previous section. After incubation with

phenanthrene the hydrocarbonoclastic bacteria in both the *L. polyedrum* and *S. costatum* cultures appeared to be arranged in clusters (or arranged in streaks) of bacteria, where previously (on day 0) they were present as single cells, sometimes appearing near micro-algal cells but in other cases unassociated with micro-algae and seemingly free-living. These micro-aggregate (<5 – 500 μm) arrangements of bacteria and micro-algae are also found in the literature (Simon *et al.*, 2002a). Their appearance on the filters in this chapter is not an even distribution compared with the general bacteria (DAPI) distribution, which suggests that the hydrocarbonoclastic bacteria are held together by transparent exopolymers (TEP) as proposed by Thornton (2002), limiting their free movement around the algal media and keeping the bacteria on or within the EPS or near the micro-algal cells. This is an important aspect of the relationship between hydrocarbonoclastic bacteria and micro-algae. EPS flocs are responsible in the marine environment for holding a variety of bacteria, biota, detritus and other particulate organic matter (POM) together as mucus webs or sticky glue and the formation of marine oil snow (MOS) in response to petroleum hydrocarbon enrichment has been previously described (Daly *et al.*, 2016; Passow *et al.*, 2012; Mishamandani *et al.*, 2016; Simon *et al.*, 2002a). These results show that these two PAH-degraders may be associated with micro-algae in order to gain increased access to the necessary hydrocarbons they require for growth and that the carbon fixed by the micro-algae provides a significant contribution to the EPS biomass, which also supports other heterotrophic bacteria (Mishamandani *et al.*, 2016). The spatial arrangement of hydrocarbonoclastic bacteria and algae has been further investigated in Chapter 5. These results warranted an investigation into the effects of micro-algae on PAH-dissolution and also into the nutritional value of diatom-derived extracellular substances to PAH-degrading bacteria.

The presence of *T. pseudonana* in the phenanthrene media (Section 2.3.2.2) increased the concentration of phenanthrene in the F/2+Si media (from 0.25 mg L^{-1} in the control to 0.29 mg L^{-1}) after extraction of the large algal cells and organic matter using GF/C filters (>0.25 μm^{-3} size particles according to Nagata, 1986). This means that micro-algal presence or micro-algal-derived extracellular compounds increased the solubility of phenanthrene in the F/2+Si media possibly by sorption, binding or inclusion complex formation with phenanthrene (Savjani *et al.*, 2012). The increase in phenanthrene concentration in the filtrate from the *C. calcitrans* culture was not quite significantly different ($p = 0.06$) from the control although this was probably due to the variation in

the control. It is highly likely that there would also have been even more phenanthrene adsorbed to algal cells and larger masses of EPS (>0.25 μm^{-3}) that would have been retained by the GF/C filter (Andelman and Suess, 1970; Kowalewska, 1999). EPS molecules may be partly responsible for this increase in phenanthrene concentration, possibly by phenanthrene complexation or emulsification with EPS produced by the diatom, although EPS contribution was not analysed in this study. This theoretical PAH-emulsification would allow EPS or aggregate-associated hydrocarbonoclastic increased access to hydrocarbons. The release of EPS by phytoplankton in response to petroleum hydrocarbons has been described recently by Passow (2016), whereas emulsification of phenanthrene has been detected previously by bacterial-derived EPS (Cuny *et al.*, 2004; Henry *et al.*, 2011; Toren *et al.*, 2002) and emulsification solely by micro-algal EPS has not been shown before. This algal-derived EPS is likely to be an important factor in the relationship between micro-algae and hydrocarbonoclastic bacteria in the phycosphere. A future experiment should aim to separate the effects of EPS and other extracellular products on PAH dissolution. This would involve extracting and characterising *T. pseudonana* EPS and subsequently subjecting this EPS to crystalized PAH molecules in closed systems.

Hydrocarbonoclastic bacterial relationships with micro-algae are also likely to be variable between species. Four species of hydrocarbonoclastic bacteria were tested for colony formation on agar containing a variety of algal-derived nutrients (Section 2.3.2.3). For *A. aromaticivorans* (DG1253) the only plate to exhibit strong growth contained the autoclaved soluble algal EPS (treatment 1 from *C. calcitrans*), whereas *P. algicola* only formed colonies on the control (pyruvate-amended) agar plate. These bacteria are known to exhibit narrow nutritional spectra (Gutierrez *et al.*, 2012b; 2013b). Treatment 1 consisted of autoclaved soluble (<0.22 μm) algal EPS and this heat and pressure treatment would have thermally modified the structures of lipids, carbohydrates, proteins and other complex molecules, which may have allowed *A. aromaticivorans* to make better use of the nutrients (Beaudet *et al.*, 2011; Hefnawy, 2011; Niemz *et al.*, 2010; Yu and Damiran, 2011). Treatments 3 and 4 contained autoclaved diatom cultures at different concentrations and autoclave treatment would have destroyed cell membrane integrity, releasing the intracellular contents of the diatom cells. *A. algicola* (TG409) and *Marinobacter* sp. (MCTG268) produced colonies on all four treatments (except for *A. algicola* on the dilute treatment 4 agar from *T. pseudonana*), suggesting these organisms are likely to have a broader

nutritional range, which fits in with published literature for members of their respective genera (Green *et al.*, 2006; Gutierrez *et al.*, 2014; Yakimov *et al.*, 2007). It should be noted that all species here are likely to be maintained by algal-derived carbon nutrients in some way because they were all were isolated from laboratory cultures of micro-algae. These results highlight the potential benefits of micro-algal-association to hydrocarbonoclastic bacteria. The inability of *P. algicola* to utilize the algal-derived nutrients here is interesting because it leads to speculation that this organism derives carbon from *S. costatum* possibly as a result of nutrient sharing with the other microbial flora in the CCAP1077/1C culture; a diverse range of bacterial groups (including many hydrocarbonoclastic species) is found in this culture (Mishamandani *et al.*, 2016). The results in Section 2.3.2.4 show that, despite not forming colonies on the 1-hydroxy,2-naphthoic acid, salicylic acid or 9,10-phenanthrenequinone amended agar plates, *P. algicola* did show some versatility in converting 1,2-dihydroxynaphthalene, diphenic acid and phthalic acid into biomass. It is a possibility that *P. algicola* may have utilised impurities present in the intermediate compounds rather than the compounds themselves to produce colonies (e.g. diphenic acid was purchased at ≥96.5% purity). Analysis of the *P. algicola* genome may clarify which compounds it can utilise as a carbon source, and further elucidate this organism's ecology.

CHAPTER 3: SEARCHING THE *POLYCYCLOVORANS ALGICOLA* GENOME FOR HYDROCARBON DEGRADATION GENETIC POTENTIAL

3.1 Introduction

Several lines of evidence warrant an investigation into the genome of the PAH-degrading bacterium *P. algicola* (strain TG408). This organism produces clearing zones on agar plates sprayed with a layer of phenanthrene crystals (Gutierrez *et al.*, 2013b), however it does not produce visible colonies. This possible limited conversion of PAH to biomass for this molecule coupled with degradation of the compound is supported by the limited growth found in phenanthrene-ONR7a medium measured by OD600 (Appendix B.1) and the undetectable ^{13}C-incorporation found using Raman in Chapter 2 (Section 2.3.1.5). The results from Section 2.3.2.4 also suggested that smaller one or two ring aromatic molecules (1,2-dihydroxynaphthalene, diphenic acid and phthalic acid) are converted more readily into biomass by *P. algicola*. Importantly, however, this organism was isolated from the diatom culture *S. costatum* (CCAP1077/1C) and not from a petroleum-contaminated site. The lack of *P. algicola* growth on filtered or autoclaved diatom growth-medium extracts was a surprising result (Section 2.3.2.3) and prompted the question: what is the ecological niche of this organism? It may be possible that the aromatic carbon nutrients (e.g. partially degraded naphthoquinones) or simpler acids (e.g. succinate) are provided to *P. algicola* by other bacteria in the *S. costatum* culture. The genome of *P. algicola* may only contain enzymes for certain stages of phenanthrene (or other hydrocarbon) degradation and require other hydrocarbonoclastic bacteria to completely mineralize substrates. In order to understand the genetic capability of *Polycyclovorans algicola* within the context of its ability to degrade hydrocarbons and its association with *S. costatum* and other marine micro-algal species, total DNA from this bacterium was extracted for whole genome sequencing and analysed in this chapter. The primary aim for this section was to investigate the complete genome sequence of *P. algicola* in search of PAH-degradation potential. The hazards that PAHs pose to the environment have been described in Chapter 1 and any novel ways of detoxifying PAHs that may be found in the genome of *P. algicola* could benefit our understanding of PAH remediation/degradation. There may be unique genes or operons involved with aromatic hydrocarbon degradation. Genome analysis might also uncover clues as to the ecology or niche of *P. algicola* (in terms of carbon utilization) and it may share genetic similarities with other

hydrocarbonoclastic bacteria. Additionally information was collected pertaining to possible relationships of *P. algicola* with other bacteria and symbiotic interactions (e.g. with *S. costatum*).

3.2 Materials and Methods

A volume of 1 L of pure *P. algicola* culture was grown and the ionic detergent cetyltrimethylammonium bromide (CTAB) was used to gently extract highly polymerized (intact) DNA. Firstly, in a laminar flow cabinet, a *P. algicola* colony was used to inoculate a test tube containing 3 ml of ONR7a medium amended with 0.1% sodium-pyruvate. Once in exponential-phase this volume was then used to inoculate a conical flask containing 1 L of the same medium. This was placed on a shaker (80 rpm) in the dark at 24°C and grown until at early stationary phase. The culture was divided among several 50-ml sterile centrifuge tubes (Falcon) and centrifuged (3,000 *g*, 10°C, 20 min) to recover the cells as pellets. The cells pellets were combined in a single 50 ml tube for subsequent DNA extraction.

DNA extraction was performed using the method outlined by the Department of Energy (DOE) Joint Genome Institute (JGI) (William *et al.*, 2004). For this, the bacterial pellet was re-suspended and adjusted to an OD600 of 1 in TE buffer (10 mM Tris; 1 mM EDTA, pH 8.0). To this volume (24.7 ml), 666.7 µg of lysozyme was then added (100 mg ml^{-1}) and the lysozyme-cell suspension incubated in a hot water bath at 37°C for 30 min. Solutions of SDS (10%, 1.33 ml) and Proteinase K (10 mg ml^{-1}, 266.7 µl) in nuclease free water were then added and incubated at 56°C for 3 h. A solution of NaCl (5 M, 3.33 ml) and a solution of hexadecyltrimethyl ammonium bromide (CTAB, 10% w/v) with NaCl (4.1% w/v) (3.33 ml heated to 65°C for 3 h with stirring) were then added to this high salt content buffer and mixed well. This was left at 65°C for 10 min. Chloroform and isoamyl alcohol were added at a ratio of 24:1 (16.67 ml) before centrifugation (13,000 *g*). The aqueous phase was transferred to a clean tube and phenol, chloroform and isoamyl alcohol were added at a ratio of 25:24:1 (16.67 ml). Once again the solutions were mixed, centrifuged and the aqueous layer was transferred to a clean tube, where nucleic acids were precipitated overnight (at -20°C) with 0.6 volumes of isopropanol. The sample was then centrifuged for 15 min and the pellet was washed with cold ethanol (70%, -20°C) before another 5 min centrifugation. The supernatant was discarded and the pellet was dried under a vacuum before being

transferred into a microfuge tube and re-suspended in 170 µl DNase-free water. RNAse I buffer was added and the sample was incubated at 37°C for 1 h (this process was repeated as a traces of RNA were persistent after agarose gel electrophoreses). RNase was inactivated by heating to 70°C for 15 min. The sample was placed on ice and 1/10 volume of sodium acetate (3 M) and 2.5 volumes of ethanol were added. DNA precipitation was complete after 30 min at -80°C. The sample was centrifuged (13,000 *g*) at 4°C for 20 min. The supernatant was carefully discarded, and the sample washed again in ethanol (70%) and centrifuged (13,000 *g*). The ethanol was then carefully removed and the DNA pellet dried under a vacuum and re-suspended TE buffer. Agarose gel electrophoresis was used to check for quality of the extracted DNA. The DNA solution was adjusted to a concentration of 500 ng/µl (500 µl) using picogreen and Nanodrop 3300 before being shipped on dry ice to the JGI for whole-genome sequencing.

The complete genome sequence for *P. algicola* was generated at the JGI as described in (Gutierrez *et al.*, 2015). Briefly, reads were assembled using hierarchical genome-assembly process (HGAP) to produce *de novo* genome sequence of accuracy greater than 99.9999% (Chin *et al.*, 2013). The genomes online database (GOLD) project ID is Ga0004718 and the NCBI taxon ID is 1415779. The genome was annotated using the bacterial annotation system (BASys), which uses Gene Locator and Interpolated Markov ModelER (Glimmer) to identify genes and over thirty programs to determine function (COG and GO), gene/protein name, operon structure, pathways and possible paralogues/orthologues (Van Domselaar *et al.*, 2005). Operons are assigned by BASys if neighbouring coding regions are on the same strand, within 30 bases of each other and uninterrupted by coding regions on the complementary DNA strand as per the method of Salgado *et al.* (2000), which has an accuracy maximum of 88%: this is a simple heuristic, which doesn't take into account gene names, promoters or Shine-Dalgarno sequences (ribosomal binding sites). *P. algicola* is classed as an obligate hydrocarbon degrader with a DNA G+C content of 63.8% (Gutierrez *et al.*, 2013b). This G+C content puts the *P. algicola* genome at the threshold level where Glimmer (the gene prediction program used by BASys) may produce high levels of false positives, and therefore the gene predictions provided by BASys were viewed with some degree of caution; BLAST searches of gene coding regions (both nucleotide and translated amino acid sequences) were double-checked against specialized databases UniProt (http://www.uniprot.org/blast/), and PDB (http://www.rcsb.org/pdb/home/

home.do) to ensure high E-values and Bit-scores (Pearson, 2013; Van Domselaar *et al.*, 2005). Gene homology with other species was confirmed by E-values smaller than 10^{-10} and Bit-scores larger than 50 as per Pearson, (2013).

3.3 Results and Discussion

The genome of *P. algicola* analysed using BASys was a total of 3,653,213 base pairs (bp) in length with 3920 identified and annotated genes. There were eight operons identified for the degradation of aromatic compounds (defined as per Salgado *et al.*, 2000) which are listed below. Genes in the eight operons exhibited small E-values ($<10^{-10}$) and high bit scores (>50) and were therefore the major focus of this chapter along with gene clusters, as in Pinyakong *et al.* (2003).

- **Operon 1: *lapF*; *lapG*; BASYS00867; *xylX*** (or Acetaldehyde dehydrogenase; 4-hydroxy-2-oxovalerate aldolase; Aromatic-Ring-Hydroxylating Dioxygenase Subunit Beta; Toluate 1,2-dioxygenase subunit alpha) (base pairs 797739 - 801522 forward strand) (Figure 11)
- **Operon 2: *bphC*; *nahD*** (or Biphenyl-2,3-diol 1,2-dioxygenase; 2-hydroxychromene-2-carboxylate isomerase) (803112 - 804735 forward strand) (Figure 11)
- **Operon 3: *bphC*; *cmtB*; *bphA3*** (or Manganese-dependent 2,3-dihydroxybiphenyl 1,2-dioxygenase; 2,3-dihydroxy-2,3-dihydro-p-cumate dehydrogenase; Biphenyl dioxygenase ferredoxin subunit) (884640 - 886685 forward strand)
- **Operon 4: *bphR*; *bphA*; *bphE*; *bphF*; *bphG*** (or Uncharacterized HTH-type transcriptional regulator; Biphenyl dioxygenase subunit alpha; Biphenyl dioxygenase subunit beta; Biphenyl dioxygenase system ferredoxin subunit; Biphenyl dioxygenase system ferredoxin-NAD (+) reductase component) (1683394 - 1687790 forward strand)
- **Operon 5: *bphB*; *bphC*** (or Cis-2,3-dihydrobiphenyl-2,3-diol dehydrogenase; Biphenyl-2,3-diol 1,2-dioxygenase) (1687826 - 1689546 forward strand)
- **Operon 6: *dmpL*; *dmpM*; *dmpN*; *dmpO*; *dmpP*** (or Phenol hydroxylase proteins P1 – 5) (2159308 - 2163795 forward strand)

- **Operon 7: BASYS02338; *dmpC*** (or Hypothetical Protein Lcho; 2-hydroxymuconic semialdehyde dehydrogenase) (2170954 - 2172878 forward strand)
- **Operon 8: *vanA*; BASYS02345; *lapF*; *mhpE*; *vanA*** (or Vanillate O-demethylase oxygenase subunit; Hypothetical Protein; Acetaldehyde dehydrogenase; 4-hydroxy-2-oxovalerate aldolase 5; Vanillate O-demethylase oxygenase subunit) (2174713 – 2179396 forward strand)

Operon 1 can be seen in Figure 11 preceded by *xylB* and 'BASYS' genes of unclassified function and followed by *aldA* and Operon 2 on the forward strand. Also visible on the reverse strand are *xylA*, *xylM* and *fadH* genes. At start of the operon (797739-798656) is an acetaldehyde dehydrogenase enzyme (*lapF*), which has 3 paralogs elsewhere in genome. The closest match of this *lapF* gene was an 89.8% identity (E-value: 0.0, Bit-score 1411) with unknown bacterium (bacterium 16 taxon ID: 1748268), and close second and third with *Azoarcus* and *Thauera* spp. (genes code for the same protein). However the best protein sequence match was an aldolase-dehydrogenase complex (4JN6) (E-value: 7.8 × 10-83, Bit-score 305), which is a gene from a cholesterol degradation pathway of *Mycobacterium tuberculosis*, a species able to store and utilize cholesterol, a lipid alcohol molecule present in animal cell membranes (Brzostek *et al.*, 2009). This is an example of the versatility of enzymes for lipid degradation for application in petroleum-hydrocarbon degradation. The closest BLAST match for the translated gene sequence of BASYS00867 was 38% sequence identity (E-value: 8.2×10^{-24} Bit-score: 107) with only 1 gap in the 143 sequence with a putative aromatic-ring-hydroxylating dioxygenase from bacterium *Novosphingobium aromaticivorans*. This gene was unnamed due to the lower identity compared to the *lapF* starting gene. The gene sequence itself had a maximum of 45.8% identity with *ortho*-halobenzoate 1,2-dioxygenase from *Collimonas arenae* (E-value: 180×10^{-39}, Bit-score: 347).

Operon 2 can also be seen in Figure 11 preceded by *aldA* and followed by naphthalene dioxygenase subunits *ndoB* and *ndoC*, as well as *benD*, *hcaE* and BASYS00879 gene, the latter being a putative aromatic-ring-hydroxylating dioxygenase. The gene *bphC* has sequence identity of identity of 71.3% with 2,3-dihydroxybiphenyl 1,2-dioxygenase from *Thalassospira* sp. Nap_22 (E-value: 2.1×10^{-165}, Bit-score: 1,220), and an identity of 72.5% (E-value: 6.4×10^{-162}, Bit-score: 1197) with dihydroxy naphthalene/biphenyl dioxygenase from *Sphingomona*s sp. LH128, a bacterium capable of oxidizing LMW

PAHs and halogenated hydrocarbons (Schuler *et al.*, 2009). Both species above are of the class *Alphaproteobacteria*, as were the top ten similar gene sequences on the Uniprot database, whereas *P. algicola* is of class *Gammaproteobacteria*. The translated amino-acid sequence revealed 66% identity with a type I extradiol dioxygenase targeting catechol (*akbC*) in *Rhodococcus* sp. strain DK17 (E-value: 5.81×10^{-118}, Bit-score: 422) with 0% gaps in the 298 length amino acid sequence (Cho *et al.*, 2010). This bacterium belongs to the phylum *Actinobacteria*. The next most similar protein was 1,2-dihydroxynaphthalene dioxygenase from *Pseudomonas* sp. strain C18. The *bhpC* gene encodes an enzyme responsible for cleaving the aromatic ring of dihydroxybiphenyl (Novakova *et al.*, 2010). Three paralogues were recognized for this gene in the *P. algicola* genome: biphenyl-2,3-diol 1,2-dioxygenase (*bhpC*), iron-dependent extradiol dioxygenase (*hsaC*), and manganese-dependent 2,3-dihydroxybiphenyl 1,2-dioxygenase (*bhpC*). These results highlight the possibility of *P. algicola* catabolic activity on a number of aromatic diols or possibly an aromatic diol subgroup. The gene *nahD* in Operon 2 has a gene sequence identity of 59.1% with an uncharacterized protein from (*Rhodocyclaceae* bacterium PG1-Ca6), but 56.2% with enzyme 2-hydroxychromene-2-carboxylate isomerase from *Hydrocarboniphaga effusa* AP103 (both E-values in region of 10^{-78}), the latter being one of the closest relatives of *P. algicola* (Gutierrez *et al.*, 2013b). The former is a pyrene degrader and the latter is an *n*-alkane degrader also implicated in aromatic hydrocarbon degradation (Palleroni *et al.*, 2004; Singleton *et al.*, 2015). Analysis of the translated amino acid sequence using PDB resulted in a closest match with 49% sequence identity and only 2% gaps over the 189bp gene (E-value : 3.3×10^{-48}, Bit-score: 189) to the enzyme 2-hydroxychromene-2-carboxylic acid (HCCA) isomerase in *Pseudomonas putida*, which catalyzes the inter-conversion of HCCA and trans-*o*-hydroxybenzylidene pyruvic acid (tHBPA) in the naphthalene catabolic pathway. Operon 2 is immediately followed by *ndoB* and *C* (Naphthalene 1,2-dioxygenase subunits *alpha* and *beta*), which may be transcribed at the same time as Operons 1 and 2.

Operon 3 is preceded by clusters of genes involved in aromatic compound degradation (*xyl*, *bph*, *ben*, *dmp* and *nah*). Also visible on the reverse strand is BASYS00949 (*ins* for transposase IS4 family) and the neighbouring *xylA* gene. The first gene in Operon 3 (*bphC*) had a translated protein sequence identity of 31% (E-value: 5.30349E-27 Score: 119.398bits) with Mn(II)-bound glyoxalase from *Novosphingobium aromaticivorans* and gene sequence identity of 59.2% (E-value: 17×10^{-120}, Bit-score:

919) with an uncharacterized protein (from *Variovorax paradoxus*). However three of the next five most similar genes were all from *Pseudomonas putida*. Two paralogs identified for this *bphC* were classified as metapyrocatechase. The *cmtB* gene had sequence identity of 66.4% (E-value: 2.9×10^{-117}, Bit-score: 892) with 2,3-dihydroxy-2,3-dihydro-p-cumate dehydrogenase (*Bradyrhizobium* sp. LTSPM299).

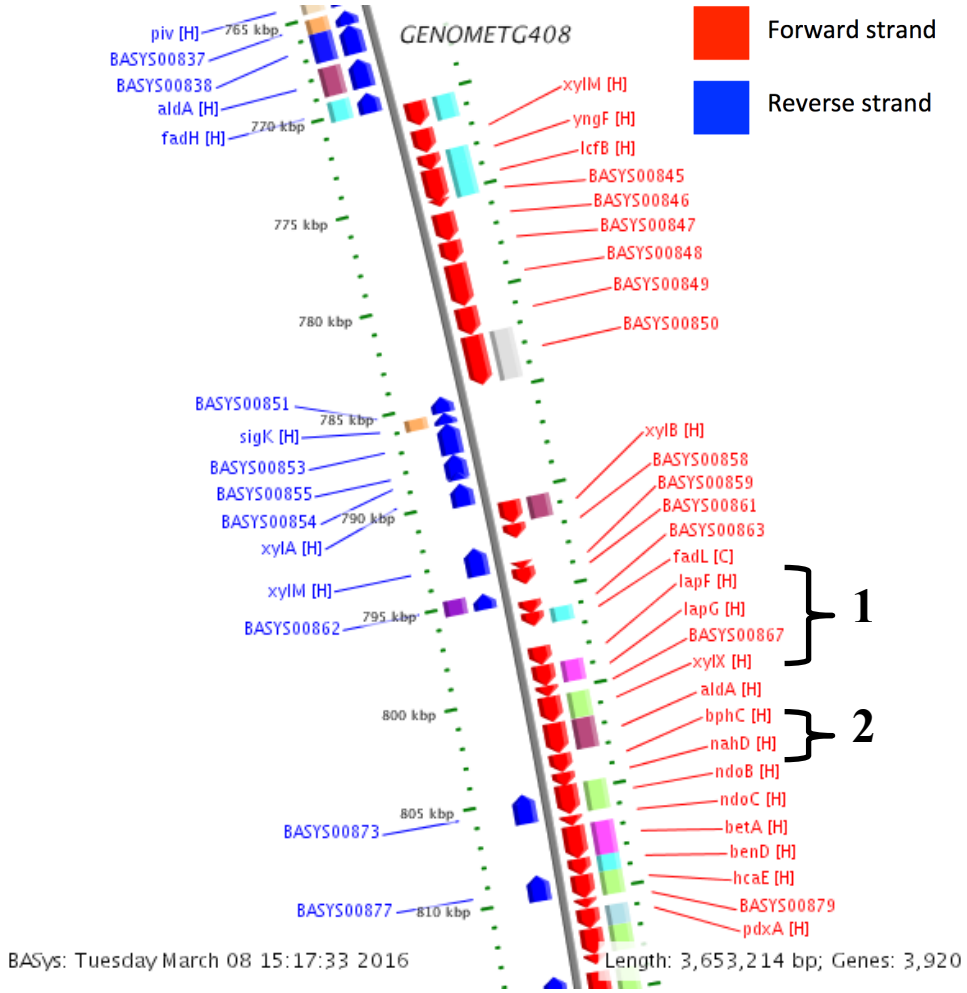

Figure 11. Annotated map of *P. algicola* strain TG408 chromosome region (765 – 810 kbp). Braces highlight the positions of Operons 1 and 2 on the forward (red) strand involved in aromatic compound catabolism, also visible are other genes (e.g. *xyl*, *hca* and *fad*) possibly involved in hydrocarbon degradation.

Operon 4 and 5 are neighbouring sequences on the same DNA strand.

The first gene *bphR* is an uncharacterized helix-turn-helix (HTH) -type transcriptional regulator. The *bphA* translated amino-acid sequence revealed sequence identity of 66% (Bit-score: 631) with Biphenyl dioxygenase (BphA1A2) from *Rhodococcus* sp. Strain RHA1 (phylum *Actinobacteria*) (Furusawa *et al.*, 2004). The closest match in gene

sequence identity was 81% (Bit-score: 2101) to *Cupriavidus* sp. WS (class *Betaproteobacteria*) capable of degrading biphenyl esters (Wang *et al.*, 2015). After *bphA* came the biphenyl dioxygenase subunit beta (*bphE*). In Pinyakong *et al.* (2003) the *bph* cluster of genes are proposed to be effective in naphthalene, phenanthrene and anthracene as well as biphenyl pathways, and therefore this arrangement of genes in Operons 4 and 5 may be have a broad compound specificity for more than one substrate. Unlike pathway proposals from Pinyakong *et al.* (2003) the *bph* operons are not interspersed or combined with *nah* (D/E/F)*, nca* (C/D/E) or *ahd* genes. Operon 5 is transcribed after Operon 4 but contains *bphB* and *C*. Pinyakong *et al.* (2003) propose that *bphB* converts a range of PAH-dihydrodiols into their corresponding dihydroxy-PAH forms (re-aromatization) before *bphC* oxidises these substrates further forming carboxyl groups. The gene following Operon 4 (and possibly transcribed at the same time) is *bphD* or 2-hydroxy-6-oxo-6-phenylhexa-2,4-dienoate hydrolase, which forms an aldehyde according to Pinyakong *et al.* (2003). The genes in Operons 4 and 5 are involved in the metacleavage pathway of biphenyl and polychlorinated biphenyl degradation by *Pseudomonas* sp. strain KKS102 (Kikuchi *et al.*, 1994).

Operon 6 is preceded by *xylR* (transcriptional regulatory protein) on the reverse strand and *dmpK* (Phenol hydroxylase P0 protein) on the forward strand. It encodes the phenol hydroxylase operon *dmp(K)LMNOP* for complete conversion of phenol to catechol, an operon which is also found in *Pseudomonas* sp. Strain CF600 (Shingler *et al.*, 1992). However in *Pseudomonas* sp. Strain CF600 the operon is longer (*dmpKLMNOPQBCDEFGHI*) where *dmpQBCDEFGHI* convert catechol to an acyl coenzyme A ester (*dmpF* performs the final stage) (Shingler *et al.*, 1992). The genes *dmpHDC* and *L* are found elsewhere in the *P. algicola* genome, with *dmpC* found in Operon 7 (located directly after Operon 6) and *xylJ and dmpH* directly after Operon 7 and directly before Operon 8. The *P. algicola* genome did not contain *dmpF*, for example, and so may have other genes for degradation of catechol. A good example is one we have already seen in the translated protein sequence of *bphC* in Operon 2 above (an enzyme with possibly more than one function, also exhibiting a paralog in Operon 3). Between Operons 6 and 7 is an HTH-type transcriptional regulator (*benM*), found on both forward and reverse strands. In Operon 7 the gene BASYS02338 revealed a sequence identity of 64.8% (E-value: 30×10^{-57}, Bit-score: 468) with bacterium 16 (taxon ID: 1748268, the same as *lapF* in Operon 1). Operon 8 starts and ends with the *vanA* (Vanillate demethylase oxygenase subunit): an enzyme that is found in

Pseudomonas spp.; vanillate is a possible intermediate of aromatic compound degradation and also a compound produced synthetically through lignin and/or petroleum hydrocarbon breakdown for use in foods and fragrances (Brunel and Davison, 1988; Priefert *et al.*, 1997). The gene sequence of hypothetical protein BASYS02345 shared highest sequence identity once again with bacterium 16 (taxon ID: 1748268). Directly downstream of Operon 8 is *nahH* (metapyrocatechase), which may be a part of the same operon unidentified by BASys.

There were four other regions present in the *P. algicola* genome that were not identified as operons by BASys but that contained clusters of genes that function in aromatic compound degradation. These are listed below:

- **1. Forward strand 790427 – 815836: *xylB*; *lapF*; *lapG*; *xylX*; *aldA*; *bphC*; *nahD*; *ndoB*; *ndoC*; *betA*; *benD*; *hcaE*; *pdxA*; *bedC1*; *hcaE*; *hcaF***

The protein function for the above genes are as follows: Aryl-alcohol dehydrogenase; Acetaldehyde dehydrogenase; 4-hydroxy-2-oxovalerate aldolase 1; Toluate 1,2-dioxygenase subunit alpha; Putative aldehyde dehydrogenase *AldA*; Biphenyl-2,3-diol 1,2-dioxygenase; 2-hydroxychromene-2-carboxylate isomerase; Naphthalene 1,2-dioxygenase subunit alpha; Naphthalene 1,2-dioxygenase subunit beta; Choline dehydrogenase; 1,6-dihydroxycyclohexa-2,4-diene-1-carboxylate dehydrogenase; 3-phenylpropionate/cinnamic acid dioxygenase subunit alpha; 4-hydroxythreonine-4-phosphate dehydrogenase; Benzene 1,2-dioxygenase subunit alpha; 3-phenylpropionate/cinnamic acid dioxygenase subunit alpha; 3-phenylpropionate/cinnamic acid dioxygenase subunit beta.

- **2. Reverse strand 829583 – 842706: *limA*; *bedC2*; *bphA*; *bphF*; *hpcG*; *dmpD*; *dmpH*; *xylJ*; *dmpC*; *dmpL*; *xylR*; *gstB*; *bphB*; *nahE***

The protein function for the above genes are as follows: Limonene-1,2-epoxide hydrolase; Benzene 1,2-dioxygenase subunit beta; Biphenyl dioxygenase subunit alpha; 4-hydroxy-2-oxovalerate aldolase; 2-oxo-hepta-3-ene-1,7-dioic acid hydratase; 2-hydroxymuconic semialdehyde hydrolase; 4-oxalocrotonate decarboxylase; 2-hydroxypent-2,4-dienoate hydratase; 2-hydroxymuconic semialdehyde dehydrogenase; Phenol hydroxylase P1 protein; Transcriptional regulatory protein *xylR*; Glutathione S-transferase GST-6.0; Cis-2,3-dihydrobiphenyl-2,3-diol dehydrogenase; Trans-O-hydroxybenzylidenepyruvate hydratase-aldolase.

- **3. Forward strand 847884 – 862438: *bsdC*; *pchF*; *bsdB*; *ywfA*; *yeaW*; *fabG*; *yliJ*; *hcaE*; *bphE*; *yxbG*; *yxbG*; BASYS00944**

The protein function for the above genes are as follows: Phenolic acid decarboxylase subunit C; 4-cresol dehydrogenase [hydroxylating] flavoprotein subunit; Phenolic acid decarboxylase subunit B; Uncharacterized MFS-type transporter *ywfA*; Putative dioxygenase subunit alpha *yeaW*; 3-oxoacyl-[acyl-carrier-protein] reductase *FabG*; Uncharacterized GST-like protein *yliJ*; 3-phenylpropionate/cinnamic acid dioxygenase subunit alpha; Biphenyl dioxygenase subunit beta; Uncharacterized oxidoreductase *yxbG*; Uncharacterized oxidoreductase *yxbG*; Uncharacterized *BphX*-like protein Bxeno_C1129.

- **4. Forward strand 867969 – 876384: *xylM*; *xylM*; *benA*; *xylY*; *xylB*; *xylE*; *dmpD***

The protein function for the above genes are as follows: Xylene monooxygenase subunit 1; Xylene monooxygenase subunit 1; Benzoate 1,2-dioxygenase subunit alpha; Toluate 1,2-dioxygenase subunit beta; Aryl-alcohol dehydrogenase; Metapyrocatechase; 2-hydroxymuconic semialdehyde hydrolase.

Taking a closer look at one of the *xylM* (Xylene monoxygenase subunit 1) genes from bullet-point 4 above we find that there are seven paralogs named *xylM* in the *P. algicola* genome. In the TOL (oxidative catabolism of toluene system) plasmid pWW0 of *Pseudomonas putida* the second subunit for this enzyme is *xylA*, which together code for the broad specificity xylene monooxygenase enzyme that additionally oxidizes a) (methyl) benzyl alcohols to (methyl) benzaldehydes and b) indole to indoxyl, according to Suzuki *et al.* (1991). Indole is an example of an intercellular bacterial signalling molecule. There were 4 paralogs named *xylA* in the *P. algicola* genome, but the two genes (*xylM* and *xylA*) were only found directly next to one another twice in the *P. algicola* as in the TOL system. The *xylM* paralogs exhibit varying sequence identities of 73 - 31% (E-value range: $1 \times 10^{-167} – 7 \times 10^{-46}$). Interestingly yet more paralogs for this gene with lower sequence identity (around 30% identity, E-values $<<10^{-10}$) were designated as other genes for example *alkB1* (Alkane 1-monoxygenase). It is unknown whether the function of these genes are orthologous of paralogous to *xylM* and incorporated into new functional gene clusters around the genome or are randomly distributed and non-functional.

Another enzyme example of relaxed substrate specificity is toluate 1,2-dioxygenase (TADO) encoded by *xylXYZ* genes, which are also part of the TOL system (Ge *et al.*, 2002; Harayama and Rekik, 1990). The subunits for said enzyme (*xylX* and *xylY*) are also found in *P. algicola* but don't appear in the same gene clusters (bullet-points 1 and 4 above respectively) and the gene *xylZ* was not found. Again these aromatic compound catabolism enzymes may have paralogous functions in this organism. The oxidoreductase (*yxbG*) genes in bullet-point 3 above share a sequence identity of 73.4% (E-value: 140×10^{-129}, Bit-score: 960) with a short-chain dehydrogenase from *Cycloclasticus* sp. Phe_18 involved in fatty acid metabolism. There were 35 other oxidoreductases found in the *P. algicola* genome. Toluene-4-monooxygenase electron transfer component (*tmoF*) is another case of a gene with possible multi-function. McClay *et al.* (2000) states that toluene monoxygenases, which hydroxylate the aromatic ring, were also effective in alkene and choro-alkene epoxidation. This gene in *P. algicola* was found directly on the opposite strand to *ndoR* (Naphthalene 1,2-dioxygenase system ferredoxin--NAD(+) reductase component) and *nahR* (HTH-type transcriptional regulator).

A gene of interest in bullet-point 2 above is limonene-1,2-epoxide hydrolase (*limA*), the gene transcribed last in this sequence and which converts the limonene epoxide into a diol. Epoxide hydrolases are involved in bacterial degradation of hydrocarbons, although are also involved in epoxide detoxification and hormone biosynthesis in plants and animals (van der Werf *et al.*, 1998; Touhara and Prestwich, 1993). In *Rhodococcus erythropolis limA* was found to be the first finding of a new class of chemicals and the translated amino acid sequence from *P. algicola* had closest match to this species, but the gene sequence had most identity *limA* from *Cycloclasticus* sp. Phe_18, the same strain match as for the *yxbG* gene above (Barbirato *et al.*, 1998). Limonene is not an aromatic but a cyclic terpene with a C=C double bond in the carbon ring. It is found in citrus fruits and used a flavoring, but also has possible therapeutic biological effects, for example arresting gliomagenesis of a very similarly structured monoterpene perillyl alcohol (da Fonseca *et al.*, 2011). Another pair of genes of similar interest in the gene cluster in bullet-point 1 above are *hcaE* and *F* (cinnamic acid dioxygenase subunits *alpha* and *beta*). Cinnamic acid (a possible product of aromatic hydrocarbon degradation) is a mono aromatic, unsaturated carboxylic acid that has an extensive range of applications and biological activities (e.g. precursor to alkaloids); cinnamic

acid and its derivatives are found in many plant species and are dietary phenolic compounds (Sharma, 2011).

As an extra note the *P. algicola* genome contained a cluster of cobalamin (vitamin B_{12}) synthesis genes from 2914988 – 2927745 bp on the reverse strand (*cobT*; *cobP*; *cobQ*; *cobC*; *cobD*; *btuF*; *bluB*; *cobB*; *cobO*; *btuB*; *cobS*). Also the genes *BioFAD* and *B* (although BioA was in a different genome region) were observed, which are involved in the biotin (vitamin B_7) synthesis.

Multiple diol-dioxygenases were detected in the *P. algicola* genome e.g. *bphC* in Operons 2, 3, 5 and bullet-point 1, and its various paralogues including *hscA* (an extradiol dioxygenase), and also possibly BASYS00879 (a putative aromatic-ring-hydroxylating dioxygenase following Operon 2). This may go some way to explaining why (in Section 2.3.2.4) *P. algicola* was able to form colonies on agar where 1,2-dihydroxynaphthalene was the sole carbon source. The intermediates from PAH degradation are environmentally relevant due to their possibly increased toxicity to organisms (Zielinska-Park *et al.*, 2004). The results above show that *P. algicola* can degrade a range intermediates. Other compounds that are intermediates of PAH degradation, but also possible industrial intermediates from the food or pharmaceutical industries (e.g. vanillate, limonene, cinnamic acid, salicylic acid), are also biologically active and may be present as environmental contaminants. Pharmaceuticals can be persistent contaminants in aquatic environments and are of global concern (Crane *et al.*, 2006; Zuccato *et al.*, 2006). If hydrocarbon degradation genes/enzymes found within hydrocarbonoclastic bacteria exhibit broad substrate specificity then they may be expected to play a significant role in the degradation of other related chemical compounds.

The aromatic degradation genes highlighted in this results and discussion section indicate a versatility in degrading two-ringed PAHs (biphenyl and naphthalene) as was found by Gutierrez *et al.* (2013b). Specific phenanthrene targeting genes were unidentified, which infers that this organism may have novel mechanisms for phenanthrene oxidation or possibly use more relaxed or broad specificity enzymes. Examples of putative broad specificity enzymes in the genome include *lapF* in Operon 1, which exhibited highest protein sequence identity with a cholesterol degradation enzyme; there are structural similarities between cholesterol and steroids found in crude

oil (Yang *et al.*, 2013). Also the *bhp* genes in Operons 4 and 5 and the *xylM* and *A* genes (possibly from the *Pseudomonas* TOL plasmid) may exhibit broad specificity (Kikuchi *et al.*, 1994; Pinyakong *et al.*, 2003; Suzuki *et al.*, 1991; Wang *et al.*, 2015). In the phenanthrene-degrader *Cycloclasticus* sp. strain A5, the genes *phnA1-A4* coding for PAH dioxygenase are found in rearranged orders and sequences to previous findings (Kasai *et al.*, 2003). Genes *phnA1-A4* were absent in *P. algicola* although, in similarity to the finding of Kasai *et al.* (2003), some other aromatic compound degradation genes (e.g. *xylX* and *xylY*) were found in different sequences and re-arranged orders to previous known hydrocarbon degraders (Ge *et al.*, 2002; Harayama and Rekik, 1990). Genes encoding naphthalene dioxygenase (*nahAa-Ad*) found in *Pseudomonas* strains were also absent in *P. algicola* (Simon *et al.*, 1993). However the transcriptional regulator for these genes *nahR* found in *Pseudomonas putida* was present in *P. algicola* on the reverse strand immediately upstream of *ndoR* (Naphthalene 1,2-dioxygenase system ferredoxin--NAD(+) reductase component) (Hedlund *et al.*, 1999). Other *nah* were found interspersed in the genome: *nahD* in Operon 2 and gene cluster bullet point 1, *nahE* in bullet point 2, *nahH* directly after Operon 8 and *nahM* was situated upstream of Operon 3.

The gene *nahD* had sequence most similar to *P. algicola*'s closest 16S rRNA relative *Hydrocarboniphaga* (there was also an *nahD* paralog elsewhere in the genome), however certain aromatic compound-targeting genes were more closely related in gene and translated amino-acid sequence to other genera, and sometimes to species in a different phylum or class. For example, the gene sequence for *bphC* had the closest match in two members of class *Alphaproteobacteria*, while the protein sequence exhibited greatest similarity to a member of the phylum *Actinobacteria* (*Rhodococcus* sp.). Likewise the gene sequence for *bphA* had a best match in class *Alphaproteobacteria* and protein sequence match in the phylum *Actinobacteria* (again *Rhodococcus* sp.). Other notable examples were the genes *yxbG* and *limA*, both of which were homologous to *Cycloclasticus* sp. Phe_18. Many other genes in this chapter were closely related to those of *Pseudomonas putida*. These examples of various genes exhibiting high (>70%) sequence identity (a proxy for evolutionary distance) to diverse groups of bacteria may suggests multiple historic horizontal transfer events involving *P. algicola* (Louvado *et al.*, 2015; Pearson, 2013), although this is yet to be investigated.

It has been established that in the phycosphere, specifically on the surface of micro-algal cells and in marine snow, complex interactions (e.g. chemical release regulated by quorum sensing) take place between closely associated bacterial species (see Chapter 1). Evidence from the genome of *P. algicola* suggests this organism may be receptive to compounds involved in bacterial communication, e.g. *xylM* and *xylA* convert indole (bacterial signalling molecule) and *limA* targets limonene (a possible inducer of bacterial PCB breakdown) (Biswas *et al.*, 2015; Melander *et al.*, 2014; Suzuki *et al.*, 1991; Tandlich *et al.*, 2001). There are also instances in the *P. algicola* genome directly before or after aromatic degradation genes where clusters of insertion sequences are found that are specific transposase enzymes (e.g. *insH10* and *insF1*). In theory, if bacteria in the phycosphere (either attached to micro-algae or marine snow/EPS) contain plasmids coding the specific insertion sequences in *P. algicola*, they could transfer aromatic catabolic genes within transposable elements at times of stress (e.g. in an oil spill), further evolving and adding to the aromatic degradation capabilities of the *P. algicola* genome (Capy *et al.*, 2000).

The provision of EPS by micro-algae, as discussed in Chapter 2, may provide the ideal habitat for the survival and growth of hydrocarbon-degrading bacteria like *P. algicola*. Many algae are cobalamin (vitamin B_{12}) auxotrophs (Croft *et al.*, 2006). *S. costatum* and *T. pseudonana* are thought to be cobalamin auxotrophs (or partial auxotrophs) (Sañudo-Wilhelmy *et al.*, 2006; Swift and Guillard, 1978; Tang *et al.*, 2010). The *bioD* gene for biotin (vitamin B_7) is not present in the *T. pseudonana* genome. The presence of cobalamin and biotin production pathways in *P. algicola* shown in this chapter may shed light on a possible mutualistic relationship between *P. algicola* and diatoms, although this is as of yet unconfirmed. Further analysis of this genome may uncover more information about the relationship between hydrocarbonoclastic bacteria in the phycosphere and possibly also uncover novel aromatic catabolic genes, which may have useful applications in the fields of bioremediation and bioaugmentation of petroleum hydrocarbons in the marine environment.

CHAPTER 4: ENHANCED CRUDE OIL BIODEGRADATIVE POTENTIAL OF HYDROCARBONOCLASTIC BACTERIA ASSOCIATED WITH NATURAL POPULATIONS OF PHYTOPLANKTON

4.1 Introduction

The importance of the role played by marine eukaryotic phytoplankton (micro-algae) at the base of the marine food web has been described in Chapter 1 of this thesis. These organisms provide the organic carbon and oxygen necessary for ecosystems to flourish (Ducklow *et al.*, 2001; Field *et al.*, 1998). Defined as the zone around micro-algal cells where bacteria are found attached, the phycosphere is an important site where interactions take place between microbes and molecules that are fundamental to the global carbon cycle (Bell and Mitchell, 1972; Kujawinski, 2011). Bacteria are the primary colonizers of micro-algae and rely heavily on algal-derived extracellular polymeric substances (EPS) (Goecke *et al.*, 2013; Lachnit *et al.*, 2011). These algal-bacterial communities, including macro-aggregates formed of these organisms, often due to the release of EPS, drive the biological pump, transporting organic and inorganic carbon to the seafloor where it can become buried and trapped for millions of years (Ducklow *et al.*, 2001; Wong and Crawford, 2002). Furthermore, complex molecular interactions involving hydrocarbon signalling molecules (like the diatom pheromone fucoserratene) take place on the phycosphere because of the nature of the diffusive boundary layer, where advective mixing does not take place (Amin *et al.*, 2012).

Contamination of the marine environment by crude oil can cause significant impacts to local ecosystems, which is often due to the toxic effects of certain hydrocarbon constituents of the oil (Sikkema *et al.*, 1995; Turner *et al.*, 2014). Crude oil is a heterogeneous mix of thousands of chemical components each with their individual physico-chemical properties, some soluble and volatile, others recalcitrant and heavy (Haritash and Kaushik, 2009; Huba *et al.*, 2016; Sauer and Boehm, 1991). Crude oil (and the dispersants used to remediate oil spills) cause structural shifts in both phytoplankton and bacterial communities (Bælum *et al.*, 2012; Özhan and Bargu, 2014b; Yakimov *et al.*, 2004a). Aromatic hydrocarbons (e.g. PAHs), as touched upon in Chapter 2, can have variable effects on the growth of organisms in the phycosphere (Haritash and Kaushik, 2009; Özhan and Bargu, 2014a). Whilst low levels ($\leq$1 mg L^{-1}) of crude oil pollution (Özhan *et al.*, 2014, and references therein) can in some cases

stimulate phytoplankton, higher concentrations cause sub-lethal or lethal effects to phytoplankton (Adekunle *et al.*, 2010; D'souza *et al.*, 2016; Gilde and Pinckney, 2012; Johansson *et al.*, 1980; Özhan and Bargu, 2014b,c; Prouse *et al.*, 1976). In the presence of crude oil, phytoplankton and bacteria have been reported to participate in the formation of marine oil snow (MOS) (van Eenennaam *et al.*, 2016; Passow *et al.*, 2012; Mishamandani *et al.*, 2016). The subsequent sedimentation of rapidly sinking MOS has been described as a mechanism that can contribute importantly to transporting large quantities of oil to the sea floor (Daly *et al.*, 2016; Passow, 2016).

Factors affecting the rate of crude oil degradation include temperature, nutrient availability, dispersants, photo-oxidation and most importantly bacterial community composition (Atlas, 1981; Bagi *et al.*, 2014; Leahy and Colwell, 1990; Siron *et al.*, 1995; McGenity *et al.*, 2012). Previous microbial community studies of crude oil contaminated marine environments have revealed that the bacteria comprising the orders *Thiotrichales*, *Alteromonadales* and *Oceanospirillales* (all *Gammaproteobacteria*) are primarily responsible for the removal of petroleum hydrocarbons from contaminated marine environments (Bælum *et al.*, 2012; Gerdes *et al.*, 2005; Hazen *et al.*, 2010; Redmond and Valentine, 2012; Yang *et al.*, 2016). New oil-degrading taxa continue to be discovered, offering a range of potential commercial and biotechnological applications, including novel bio-surfactant and bio-emulsifying molecules that these types of microorganisms are commonly found to produce (Gutierrez *et al.*, 2013a; Yakimov *et al.*, 1999). The marine environment is so far the only known ecosystem where obligate hydrocarbonoclastic bacteria have been isolated and described (Head et al. 2006; Yakimov *et al.*, 2007). Recently, novel hydrocarbonoclastic bacteria have been isolated from laboratory cultures of marine micro-algae (Green *et al.*, 2006; Gutierrez *et al.*, 2012b,c,2013b,2014). These studies suggest that the phycosphere is an important biotope for hydrocarbonoclastic bacteria and a source of novel bacterial taxa, although to date the relative importance of their contribution to crude oil decontamination (relative to free-living bacteria) in the marine environment is poorly understood.

There are multiple explanations that may help to explain this relationship. Adsorption of hydrocarbons to the cell surface of micro-algae, addressed in Chapter 2, may potentially increase their concentration at this cellular site (Andelman and Suess, 1970; Schmidt *et al.*, 2004; Sikkema *et al.*, 1995; Yamada *et al.*, 2003). This enrichment of

hydrocarbons may provide phycosphere-associated hydrocarbonoclastic bacteria with a supply of carbon and energy needed to maintain them under oligotrophic conditions and when there is no source of oil hydrocarbons. Micro-algae have also been shown to produce hydrocarbons, including PAHs, quinones and isoprene (Borneff *et al.*, 1968; Dawson *et al.*, 2013; Exton *et al.*, 2012; Nowicka and Kruk, 2010). In fact all three domains of life produce isoprenoids (Dawson *et al.*, 2013; Fall and Copley, 2000; Kuzma *et al.*, 1995; Rontani *et al.*, 2003). Complex communities of micro-organisms may therefore produce the hydrocarbons necessary for maintaining populations of hydrocarbonoclastic bacteria in the laboratory cultures mentioned above, and likewise the signalling molecules or secondary metabolites in marine snow (e.g. fucoserratene, phenol, salicylic acid, limonene, isoprene) may themselves act as a carbon source utilized by hydrocarbonoclastic bacteria (Amin *et al.*, 2012; Fall and Copley, 2000; Gram *et al.*, 2002; Singer *et al.*, 2003; also see Chapter 3 on *P. algicola* genome analysis). In addition, the porous frustules of diatoms absorb crude oil, which may be an attractive prospect for the adhesion of hydrocarbonoclastic bacteria using their 'sticky' glue-like EPS (Daly *et al.*, 2016; Gärdes *et al.*, 2011; Özhan *et al.*, 2014). The hydrocarbonoclastic bacteria might (like other heterotrophic bacteria) be partaking in a mutualistic relationship be providing some nutrient to the phytoplankton (e.g. ammonia or cobalamin) (Croft *et al.*, 2005; Dashti *et al.*, 2015), or they may simply be lying dormant waiting for a crude oil enrichment event. Whatever the underlying reasons for the relationship between hydrocarbonoclastic bacteria and marine eukaryotic micro-algae, an investigation into the role of algal-associated hydrocarbonoclastic bacteria in oil spills is warranted.

Cultures containing combinations of hydrocarbonoclastic bacteria and aquatic or soil algae have demonstrated increased degradation compared to without algae or algal exudates (possibly due to algal oxygen provision), although these studies all used artificial microbial communities and none were marine (Borde *et al.*, 2003; Muñoz *et al.*, 2003; Safonova *et al.*, 1999; Warshawsky *et al.*, 2007). The intrinsic potential for hydrocarbon degradation in many areas of the marine environment (sediment, sea ice, coastal water) has been demonstrated in a number of studies using oil-amended mesocosm experiments, however to date none have shown if these bacteria are free-living or phytoplankton associated (Brakstad *et al.*, 2008; Gertler *et al.*, 2012; Suárez-Suárez *et al.*, 2011; Yakimov *et al.*, 2004a). In an attempt to quantify the significance of the phytoplankton-hydrocarbonoclastic bacterial relationship in a crude oil spill, the

following experiment was designed. A natural bacterial-phytoplankton assemblage from the west coast of Scotland (Loch Creran) was collected and its effectiveness at degrading crude oil was compared with the free-living (non micro-algal associated) bacterial population. The objectives of the present study were: a) to find out if phytoplankton presence impacts aliphatic and aromatic hydrocarbon degradation, b) to determine whether phytoplankton presence influences bacterial community compositional changes in response to crude oil enrichment, and c) to identify any novel taxa of hydrocarbonoclastic bacteria associated with phytoplankton. To address these aims, bacterial community 16S rRNA sequence analysis (using Illumina MiSeq technology) and also individual hydrocarbon concentration analysis (using GC-MS) were performed.

4.2 Materials and Methods

4.2.1 Field sample collection and crude oil enrichment setup

Loch Creran, a marine special area of conservation (mSAC) on the west coast of Scotland (designated as such for its *Serpula vermicularis* and horse mussel *Modiolus modiolus* reefs), was chosen as the site of investigation for its high algal abundance (Tett and Edwards, 2002). Loch Creran is a tidal marine body of water and receives seawater from the Atlantic, via Loch Linnhe. Water was collected in late May 2013 using the *RV Serpula* vessel at coordinates 56º30' 820N, 5º22' 817W, from which a phytoplankton net was trawled for a few minutes at a depth of one meter. This was added to an additional 10-L seawater sample collected with a Niskin bottle at the same location. The two samples were combined and passed through a 125-µm metal mesh filter to remove meso-zooplankton and stored at 4°C. A sub-sample (10 ml) of this 'stock-inoculum' was sent to the Scottish Environmental Protection Agency (SEPA) for micro-algal species identification using a Sedgewick Rafter.

The crude oil used for enrichment was Heidrun (Statoil; low-sulphur oil, density = 860.8 kg m^{-3}), which was sourced form the Norwegian Sector of the North Sea. Before use, it was sterilized by filtering through polycarbonate Isopore membrane (0.2 µm) filters.

To compare the microbial responses of the stock-inoculum, with and without micro-algae, to seawater enrichment with crude oil, three types of treatment, each in triplicate,

were set up: PHY treatment, which comprised solely the stock seawater inoculum; BAC treatment, which comprised the stock-inoculum of seawater after it had been filtered though 2 μm polycarbonate filters (Whatman, Nuclepore) to remove phytoplankton and associated bacteria; and CON treatment, which comprised the stock inoculum (no Heidrun crude oil was be added to this control treatment). In triplicate setup, 350 ml of PHY, BAC and CON inoculum was added to each conical flask. Crude oil was added to PHY and BAC treatments at a concentration of ca.1.5 parts per thousand (ppt) (v/v), whereas no oil was added to the control (CON) treatment. To determine changes in the crude oil composition due to microbial hydrocarbon degradation in PHY and BAC treatments throughout the 40 day experiment four additional treatments were included (also in triplicate): PHY, PHY+acid, BAC and BAC+acid (85% phosphoric acid [3% v/v]). These twelve extra conical flasks were sampled after 40 days (see Section 4.2.2) for total petroleum hydrocarbon (TPH) analysis. All flasks were incubated at 15ºC on a 12-h light/dark cycle (light intensity ~100 μmol m^{-2} s^{-1}) with a magnetic stir bar in each. On each sampling day contents were stirred using the magnetic stir bar for 30 seconds to completely mix the oil and seawater. The conical flasks were tilted to create a clearing in the oil into which a glass serological pipette was placed (to a depth of ~ 1 cm). Volumes of seawater were extracted and these samples were used for analysis of nucleic acid (Section 4.2.3) and bacterial and phytoplankton quantification (Section 4.2.4).

4.2.2 Hydrocarbon analysis

At the end of the experiment (day 40) the contents of conical flask for TPH analysis were poured into a 250 ml separatory funnel with 20 ml dichloromethane (DCM) and shaken. The denser organic DCM phase was collected into a round-bottom flask. Then 20 ml of fresh DCM was added to the flask and shaken to extract the remaining crude oil, and this was repeated twice. The supernatant oil was removed from the separated oil-water mixture using a pipette. Residual oil was dissolved in petroleum ether and added to the supernatant oil. The oil sample was then diluted with DCM to ca. 5 ml and dried by the addition of anhydrous sodium sulphate (ca. 1 g). The sample was removed from the sodium sulphate. The sodium sulphate was washed 4 times with ca. 5 ml amount of DCM and the washings were combined with the dilute oil sample. Sample volume was reduced to ca. 2-3 ml, transferred to a measuring cylinder and diluted to 5 ml. An aliquot of known volume was removed, evaporated to dryness and weighed.

The gravimetric data were used to calculate the original sample weight and the weight of oil remaining.

Before commencement of *n*-alkane analysis a known aliquot corresponding to ca. 30 mg was taken from the remaining TPH sample and transferred to a 10 ml vial. An aliquot of the reference oil was weighed directly into a vial and diluted with ca. 0.3 ml DCM. Squalane and 1,1'-binaphthyl were added as surrogate standards at ca. 0.5% and 0.05% by weight of the oil, respectively. One sample was analysed in triplicate and the reference oil was analysed in duplicate. A procedural blank including the standards was also prepared. A small amount (ca. 2g) of alumina was added to the vial and solvent was removed under gentle stream of nitrogen; the alumina was stirred during the evaporation of solvent to ensure an even distribution of sample on the alumina. A chromatographic column was prepared using silica topped with alumina. Both sorbents were pre-extracted with DCM and activated at 120°C prior to use. The sorbents were introduced as slurries in petroleum ether (BP range 40-60°C). The sorbed sample was applied to the top of the column. The total hydrocarbon (THC) fraction was eluted with 50 ml petroleum ether followed by 70 ml petroleum ether/DCM (2:5). Solvent was reduced to ca. 2 ml using a Heidolph rotary evaporator. The sample was transferred to a vial and diluted to 3.4 ml, and an aliquot was removed for gas chromatographic analysis. The samples were analysed on a Hewlett Packard 5890 GC fitted with a split/splitless injector (300°C), a flame ionisation detector (FID) (310°C) and an HP-5 capillary column (J&W, 30 m × 0.25 mm i.d. × 0.25 μm film thickness). Samples were injected using a Hewlett Packard 6890 automatic injector. The oven programme was 50°C (2 min) – 5°C min^{-1} – 300°C (20 min) giving a total run time of 74 min. The chromatographic data were acquired and processed using an Atlas 8.3 Chromatographic Data System (Thermo Scientific). Peak areas for individual C8 to C35 *n*-alkanes; the isoprenoids, pristane and phytane; and for the surrogate standard squalane were obtained. The total hydrocarbon content was calculated using the manually integrated area under the whole chromatogram, drawing a horizontal baseline from the start of the solvent peak to the end of the acquisition. The corresponding total area for the procedural blank (which also contained the surrogate standards) was then subtracted from the total area obtained for the samples and reference oil. Analyte concentrations were measured using the areas of the added standards, assuming a response factor of one.

The aromatic hydrocarbons in the TPH fractions were analysed by GC-MS on an Agilent 7890A GC fitted with a split/split less injector (at 280°C) linked to an Agilent 5975C MSD, with data acquisition and processing by Agilent Chemstation software. Selected samples were analysed in full scan mode (50-600 amu/sec) but all samples were analysed in selected ion monitoring (SIM) mode using the analyte aromatic hydrocarbon molecular ions or major fragment ions. An aliquot (1 µl) of the TPH fraction diluted in hexane/dichloromethane was injected in split/splitless mode using an Agilent 7683B autosampler and the split opened after 1 min. Separation was performed on an Agilent fused silica capillary column (30 m x 0.25 mm i.d) coated with 0.25 µm 5% phenylmethylpolysiloxane (HP-5) phase. The GC was temperature programmed from 50 – 310°C at 5°C min^{-1} and held at final temperature for 10 min with helium as the carrier gas (flow rate of 1 ml min^{-1}, initial inlet pressure of 50 kPa, split at 30 ml min^{-1}). Individual aromatic hydrocarbon analytes were semi-quantitatively determined by comparison of their peak areas in their respective ion chromatograms with that of the added 1,1'-binaphthyl standard (*m/z* 253) assuming a response factor of one. Concentrations of aliphatic and aromatic hydrocarbons that were biodegraded after 40 days were calculated by averaging hydrocarbon concentrations in the two triplicate treatments (PHY and BAC) and in their respective triplicate acidified controls. Students T-tests were performed to test for significant differences ($p < 0.05$) between the live (PHY or BAC) treatments and their acidified (PHY+acid or BAC+acid) controls. Significant results were expressed as percentage degradation in PHY and BAC treatments relative to the respective acidified controls.

4.2.3 Nucleic acid extraction

On days 0, 8, 14, 24 and 40, sub-samples were taken from the PHY, BAC and CON treatments for collection of all biomass for subsequent DNA extraction as outlined in Section 4.2.1. For this, sub-samples were passed through a glass vacuum filtration system (Millipore) with 25 mm polycarbonate Isopore membrane (0.2 µm) filters. After storage at -20°C the polycarbonate membranes were placed into 1.5 ml microfuge tubes containing 200 µl extraction buffer (10 mM Tris; 1 mM EDTA; 0.5% [w/v] SDS; 50 µg ml^{-1} proteinase K). Tubes were gently vortexed and incubated for 30 min at room temperature. Polycarbonate filters were dissolved after addition of 200 µl of pH 8 equilibrated phenol:chloroform:isoamyl alcohol (25:24:1), which was left for 5 min at room temperature. Reactions were centrifuged for 5 min (13,000 *g*). Nucleic acid in

the aqueous top phase was transferred to a clean tube before TE (200 µl) was added into the original tube and centrifuged a second time to capture the remaining nucleic acid. The aqueous phases were combined and nucleic acid was precipitated by addition of 10% NaCl and 2.5× volumes of isopropanol for 30 min at -20ºC. The nucleic acid was pelleted by centrifugation (13,000 *g*), washed with 70% ethanol and then resuspended in 50 µl of TE.

4.2.4 Quantification of phytoplankton using chlorophyll-a measurements and the bacterial population using real-time PCR

The following method was included in order to monitor phytoplankton growth in the PHY and CON treatments. On days 0, 2, 5, 8, 11, 14, 23 and 40, chlorophyll-*a* (Chl-*a*) was extracted using a modified version of EPA Method 445 (Arar and Collins, 1997). Seawater (2 ml) from each conical flask was filtered through GF/C glass fiber filters (25 mm) using a glass vacuum filtration system (Millipore) before being placed into 10 ml of 90% acetone. Samples were sonicated in an ice-water bath for 10 min in the dark, then placed in a -20°C freezer for approximately 20 h before analysis. Samples were then centrifuged and allowed to equilibrate in the dark at room temperature prior to fluorometric analysis. Fluorescence of the extracted samples was measured using excitation and emission wavelengths of 485 nm and 685 nm respectively in quartz cuvettes on a Fluoromax-4 fluorometer (Horiba Scientific) with a pre-programmed Chl-*a* calibration curve (Welschmeyer, 1994).

The bacterial population was also monitored on days 0, 2, 5, 8, 11, 14, 23 and 40 by cell counting with the use of the DNA stain 4',6-diamidino-2-phenylindole (DAPI). However, due to large aggregates containing dense clusters of uncountable prokaryotes, this method produced an inaccurate total quantification. Therefore to focus on bacteria, the nucleic acid extracts from triplicate PHY, BAC and CON treatments from Section 4.2.3 were used to quantify the number bacterial 16S rRNA genes on days 0, 5, 8, 14, 23 and 40 using quantitative PCR (qPCR) with primers targeting the bacterial V3 and V5 16S rDNA regions: (341f – 5' CCT ACG GGA GGC AGC AG-3' and 518r – 5' ATT ACC GCG GCT GCT GG 3') (Muyzer *et al.*, 1993) adjusted to 4 µM. The template DNA (0.5 µl) was added in triplicate to 20 µl reactions containing forward and reverse primers (341f and 518r) (1 µl each), DMSO (0.6 µl), 5xMyTaq buffer (4 µl) (Bioline), 5U/µl MyTaq polymerase (4 µl) (Bioline), 5xSYBR Green (4 µl) (Thermo Fisher) and

nuclease-free H_2O. Each plate also contained a triplicate dilution series of *E. coli* 16S rDNA amplicons (using the same primer set) of known DNA concentration (measured with NanoDrop 3300) to provide a calibration curve. PCR was done with the following program using a StepOne (Applied Biosystems) Real-Time PCR System: initial denaturation of 20 seconds at 95°C followed by 30 cycles of denaturation at 95°C (3 s) and annealing at 58°C (20 s). A melting curve was then produced between and 58 and 95°C. The threshold cycle (Ct) for each sample was automatically determined by the instrument. The calibration curve copy number range was from $3.1 \times 10^5 – 3.1 \times 10^8$ μl^{-1} and the regression fit (R^2) was 0.998. The standard curve for quantifying bacterial 16S rDNA gene copy number is described by the following equation:

$$\text{Log}_{10} \text{ gene copy number} = [(\text{Ct value}) – 45.49)] / -4.853$$

4.2.5 Barcoded amplicon metagenomic sequencing and analysis

MiSeq 16S rRNA gene sequencing was conducted for duplicate PHY, BAC and CON treatments on days 0, 8, 14 and 40 in order to monitor bacterial community change. Almost full length 16S rRNA sequences were amplified using the 27f (5' AGA GTT TGA TCM TGG CTC AG 3') and 1492r (5' GGT TAC CTT GTT ACG ACT T 3') (Weisburg *et al.*, 1991) primers (20 µM) in 50 µl reactions containing 45 µl Supermix (IDT Invitrogen) and 1 µl of the nucleic acid extracts from Section 4.2.3. The Veriti (Applied Biosystems) 96-Well Thermal Cycler was used to perform an initial extension of 1 minute at 94°C followed by 35 PCR cycles (45 seconds at 94°C; 45 seconds at 45°C; 1 minute at 72 °C) and a final extension stage of 5 min at 72°C. PCR products were then cleaned by addition of 5 µl FastAP ($1U\ L^{-1}$) and 7.5 µl Exonuclease I ($1U\ L^{-1}$) (Life Technologies) (45 min at 37°C; 15 min at 85°C). A second round of PCR targeting the hypervariable V3 and V4 regions was performed using MiSeq forward (5' AAT GAT ACG GCG ACC ACC GAG ATC TAC AC <8-nt i5 barcode> TAT GGT AAT TGT ACW CCT RCG GGW GGC WG 3') and reverse (5' CAA GCA GAA GAC GGC ATA CGA GAT <8-nt i7 barcode> AGT CAG TCA GCC ACC AGG GTA TCT AAK CCT G 3') primers (20 µM). Primers were added to a tube containing 5 µl of cleaned PCR product, MyTaq polymerase (5 U), MyTaq reaction buffer (1x) and DMSO (1.5%) (total of 20 µl reaction). For this round an initial extension of 3 min at 95°C followed by 28 PCR cycles (15 seconds at 95°C; 15 seconds at 55°C; 1 minute at 72°C) and a final extension stage of 5 min at 72°C was performed. Once again the PCR

product was cleaned by addition of 2 µl FastAP (1U L^{-1}) and 3 µl Exonuclease I (1U L^{-1}) (45 min at 37°C; 15 min at 85°C). The expected length of the amplicon after the second round was ca. 450 mer. Samples were sequenced via the Illumina MiSeq platform at the University of Liverpool Centre for Genomic Research where a final 8 cycles of PCR were preformed with Illumina Nextera XT forward and reverse primers containing an adapter, a 2 bp linker (written in bold) and finally the 16S primer sequence (forward Primer = 5' T CGT CGG CAG CGT CAG ATG TGT ATA AGA GAC **AG** CCT ACG GGN GGC WGC AG) (reverse Primer = 5' G TCT CGT GGG CTC GGA GAT GTG TAT AAG AGA **CA** GGA CTA CHV GGG TAT CTA ATC C). Final amplicons were quality controlled using Qubit and Bioanalyzer, pooled and run on a 2 × 444 paired-end run of the MiSeq using v3 reagents (Illumina).

Raw Illumina fastq forward and reverse files were merged via Pandaseq and sequences smaller than 400 mer were trimmed using Prinseq (~80% of sequences were conserved). This produced a total of 3,140,774 raw reads. QIIME software was used to cluster the sequences into operational taxonomic units (OTUs) based on 97% sequence identity. The most abundant sequence in each OTU cluster was selected as the representative OTU sequence. Representative sequences were blasted and the GreenGenes database was used to assign taxonomy to the representative strain/OTU cluster. Data were normalised by expressing the number of sequences in each OTU cluster as a percentage of total sequences in a given treatment at a given time (i.e. percentage abundance). Chloroplast 16S rRNA sequences were deleted and percentage abundances of bacterial 16S rRNA sequences were adjusted accordingly. A heatmap was produced manually using Microsoft Excel and all included OTUs that had a relative abundance of >1% and that had also exhibited increased relative abundances in the Heidrun crude oil treatments. Representative OTUs of unknown phylogenetic classification were checked known sequences using RDP and BLASTn.

4.2.6 Phylogenetic tree

Representative 16S rRNA gene sequences of OTUs identified by MiSeq analysis that were enriched in crude oil-containing treatments (belonging to putative and recognized hydrocarbonoclastic taxa) were aligned using CLUSTAL_X programme (Thompson *et al.*, 1997). Sequences and type strains with the highest sequence similarity from GenBank were also used for tree construction. A neighbour-joining tree was

constructed with TREEVIEW (WIN32) version 1.5.2 and bootstrap replication (n=1000) (Page, 1996). The archaeal species *Methanobacterium aarhusense* (AY386124), *Methanobacterium flexile* (NR116276) and *Methanobacterium paludis* (NR133895) were used as the out-group.

4.3 Results

4.3.1 Degradation of Heidrun crude oil

The Heidrun crude oil inoculated into the conical flasks on day 0 contained 3.8% *n*-alkanes ($C_8 - C_{35}$) and 15% aromatic hydrocarbons. A GC-FID chromatogram for the Heidrun crude oil at the time of inoculation can be found in Appendix F, Figure 35. Cyclic and branched alkanes (and NSO compounds including asphaltenes) were not quantified. Ratios of *n*-alkanes to acyclic isoprenoid hydrocarbons (nC_{17}/pristane and nC_{18}/phytane) were used as convenient indicators of biological degradation, due to the recalcitrance imparted by the branched structure of the isoprenoid biomarkers (Dawson *et al.*, 2013; Papazova and Pavlova, 1999; Sauer and Boehm, 1991). Similarly for aromatic hydrocarbon analysis live treatments (BAC or PHY) were compared to their acid-inhibited controls for 7 parameters/ratios indicative of biodegradation (naphthalene/2-methylnaphthalene; 2-methylnaphthalene/1-methylnaphthalene; 2-ethylnaphthalene/2,6+2,7-dimethylnaphthalene; 2-methylnaphthalene/2,6+2,7-dimethylnaphthalene; phenanthrene/9-methylphenanthrene; 3+2-methylphenanthrene/9+1-methylphenanthrene; 3-methylphenanthrene/9-methylphenanthrene). Students T-tests ($\alpha = 0.05$) confirmed that there were significant differences between control and PHY treatments for 5 of the parameters listed above (Figure 12), specifically reductions in both nC_{17} and nC_{18} aliphatic hydrocarbons and reductions in 2-methylnaphthalene and phenanthrene. In comparison BAC treatments displayed significant reductions compared to their controls in just a single parameter indicative of biodegradation (i.e. 2-methylnaphthalene/2,6+2,7-dimethylnaphthalene [2MN/26+27DMN]) (Figure 12). These results suggested that biodegradation had occurred to a greater extent in the PHY (with phytoplankton) than in BAC (without phytoplankton) treatments for both aliphatic and aromatic hydrocarbons.

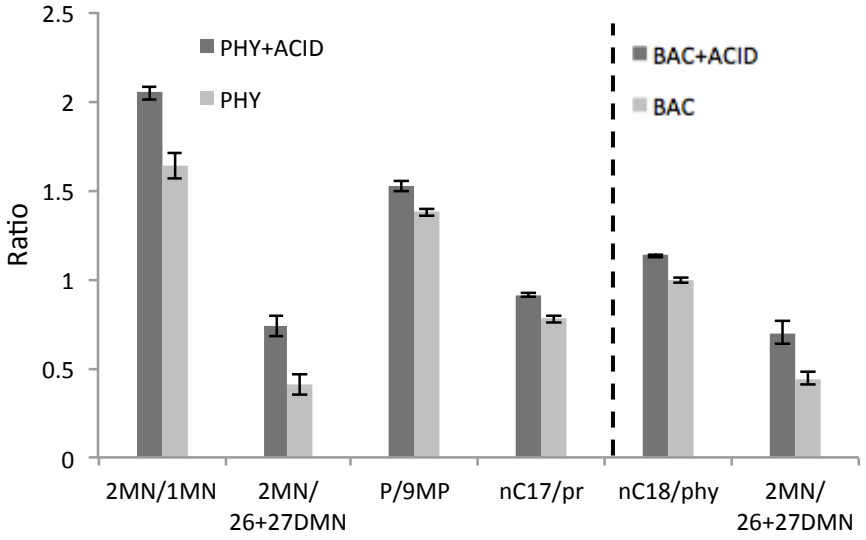

Figure 12. Differences in hydrocarbon ratios (significant results only, Students T-test, $\alpha = 0.05$) comparing live treatments (BAC or PHY) to their acidified controls for five characteristic parameters indicative of biodegradation: 2-methylnaphthalene/1-methylnaphthalene (2MN/1MN), 2-methylnaphthalene/(2,6+2,7)-dimethylnaphthalene (2MN/26+27DMN), phenanthrene/9-methylphenanthrene (P/9MP), nC$_{17}$/pristane (nC$_{17}$/pr), nC$_{18}$/phytane (nC$_{18}$/phy). Values are averages of the triplicate treatments. Error bars show standard error. The dashed line shows the division between PHY and BAC treatments.

To further investigate this effect of increased hydrocarbon degradation in the phytoplankton (PHY) treatments, the live treatments (BAC or PHY) were compared to their acid-inhibited controls (using Students T-tests, $\alpha = 0.05$) for concentrations of a total of 28 *n*-alkanes (nC$_8$-nC$_{35}$), 12 naphthalenes (C$_0$-C$_3$ alkylnaphthalenes, *m/z* 128, 142, 156, 170), 17 phenanthrenes (C$_0$-C$_3$ alkylphenanthrenes, *m/z* 178, 192, 206, 220), 14 dibenzothiophenes (C$_0$-C$_2$ alkyldibenzothiophenes, *m/z* 184, 198, 212), 12 monoaromatic steroids (*m/z* 253) and 9 triaromatic steroids (*m/z* 231). Phytoplankton treatments (PHY) exhibited significant degradation in relation to its acidified control for 9 alkanes nC$_{20}$ – nC$_{31}$ although strangely not including nC$_{29}$ – nC$_{30}$ (Table 3). Bacterial treatments without phytoplankton (BAC) exhibited significant degradation of 8 alkanes nC$_{16}$ – nC$_{24}$ although not including nC$_{18}$. For alkanes significantly degraded in both treatments the extent of degradation (mean percentage values) were consistently greater in PHY treatments compared to BAC treatments (Table 3). These results suggest an enhanced ability of phytoplankton-associated microorganisms (likely bacteria) in degrading longer chain alkanes and indicate a preference for shorter chain alkane by the

free-living bacterial fraction. Similarly, aromatic hydrocarbon analysis revealed more extensive degradation in the PHY treatments. Table 3 highlights 16 PAH compounds that were significantly degraded in the PHY treatments compared to 13 in the BAC treatment. Biodegradation by the free-living bacterial population displayed a preference for the LMW-PAHs (i.e. naphthalenes), while the phytoplankton-associated bacteria also exhibited significant degradation in 4 phenanthrenes, 3 dibenzothiophenes, 1 monoaromatic steroid and 2 triaromatic steroids. Once again, where PAHs were degraded in both PHY and BAC treatments, the extent of degradation (mean % values) was consistently greater in PHY treatments. The alkanes nC$_8$, nC$_9$ and nC$_{10}$ were likely to have been completely evaporated or biodegraded as these hydrocarbons were not detected in any of the live or acid-inhibited treatments, but were present in the reference oil.

Table 3. Aliphatic and aromatic hydrocarbon biodegradation during enrichment of the phytoplankton (PHY) and free-living bacterial (BAC) treatments with Heidrun crude oil. Values are expressed as average (Avg) percentage (%) reduction after 40 days relative to acidified controls ± standard error (SE).

Hydrocarbon group	**Avg % (±SE) of biodegradation in treatment[a]**	
	PHY	**BAC**
***Aliphatics**:*		
C$_{16}$		14.9 ± 3.9
C$_{17}$		11.5 ± 2.0
C$_{19}$		8.9 ± 1.7
C$_{20}$	11.3 ± 2.0	10.8 ± 1.1
C$_{21}$	10.8 ± 1.6	8.4 ± 2.4
C$_{22}$	9.9 ± 1.9	5.6 ± 1.5
C$_{23}$	9.5 ± 1.7	6.4 ± 1.5
C$_{24}$	7.0 ± 1.7	4.9 ± 1.9
C$_{25}$	6.0 ± 2.5	
C$_{27}$	5.9 ± 1.6	
C$_{28}$	10.3 ± 2.6	
C$_{31}$	17.1 ± 4.0	
Aromatics:		
2-methylnaphthalene	61.6 ± 6.8	45.3 ± 3.3
1-methylnaphthalene	52.4 ± 6.6	35.0 ± 10.3
2-ethylnaphthalene	35.7 ± 6.5	26.4 ± 5.2

1-ethylnaphthalene	32.3 ± 3.5	19.9 ± 5.9
(2,6+2,7)-dimethylnaphthalene	30.7 ± 2.2	13.7 ± 1.4
(1,3+1,7)-dimethylnaphthalene		15.7 ± 3.3
1,6-dimethylnaphthalene		13.2 ± 2.4
(1,4+2,3)-dimethylnaphthalene		14.9 ± 0.9
1,2-dimethylnaphthalene	25.4 ± 2.2	16.3 ± 3.8
phenanthrene	17.5 ± 1.9	8.2 ± 1.0
3-methylphenanthrene		9.1 ± 1.8
2-methylphenanthrene	14.5 ± 3.1	
9-methylphenanthrene	9.0 ± 1.0	
1-methylphenanthrene	9.8 ± 1.19	
(unconfirmed)-phenanthrene		29.8 ± 5.8
dibenzothiophene	23.2 ± 3.7	
4-methyldibenzothiophene	7.9 ± 1.3	
4-ethyldibenzothiophene	10.9 ± 1.2	
$C_{27}\beta$ monoaromatic steroid		8.1 ± 2.1
$C_{29}\alpha$ monoaromatic steroid	14.7 ± 3.1	
C_{28}S-triaromatic steroid	10.3 ± 1.3	
(unconfirmed)-triaromatic steroid	16.0 ± 5.2	

[a] Values are the average (Avg) from triplicate measurements.

4.3.2 Phytoplankton and bacterial community dynamics

The assemblage of phytoplankton was typical for spring-summer with the diatoms *Thalassiosira, Chaetoceros* and *Skeletonema* dominating. A full list of phytoplankton species present is shown in Table 4. Diatoms dominated the 'high' (≥1000 cells ml^{-1}), 'moderate' (20 – 999 cells ml^{-1}) and 'low' (<20 cells ml^{-1}) abundance groups, whilst there were also some species of dinoflagellates also in 'low' abundance. Also present in the Loch Creran seawater sample were indeterminate micro-flagellates (moderate abundance), indeterminate ciliate micro-zooplankton (moderate), indeterminate amoeba (low) and the silicoflagellate *Dictyocha speculum* (low).

Table 4. Abundance of eukaryotic phytoplankton taxa morphologically identified at high (≥1000 cells ml^{-1}), moderate (20 – 999 cells ml^{-1}) or low (<20 cells ml^{-1}) abundance at Loch Creran in May 2013 by Malcolm Baptie at SEPA.

Taxon	Group	Abundance
Chaetoceros spp. (subgenus *Hyalochaete*)	diatom	high
Skeletonema spp.	diatom	high
Thalassiosira cf nordenskioeldii or *aestivalis*	diatom	high
Thalassiosira spp.	diatom	high
Chaetoceros curvisetus	diatom	moderate
Chaetoceros laciniosus	diatom	moderate
Chaetoceros decipiens	diatom	moderate
Thalassiosira cf *rotula* or *gravida*	diatom	moderate
Asterionellopsis glacialis	diatom	low
Cerataulina pelagica	diatom	low
Ceratulus turgidus	diatom	low
Ceratoneis closterium	diatom	low
Nitzschia longissima	diatom	low
Chaetoceros affinis	diatom	low
Chaetoceros didymus	diatom	low
Chaetoceros protuberans	diatom	low
Ditylum brightwellii	diatom	low
Guinardia delicatula	diatom	low
Gyrosigma spp.	diatom	low
Leptocylindrus danicus	diatom	low
Licmophora spp.	diatom	low
Pleurosigma spp.	diatom	low
Pseudonitzschia delicatissima	diatom	low
Pseudonitzschia seriata	diatom	low
Thalassiosira punctigera	diatom	low
Diplopsalis group	dinoflagellate	low
Indeterminate armoured dinoflagellate	dinoflagellate	low
Indeterminate naked dinoflagellate	dinoflagellate	low
Prorocentrum lima	dinoflagellate	low
Prorocentrum micans	dinoflagellate	low
Protoperdinium spp.	dinoflagellate	low
Protoperidinium thorianum	dinoflagellate	low
Scrippsiella spp.	dinoflagellate	low

Visual inspection of the PHY treatment revealed the phytoplankton cells to be bleached by day 7 with noticeably more flocculent off-white organic material developing as the experiment progressed, when compared with the BAC treatment. From an initial concentration of 8.5 ± 0.5 μg l^{-1} at day 0 in the PHY treatment, chlorophyll-*a* concentrations had decreased to below 0.7 ± 0.2 μg l^{-1} by day 14 (1-way ANOVA with Tukey's *post hoc* test, $p < 0.001$) and did not thereafter increase, which suggests that the Heidrun crude oil has a toxic effect on the micro-algae (Figure 13). On the other hand the CON treatments showed an increase in chlorophyll-*a* concentration from day 2 until day 8 reaching a maximum of 54.0 ± 3.7 μg l^{-1}, after which point chlorophyll-*a* concentration started to decline until returning to day 0 levels on day 24 which peristed until day 40 (1-way ANOVA with Tukey's *post hoc* test, $p < 0.001$).

As explained in Section 4.2.4, accurate bacterial DAPI cell counts were impossible to obtain due to the aggregations of bacterial cells (Figure 14A). Shown in Figure 13 are the bacterial 16S rRNA gene abundance dynamics (used as a surrogate for bacterial biomass) in all three treatments (PHY, BAC and CON) over the course of 40 days. There were no significant changes in $\log_{10}$ gene number in the PHY treatments over the course of the experiment. Results of Student's *t* tests comparing day 5 $\log_{10}$ gene numbers with day 8 confirmed that there was no increase in gene numbers in this time period for any of the treatments PHY, BAC or CON (a time period coinciding with the chlorophyll-*a* increase in the CON treatments). The significant differences in gene number were between day 0 and day 40 in BAC ($p < 0.01$) and CON ($p < 0.01$), which showed decreases in gene number not uncovered in the PHY treatment. In the control treatments without oil (CON) this decline was most likely due to grazing from nano- (2 – 20 μm) or micro- (20 – 200 μm) zooplankton/protozoa (Figure 14B) (Frost, 1987). Protist grazing by may also explain the rapid decline in chlorophyll-*a* concentration in the CON treatments after day 8.

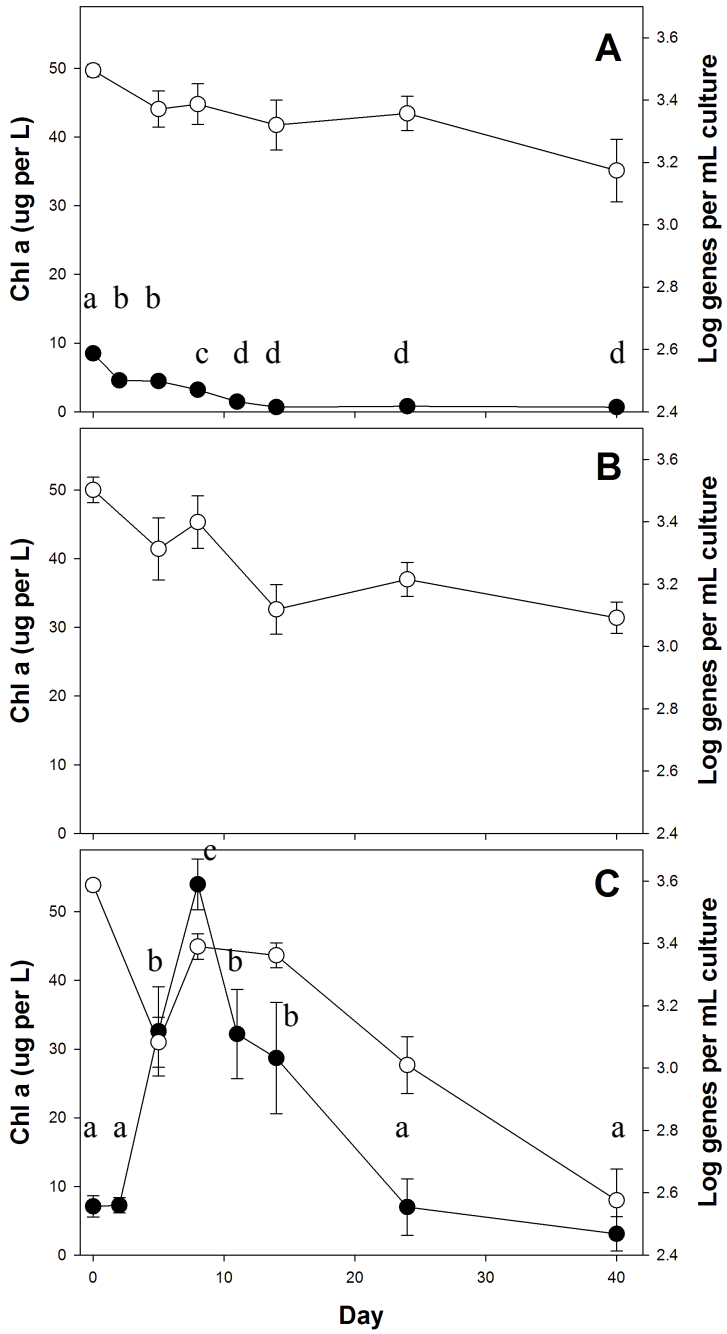

Figure 13. Chlorophyll-*a* concentrations (left-hand y-axis and solid circles) and bacterial 16S rRNA gene concentrations (right-hand axis and open circles) in PHY (A), BAC (B) and CON (C) treatments. Each point represents the mean and standard deviation (error bars) of triplicate Chl-*a* or qPCR measurements. Chlorophyll-*a* was not detected in the BAC treatments. Lower case letters show the results of Tukey's *post hoc* test on chorophyll-*a* concentrations (solid circles): a treatment sharing the same letter with another treatment denotes the treatments were not significantly different from each another.

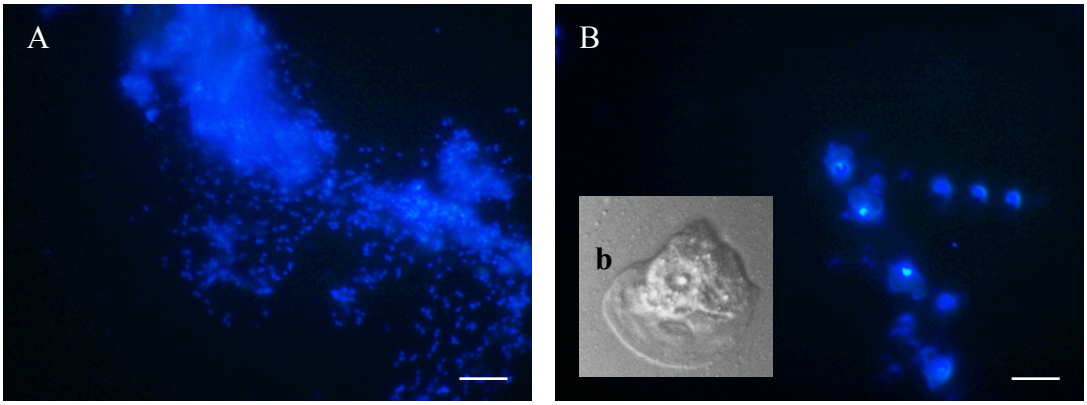

Figure 14. Epifluorescence micrographs of a DAPI stained aggregation of bacteria in a PHY treatment on day 14 (A) and DAPI stained cell nuclei of 8 *Vannella*-like species in a CON treatment day 8 (B); inset (b) shows an example of *Vannella* (*Gymnamoeba*) from Anderson and Rogerson, (1995). White scale bar = 20 μm.

4.3.3 Bacterial community analysis

Metagenomic abundance data were collected from duplicate treatments and were therefore not checked for statistical significance against the qPCR bacterial abundance data from the previous section. Taxonomic assignments of OTUs (on days 0, 8, 14, 24 and 40) using the Greengenes database revealed that free-living (BAC) and phytoplankton-associated (CON and PHY) bacterial communities were dominated by members of class *Gammaproteobacteria*. The order *Vibrionales* (families *Pseudoalteromonadaceae* and *Vibrionaceae*), comprised ca. 80% of total 16S rRNA gene sequence reads in each library on day 0 (Figure 15). The genus *Pseudoalteromonas* was almost the sole contributor to its family's abundance. Also present on day 0 in all treatments were the *Piscirickettsiaceae*, *Vibrionales*, *Oceanospirillales*, *Psychromonadaceae*, *Colwelliaceae, Alteromonadaceae*, including other members of the order *Alteromonadales*. Finally *Rhodobacterales* (<4%) and *Flavobacteriales* (<4%) were present on day 0. On day 8, the *Pseudoalteromonadaceae* and *Vibrionaceae* had declined dramatically in all three treatments, but most notably in the CON treatment. The abundance of these two families continued to decline to less than 1% by day 40 in all treatments.

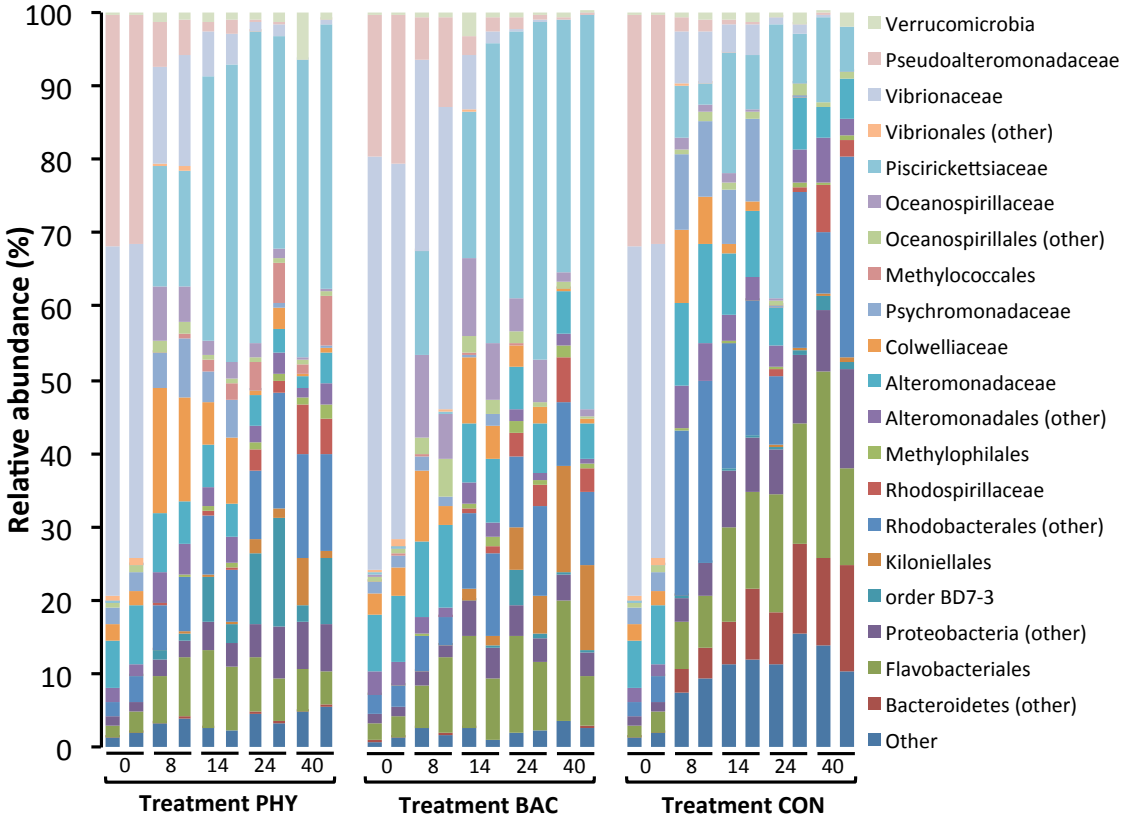

Figure 15. Relative abundances of bacteria taxa (≥1%) in duplicate the phytoplankton treatments with crude oil (PHY), the free-living bacterial treatments with crude oil (BAC) and the control treatments containing phytoplankton without crude oil (CON) on days 0, 8, 14, 24 and 40. Taxonomy was assigned by comparing the 16S rRNA gene MiSeq reads to the Greengenes 16S rRNA database (DeSantis *et al.*, 2006). Sequences were classified to family-level taxonomy when possible and otherwise a higher-level classification is shown.

From day 8 onwards members of the *Piscirickettsiaceae* displayed the most dramatic increase in abundance, which was delayed in just one of the BAC replicates (although also reaching the highest maximum abundance of over 50% on day 40 in one of the BAC replicates). The *Colwelliaceae* exhibited the largest increase in the PHY treatments from day 0 to day 8 (from ~2 – 15%). The most pronounced increase on day 8 for the *Rhodobacterales* was in the CON treatments comprising over 20% of gene sequence reads, which persisted until day 40. This group was also present in PHY and BAC treatments. Similarly, the *Flavobacteriales* were constant members of the community, as were also the *Alteromonadaceae*. The *Oceanospirillaaceae* and other members of the order *Oceanospirillales* showed an increase in abundance on days 8

through 24 in both of the oil amended treatments (PHY and BAC) compared with the control (CON). The *Kiloniellales* displayed highest abundance in the BAC treatments on day 40. By day 40 the *Piskirickettsiaceae* dominated the bacterial communities in both crude oil treatments (PHY and BAC). Notably, an increase in abundance of order BD7-3 (days 8 – 40) appeared to be limited to PHY treatments, except for a single BAC replicate on day 24.

A total of 20 OTUs were identified as enriched by the presence of Heidrun crude oil, which are shown in Figure 16. In the BAC treatments, *Methylophaga* (OTU-9) was the most abundant organisms reaching as high as 53% abundance, whereas in PHY treatments other unclassified members of the *Piskirickettsiacea* (OTU-8) accompanied *Methylophaga*. Phytoplankton presence in crude oil treatments (PHY) was shown to induce patterns of bacterial enrichment not found in the BAC and CON treatments: firstly, members of the genus *Cycloclasticus* (OTU-6) were only found in PHY treatments; secondly the genus *Verrucomicrobium* (OTU-20) was a late enrichment unique to a single PHY replicate; thirdly, *Alcanivorax* (OTU-12) was slightly enriched on day 8 and, as mentioned above, the order BD7-3 (OTU-1) was considerably more pronounced in the PHY treatments (Figure 16). Unique to a single BAC replicate was an enrichment of *Halomonas* (OTU-13). Both oil-amended treatments (BAC and PHY), however, included enrichments of *Thalassospira* (OTU-4), *Oleispira* (OTU-10), *Marinomonas* (OTU-11), *Olleya* (OTU-17), *Winogradskyella* (OTU-18), and *Methylotenera* (OTU-19) when compared to the CON treatment with no oil. *Shewanella* (OTU-14) were present in both crude oil treatments but were also enriched in the CON treatments, as were *Hyphomonadaceae* (OTU-2)*, Rhodobacteraceae* (OTU-3), *Phaeobacter* (OTU-5), *Colwelliaceae* (OTU-7), *Psychromonas* (OTU-15) and *Flavobacteriaceae* (OTU-16). The 16S rRNA gene sequence reads of the above twenty OTUs were compared with related GenBank sequences, including sequences belonging to related HCB (Figure 17).

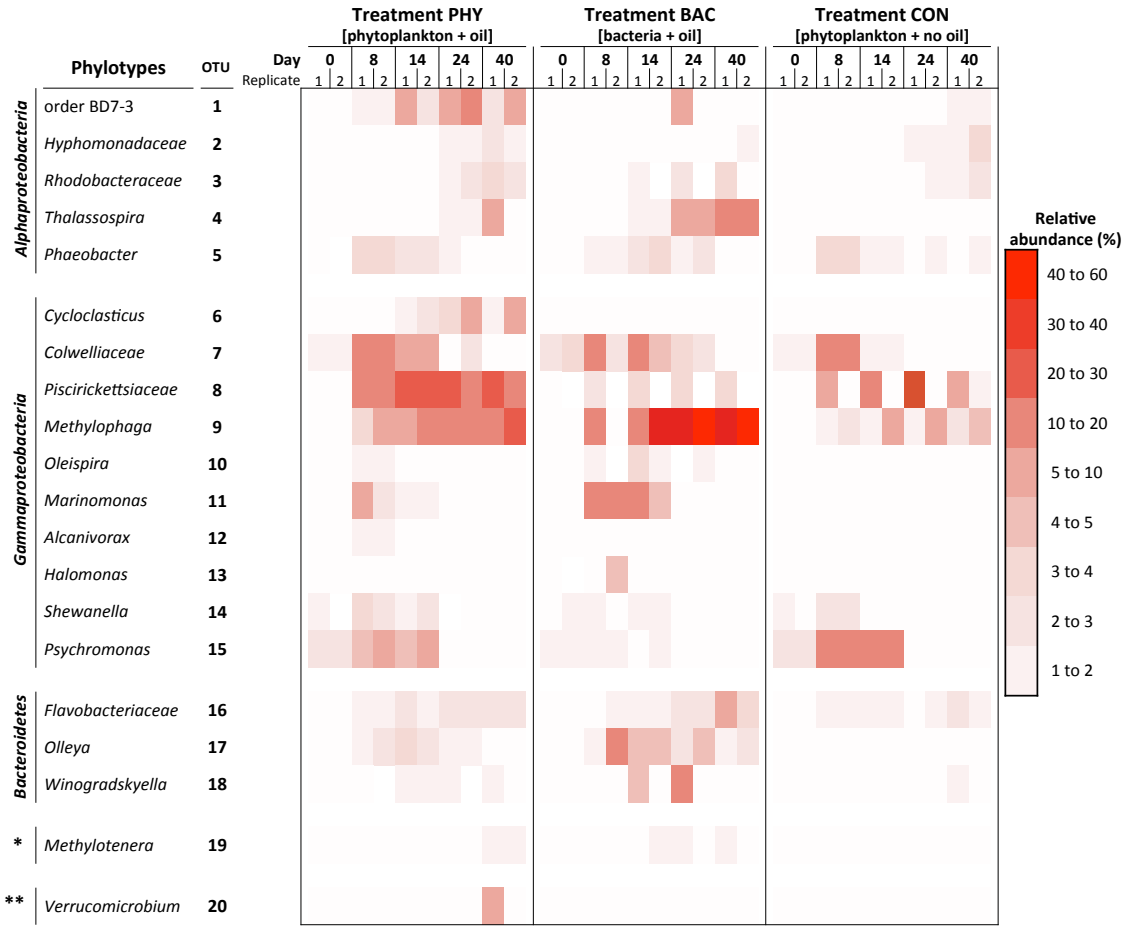

Figure 16. Heatmap of all OTUs enriched in PHY or BAC treatments by at least 1% relative abundance compared to a previous time point for at least one of the duplicate incubations. Colour key indicates relative abundance (%). Prefix PHY = phytoplankton incubation with oil, BAC = free-living bacterial incubation with oil, CON = phytoplankton incubation without crude oil. (* - *Betaproteobacteria*, ** - *Verrucomicrobia*).

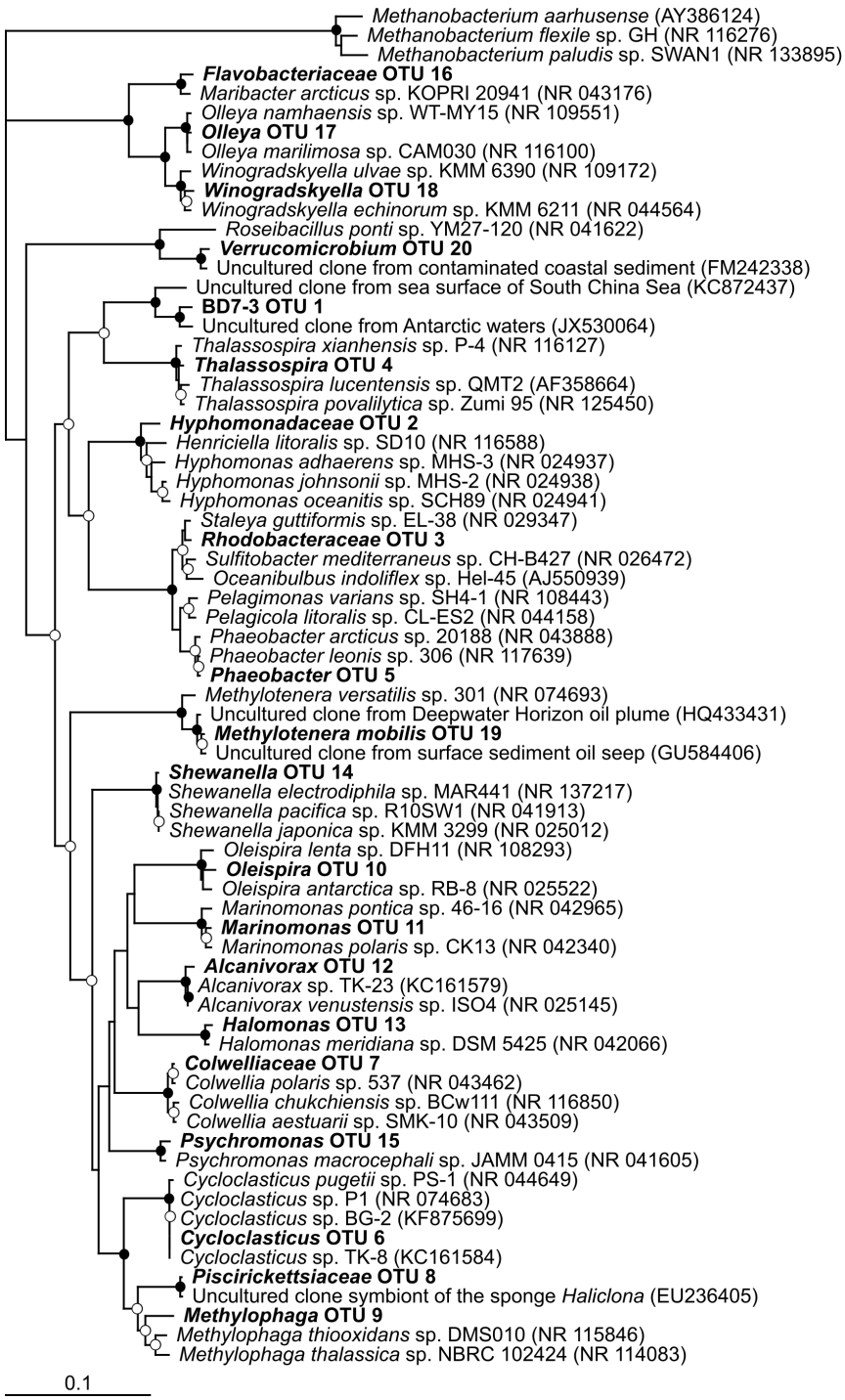

Figure 17. Neighbour-joining phylogenetic tree based on 16S rRNA gene sequences (>1,200 bp), showing the 20 OTUs enriched (in bold) in the Heidrun crude oil-amended incubations alongside representatives of related taxa. Filled circles indicate nodes with bootstrap values (1,000 bootstrap replications) greater than 90%; open circles indicate bootstrap values greater than 60%. GenBank accession numbers are shown in parentheses. The scale bar indicates the number of substitutions per site.

4.4 Discussion

The diatom community (dominated by *Thalassiosira, Chaetoceros* and *Skeletonema*) was typical of the euphotic zone in Loch Creran during late Spring (Lappalainen and Tett, 2014). The Heidrun crude oil had a severe impact on the phytoplankton from Loch Creran, which was shown by the significant decrease in chlorophyll-*a* concentrations in the PHY treatments. In the CON treatments chlorophyll-*a* concentrations increased, which showed that cultures were not nutrient-limited. The diatom-dominated Loch Creran sample could not tolerate the Heidrun crude oil, and chlorophyll-*a* concentrations became gradually lower until day 14. As in the mesocosm study of Brussaard *et al.*, (2016), a decrease in chlorophyll-*a* concentration of ~50% was detected in oil incubations after just 2 days. Brussaard *et al.*, (2016) found that the disappearance of chlorophyll-*a* was down to a decrease in eukaryotic phytoplankton. Crude oil toxicity mechanisms in phytoplankton include not just detrimental effects to cell membranes, as mentioned above, but also disruption to photosystem II and electron transfer and silica frustule absorption (Aksmann and Tukaj, 2008; Gilde and Pinckney, 2012; Özhan *et al.*, 2014; Sikkema *et al.*, 1995). Crude oil concentrations as low as 1 mg L^{-1} (roughly one part per million [ppm]) can induce algal toxicity in phytoplankton (Özhan *et al.*, 2014, and references therein). Heidrun crude oil was used at a concentration of 0.142% (v/v) in this study. Mono- and poly-aromatics are considered the main toxic components in crude oil (Boehm *et al.*, 2007; Boehm and Page, 2007; Brussaard *et al.*, 2016). In Chapter 2, *T. pseudonana* was resistant to phenanthrene but much more susceptible to naphthalene toxicity. Analysis of Heidrun crude oil shows it to consist of ~15% aromatics, but more specifically ~10.5% naphthalenes. Therefore, upon incubation (day 0) the phytoplankton would have experienced ca.142 ppm naphthalenes. These compounds likely contributed greatly to the phytoplankton toxicity witnessed in PHY treatments.

The death of phytoplankton was also witnessed by looking at the bleached PHY conical flasks, which was accompanied by a build up of off-white flocculent material also known as marine oil snow (MOS) (Mishamandani *et al.*, 2016). The diatom-dominated PHY treatment produced visibly more MOS than the BAC treatment. Passow *et al.* (2012) has previously demonstrated diatom MOS contribution and there is also evidence provided for this in Chapter 2. According to van Eenennaam *et al.* (2016), the diatom *Phaeodactylum tricornutum* can produce EPS within days, which was the case in the Loch Creran sample as by day 14 there was very little chlorophyll-*a* measured in

the seawater and thus little CO_2 fixation. However, bacteria associated with phytoplankton also make a contribution to the MOS formation (van Eenennaam *et al.*, 2016). There were noticeable clusters of MOS to a lesser extent in the BAC treatments. Members of bacterial groups *Alteromonas, Halomonas, Colwellia* and *Pseudoalteromonas* are known EPS producers (Gutierrez *et al.*, 2013a; Gutierrez *et al.*, 2008). *Halomonas* (OTU-13) was enriched in the BAC treatment alone while the *Colwelliaceae* (OTU-7) and the *Pseudoalteromonadaceae* possibly contributed to MOS formation in both PHY and BAC treatments. Sikkema *et al.* (1995) mentions the reduction of toxic effects in bacteria by immobilization on adsorbent surfaces. The MOS may act as a surface in this respect, limiting damage to bacterial cell membranes and allowing hydrocarbon degradation to progress. Increased MOS production in PHY treatments might therefore be a factor enhancing petroleum hydrocarbon degradation.

The bacterial community in the PHY crude oil incubations did not significantly decrease over time. On the other hand the BAC (with oil) and CON (phytoplankton with no oil) treatments did exhibit significant reductions in the bacterial community between day 0 and day 40. These reductions are likely to be due to different factors; for example, due to the extraction of phytoplankton in the BAC treatment the PHY would have had added nitrogen and phosphorus (not measured) possibly resulting from micro-algal lysis. Also MOS production was different in these two treatments, possibly impacting bacterial resistance to oil. Competition between bacterial species and variations in intermediate products (also not measured) are other factors that may have contributed to the different bacterial community dynamics that were detected. In the CON treatment protists may have also reduced bacterial numbers (see the end of this discussion). The large decreases of relative abundances of *Pseudoalteromonadaceae* and *Vibrionaceae* from days 0 – 8 (significance not determined due to limited replication) may demonstrate the susceptibility of these groups to hydrocarbons, although these groups decreased in CON treatments alike. Mechanisms of toxicity of hydrocarbons include accumulation in the lipid bilayer, membrane structure alteration, subsequent loss of proton motive force and impairment of homeostasis and membrane protein function (Sikkema *et al.*, 1995). Additionally (although not measured in this study), as was investigated in Chapter 2, the production of reactive oxygen species/intermediate metabolites (e.g. quinones) during the breakdown of hydrocarbons can produce compounds that are genotoxic (Kanaly and Harayama, 2000; Hu *et al.*, 2012; Zielinska-Park *et al.*, 2004). Sikkema *et al.* (1995) highlight the adaptability of

bacterial membrane phospholipid composition and its role in changing the partition coefficients of hydrocarbons, possibly leading to resistance. The maintenance of bacterial gene numbers in the PHY treatment alone might be explained by alteration of cellular membrane composition, resistance of hydrocarbon tolerant bacterial strains or growth of hydrocarbonoclastic bacteria. Increases in relative abundance of the bacterial groups *Piscirickettsiaceae*, *Colwelliaceae*, *Oceanospirillales*, *Rhodobacterales* and *Alteromonadales* were detected in both of the crude oil treatments (PHY and BAC). These detected enrichments have been found previously in crude oil enrichment experiments in the marine systems: *Oceanospirillales, Piscirickettsiaceae* and *Colwelliaceae* have been detected in numerous studies (Mishamandani *et al.*, 2016; Wang *et al.*, 2016a; Yang *et al.*, 2016). For examples, Brakstad *et al.* (2015) detected *Rhodobacterales*, and Wang *et al.* (2016a) detected *Alteromonadales* in response to crude oil.

Hydrocarbon degradation was enhanced in the PHY treatments. Degradation in BAC and PHY treatments was calculated by comparing hydrocarbon compound concentrations to those in acid-inhibited BAC and PHY controls spiked with equal amounts of crude oil. This method was instead of comparison with the reference Heidrun crude oil at the time of incubation to ensure that the acid-inhibited controls were realistic surrogates (with regards to biological sample matrix) of the PHY and BAC treatments, as the sample matrix can influence oil recovery efficiency. A spike-recovery test (Andreasson *et al.*, 2015) was not conducted in this study. From the 28 *n*-alkanes and 64 aromatic compounds that were analysed, only eight aliphatic and 13 aromatic hydrocarbons were significantly degraded in BAC treatments, and in the PHY treatment nine aliphatic and 16 aromatic compounds were degraded. The mean percentage degradation values were consistently higher in the PHY versus the BAC treatments. Furthermore, both the nC_{17}/pristane and the nC_{18}/phytane ratios were lower in the PHY relative to acid inhibited controls, along with 2-methylnaphthalene/1-methylnaphthalene, 2-methylnaphthalene/(2,6+2,7)-dimethylnaphthalene and phenanthrene/9-methylphenanthrene (P/9MP) ratios, whereas only the 2-methylnaphthalene/(2,6+2,7)-dimethylnaphthalene ratio was lower in the BAC treatments. This enhanced degradation highlights the importance of the micro-algal-attached bacterial communities in the decontamination of petroleum in the marine environment. There was an apparent biodegradation preference (presumably attributed to hydrocarbonoclastic bacteria) in PHY and BAC treatments for the lower molecular

weight PAHs (displaying higher mean % degradation values), specifically methyl- and ethyl-naphthalenes. As mentioned before, these are the compounds with high acute toxicity to phytoplankton (Yamada *et al.*, 2003) although their degradation may produce toxic mono-aromatic derivatives, which may have increased toxic effects on phytoplankton mentioned above. Naphthalene concentrations were very low in acid-inhibited controls (due to volatilization), resulting in no significant differences between live and acid inhibited treatment naphthalene degradation. BAC treatments displayed significant degradation of shorter chain alkanes and lower molecular weight aromatic molecules. The free-living bacterial fraction in the BAC treatments may be pre-adapted to degrading LMW hydrocarbons due to their comparatively increased aqueous solubility (Vandermeer and Daugulis, 2007), while HMW may partition onto aggregates or cells where they may be degraded by aggregate-associated bacteria (e.g. in the PHY treatments). Triaromatic steroids were significantly degraded in the PHY treatments, which is a strange result as these molecules are recalcitrant to biodegradation (Radović *et al.*, 2014). Although triaromatic steroid depletion has been detected before in the laboratory and in the field (Barakat *et al.*, 2002; Díez *et al.*, 2005; Radović *et al.*, 2014) these cholestane-derivatives usually become depleted after extensive degradation of oil, and in the Heidrun crude oil sample there were still LMW-PAH present after 40 days. It may be possible that hydrocarbonoclastic bacteria present associated with phytoplankton are pre-adaptated for steroid-degradation due to broad specificity enzymes targeting cholesterols, which are found in the cell membranes of marine diatoms (Ponomarenko *et al.*, 2004), although this is as of yet unknown. The irradiance (although low intensity of ~100 μmol m^{-2} s^{-1}) provided in this experiment may have enhanced triaromatic steroid biodegradation by photo-oxidation (Charrié-Duhaut *et al.*, 2000; Radović *et al.*, 2014).

Although the results show incomplete Heidrun crude oil degradation in both PHY and BAC treatments, the improved PHY treatment degradation is likely to be partially due to the enriched bacterial OTUs in the PHY treatment (with phytoplankton) that were not enriched in the BAC treatment (phytoplankton removed). Firstly, *Cycloclasticus* (OTU-6), a genus well known for its almost exclusive preference for utilising PAHs as a sole source of carbon and energy, had a sequence match of 100% with the strain *Cycloclasticus zancles* 7-ME, which was isolated from sediment from the MT Haven oil tanker shipwreck (Cui *et al.*, 2014; Louvado *et al.*, 2015; Valentine *et al.*, 2010). This may explain the enhanced PAH degradation in the PHY treatments. Also strong

enrichment in the order BD7-3 (OTU-1) and the weaker enrichment (in just one replicate) designated *Verrucomicrobium* (OTU-20) using GreenGenes both had closest sequence matches of just 88%. These two taxa have never been enriched in hydrocarbon degradation studies before, however they may belong to unknown taxa as it is not possible to infer phylogeny based on 88% 16S RNA sequence identity. Finally, *Alcanivorax* is well known oil-degrading genus that has also been found associated with toxin-producing dinoflagellates (Kostka *et al.*, 2011; Harayama *et al.*, 1999; Green *et al.*, 2004). *Alcanivorax* (OTU-12) shared a sequence identity of 97% with *Alcanivorax dieselolei* B5, a strain isolated from oil contaminated surface waters, which can utilize C5 – C36 alkanes as sole carbon sources (Lai *et al.*, 2012).

Unique to a single BAC replicate was an enrichment of *Halomonas* (OTU-13), a group that has been isolated from oil contaminated marine environments (Gutierrez *et al.*, 2013a; Hazen *et al.*, 2010; Melcher *et al.*, 2002; Zhao *et al.*, 2009). Interestingly, both the PHY and BAC treatments contained OTUs that were not enriched in the control (CON) treatments. For example, *Marinomonas* are a group of putative hydrocarbon degraders (Dong *et al.*, 2015; Melcher *et al.*, 2002) and OTU-11 (*Marinomonas*) had highest sequence identity of 98% indicating this may be a novel strain. *Thalassospira* (OTU-4) (maximum sequence identity of 99%) were enriched to the greatest extent in the BAC treatments, but only in one of the PHY replicates on the day 40. Members of this genus are known to degrade a range of PAHs present in crude oil (e.g. pyrene, naphthalene and phenenathrene) and also diesel oil (Kodama *et al.*, 2008; Liu *et al.*, 2007; Zhao *et al.*, 2010). *Oleispira* have been detected previously in oil contaminated environments (Wang *et al.*, 2016a), and it is a genus that includes obligate hydrocarbonoslastic bacteria, some of which are psychrophilic (Gentile *et al.*, 2016; Hazen *et al.*, 2010; Yakimov *et al.*, 2004a). *Oleispira* (OTU-10) had a 99% sequence identity match with *Oleispira antarctica* strain RB-8 isolated from crude oil enrichments (Yakimov *et al.*, 2003). This is a surprising result as the incubation temperature of this study was 15 ºC whereas this genus is usually found at colder temperatures. *Olleya* have been found previously in oil degradation studies (Isaac *et al.*, 2013; Okai *et al.*, 2015;). Some members of the *Flavobacteriaceae* can degrade hydrocarbons or possibly intermediates resulting from petroleum hydrocarbon degradation so this also cannot be ruled out for *Olleya* (OTU-17) (maximum sequence identity of 99%) (Gertler *et al.*, 2012; Gutierrez *et al.*, 2014). *Methylotenera* have been found in crude oil contaminated environments before (Gründger *et al.*, 2015).

Methylotenera (OTU-19) had a sequence identity of just 96% with *Methylotenera mobilis*, a utilizer of simple amines, and may possibly utilize products produced by hydrocarbonoclastic bacteria although this is unknown (Kalyuzhnaya *et al.*, 2006).

Previously *Methylophaga* have become enriched briefly by crude oil enrichment of a *Skeletonema costatum* laboratory culture (Mishamandani *et al.*, 2016), and in the present study in Loch Creran this genus was enriched also, however much later and becoming more abundant as the experiment progressed. In the BAC treatments, *Methylophaga* (OTU-9) was the most abundant OTU reaching as high as 53% abundance in one replicate. Additionally to OTU-9, PHY treatments also had more pronounced enrichments of unclassified members of the *Piscirickettsiacea* (OTU-8). It should be noted that OTUs 8 and 9 were also both enriched to a lesser extent in the control incubations without Heidrun crude oil (CON), highlighting the dietary versatility in carbon source utilization of these two groups. The *Piscirickettsiacea* (OTU-8) and *Methylophaga* (OTU-9) had maximum sequence identities of 93% and 97% respectively with *Methylophaga thiooxydans* strain DMS010^{T}, although OTU-8 had the same identity with *Cycloclasticus zancles* (Boden *et al.*, 2010). The *Methylophaga* genus is a genus known for its C_1 compound utilization although recently it has been implicated in hydrocarbon degradation (Janvier and Grimont, 1995; Mishamandani *et al.*, 2014; Mishamandani *et al.*, 2016).

The occurrence of OTUs that were enriched in all three (PHY, BAC and CON) treatments does not rule these OTUs out of Heidrun crude oil utilization in the PHY and BAC treatments. A member of the *Shewanella* genus (*Shewanella* sp. GA-22,) is a psychrophilic hydrocarbonoclastic bacterium (Gentile *et al.*, 2003). OTU-14 (*Shewanella*) had a closest sequence match of 98% with *Shewanella* sp. Strain P1-14-1 (Rischer *et al.*, 2016). Members of the *Colwelliaceae* are putative oil degraders (Hazen *et al.*, 2010; Yakimov *et al.*, 2004a). The presence of *Colwelliaceae* (OTU-7) (maximum sequence identity of 94%) in incubations with crude oil as well as in control incubations may infer nutrient sharing by this organism or a broad nutrient degradation spectrum. *Rhodobacteraceae* (OTU-3) and *Phaeobacter* (OTU-5) both have a maximum sequence identity of 99% with *Sulfitobacter guttiformis* KCTC 32187 and *Phaeobacter arcticus* DSM 23566 respectively, putting them both in the *Roseobacter* clade (Ankrah *et al.*, 2014; Freese *et al.*, 2013; Kwak *et al.*, 2014; Wang *et al.*, 2016b). *Sulfitobacter* is a genus enriched previously in crude oil enrichments (Prabagaran *et al.*,

2007), and some *Sulfitobacter* members contain aromatic hydrocarbon degradation genes (Mas-Lladó *et al.*, 2014). The *Roseobacter* clade in general is commonly found associated with phytoplankton (although its members can be free-living) and may also consume EPS along with hydrocarbons (Geng and Belas, 2010; Arnosti *et al.*, 2015), and members of this clade were found to some extent in all treatments. As described in Chapter 1, members of the *Roseobacter* clade can interact with algae either in a growth stimulating way or produce algicides (Cooper and Smith, 2015; Wang *et al.*, 2016b). The four other OTUs enriched in all treatments (PHY, BAC, and CON) may or may not be linked to the presence of crude oil. *Flavobacteriaceae* (OTU-16) had a sequence identity of 97% with *Maribacter antarcticus* DSM 21422. *Winogradskyella* (OTU-18) of the *Flavobacteriaceae* family is a genus previously found in oil contaminated environments (Bacosa *et al.*, 2015; Wang *et al.*, 2014) and OUT-18 had a closest match of 98%. *Hyphomonadaceae* (OTU-2) had a match of 98% to *Hyphomonas johnsonii* MHS-2 (Weiner *et al.*, 2000), and *Psychromonas* (OTU-15) shared a 98% match with *Psychromonas* sp. CNPT3 (Lauro *et al.*, 2013).

As a final detail, on the day of sampling in Loch Creran there was a strong wind and a rising tide, which likely introduced nutrients from the Atlantic and sediment mixing into the water column. Also the River Creran and its tributaries around Beinn Sculaird bring nutrients from the land into the Loch (Loh *et al.*, 2014). The result in the control (CON) incubations without crude oil was a small phytoplankton bloom as shown in the chlorophyll-*a* data on day 8. The total bacterial 16S rRNA gene sequence abundance also increased at this point, possibly due to the increased quantities of labile fixed carbon produced by the phytoplankton, and this increased was maintained slightly longer than the phytoplankton. Such fluctuations are commonplace in the marine environment (Chang *et al.*, 2003; Riemann *et al.*, 2000; Turley *et al.*, 2000). The bacterial taxa in CON treatments were typical of phytoplankton associates: *Bacteroidetes, Flavobacteriales, Alphaproteobacteria, Rhodobacterales* and *Gammaproteobacteria* (Pinhassi *et al.*, 2004). Members of these groups are also associated with protists, with some (e.g. *Bacteroidetes*) able to adapt and resist protozoan grazing (Baña *et al.*, 2014; Chavez-Dozal *et al.*, 2013; Gong *et al.*, 2016; Tully *et al.*, 2014). Amoeba are known to be bacterivorous and they were photographed in the CON treatments on day 8 (Caron *et al.*, 1982; Mayes *et al.*, 1998). The data from SEPA show other protozoa were also present in PHY and CON treatments. Dinoflagellates can also be heterotrophic, feeding on bacteria (Almeda *et al.*, 2013).

Protozoa would likely have experienced some toxic effects from the crude oil (at 0.142% [v/v] oil concentrations) in the PHY treatments although this was not monitored (Almeda *et al.*, 2014; Johansson *et al.*, 1980; Rogerson and Berger, 1981,1982). The nano- and micro-zooplankton present in the CON treatments (Section 4.3.2 and Figure 14B) my have contributed to the rapid decrease in bacterial abundance, and possibly also the phytoplankton, although nutrient limitation may have also started the decline of phytoplankton (Adiba *et al.*, 2010; Miki and Jacquet, 2008; Sherr and Sherr, 1988; Stel'makh *et al.*, 2009). The possibility of hydrocarbonoclastic bacteria associated with other non-photosynthetic eukaryotic marine organisms will be further investigated in the next chapter.

The range of sequence identities in the 20 enriched OTUs, from as low as 88% in order BD7-3 (OTU-1), means that there are novel species unearthed in this study. This demonstrates the treasure-trove of organisms and genetic diversity harbored in the marine phycosphere and supports the description of the phycosphere as an underexplored biotope that harbours hydrocarbonoclastic bacteria (Gutierrez *et al.*, 2012b,2013b,2014; Mishamandani *et al.*, 2016). The evidence presented here confirms the significant impact of phytoplankton-associated hydrocarbonoclastic bacteria on crude oil degradation, especially the more harmful aromatic compounds and recalcitrant HMW hydrocarbons. In conclusion, crude oil presence had a marked negative effect on micro-algal and bacterial populations. Micro-algal presence was a definitive factor shaping microbial response to crude oil enrichment, with members of the order BD7-3, phylum *Verrucomicrobia* and *Methylotenera* identified in this study as putative novel hydrocarbonoclastic bacteria.

CHAPTER 5: PROBING THE NORTH EAST ATLANTIC FOR EPIBIOTIC *MARINOBACTER*

5.1 Introduction

The following chapter focuses on the *in situ* detection of epibiotic *Marinobacter* associations in two niches present in the northeastern Atlantic: the open-ocean sea surface (photic zone) and the deep-sea cold coral reefs (specifically *Lophelia pertusa* corals). The *Marinobacter* genus is important because it is a versatile group of oil degraders that have commonly become enriched during crude oil contamination of the marine environment (Head *et al.*, 2006; Yakimov *et al.*, 2007). The *Marinobacter* members are also ubiquitous in the marine environment and thought to be important in global biogeochemical cycling (carbon, manganese, nitrogen, phosphorus and iron) (Handley and Lloyd, 2013; Singer *et al.*, 2011). *Marinobacter* have been found in a range of marine habitats including beaches, the open-ocean, tropical waters, deep sea cold seeps, sediments, Arctic and Antarctic waters (Bowman *et al.*, 1997; Kostka *et al.*, 2011; Zhang *et al.*, 2016). They have even been found on dust particles collected above Kuwait City (Al-Bader *et al.*, 2012). *Marinobacter* are an important group when considering the relationships of hydrocarbonoclastic bacteria with marine eukaryotes, having been found ubiquitously associated with marine eukaryotic microalgae including toxic dinoflagellates, and can be extremely halotolerant, light tolerant and dessication tolerant (Amin *et al.*, 2009; Coulon *et al.*, 2012; Gauthier *et al.*, 1992; Green *et al.*, 2006; McKew *et al.*, 2011). They are also associated with marine oil snow (Arnosti *et al.*, 2015) and are able to utilize a broad range of carbon sources, including lipid compounds, acyclic isoprenoids, aliphatic, monoaromatic and polycyclic aromatic hydrocarbons (PAH) (Bonin *et al.*, 2015; Duran *et al.*, 2015; Fathepure, 2014; Kostka *et al.*, 2011; Yakimov *et al.*, 2007). Klein *et al.*, (2008) found that the type strain *Marinobacter hydrocarbonoclasticus* (SP17) formed biofilm at the interface between oil and the aqueous phase while biofilm cells accumulated wax esters in the cytoplasm. The same strain exhibited increased protein expression in biofilm compared with free-living cells, and the type VI secretion system was overexpressed in biofilm cells (important in symbiotic interactions with host organisms and virulence) (Vaysse *et al.*, 2009). *Marinobacter* have been reported to use nitrate as an electron acceptor and acetate as an electron donor under anaerobic conditions, highlighting the importance of *Marinobacter* involved in oil degradation at redox interfaces (Duran, 2010). Also *Marinobacter* can produce synergic effects on PAH degradation when incubated with

other hydrocarbonoclastic bacteria (Cui *et al.*, 2014). Studying the associations of epibiotic *Marinobacter* may enhance our understanding of the ecology of these important organisms.

5.1.1 Marinobacter associations in the photic zone

Previous research on oil spills in the marine environment (and results presented in Chapter 4) has demonstrated the intrinsic capacity a body of seawater may have to support a natural population of indigenous hydrocarbonoclastic bacteria (Bælum *et al.*, 2012; Kostka *et al.*, 2011; Wang *et al.*, 2016a; Yang *et al.*, 2016). Chapters 2 and 4 highlighted the important role that phytoplankton play in this capacity, with phytoplankton-bacterial associations being particularly beneficial to oil degradative processes in the marine environment. This section will once again focus on photic zone organisms, building on the use of fluorescent probing to detect the location of PAH-degraders on laboratory cultures of *L. polyedrum* and *S. costatum* in Chapter 2. Here, due to the low numbers of signals detected from the fastidious PAH-degraders before PAH enrichment in Chapter 2, the focus was on a hydrocarbonoclastic bacterial taxonomic group that is more widespread and generalist (i.e. *Marinobacter*) (Handley and Lloyd, 2013; Singer *et al.*, 2011).

Many strains of *Marinobacter* have been isolated from a variety of micro-algal cultures and as a genus *Marinobacter* has been shown in some cases to dominate the phycosphere (Amin *et al.*, 2009; Lupette *et al.*, 2016; Sonnenschein *et al.*, 2011; Sonnenschein *et al.*, 2012). *Marinobacter* have been previously identified as putative micro-algal symbionts in numerous studies. They exhibit chemotactic responses to *Thalassiosira weissflogii* and interact with *T. weissflogii* to form aggregates (Sonnenschein *et al.*, 2011; Sonnenschein *et al.*, 2012). They have also been shown to produce iron chelating siderophores in a mutualistic interactions whereby a vibrioferrin provided by *Marinobacter* binds iron, which is a limiting algal-growth factor in the oceans, and promotes dinoflagellate and coccolithophore iron uptake (Amin *et al.*, 2009; Barker *et al.*, 2015; Cooper and Smith, 2015; Landry *et al.*, 2000a,b). *Marinobacter* are thought to play a direct role in supplying vitamins (e.g. B1 and B12) to the micro-algae *Lingulodinium polyedrum* and *Eutreptiella* sp. (Cruz-López and Maske, 2016; Kuo and Lin, 2013). It is unknown in the case of Sonnenschein *et al.* (2012) whether *Marinobacter* is parasitic, but as a genus they degrade a wide range

aliphatic substances and possibly benefit from algal EPS production (Handley and Lloyd, 2013; Mounier *et al.*, 2014). None of the above authors have identified the degree of association of *Marinobacter* with micro-algae in an environmental sample of seawater.

We have seen in previous chapters that bacteria can be associated with tightly or loosely-bound EPS, which is produced by a wide range of micro-organisms (Zhao *et al.*, 2015). Bacteria are also associated with suspended particulate organic matter (sPOM) (Freiwald and Roberts, 2005). Flow-cytometry is a quantitative single particle/cell analysis method of counting and detecting other characteristics of individual particles, which can be smaller than bacterial cells (Steen, 2004). In a flow cytometer particles are passed through laser beams and the beam disturbance is measured in a number of ways and used to deduce particle features. This method can be combined with fluorescence *in situ* hybridization (Flow-FISH) to identify particles or cells with fluorescent characteristics. Accurate quantification of selected bacterial taxa within communities has previously been achieved by this method (Amann *et al.*, 1990; Friedrich and Lenke, 2006; Nettmann *et al.*, 2013; Wallner *et al.*, 1993). A variety of marine micro-algae have also been analysed in a quantitative fashion using Flow-FISH, however, so far no reports have examined the degree or extent of epibiotic bacterial associations on micro-algae by detecting both bacterial and micro-algal characteristics using Flow-FISH. In the present study Flow-FISH was employed to determine the level of association of *Marinobacter* cells to micro-algae and to quantify the relative numbers of loosely and tightly bound *Marinobacter* cells. McKay *et al.* (2016) developed a probe that could target 62.5% of the *Marinobacter* genus (MRB625a) along with a competitor probe blocking hybridization to six *Halomonas* species, which share a one base pair mismatch. This probe has never been used for Flow-FISH in this way. Hitherto, no reports have previously reported attempts to determine the association of *Marinobacter* with micro-algae in field samples.

5.1.2 Marinobacter associations with deep-sea corals

The symbiotic microbial assemblages associated with corals are thought to perform many important ecosystem functions (Ainsworth *et al*. 2010). The microbial communities may be as important as plant communities in driving ecosystem processes (Allison and Martiny, 2008). Microbes are thought to both prevent and cause disease,

and drive nutrient cycles (Ainsworth *et al*. 2010). Much research in the field of coral symbioses has focused on microorganisms associated with shallow-water corals confined to the tropics; many hermatypic corals (reef building corals of order *Scleractinia*) living in nutrient-poor coastal waters contain symbiotic dinoflagellate algae called zooxanthellae that provide a source of fixed carbon for the corals in return for a protected environment to live in (Falkowski *et al*. 1993). Complex interactions have been shown to occur in these corals, including the cnidarian hosts controlling the density of zooxanthelle cells within their own cells (Falkowski *et al*. 1993). Previous studies have suggested that bacterial communities associated with corals may benefit the coral by nutrient cycling, antibiotic production and chelating iron (Kellogg *et al.*, 2009. Compared to the amount of information scientists have collected regarding symbiosis in zooxanthellate (photosynthetic) corals very little is known about the composition and function of microbial communities associated with deep-water corals.

Lophelia pertusa is arguably one of the most widespread and common reef framework-forming cold-water corals on the planet (Freiwald *et al.*, 2002; Freiwald and Roberts, 2005; Roberts *et al.*, 2003). Reef-forming corals provide niches for a range of organisms and are important as a nursery for juvenile fish (Foley *et al.*, 2010; Howell *et al.*, 2011). Deep-sea cold water reefs are a nursery for commercial fish species (Foley *et al.*, 2010), therefore it is in the interest of the public to protect and investigate *L. pertusa*. Reef forming corals are an 'essential reef habitat' with damage of habitat resulting in lower fish abundance and spawning (Foley *et al.*, 2010). Creating marine reserves and prohibiting trawling around these reef forming species benefits can benefit fisheries, by lowering catch effort (Costello, 2014). Fishermen claim catches are significantly lower where reefs are damaged (Fosså *et al.*, 2002). *L. pertusa* reefs also act as a paleoindicator (interpretation of $CaCO_3$ skeletons to infer historical environmental conditions), a CO_2 sink and also place to find new pharmaceutical compounds (Foley *et al.*, 2010). But this species is threatened by ocean acidification and climate change, along with destructive fishing practice (Dodds *et al.*, 2007; Rogers, 1990). Very little information is currently known about the impact of the petroleum industry on *L. pertusa* although this is regarded as a potential threat.

Interestingly, *L. pertusa* has been found on underwater oil and gas platforms 100 m deep in the North Sea (Gass and Roberts, 2006). Drill cutting marks have been found in living *L. pertusa* communities, which can grow on active oil and gas platforms (Gass

and Roberts, 2006). However, no *L. pertusa* was found in the North Sea prior to the oilrig constructions. Rogers (1990) raised concerns about the impact of UK industry expansion from North Sea to west of Shetland and the northeast Atlantic on *L. pertusa*. In the Gulf of Mexico after the Deepwater Horizon oil spill a brown flocculent material was found covering *L. pertusa*, which contained hopanoid biomarkers linking this oil to the Macondo well (White *et al.*, 2012). Many other signs of stress were seen at this time (3 – 4 months after the well was capped) (White *et al.*, 2012). Further away (>20 km) there were healthy corals, seemingly unchanged from sampling before the well. These results show that oil can negatively impact deep-water communities but also that *L. pertusa* has the capacity to cope to some extent. For slow-growing cold-water species like this, the impact of oil pollution could be long-term and may therefore be more serious (Brooke and Young, 2009; Clark, 1992).

The discovery of oil-degrading bacteria closely associated with marine algae served as motivation to search for similar associations of such bacteria with other marine eukaryotic organisms. If *Marinobacter* are ubiquitous in the marine environment then there is a possibility that they could be found in the deep sea associated with *L. pertusa*. The arguably 'likely' association of *Marinobacter* cells in this deep sea habitat stands to reason, not only because of the likelihood of marine snow depositing organic material (possibly with *Marinobacter* attached) to sediment, but also due to the possible nutrition provided by the coral and the generalist nature of this hydrocarbonoclastic bacterial group (Arnosti *et al.*, 2015; Handley and Lloyd, 2013; Singer *et al.*, 2011). Cnidarians produce EPS in the form of mucus and in *L. pertusa* mucus production is well regulated and linked to particle removal, feeding and possibly other functions (Neulinger *et al.*, 2009; Wild *et al.*, 2004; Zetsche *et al.*, 2016). Carbohydrates in *L. pertusa* mucus can be used by microbes as a carbon source (Wild *et al.*, 2010). As has been mentioned in Chapters 2 and 4, hydrocarbons form aggregations with EPS and they are also adsorbed to lilophilic molecules like cell membranes or possibly EPS. Oil exploration in areas close to the North East Atlantic (e.g. North Sea) and natural seeps and background oil levels Creran) could provide added carbon for epibiotic hydrocarbonoclastic bacteria associated with deep-sea corals (Mazzini *et al.*, 2003; Niemann *et al.*, 2005; OSPAR Commission, 2013; Sweeney, 1988).

In fact some previous studies have provided evidence of *Marinobacter*-coral associations. Carlos *et al.* (2013) found *Marinobacter* associated with mucus and

shallow (10 m deep) coral species (not *L. pertusa*). Juvenile coral planulae are commonly found with *Marinobacter* and *Roseobacter* (Sharp *et al.*, 2012). Alagely *et al.* (2011) showed that *Marinobacter* inhibited swarming and biofilm formation of coral parasite *Serratia marcescens,* whilst a report by Lee et al. (2012) identified *Marinobacter* on *Sarcophyton* coral. There are so far no examples in the literature of *Marinobacter-L. pertusa* associations. *L. pertusa* has shown some habitat-specific variations in the associated bacterial communities (Neulinger *et al*., 2008). Neulinger *et al.* (2008) described the microbial communities associated with *L. pertusa* as being extremely species-rich and very different from the surrounding environment; different colour-varieties of the soft coral had variations in their associated microbial communities. In the Mediterranean Sea Yakimov *et al.* (2006) found that the microbial communities on live *L. pertusa* were different from dead reef communities. Kellogg *et al.* (2009) studied the deep-sea *L. pertusa* reefs in the northeastern Gulf of Mexico at two study sites: site VK906/862 (315 m deep, 9 - 13 °C) and VK826 (500 m deep, 7 - 9 °C). The latter site had localized hydrocarbon seepage. Site VK906/862 was dominated by the *Proteobacteria* and site VK862 was dominated by previously unknown members of the *Mycoplasma* (lacking cell wall), *Tenericutes* and *Bacteroidetes.* Kellogg *et al*. (2009) also found that two groups of bacteria were specific to *L. pertusa*: 1) *Mycoplasma* spp. and 2) *Gammaproteobacteria* related to clam symbionts. Identification of 16S rRNA gene sequences from associated bacterial communities showed that some sequences were 100 % related to bacteria associated with *L. pertusa* from Norwegian fjords (Kellog *et al*. 2009). The above study of Kellogg *et al.*, (2009) used a 'Kellog sampler' to individually seal coral polyps at depth using a submersible remotely operated vehicle (ROV). This was done to minimize cross-contamination of the coral polyps with bacteria from elsewhere in the water column, a key issue with 16S rRNA gene sequencing surveys. Previous authors hadn't taken this precaution, either using nets or boxes, subjecting polyps to water column microbial sample contamination (Brück *et al.*, 2007; Lee *et al.*, 2012; Neulinger *et al.*, 2008,2009; Penn *et al.*, 2006; Yakimov *et al.*, 2006).

The aim of the work presented in this chapter was to determine if *Marinobacter* is found either externally or internally associated, or both, with coral polyps of *L. pertusa* at three reef sites (Longachev, Mingulay, Pisces) in the northeastern Atlantic. This is important not only for identification of putative hydrocarbonoclastic bacterial seed population at the start of sporadic pollution events but also in terms of the

hydrocarbonoclastic bacterial-host interactions that are the focus of this thesis. Putative symbiotic relationships of hydrocarbonoclastic bacteria with higher organisms, such as with *L. pertusa*, may be inferred by showing *in-situ* epibiotic associations between the two organisms. This study may instigate further research to uncover the mechanistic processes underlining intricate hydrocarbonoclastic bacterial associations. Research into the microbes (possibly endolithic) associated with *L. pertusa* is still in its infancy (Neulinger *et al*. 2009); no information currently exists on the microbial communities associated with *L. pertusa* from the northeastern Atlantic. Any improved understanding of the interactions between microbes and their cnidarian hosts will undoubtedly assist in helping us to better understand their ecology and hopefully also with plans to conserving these fragile organisms (Rosenberg 2007).

As we have seen in Chapter 2, CARD-FISH would lend itself well here because in environmental samples FISH signals are often weak due to low ribosome numbers, so amplification of signals is needed. Neulinger *et al.* (2009) has shown this method can be implemented combined with histological methods (removing skeleton of calciferous organism, cutting with microtome, etc.). Neulinger *et al.* (2009) went on to use CARD-FISH to analyse the microbial community associated with *L. pertusa*, although as mentioned above this study was subject to contamination issues. This research became possible when soft coral samples from the James Cook voyage became available for analysis in our laboratory, which were sampled using a state of the art remote operated vehicle (ROV) designed by Geoff Cook with capabilities of at-depth vacuum-packaging of coral polyps to eliminate water-column contamination. The aim was to test whether *Marinobacter* cells could be identified living associated with *L. pertusa* coral polyps using CARD-FISH, the occurrence of which might infer *L. pertusa* reefs' intrinsic capacity for oil degradation.

5.2 Materials and Methods

5.2.1 Phytoplankton field sampling and analysis

5.2.1.1 Field sample collection and fixation

A sea surface phytoplankton sample was collected on R/V Scotia during a research cruise to the Faroe-Shetland Channel (FSC) in the northeastern Atlantic on May 2, 2015 (Latitude: 60° 37.84' N, Longitude: 4° 54.60' W). At this location the sea surface temperature was 7.6°C and the depth of the water column to the seabed was 1,022 m. A

phytoplankton net (50 µm mesh size) was trawled near the sea surface (1 – 2 m depth) for several minutes to collect the phytoplankton community (the limitation of this method is that it only sampled predominantly the larger phytoplankton species with the smaller species passing through the net). Equal sized portions (~100 µl wet volume) of the collected phytoplankton haul were placed into 1.5 ml microfuge tubes (twelve separate samples) and fixed using paraformaldehyde (3% v/v) in filter sterile (0.2 µm) PBS (1x) for 30 min at ambient temperature. The paraformaldehyde was removed by washing the cell suspensions with PBS at least 3 times by centrifugation (8000 *g*; 10 min). The 12 fixed phytoplankton samples were stored at -20°C in 1:1 (v/v) PBS and ethanol for subsequent analysis by Flow-FISH (see below).

5.2.1.2 FISH procedure

In order to test experimental conditions and for the purpose of a positive control *Marinobacter algicola* were grown on sterile artificial seawater medium (ZM/10) on a shaker (80 rpm) in the dark at 16°C. The cells were fixed using the same method as outlined above. The 12 field samples were removed from the freezer and washed with 250 µl PBS (8,000 ×g/ 10 min/ room temperature). The hybridization was performed in very dark conditions as to maintain fluorophore intensity. The hybridization buffer and conditions used were a modified version of the Flow-FISH protocol described in Nettmann *et al.* (2013) using the entire 1 ml samples. The 12 field samples and the *M. algicola* sample were centrifuged at 8,000 ×*g* (10 min) and re-suspended in 221 µl of 46°C preheated hybridization buffer, which contained 900 mM NaCl, 20 mM Tris/HCl (pH 7.2), 0.1% SDS, 25% formamide (McKay *et al.*, 2016) and 21 µl of each FISH probe (50 ng μl^{-1}) (see Table 5). Samples were incubated at 46°C for 2 h inverting periodically. After hybridization samples were centrifuged as before, the supernatant discarded and 500 µl washing buffer (0.149 M NaCl, 20 mM Tris/HCl (pH 7.2), 5 mM EDTA) preheated to 48°C was added to the microfuge tubes (NB: this washing buffer maintained slightly more stringent conditions than hybridization buffer). Samples were incubated for 15 min at 48°C. They were subsequently washed twice with 0.05 M PBS (pH 7.0) (Nettmann *et al.*, 2013). The contents of the 12 field-samples (treatments A – D) and single *M. algicola* (treatment E) hybridization contents are outlined in Table 5. The two Cy3-labelled probes and the *Halomonas* competitor probe for MRB625a from Table 5 are listed below and were purchased from Integrated DNA Technologies (IDT).

NON338 Cy3-5' - ACT CCT ACG GGA GGC AGC - 3' Nonsense probe (Wallner *et al.*, 1993)

MRB625a Cy3-5' - CAG TTC GAA ATG CCG TTC CCA - 3' *Marinobacter* probe (McKay *et al.*, 2016)

HAL625a 5' - CAG TTC CAA ATG CCG TTC CCA - 3' – MRB625a competitor probe (McKay *et al.*, 2016)

Table 5. Details of the probes used during hybridization of the triplicate field samples (treatments A – D) and *M. algicola* control sample (treatment E) and reasons for performing hybridizations.

Treatment	Hybridization and probe selection	Replicates	Explanation
A	MRB625+Cy3; HAL625c	3	experimental sample
B	MRB625+Cy3; HAL625c; enriched with fixed *M. algicola*	3	positive control
C	NON338+Cy3	3	nonspecific binding quantification
D	probe absent	3	autofluorescence
E	*M. algicola* PFA-fixed culture MRB625+Cy3; HAL625c	1	validation and cell enrichment

The *M. algicola* cell suspension was visualized under a Zeiss epifluorescence microscope (Axio Scope.A1) to confirm successful hybridization. A small volume (10 µl) of this was added to the positive control triplicate treatments. All 12 phytoplankton hybridizations and the single Cy3-hybridized *M. algicola* sample were shipped immediately to the Iain Fraser Cytometry Centre (University of Aberdeen) at 4°C (in ice box), where analysis (Section 5.2.1.3) took place the following day. Before analysis DAPI (4', 6-diamidino-2-phenylindole) as indicator for DNA-containing species was added to all samples to a final concentration of 1 µg ml^{-1}. Samples were passed through a 70 µm nylon mesh to get single cell suspension and to prevent clumping (the limitation of this method is that the phytoplankton analysed were predominantly between 50 and 70 µm due firstly to the net trawl and secondly the nylon mesh). For determining the relative size of particles in the samples, the flow cytometer was set-up to the most useful scatter profile by using size standardized beads covering a range of 1.3 µm, 6 µm and 15 µm (Thermo Fisher Scientific Ltd).

5.2.1.3 Laser/Channel selection and flow-cytometric analysis

Samples were analysed using a BD LSR Fortessa Flow Cytometer with five lasers (λ_{ex}: 355 nm, 405 nm, 488 nm, 561 nm and 640 nm) and 18 fluorescence detection units in addition to the scatter parameter FSC (Forward Scatter) and SSC (Side Scatter). FSC is the scattered light in forward direction and the signal is proportional to cell size. Side Scatter (SSC) signal intensity (measured at 90° to the FSC signal) is proportional to cell complexity/granularity. Scatter profiles (FSC and SSC) were optimized by measuring the background using filtered solutions (0.22 μm for Sheath fluid and 0.1 μm for dH_2O and PBS) and calibration beads in order to obtain the proper information about the size and complexity of each cell in the sample. The phycoerythrin (PE) channel was used for Cy3 fluorescence (λ_{ex}= 561 nm [yellow/green laser] and a 585/15 nm emission band-pass filter), whilst the peridinin-chlorophyll protein (PerCP) channel was used to measure chlorophyll (Chl) auto-fluorescence of phytoplankton/micro-algae (λ_{ex} = 488nm [blue laser] and a 670/14 nm emission band pass filter). Spectral overlay of the Cy3 into the Chl channel and vice versa was compensated by using a sample of marine bacteria single-stained with Cy3 and a marine phytoplankton sample for chlorophyll auto-fluorescence. DAPI was excited by a 355nm UV laser and measured using an emission filter 450/50 nm.

5.2.1.4 Flow-FISH data analysis

For each particle/cell that passes through the flow-cytometer, information from all five signals (FSC, SSC, Cy3, Chl and DAPI) of the above channels/lasers was collected and saved as FCS (Flow Cytometry Standard) file. To analyse the flow-cytometric data a series of gating strategies were used. 'Gating' is the process of virtually selecting cells/particles of interest from a large set of particles to analyse the cells in detail and to obtain statistical parameter. Gates, or regions are drawn manually on histograms and on bivariate scatter or fluorescence plots. These gates can then be applied to view and to get the statistics such as the frequency or Mean Fluorescence Intensity (MFI). In the present study bivariate plots could be produced using any two of the five channels selected.

Firstly, to obtain a general description of the contents of the phytoplankton sample (e.g. number of particles, number of DAPI positive particles, size of particles) and the quantities of Cy3 particles (*Marinobacter)* detected by the flow cytometer **Strategy 1** was employed as outlined:

- The 1st plot, scatter plot, gated a range of 53.7 ± 13.7% (SD) of the total particles using the scatter plot of size (FSC) against complexity (SSC) taking into account large and small particles over a range of complexities (e.g. Figure 19), eliminating the majority of unknown artifacts and background noise present in the filtered PBS and bead calibrations (Donnenberg and Donnenberg, 2015). This population was named 'Scatter Species' and has been used for further analysis in the 2nd Plot.
- In the 2nd plot, size (FSC) was plotted against DAPI fluorescence, which once again eliminated DAPI-negative artifacts present in controls. A gate was drawn around DAPI-positive particles and this was divided into two populations, 'big' and 'small', based on a bacterial-size control (i.e. any particles bigger than single bacteria were in the 'big' gate). These gates were termed 'Small DAPI+' and 'Big DAPI+'.
- In the 3rd and 4th plots the gates from the 2nd plot were analysed further to identify phytoplankton by chlorophyll and *Marinobacter* by Cy3 fluorescence. The particles from 'Small DAPI+' (3rd plot) and 'Big DAPI+' (4th plot) were gated at exactly the same fluorescence intensities. Three gates were drawn in each plot to analyse following the populations and results: chlorophyll positive phytoplankton without *Marinobacter* called 'Chl+', only *Marinobacter* called 'Cy3+' and a double-positive gate representing *Marinobacter* together with phytoplankton called 'Chl+Cy3+'.

Secondly, to count the total phytoplankton cells and subsequently identify the proportion of them that were positive for *Marinobacter* cells (Cy3), **Strategy 2** was employed as outlined:

- In the 1st plot the fluorescence intensity of chlorophyll-*a* (PerCP Channel, 670 nm emission) was plotted against FSC. Phytoplankton (called 'Big Chl+' in the results section) were discriminated using chlorophyll fluorescence (Chl) and 'big' size (FSC); this population was determined by using the *M. algicola* (treatment E, Table 5), which was negative for chlorophyll.
- In the 2nd plot the previous gated population 'Big Chl+' was further analysed for the presence of Cy3 fluorescence intensity against the DNA dye DAPI. Analyzing the negative control treatments C and D (Table 5) as well as the positive sample of *M. algicola* cells determined positive Cy3 signals. Particles

of interest were labelled 'Cy3+ DAPI+', and this gate represents the presence of *Marinobacter* together with phytoplankton.

By this second gating strategy, the frequency (%) of viable (DAPI+) Cy3 positive (*Marinobacter*) bacteria that were within the gate 'Big Chl+' (containing micro-algae) was determined. Dr. Raif Yuecel performed the above gating strategies at the University of Aberdeen Iain Fraser Cytometry Centre. Importantly, throughout this section where particles are referred to as 'small' (e.g. bacteria or achaea, ca.1 μm): these small particles are assumed to be cells that were originally attached to the larger particles (ca. 50 – 70 μm) (e.g. micro-algal cells, particle clusters or marine debris) that have become disassociated from the larger particles (i.e. loosely associated). This is due to the 50 μm phytoplankton net trawl that did not sample the free-living bacterial community.

5.2.1.5 Statistical analysis:

One-way ANOVA was used with Tukey's *post hoc* test was used to compare groups using SPSS statistical package. For comparing two groups T-tests were used. When necessary data were $\log_{10}$-transformed in order to conform to parametric assumptions of normality and homogeneity of variance.

5.2.2 Lophelia pertusa field sampling and analysis

5.2.2.1 Sample collection and fixation

Three coral mounds (Longachev, Mingulay and Pisces) in the northeast Atlantic were visited during the RRS James Cook 073 cruise from the 18th May – 15th June 2012. Reef location maps and metadata for *L. pertusa* sampling can be found online at https://www.bodc.ac.uk/resources/inventories/cruise_inventory/reports/jc073.pdf. Polyps were cut and collected by the remotely operated vehicle (ROV) and packaged using the Cook Sampler (named after its creator Dr Geoff Cook), a unique piece of equipment that hydraulically sealed the samples at depth to avoid contamination from the water column. From each *L. pertusa* colony visited with the ROV three samples were taken, which included one sample from the top or apex of the colony, one from the middle section, and a third from the bottom of the colony nearer to the sediment. The total number of samples obtained from Longachev, Mingulay and Pisces for the CARD-FISH was 21, 18 and 9 respectively. Once on deck coral polyps were immediately

photographed and placed into canisters (~5 ml). They were fixed on deck immediately for 3 h in filter sterile (0.22 μm) 3% paraformaldehyde (PFA) and washed with filter-sterile PBS three times (1 min) before being immersed in 1:1 (v/v) ethanol (99%) and PBS (1x) and stored at -20°C. The polyps were transported back to the laboratory for subsequent analysis.

5.2.2.2 Polyp storage solution analysis

In the laboratory two polyp canisters (one from top and one from bottom region) were selected from each reef site. From the polyp storage solution (1:1 of ethanol:PBS), a 2 ml volume was very gently passed through a white polycarbonate membrane (0.22 μm) with a GF/C filter laid underneath. A mounting solution containing DAPI (described in CARD-FISH methods below) was then applied. Seventeen fields of view (FOV) were selected at random for quantification of bacterial and coral cells. An epifluorescence microscope (AXIOScopeA1), a fluorescence imaging camera (MRm) and the Zen Blue2011 image analysis software were used to quantify cells.

5.2.2.3 Decalcification and sectioning

The *L. pertusa* polyp branches were decalcified in 20% (wt/vol) EDTA in PBS (pH 8.3). This solution was renewed two to three times over 2 days until the coral skeleton had completely dissolved. Polyps were separated and dehydrated in a graded ethanol-xylene series (ethanol at 70, 90, and 95% and twice at 100%; xylene, three times at 100% [vol/vol]) at room temperature for 20 min each step. Two infiltrations with paraffin were performed at 60°C for 10 min each time. The polyps were allowed to solidify in paraffin blocks before being cut from oral to aboral end as shown in Figure 18. The center face (black and red dotted line in Figure 18) of each polyp was placed face down in cuboid tin molds and covered in molten paraffin so that, when cut using a microtome, sagittal sections slices (10 μm thick) started from the center of the polyp. Sections were placed on Superfrost-plus glass slides.

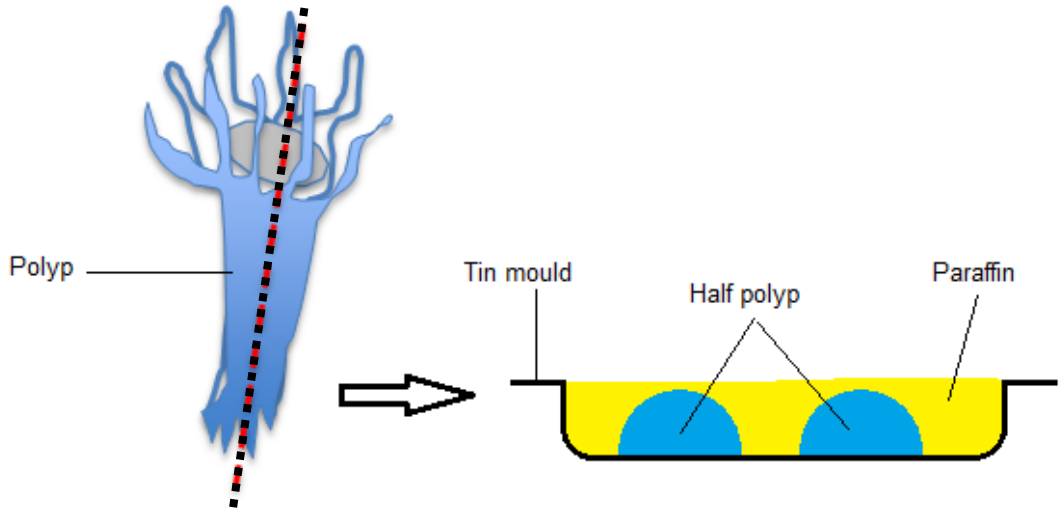

Figure 18. Paraffin block preparation in tin moulds. Once solidified at room temperature sagittal sections were cut using a microtome.

5.2.2.4 CARD-FISH analysis

L. pertusa polyp sections were deparaffinated by heating to 60°C and immediately washing in pure xylene (60°C) and ethanol (100% and 70%) and H_2O for 30 seconds each step. To avoid loss of loosely associated bacteria, slides were dipped in 0.2% (wt/vol) agarose in deionized water and air-dried (Pernthaler *et al.*, 2002). In order to detect putative hydrocarbonoclastic bacteria from the *Marinobacter* genus the MRB625a was selected (McKay *et al.*, 2016). The horseradish peroxidase (HRP) labelled probe had not been optimized for CARD-FISH previously so a melting curve using hybridization buffers at various formamide concentration (0 – 70%) was performed (as outlined in Appendix D) using *M. algicola* as the target species. A formamide concentration of 55% was used for the *L. pertusa* polyp hybridizations in order to obtain maximum fluorescence and to minimize non-specific binding. Cells were permeabilized and hybridized using the same method as is described in Appendix D. Hybridization buffers consisted of 55% formamide (Appendix D), and the MRB625a probe and HAL625a competitor probes were used in equimolar amounts. Samples were visualized using a Zeiss (Axio Scope.A1) epifluorescence microscope fitted with Carl Zeiss Filter Sets 01, 09 and 15 (for use with DAPI, Fluorescein and Cy3 respectively) and a Zeiss digital fluorescence imaging camera (AxioCam MRm). Epifluorescence micrographs were overlaid using Zeiss Zen-Blue (2012) image processing module. EUB338-I, -II and -III probe mix and NON338 were used to confirm successful hybridization and absence of nonspecific binding, respectively. NON338 hybridizations were inspected for absence of fluorescent signals.

5.2.2.5 Autofluorescence detection using confocal laser scanning microscopy

A LEICA TCS SP2 confocal laser scanning microscope was used to determine autofluorescence of a deparaffinated coral tissue sample (10 μm thick section). Seven excitation wavelengths ranging from 458 – 633 nm were used and fluorescence emission from coral tissue detected at 5 nm intervals. Excitation laser power was adjusted for each of the 7 wavelengths to avoid over-exposure (e.g. 25% power @458 nm, 50% @ 514 nm, 80% @ 633 nm).

5.3 Results

5.3.1 Detection of Marinobacter associated with phytoplankton

In this section the main focus was to detect epibiotic *Marinobacter* cells (hybridized with Cy3-labelled MRB625a oligonucleotide probes) in a phytoplankton trawl sample and attempt to identify the characteristics of the particles that the *Marinobacter* are associated with. These particles might be large or small clusters of bacterial (or archaeal or fungal) cells (and thus test positive for fluorescence imparted by DAPI staining), or they may be marine micro-algae (and thus test positive for chlorophyll fluorescence). The particles collected in the trawl may be some other kind of marine debris or suspended particulate organic matter (sPOM) and thus be detected in the FSC and SSC channels. To assess the quality of the phytoplankton sample and count *Marinobacter* cells two gating strategies were adopted. The first strategy focused on a random selection of particles to assess particle characteristics in a general sense and to quantify Cy3-positive particles (Section 5.3.1.1). The second strategy looked more specifically at micro-algal associated epibiotic *Marinobacter* (Section 5.3.1.2).

5.3.1.1 Strategy 1

To recap, the aim here was to obtain a general description of the contents of the phytoplankton sample (e.g. number of particles, number of DAPI positive particles, size of particles) and count the number of Cy3 particles (*Marinobacter*) detected by the flow cytometer. The first gate of Strategy 1 takes a random selection of particles (Figure 19 'Scatter Species', example from treatment A) in the forward (FSC) and side (SSC) bivariate scatter-plot, the shape of which eliminated the majority of unknown signals in the filtered (PBS) (i.e. artifacts of the flow-cytometer). There were ~20000 particles (53.7 ± 13.7% of total particles) gated in the 1st gate 'Scatter Species' in all treatments

(A – D) from Table 5 ($p = 0.529$). Similarly, in the second plot there was no difference between the number of particles in each gate, 'Small DAPI+' (~14,000 particles, $p = 0.708$) or 'Big DAPI+' (~5,500 particles, $p = 0.43$), in each of the treatments A – D. The particles gated within the 'Big DAPI+' and 'Small DAPI+' gates in Figure 19 were combined and analysed for total Cy3+ particles. One way ANOVA with Tukey's *post hoc* test showed that treatments A and B had significantly higher numbers of Cy3+ particles than treatments C and D (negative controls) ($p < 0.01$), which confirmed higher Cy3 fluorescence in treatments containing the MRB625a+Cy3 oligonucleotide probe. Within the treatment A 'Big DAPI+' gate (Figure 19, 4th plot) the number of double-positive particles (Cy3+ Chl+) 79.6 ± 27.31 was the same as the number of single positive particles lacking chlorophyll (Cy3+) 98 ± 36.3 (T-test, $p = 0.523$). In other words, the number of large photosynthetic (e.g. micro-algae) particles was the same as the number of large non-photosynthetic particles (e.g. sPOM) with *Marinobacter* positive (Cy3) signals in the phytoplankton net trawl.

Treatment A was analysed further, comparing the 'Small DAPI+' and 'Big DAPI+' gates (Figure 19, 3rd and 4th plots). Firstly, the Cy3-negative gates (Chl+) were analysed. There were significantly more chlorophyll-positive particles without Cy3 fluorescence in the 'Big DAPI+' plot (1968 ± 1020) than in the 'Small DAPI+' plot (75 ± 31.7) ($p < 0.01$). This means that there were more big photosynthetic (e.g. eukaryotic micro-algae) particles without strong Cy3 signals than small photosynthetic particles (e.g. cyanobacteria). Secondly the chlorophyll-negative gate (Cy3+) was analysed. There were more 'Small DAPI+' (289.6 ± 90) than 'Large DAPI+' (98 ± 36.3) ($p = 0.027$) particles. This means that, considering only the chlorophyll-negative particles, there were many more 'small' Cy3 positive (i.e. *Marinobacter* cells) than 'big' Cy3 positive particles (e.g. large sPOM with *Marinobacter* attached). Thirdly, in the double-positive (Cy3+ Chl+) gate, no significant differences were found between numbers of 'big' (79.7 ± 27.3) and 'small' (65.7 ± 18.6) particles ($p = 0.504$). The total numbers of particles in the six gates in 'Small DAPI+' and 'Big DAPI+' for all treatments (A – D) are summarized in the histograms in Figure 20.

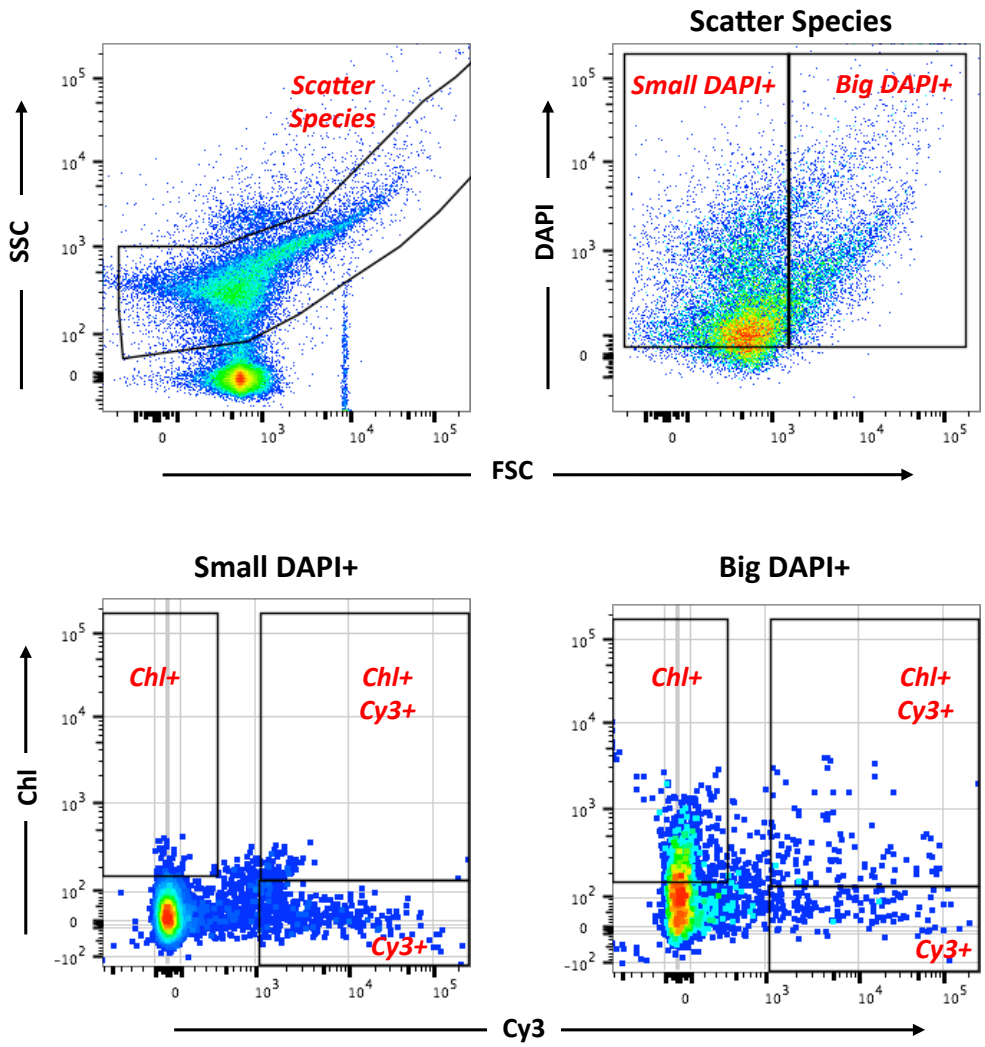

Figure 19. Strategy 1: Bivariate plot and gating sequence example from treatment A: 'experimental sample probed for *Marinobacter*'. Gate names shown in red and correspond to the titles in black above subsequent plots. The first gate was created using scatter parameters (FSC and SSC). Fluorescence parameters (DAPI, then Cy3 and chlorophyll) were then used for subsequent gates. The same bivariate plot and gating strategy was performed on all replicates from treatments A – D (the results of which have been summarized in the Figure 20. Figure produced with the assistance of Dr. Raif Yuecel.

When comparing between treatments (A – D, Table 5) for the six gates shown in 'Big DAPI+' and 'Small DAPI+' gates in Figure 19**,** significant differences in total counts were found in the 'Cy3+' (or MRB positive chlorophyll negative gate). These significant differences are shown in Figures 20C and D. This means that in both 'big' and 'small' cell gates, treatments A (experimental sample: phytoplankton sample with MRB625a probe) and B (positive control) have significantly higher positive Cy3

(MRB625a fluorescence) cell numbers than in negative control treatments (C and D) ($p < 0.01$). As can be seen, the positive control (B) has a greater number of positive signals than the experimental sample (A).

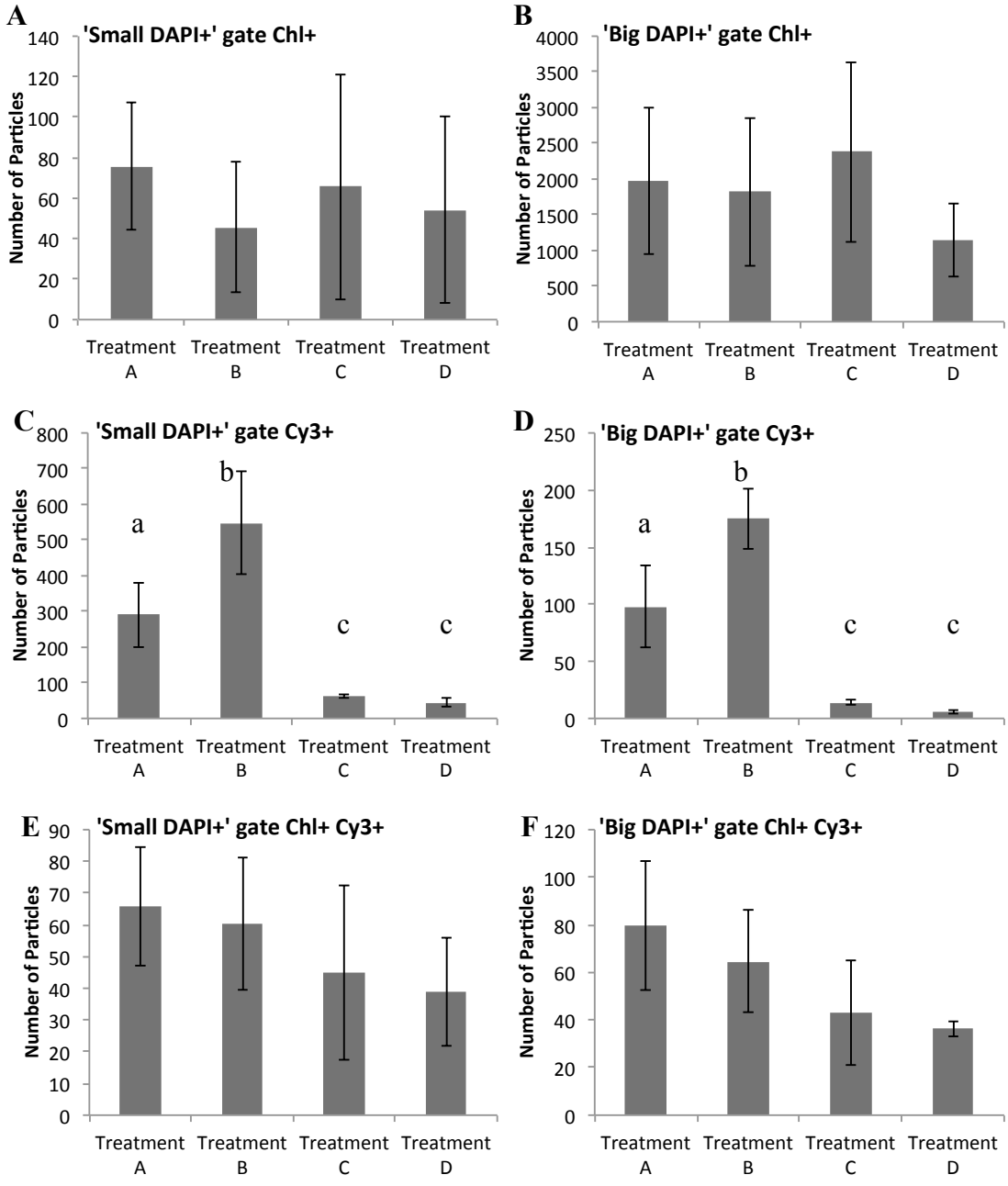

Figure 20. Total number of particles (mean values and standard deviation for three replicates) in the three 'Small DAPI+' (left hand charts) and three 'Big DAPI+' (right hand charts) gates from Strategy 1 (Figure 19) comparing treatments A – D. Lower case letters show the results of Tukey's *post hoc* test: a treatment sharing the same letter with another treatment denotes the treatments were not significantly different from each another.

5.3.1.2 Strategy 2

Due to the lack of significant differences in the double positive 'Chl+ CY3+' gate between treatments A – D (Figure 20F 'Big DAPI+' gate Chl+ Cy3+ double positive), a different gating strategy was performed that included all particles including some of the larger (FSC) more complex (SSC) micro-algal cells (Chl+) that were gated out of the random 'Scatter Species' sample in Strategy 1 (Figure 19). To recap, the aim here was to count the total algal cells and subsequently measure the proportion of them that were positive for epibiotic *Marinobacter* cells (Cy3). As observed in Figure 21, the micro-algae ('Big Chl+', left hand plot) were first gated, and subsequently data from this gate were further analysed for *Marinobacter* using high Cy3 (y-axis) and DAPI viability (x-axis), which can be seen in the 'Cy3+ DAPI+' gates in the right hand plots (Figure 21, Treatments A – D). Clearly the negative controls treatments (C and D) show a lack of particles in the final gate, and $\log_{10}$-trasformed data confirm that the number of particles were significantly lower than treatments A and B ($p < 0.01$). Results of Tukey's *post hoc* test are shown in Figure 22. To summarize the data from the experimental treatment of interest (Treatment A), a total of 1.55 ± 1.33% of 'micro-algal' cells (Big Chl+) tested positive for the *Marinobacter* Cy3 signal. This compares to 0.176 ± 0.06% in the nonsense treatment (C).

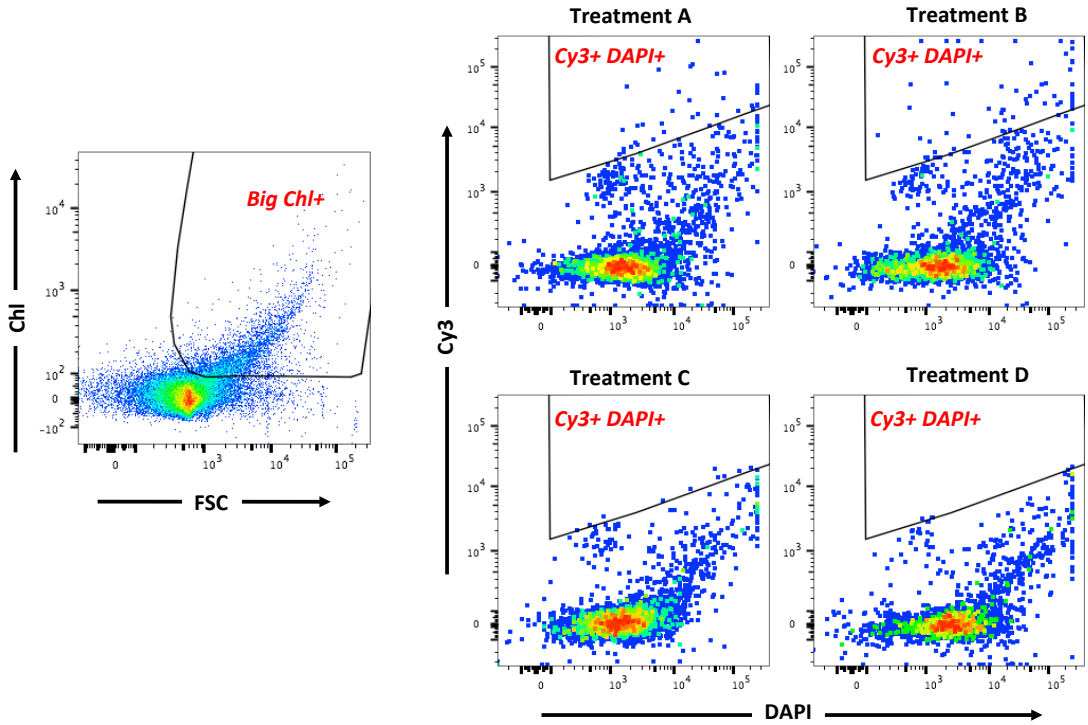

Figure 21. Strategy 2: Bivariate plot and gating sequence using firstly scatter (FSC) and chlorophyll (Chl) parameters to gate big phytoplankton (Big Chl+), followed by fluorescence (DAPI and Cy3) parameters to gate viable (DAPI+) *Marinobacter* cells (Cy3+) in gate Cy3 DAPI+ (examples from treatments A – D). Gate names shown in red and titles in black (in right hand plots) correspond to the treatments in Table 5. Nonsense probe and negative control treatments (C and D) clearly contain less Cy3 fluorescence in gate 'Big Chl+'. Total particles in 'Big Chl+' gates are shown in Figure 22. Figure produced with the assistance of Dr. Raif Yuecel.

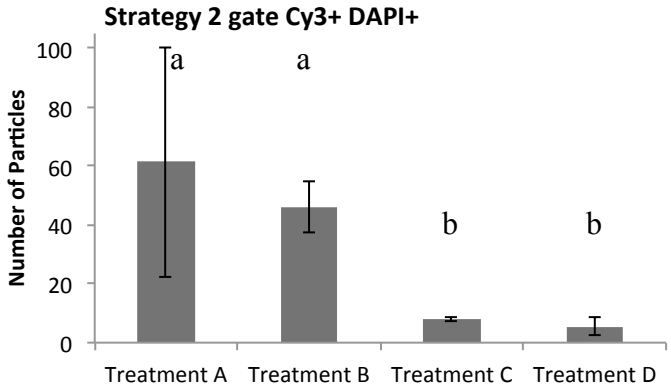

Figure 22. Total number of particles (mean values and standard deviation for three replicates) in the final gate of Strategy 2 from Figure 21 comparing treatments A – D. Lower case letters show the results of Tukey's *post hoc* test: a treatment sharing the same letter with another treatment denotes the treatments were not significantly different from each another.

5.3.2 Detection of Marinobacter associated with Lophelia pertusa

5.3.2.1 Analysis of the L. pertusa polyp storage solution

L. pertusa polyp branches were preserved on board the RRS James Cook. In order to address fears of possible bacterial cell loss during transportation and processing on board the vessel the storage solution (ethanol/PBS [1:1]) from selected polyps was passed through 0.22 μm filters to collect any lost cells and stained using DAPI to identify DNA. The filtration of the polyp storage solution demonstrated that not only bacteria but also surprisingly coral cells had become dissociated from the polyps (Figure 23). One sample solution was devoid of coral and bacteria cells (ROV19 C6), but others contained more dissociated coral nuclei than bacterial cells (e.g. ROV5 C3). There were no significant differences between mean dissociated bacterial cells and mean coral cell nuclei per polyp.

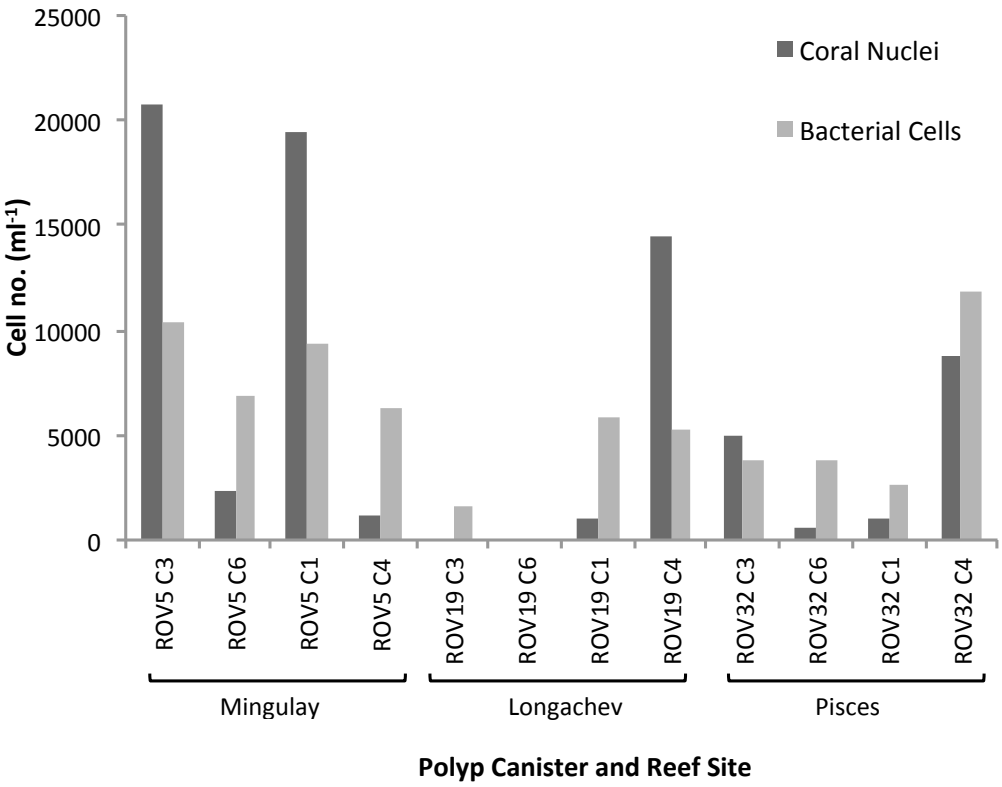

Figure 23. Mean bacterial and coral cell numbers (ml^{-1}) across 17 randomly selected fields of view counted on filtered coral polyp storage solutions that contained 12 polyp branches from Mingulay (ROV5), Longachev (ROV19) and Pisces (ROV32) reef sites (C = canister number).

5.3.2.2 Autofluorescence detection using confocal laser scanning microscopy

The tissue of *L. pertusa* was found to be fluorescent over a broad range of photon wavelengths (Figure 24). This meant that visualizing the *Marinobacter* for the following study would be difficult if they were lying on the connective tissue. Conversely, cells lying in spaces in between tissue or outside the coral tissue on the ectoderm would be easier to identify. This said, at smaller excitation wavelengths less laser power (lower photon flux) was needed to visualize a fluorescence image on the confocal LCD monitor (see Materials and Methods). This meant that the Cy3 HRP-labelled probes targeting *Marinobacter* could be used (instead of fluorescein) in order to obtain *Marinobacter*-specific fluorescent signals that are more easily visible when overlaid against the autofluorscence from coral tissue.

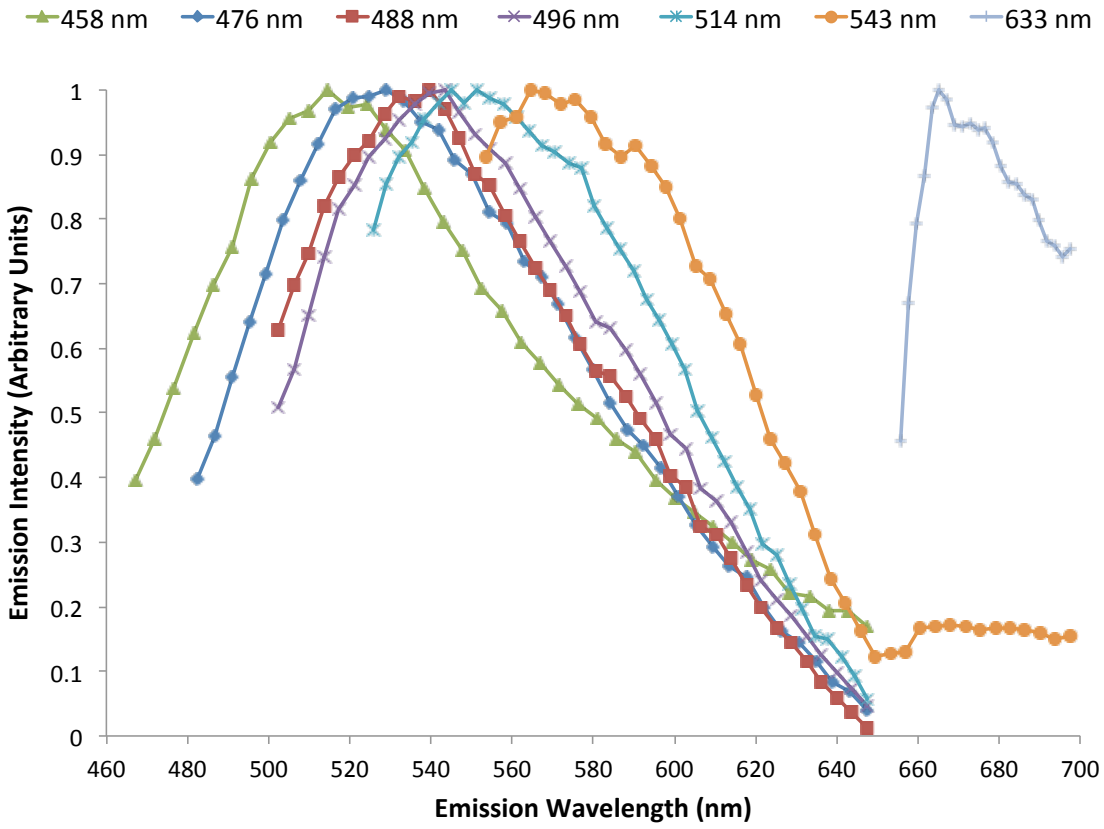

Figure 24. *L. pertusa* tissue fluorescence emission spectra produced using seven photon laser excitation wavelengths (listed above). Spectra were normalized so that maximum intensity was 1 (y-axis) (each spectrum is proportional to itself and not to the other six spectra).

5.3.2.3 Identification of Marinobacter cells associated with L. pertusa

The following Figures (25 – 27) all show the following: **i)** a micrograph of the relevant 10 μm-thick polyp sections embedded in wax (oral end at the top), with annotations in red representing fields of view (FOV) where positive MRB625a-Cy3 signals were found (image produced with/using dissection microscope) and **ii)** an example of an epifluorescence micrograph of one FOV from image **i**, using the ×100 objective lens with the epifluorescence microscope showing three-channel (blue, green, orange) emission overlays. Channels represent different dichroic filter sets with the green channel showing coral tissue autofluorescence, and orange channel (Cy3) showing *Marinobacter* cells and tissue autofluorescence, and the blue (DAPI) channel showing coral nuclei.

A middle-colony polyp from the Longachev reef is shown in Figure 25, in FOV1 the *Marinobacter* Cy3 signals appear to be either inside the mesoglea (possibly intracellular) or perhaps more likely lodged on endoderm of the gastrovascular cavity, possibly appearing intracellular in the endocoel (space between mesenterial filaments). There is a great deal of coral tissue autofluorescence (green), and judging by the close proximity of the *Marinobacter* signals it is apparent that they are very closely associated with the coral tissue. The three FOVs are all in the vicinity of the oral end of the polyp. The middle colony polyp seen in Figure 26 is from the Mingulay reef. A dense network of coral nuclei (blue) and nematocysts/cnidocysts stinging cells (green coils) can be seen surrounding the Cy3-*Marinobacter* signal. Once again this shows *Marinobacter* cells near the oral end of the polyp, but this time in the more tentacular region. Figure 27 shows a middle-colony polyp from the Pisces reef. The *Marinobacter* signals here are closely associated with the ectoderm tissue, possibly even endolithic although due to decalcification this cannot be confirmed. The HRP-labelled MRB625a probe targeted cells in all polyps from all reef mounds; *Marinobacter* cells were found in the tentacular region, the gastrodermis and on the ectoderm tissue touching the calcium carbonate exoskeleton. It is not confirmed from this data whether the cells are intracellular or extracellular.

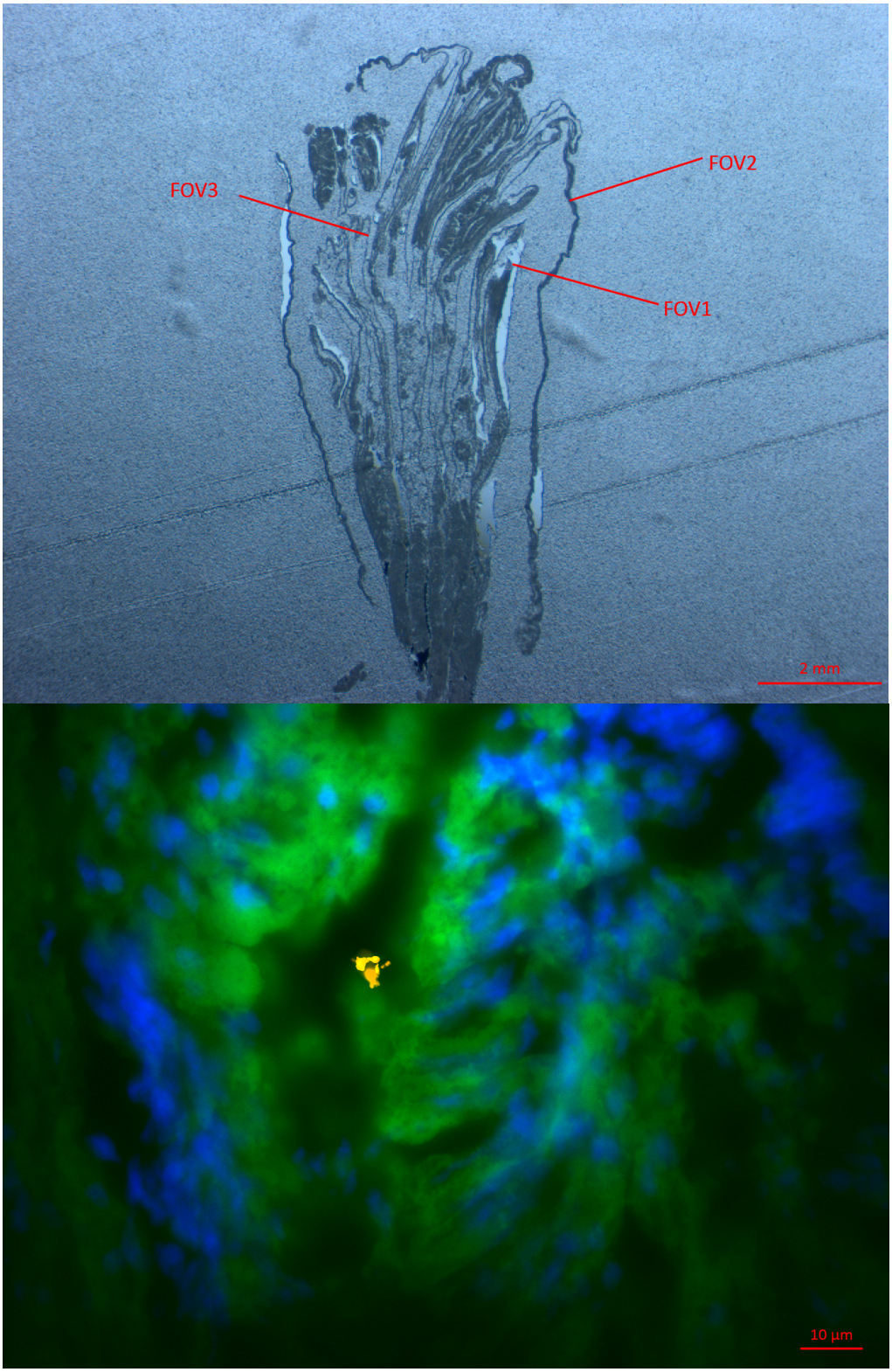

Figure 25. Micrograph of a polyp section from the Longachev reef mound showing FOVs in red (above) and an epifluorescence micrograph of FOV1 (below). *Marinobacter* (yellow-orange) cells are shown localized in a mid-tissue region. Coral nuclei appear as blue regions after counter staining with DAPI. In the bottom right hand corner of each image are scale bars (2 mm for the polyp micrograph and 10 µm for the epifluorescence micrograph).

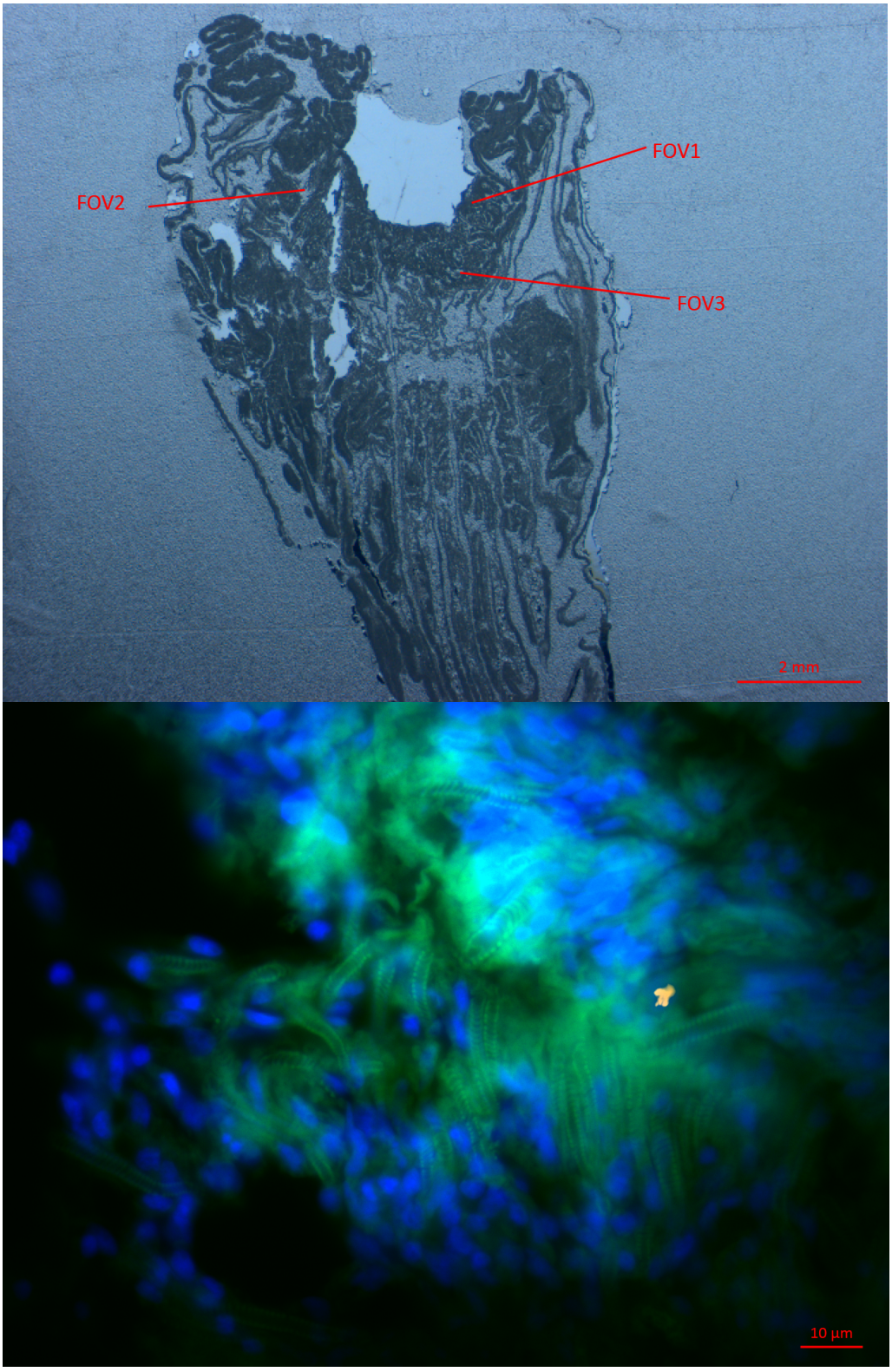

Figure 26. Micrograph of a polyp section from the Mingulay reef mound showing FOVs (above) and an epifluorescence micrograph of FOV1 (below). Here in the tentacular region (shown by the coiled nematocyst batteries in green) a dense concentration of coral cell nuclei (blue) is shown surrounding a small concentration of *Marinobacter* Cy3 signals (yellow-orange). Scale bars are shown in the bottom right-hand corners (2 mm for the micrograph and 10 µm for the epifluorescence micrograph).

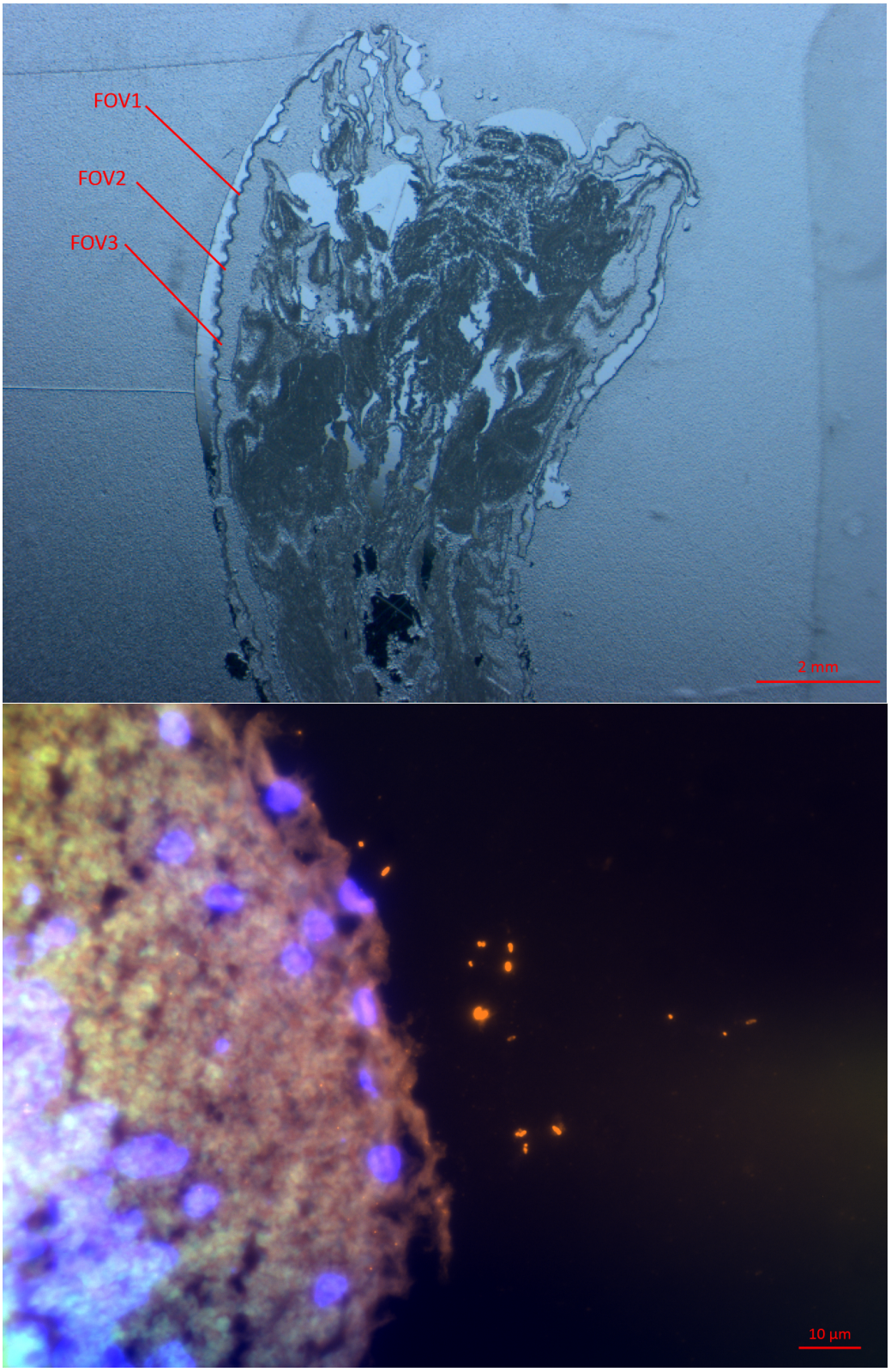

Figure 27. Micrograph of a polyp section from the Pisces reef mound showing FOVs (above) and an epifluorescence micrograph of FOV3 (below). In FOV 3 (below) MRB625a+Cy3 fluorescence can clearly be seen against a black background. Scale bars are shown in the bottom right-hand corners (2 mm for the micrograph and 10 µm for the epifluorescence micrograph).

5.4 Discussion

5.4.1 Marinobacter associated with phytoplankton in northeastern Atlantic waters

The first gating strategy showed that a) the particles collected from the phytoplankton trawl demonstrated a wide range of granularity and therefore complexity, inferring a heterogenous collection of particles, b) there were more small (ca. 1 μm), unassociated/dissociated *Marinobacter* cells than there were cells attached to larger non-phytosynthetic marine particles (e.g. sPOM or bacterial aggregations), c) there was no difference in the total number of *Marinobacter*-containing particles associated with large photosynthetic particles and large non-photosynthetic particles, and d) there were large numbers of individual *Marinobacter* cells and also *Marinobacter* cells present on non-photosynthetic particles. The second gating strategy showed that a small proportion (1.55 ± 1.33%) of the larger micro-algal cells had extremely high Cy3 fluorescence intensity, and may therefore have had multiple epibiotic *Marinobacter* cells attached to them. These results confirm the ubiquity of *Marinobacter* in the phycosphere (Amin *et al.*, 2009; Singer *et al.*, 2011); while some *Marinobacter* were more loosely associated than others they were present in single cell, bacterial-cluster-associated and algal-associated arrangements. Some of the highest Cy3 fluorescence intensities were found on large algal cells. The fluorescence intensity is proportional to ribosome number (and therefore metabolic activity) using Flow-FISH and high Cy3 intensities may indicate that some members of the *Marinobacter* genus were highly active at the time of sampling (Amann *et al.*, 1990; Nettmann *et al.*, 2013).

This is the first time epibiotic *Marinobacter* have been spatially located on micro-algae in an environmental field sample from the marine photic zone. The large numbers of *Marinobacter* that were not identified as epibiotic were nevertheless associated with the phycosphere and may have become dissociated during Flow-FISH processing, issues which will be discussed below. These results strengthen the relationship between hydrocarbonoclastic bacteria and micro-algae and are valuable in understanding the ecological relationships of *Marinobacter*, which are important organisms in global nutrient cycling (Handley and Lloyd, 2013; Singer *et al.*, 2011). The intimate associations of *Marinobacter* with phytoplankton betray intimate relationships that are likely to vary for specific *Marinobacter* species. The relationships of *Marinobacter* with phytoplankton could range from mutual symbiotic relationships to bacterivorous dinoflagellates preying on *Marinobacter* (Braun and Hantke, 2011; Cooper and Smith,

2015; Zhang *et al.*, 2013). The identification of *Marinobacter* associations with large non-photosynthetic particles and phytoplankton cells suggest that this taxonomic group is involved in a variety of aggregate formation interactions in the photic zone, a discovery that is supported by previous investigations with phytoplankton (specifically *Thalassiosira weissflogii*) and *Marinobacter*, and implicate this as an important group pertaining to the biological pump and the marine carbon flux (Gärdes *et al.*, 2011; Longhurst and Glen Harrison, 1989; Sonnenschein *et al.*, 2011). The results from Flow-FISH reiterate the intrinsic potential for the phycosphere to harbor hydrocarbonoclastic bacteria, which is extremely important for the natural decontamination of hazardous hydrocarbons. Indeed natural populations of *Marinobacter* have been found to be important hydrocarbon degraders in crude oil enriched environments worldwide (Isaac *et al.*, 2013; Kostka *et al.*, 2011; Gerdes *et al.*, 2005). Exploitation of these relationships may have ramifications in the field of bioremediation (specifically bioaugmentation) where microorganisms (typically bacterial cultures) and enzymes are used, and where results in the field have sometimes produced ineffective biodegradation of petroleum hydrocarbons (Chang *et al.*, 2000; Lü *et al.*, 2013; McKew *et al.*, 2007; Ruberto *et al.*, 2003; Venosa and Zhu, 2003). Crude oil phytoremediation using marine micro-algal cultures in combination with their natural hydrocarbonoclastic symbionts in the open ocean is an underexplored field (Lemos *et al.*, 2011; Yavari *et al.*, 2015).

With all fluorescence *in situ* hybridization there is an inherent effect of nonspecific binding, however the significant differences between negative controls and positive controls demonstrate the hybridization worked effectively and that nonspecific binding levels were acceptable. In Strategy 2 the near-complete eradication of bacterial autofluorescence provided confidence that the Cy3 channel fluorescence was probe-attributed (MRB625a), and that *Marinobacter* are very closely associated with larger photosynthetic sPOM, which are likely to be micro-algae. Although quantitative data are shown in this chapter the results are not an exact representation of the actual phytoplankton population of the northeastern Atlantic. This is partly due to removal of the >70 μm size particles by nylon mesh filtration, a step necessary to avoid blockage of the flow cell in the BD LSR Fortessa flow-cytometer, and therefore this represents a loss of the environmental particles/data (also small [<50 μm] phytoplankton were not selected by the phytoplankton net). Flow-FISH can certainly be used for obtaining a number of particles and relative abundances of a specific taxon from a mixed sample, although this may not be representative of the environment – only informative about the

environment (Sekar *et al.*, 2004). Quantitative data have been produced previously using Flow-FISH, with some studies focusing on nano- and picoplankton (Biegala *et al.*, 2003; Lebaron *et al.*, 1997; Schönhuber *et al.*, 1997; Sekar *et al.*, 2004). These authors, however, used CARD-FISH combined with flow cytometry to overcome the problem of possible low ribosome number that have been mentioned before, and they reported issues with cell aggregation and cell loss due to multiple centrifugation steps and re-suspension during hybridization. The difficulties associated with Flow-FISH processing were minimized by reducing the number of centrifugation steps and processing time using a modified version of the Nettmann *et al.* (2013) protocol (without catalyzed reporter deposition). The gentle centrifugation was intended to maintain the natural microbial assemblage as much as possible.

5.4.2 Marinobacter associated with the cold-water coral Lophelia pertusa in northeastern Atlantic waters

The results presented are the first evidence of *Marinobacter* cells associated with *L. pertusa*. These cells were found predominantly in the oral end of the polyp. These findings raise several important questions that relate to the origin, ecology and symbiotic association of *Marinobacter* with *L. pertusa*. Did these organisms evolve together and how long have they existed together? Is *L. pertusa* seeded with *Marinobacter* through vertical deposition in the water column to coral mounds on the sea floor, such as via the process of sinking marine snow particles containing communities of these bacteria? Are these associations related to hydrocarbon or lipid degradation? Clues to answering these questions may come from other studies on deep-sea corals.

As mentioned in Section 5.1 (the photic zone), *Marinobacter* are attached to sPOM and are associated with micro-algae in the phycosphere. Marine snow is ubiquitous in the marine environment and especially so during oil spills (Daly *et al.*, 2016; Simon *et al.*, 2002a; Thornton, 2002). Therefore a mechanism for transferring hydrocarbonoclastic bacteria to the deep sea exists, possibly bringing *Marinobacter* into contact with *Lophelia pertusa*. The diet of *L. pertusa* may also be informative of putative bacterial interactions. *L. pertusa* consume amphipods and copepods, which in turn eat phytodetritus (Duineveld *et al.*, 2004; Freiwald and Roberts, 2005). Stable isotope probing and lipid biomarker experiments have shown that the *L. pertusa* diet likely

fluctuates between filter feeding sPOM, micro-algae and zooplankton in a regional and temporal way (Dodds *et al.*, 2009; Duineveld *et al.*, 2004; Freiwald and Roberts, 2005). Dodds *et al.* (2009) also found that storage lipids accounted for 5-12% of *L. pertusa* ash-free dry mass. Members of *Marinobacter* have been known to degrade squalene (a polyunsaturated fat), one of the most common metazoan lipids and precursor to steroids, while *M. hydrocarbonoclasticus* degrades a broad range of lipids (Mounier *et al.*, 2014; Rontani *et al.*, 2003). This may shed some light on why we may be seeing epibiotic (possibly even intracellular) MRB625a signals from our *L. pertusa* sample, and the high lipid content of coral mucus may also explain the ectodermal *Marinobacter* location (Wild *et al.*, 2004). According to Neulinger *et al.* (2009) the bacterial aggregations around the nematocysts supports the 'sloppy eater' hypothesis where haemolymph from coral prey leaks out providing organic nutrients (fatty acids and amino acids) for bacteria. Neulinger *et al.* (2009) even argue that the presence of gastrodermis-associated bacteria would suggest exchange of metabolites with the 'host', although this is unknown in the present study.

The storage solution (Figure 23) filtration demonstrated that cells (bacterial and coral) did dissociate from these fixed samples. Possible reasons for this include soft tissue knocking against sides of containers during boat movement or transportation, causing the internal skeleton to crush and break the soft tissue mechanically, losing some coral nuclei and bacteria. Additionally Neulinger *et al.* (2009) established that the various processing stages during CARD-FISH may affect bacterial cell loss from the polyp sections. Firstly, fixing the polyps in 3% PFA before rinsing three times in PBS provides an opportunity for bacteria to potentially be washed off the polyp. Secondly, decalcification of the polyps in 20% EDTA may remove endolithic bacteria that reside between the internal exoskeleton of the coral and the soft coral tissue. Thirdly, the infiltration steps with xylene and molten paraffin followed by subsequent de-paraffination may result in bacteria becoming detached from the polyp tissue. It could be argued that the physical process of paraffin infiltration and cutting with the microtome may have dislodged some bacteria and moved (or smudged) them to a slightly different locality. This is not to mention the various washing stages in the CARD-FISH protocol itself. In order to reduce cell loss the protocol of Neulinger *et al.* (2009) was adapted in this study by dipping in 0.2% agarose solution, although this was performed after deparaffination. Importantly however, despite the above drawbacks, the fact that *Marinobacter* signals were detected associated with the various polyp

tissues analysed is substantial evidence that members of this bacterial genus are closely associated with *L. pertusa*. Indeed all three coral mound locations (Longachev, Mingulay, Pisces) sampled in the northeastern Atlantic tested positive for *Marinobacter* cells.

Autofluorescence detection using the confocal laser scanning microscope confirmed the high autofluorescence in the coral tissue. The lasers did not have UV capabilities and so UV autofluorescence was not shown in Figure 24. Nevertheless certain molecules in the coral tissue do fluoresce at this frequency, and therefore there was also substantial autofluorescence in the blue channel also. This meant it was sometimes difficult to visualize the bacterial cells, and imaging quality was greatly influenced by tissue density. There was a great deal of tissue autofluorescence shown in Figure 24 and all of the epifluorescence micrographs (Figures 25 – 27), which may be due to a number of endogenous biological fluorophores. A connective tissue present in the class *Anthozoa* is collagen (Sharabi *et al.*, 2014; Young, 1973). Collagen is a fluorescent protein containing the aromatic amino acids phenylalanine, tryptophan and tyrosine that fluoresce, as well as cross-linking fluorescent compound pyridinoline (Shoulders and Raines, 2009). Other endogenous aromatic fluorophores present in *L. pertusa* include the nicotinamide adenine dinucleotide and the flavin adenine dinucleotide (NAD and FAD). In very general terms, the observed blue autofluorescence can be explained by pyridine nucleotides (e.g. NADH) whilst green autofluorescence contributors contain flavin (e.g. flavoproteins) (Ropp *et al.*, 1995). The green fluorescent protein (GFP) was actually discovered in cnidarians (the jellyfish *Aequorea victoria*), although it is as of yet unknown whether this is present in *L. pertusa* (Chalfie, 2009). The increased fluorescence in the nematocysts cells may be explained by looking more broadly at the *Cnidaria*. *Hydra* (Phylum: *Cnidaria*) nematocyst capsules contain mini-collagen (collagen-like peptides), which are highly conserved in the class *Anthozoa* (Engel *et al.*, 2001; Kurz *et al.*, 1991; Wang *et al.*, 1995). It is unknown whether formaldehyde-induced autofluorescence contributed to any of the autofluorescence observed in this study (Schipper and Tilders, 1982).

In epifluorescence imaging micrographs where green fluorescence intensity is high (e.g. Figure 26), it should be noted that the green features (e.g. coiled stinging cells) could also be visualized in the orange (Cy3) channel. However, the exposure in the orange channel was decreased in order to draw attention to the even more intense orange

bacterial cell-like structures. The obvious absence of these cell-like structures in the green channel, even at an exposure where green structures (e.g. coiled stinging cells) were clearly visible, is further evidence that fluorescence in the orange channel is not due to general tissue autofluorescence but due to something only visible in the orange channel i.e. Cy3-labelled tyramides covalently bonded to 16S rRNA site of *Marinobacter* cells.

5.4.3 Conclusions

In the photic zone a phytoplankton net-trawl revealed that *Marinobacter* are very closely associated with micro-algae, with 1.55 ± 1.33% of micro-algal cells maintaining *Marinobacter*-association even after processing and hybridization. *Marinobacter* cells and other bacteria were also detected separate from the micro-algae in high numbers, although these may have been loosely bound to algal-EPS before processing and hybridization. This work highlights Flow-FISH as an effective method for detecting epibiotic bacteria on micro-algae, which will be a useful tool for the comparative quantification of phycosphere-dwelling hydrocarbonoclastic bacteria in the future. *Marinobacter* also live in close-association with *L. pertusa*, although their ecological or physiological role here warrants further investigating. They may have been deposited in the deep-sea in marine snow from the photic zone, and other deep-sea fauna may be introduced to hydrocarbonoclastic bacteria by this mechanism. There may be more than one distinct group of *Marinobacter* (some on ectoderm some on endoderm/or internal). It is noteworthy that this probe (MRB625a) targeted 62.5% (McKay *et al.*, 2016) of the genus so not all members will have the same ecological role. The intracellular bacteria may be parasitic and devour membrane lipids or feed on coral mucus lipids or EPS. These *Marinobacter* may be providing nutrients like vitamin B12 (Kuo and Lin, 2013). Perhaps the relationship is similar to *Marinobacter* found in mussel gills (Cappello *et al.*, 2012). The findings of this study suggest, in a similar way to Foley *et al.* (2010) that *L. pertusa* reefs (and the phycosphere) are biotopes that harbor hydrocarbonoclastic *Marinobacter*, including possibly novel members of this genus. Looking at this from left field, their isolation and cultivation in the laboratory may find a use for these organisms in a biotechnological application(s).

CHAPTER 6: CONCLUSION

Bacteria, especially in the euphotic zone in the global ocean, are supported by carbon fixed by phytoplankton and the resulting high carbon nutrient concentrations in the phycosphere (Buchan *et al.*, 2014; Field *et al.*, 1998). The relationships between eukaryotic micro-algae and hydrocarbonoclastic bacteria are likely to be dependent on temporal changes (e.g. life stage of micro-algae and seasonal factors like temperature and sunlight intensity) (Nanninga and Tyrrell, 1996; Wang *et al.*, 2016b), hydrocarbon concentrations/composition (Özhan and Bargu, 2014c), species-specific interactions (Amin *et al.*, 2015), and display variability with the community composition of both micro-algae and associated bacteria (Brakstad *et al.*, 2008; Yakimov *et al.*, 2007). A number of these details have been investigated in this thesis. Firstly, variable tolerance of micro-algal species to phenanthrene was detected in Chapter 2, with the larger diatom *Thalassiosira pseudonana* able exhibiting better growth rates and higher chlorophyll-*a* concentrations than the smaller *Chaetoceros calcitrans* cells. In previous reports, it has been postulated that larger cells display higher tolerance to petroleum hydrocarbons due to their smaller surface area to volume ratio (Del Vento and Dachs, 2002; Echeveste *et al.*, 2010), however the difference between small (<20 μm) and larger size diatoms in the literature has also shown the opposite trend (González *et al.*, 2009). An investigation into the toxicity of intermediate breakdown products (from PAH biodegradation) to the diatom *T. pseudonana* demonstrated that different metabolites exhibit contrasting metabolic effects, ranging from no observed effect over two weeks (e.g. 1-hydroxy,2-naphthoic acid) to total cessation of photosynthetic activity and cell division within four hours (e.g. 9,10-phenanthrenequinone and 1,2-dihydroxynaphthalene) at the same concentration (1.93 μg ml^{-1}). None of the six metabolites enhanced growth of *T. pseudonana*. The nature of the functional moieties of aromatic hydrocarbons is a very important factor influencing their biological effect. These results show that intermediate metabolites (quinones and diols in particular) from PAH degradation can be more toxic to marine micro-algae than their parent compounds. Variations in micro-algal tolerance to hydrocarbons are difficult to predict, possibly due to various genetic and phenotypic characteristics, and may result in either senescence/mortality at one extreme to healthy growth and cell division at the other. Other authors have found that micro-algal cellular-states can be detected by bacteria and trigger either pathogenic cellular co-ordination between bacteria or mutualistic symbiosis (Wang *et al.*, 2016b).

The fractions extracted from various stages of phenanthrene degradation by *P. algicola* also had variable effects on *T. pseudonana* growth. Fractions collected at the latter stages (days 4 and 6) of growth by *P. algicola* inhibited growth of *T. pseudonana* more than earlier (day 2) fractions. This may have been due partly to increased toxicity of metabolites from more advanced stages in the phenanthrene degradation pathway, but likely also due to synergistic effects of phenanthrene and other metabolites at various stages of degradation. During the stable isotope tracing experiment (using ^{13}C-phenanthrene) there was no identifiable evidence for the incorporation of labelled carbon from phenanthrene (or its degradation products) into *T. pseudonana*, as analysed for labeling of phenylalanine in cells by Raman spectroscopy. The toxic effects of phenanthrene and its degradation products are therefore likely to be damaging to cellular function without being metabolized by the diatom (e.g. partitioning into the cell membrane and impairing its function as described by Sikkema *et al.,* 1995). Indeed, this is supported by GC-MS analysis that showed no significant degradation of phenanthrene by *T. pseudonana*.

P. algicola was originally isolated from a laboratory culture of the marine diatom *S. costatum*. During phenanthrene enrichment of the *S. costatum* culture in Chapter 2 there was evidence of the aggregation of *P. algicola*, likely due to the release of exopolymeric substances (EPS) by the diatom – similar results were observed with *A. aromaticivorans* after phenanthrene enrichment of the *L. polyedrum* dinoflagellate culture. There are multiple examples in the literature of EPS production by diatoms (Myklestad, 1995), particularly in response to petroleum hydrocarbon contamination (Daly *et al.*, 2016; Passow *et al.*, 1994; Passow and Alldredge, 1994), and papers have also described the same for non-axenic cultures of *S. costatum* (Arnosti, 2011; Arnosti *et al.*, 2015; Gutiérrez *et al.*, 2007; Mishamandani *et al.*, 2016). Attempts to create an axenic culture of *S. costatum* using antibiotics were unsuccessful, so to obtain a more detailed assessment for the contribution of EPS production by the diatom in response to phenanthrene could not be realized. Nevertheless, it was demonstrated that the presence of *T. pseudonana* and its derived extracellular products significantly increased the dissolution of phenanthrene in the F/2+Si seawater medium. The hydrocarbon-adsorbing characteristics of diatom extracellular products are likely to be diatom species-specific, as *C. calcitrans* presence did not increase phenanthrene dissolution. It is possible that the EPS produced by *T. pseudonana* (or perhaps *S. costatum*) has an

affinity for the adsorption of phenanthrene, resulting in increasing its bioavailability for biodegradation. The microscopic identification (using CARD-FISH) of the PAH-degrading *P. algicola* in bacterial and diatom cell aggregations would support this. Although not quantified, there was an increase in the number of *P. algicola* CARD-FISH signals after five days of incubation with phenanthrene. This may mean direct conversion of phenanthrene into cell biomass or nutrient sharing with the diatom-bacterial community.

The non-axenic *S. costatum* culture (CCAP1077/1C) from which the *P. algicola* strain TG408 was isolated is a laboratory culture that has been maintained for decades (since 1970) on F/2+Si seawater medium. While there would have been no routine addition of PAHs to the culture media at the CCAP, the recipe for F/2+Si uses autoclaved filtered natural seawater, which may contain background levels of PAHs (Stagg and McIntosh, 1996). Although there is a possibility of this background PAH source sustaining *P. algicola* within the *S. costatum*-associated community, other mechanisms could be considered to why *P. algicola* is supported on the phycosphere of this diatom. These could include the potential ability of the diatom to synthesize hydrocarbons, or the sharing of nutrients as provisioned by the diatom. Although *P. algicola* produced clearing zones in phenanthrene-coated ONR7a agar plates, visible colonies were not detected in the present study nor by previous authors (Gutierrez *et al.*, 2013b), which would infer limited conversion of phenanthrene into bacterial biomass by this organism (in comparison to pyruvate-amended agar) or possibly also the excretion of extracellular enzymes responsible for phenanthrene degradation. Zoppini *et al.* (2005) have shown that extracellular enzymes are of particular importance to degradation processes in mucilaginous aggregates. The colour change (turning orange) identified in the phenanthrene media inoculated with *P. algicola*, which was accompanied by limited growth measured by changes in optical density, may support the extracellular enzyme hypothesis (Appendix B.1). Limited growth accompanied by a colour change was also reported for this strain when incubated with fluoranthene (Gutierrez *et al.*, 2013b).

In contrast, visible colonies were formed by this organism when cultured on agar plates amended with intermediate breakdown metabolites (both one and two ring aromatics) from bacterial phenanthrene degradation (phthalic acid, 1,2-dihydroxynaphthalene and diphenic acid). These intermediates are therefore more efficiently or rapidly converted into biomass by *P. algicola* than petroleum hydrocarbons themselves. It may be

possible that these compounds or similar compounds are provided to *P. algicola* by other PAH-degrading bacteria found in the *S. costatum* culture, such as *Marinobacter* spp. or *Arenibacter algicola* strain TG409 (Gutierrez *et al.*, 2014; Mishamandani *et al.*, 2016). Similarly, other hydrocarbon compounds produced via partial degradation of fatty acids, isoprenoid side chains or isoprenoid quinones (e.g. benzo- or naphthoquinones common in biological organisms) may provide nutrients that maintain *P. algicola* in the absence of any petrochemical substrates. Interestingly growth of *P. algicola* has been detected on both hexadecane and pristane as well as succinate, acetate and propionate (Gutierrez *et al.*, 2013b). Isoprene production by marine bacteria and algae has been reported (Fall and Copley, 2000; Shaw *et al.*, 2010), although *P. algicola* has not yet been screened for isoprene degradation, so this may warrant investigating.

When the genome of *P. algicola* was examined for aromatic hydrocarbon degradation potential (Chapter 3), a number of putative operons and also gene clusters were discovered encoding genes for a range of enzymes targeting monoaromatic hydrocarbons and their derivatives (e.g. benzene, catechol, xylene, toluene, vanillate, limonene) and also diaromatic compounds (naphthalene and biphenyl). However, specific phenanthrene targeting enzymes were not identified, possibly inferring broad specificity enzymes targeting this molecule; although putative aromatic degradation membrane proteins were identified. Evidence for the reorganization of aromatic degradation genes from the operons of other bacterial groups (Ge *et al.*, 2002; Harayama and Rekik, 1990) and the presence of multiple insertion sequences may infer acquisition of aromatic genes by horizontal transfer, which is a distinct possibility in aggregate-associated bacteria due to the intimate associations within bacterial clusters (Amin *et al.*, 2012; Louvado *et al.*, 2015). Some genes (e.g. *limA*) are receptive to putative bacterial signalling molecules like limonene (Tandlich *et al.*, 2001). The presence of cobalamin synthesis genes bares relevance to a possible mutualistic relationship of *P. algicola* with auxotrophic micro-algae (Croft *et al.*, 2006; Kazamia *et al.*, 2012). The prevalent lipid in diatom-derived mucilage from the Adriatic Sea is cholesterol (Pistocchi *et al.*, 2005), and the highest protein sequence identity of the *lapF* with a cholesterol degradation protein (Brzostek *et al.*, 2009) may mean that diatom-derived lipids could be a possible source of carbon supporting *P. algicola*, although this organism did not produce colonies when streaked on agar containing diatom-derived EPS from *T. pseudonana* or *C. calcitrans*. Nonetheless, the relationships between

hydrocarbonoclastic bacteria and micro-algae are likely to be highly species specific and dependent to a large extent on the genes encoded genes encoded by each organism.

Crude oil degradation in seawater samples taken from the marine environment (Chapter 4) was significantly affected by the presence or absence of phytoplankton. The presence of a phytoplankton community (dominated by diatoms) from a spring bloom in Loch Creran was shown to enhance Heidrun crude oil degradation. The endogenous communities of phytoplankton-associated hydrocarbonoclastic bacteria are thought to be responsible for this. Endogenous marine bacteria have been shown to degrade petrochemicals in a variety of marine environments (Yakimov *et al.*, 2007). However, this is the first time the influence of phytoplankton-associated bacteria on the degradation process has been compared to that of the free-living bacterial fraction. In this thesis many examples are given of hydrocarbonoclastic bacteria associated with marine micro-algae, which may partially explain the enhanced degradation measured in the Loch Creran phytoplankton samples. Bacterial taxonomic groups that were enriched in the treatments containing the phytoplankton treatment (PHY), but not in the free-living bacterial treatment (BAC), were *Alcanivorax* (OTU-12) and *Cycloclasticus* (OTU-6), presumably responsible for aliphatic and aromatic hydrocarbon degradation respectively. Also the marked relative abundance increase of sequence reads belonging to order BD7-3 (OTU-1) was much more pronounced (10 – 20% of total sequences) in PHY treatments compared to the BAC treatments and control (CON) treatments without crude oil. Order BD7-3 enrichments have not been detected in petroleum hydrocarbon degradation studies by other authors. Of these four groups, all but order BD7-3 have been found associated with marine micro-algae (Coulon *et al.*, 2012; Green *et al.*, 2015; Mishamandani *et al.*, 2016). Many bacterial groups detected in Chapter 4, including hydrocarbonoclastic bacterial groups (e.g. *Alcanivorax*), are potentially novel species (sharing <99% 16S rRNA gene sequence identity to closest type strains). A notable absent group in Loch Creran was the *Marinobacter* genus, common in phytoplankton blooms and dominant in previous crude oil degradation experiments (Brakstad *et al.*, 2015; Mishamandani *et al.*, 2016). In contrast to the ANS crude oil-stimulation of bacterial production found by Mishamandani *et al.* (2016), Heidrun crude oil did not prompt a downward trend in the total bacterial 16S rRNA gene number in phytoplankton treatments. These differences in bacterial community bloom dynamics in mesocosm experiments might be explained by a multitude of different conditions (crude oil type, light, temperature, bacterial competition for nutrients, etc.).

It is not atypical to find such a high diversity of bacteria associated with a diatom-dominated phytoplankton spring bloom because diatoms are involved in complex mutualistic nutrient sharing interactions with bacteria (Amin *et al.*, 2015; Villareal, 1990). They may absorb petroleum hydrocarbons in their porous silica frustules (Özhan *et al.*, 2014). Also, diatoms are prominent producers of EPS (Myklestad, 1995; Passow *et al.*, 1994) and can interact with bacteria by altering their EPS composition (Bruckner *et al.*, 2008). It is a possibility that the endogenous hydrocarbonoclastic bacteria in Loch Creran were supported by micro-algal derived hydrocarbons (Binark *et al.*, 2000; Borneff *et al.*, 1968), thus maintaining a population of bacteria with the potential to respond to crude oil pollution and thus enhance remediation after contamination events. Phytoplankton blooms occur periodically when nutrient and light levels allow (Buchan *et al.*, 2014), and one might hypothesize seasonal-fluctuations in the abundances of hydrocarbonoclastic bacteria following phytoplankton blooms (and possibly also resultant rates of crude oil degradation). Although not a factor examined in this thesis, seasonal fluctuations in hydrocarbonoclastic bacteria in sediments following the Deepwater Horizon oil spill were detected (Horel *et al.*, 2012). Bode *et al.* (2006) found that petroleum hydrocarbon degradation was correlated with phytoplankton biomass and total organic carbon (TOC) concentrations, and may also be linked with oxygen consumption rates. In this way spring plankton communities might be pre-adapted to remediate oil spillage.

In addition to the variability of impacts of phenanthrene (or other individual petroleum compounds) on micro-algae that were shown in Chapter 2, making predictions regarding phytoplankton response is more complicated still when considering crude oil: a complex carbon-rich mixture containing a range of hydrocarbons and other metals and non-metals. In Chapter 4, for example, the Heidrun crude oil proved to be toxic to the phytoplankton sample from Loch Creran (at a concentration of 0.142% v/v), decreasing the chlorophyll-*a* concentration from day 1. This was a very similar result to that of Brussaard *et al.*, (2016). Also when ANS crude oil was added to a culture of *S. costatum* (CCAP1077/1C) at a concentration of 1% (v/v), Mishamandani *et al.* (2016) detected growth suppression of the diatom after four days. In contrast many past experiments have uncovered micro-algal stimulation by crude oil (D'souza *et al.*, 2016; González *et al.*, 2009; Özhan *et al.*, 2014). The toxic effects in Chapter 4 were likely to be due the aromatic compounds in the Heidrun crude oil, with an increase in the

proportion of aromatic molecules possibly leading to increased toxicity to micro-algae (Özhan and Bargu, 2014a). Lower molecular weight aromatics (e.g. naphthalene) are likely to be more toxic due to their increased volatility and solubility (Turner *et al.*, 2014), and indeed naphthalene was more toxic than phenanthrene to both axenic diatoms as tested in Chapter 2. It is unknown whether phytoplankton mortality, cell lysis and release of cellular organic acids (e.g. fumaric acid) assisted in aerobic Heidrun crude oil degradation in the PHY treatments, although organic acids certainly assist in anaerobic degradation of both aliphatic and aromatic petroleum hydrocarbons (Jaekel *et al.*, 2015; Rabus *et al.*, 2011,2014).

The ecological distribution of the *Marinobacter* genus was investigated in Chapter 5. The identification of *Marinobacter* in the phycosphere using Flow-FISH, and in the deep-sea coral samples using CARD-FISH, supported the view of *Marinobacter* as ubiquitous in the marine environment (Head *et al.*, 2006; Yakimov *et al.*, 2007). In the northeastern Atlantic phytoplankton sample an endogenous population was found associated with phytoplankton cells, associated with aggregates of cells or debris with no chlorophyll-*a* signals and also loosely bound or dissociated from phytoplankton. Both phytoplankton-associated and free-living *Marinobacter* have been documented previously, and *Gammaproteobacteria* more generally have been found in aggregates (Amin *et al.*, 2009; Kellogg and Deming, 2009; Sonnenschein *et al.*, 2012). In the future, Flow-FISH could prove effective in assessing locations and comparative quantities of intrinsic hydrocarbonoclastic bacterial populations in the phycosphere. This may be useful in determining regional variations in populations of hydrocarbonoclastic bacteria throughout the oceans (i.e. pre-adapted oil-degradative potential), which may further elucidate their relationship with micro-algae. *Marinobacter* were also found associated with the coral polyp gastrovascular cavity, tentacle region and ectoderm, although fluorescent signals were scarce and limited to small clusters of cells. Polyps from three coral mounds (Longachev, Mingulay and Pisces) tested positive for *Marinobacter* associations. In some cases it was impossible to tell whether the *Marinobacter* cells were internal symbionts of *L. pertusa* because of possible folding of the two cnidarian cell layers (endoderm and ectoderm) and the complex structure of the mesenterial filaments. This discovery of *Marinobacter* associated with deep-sea *L. pertusa* polyps is new, although this genus has been found associated with shallow-dwelling species of coral and planktonic planula larvae (Carlos *et al.*, 2013; Lee *et al.*, 2012; Sharp *et al.*, 2012). It is doubtful that the presence of

Marinobacter in deep-sea environments is an indicator of hydrocarbon pollution because of the broad nutritional spectrum of this genus (Mounier *et al.*, 2014; Rontani *et al.*, 2003; Singer *et al.*, 2011) and their presence in marine snow (Arnosti *et al.*, 2015), which serves as a food source for *L. pertusa* (Dodds *et al.*, 2009; Duineveld *et al.*, 2004; Freiwald and Roberts, 2005). These results confirm the ubiquity of the *Marinobacter* genus and highlight the capacity of this genus for niche differentiation. As was mentioned before, this genus has the ability to respond to crude oil enrichment (Brakstad *et al.*, 2015; Mishamandani *et al.*, 2016) and it appears to be present and ready to degrade petroleum hydrocarbons in both shallow and deep marine habitats.

APPENDICES

Appendix A: The effect of 1-hydroxy,2-naphthoic acid on *T. pseudonana*

In this section the aim was to determine whether 1-hydroxy,2-naphthoic acid inhibits or stimulates *T. pseudonana* growth and light absorption (photosystem II photochemical efficiency, F_v/F_m). The methodology (outlined in Section 2.2.1.2) varies from the previous *T. pseudonana* incubations in Section 2.2.1.2 in that the volumes of each treatment were larger (50 ml vs. 16.5 ml) and the experiment was performed in conical flasks (rather than test tubes) on a shaker at a lower light intensity (photon flux density = 150 μmol m^{-2} s^{-1} vs. 350 μmol m^{-2} s^{-1}). Samples for analysis were taken daily for the first 10 days, as can be seen in Figures 28A and B, whereas chlorophyll-*a* concentrations were measured on the last day (day 14). No significant differences between control (0 μg ml^{-1}) and 1-hydroxy,2-naphthoic acid (0.5 – 2 μg ml^{-1}) treatment cell concentrations were detected on any day (days 1 – 14) using 1-way ANOVA with Tukey's *post hoc* test (Figure 27A). Kruskall Wallace tests performed on each day showed that there were also no differences in photosystem II photochemical efficiency (F_v/F_m) between the 4 treatment groups (Figure 28B). Each treatment showed maximum photochemical efficiency on day 2 and this decreased steadily until day 14. A 1-way ANOVA was performed on the chlorophyll-*a* data upon termination of the experiment and all treatments had roughly 1100 – 1150 μg L^{-1} of chlorophyll-*a* (Figure 28C). These results show that 1-hydroxy,2-naphthoic acid had no effect on phytoplankton growth and light absorption at all concentrations measured, indicating that *T. pseudonana* is more resistant to 1-hydroxy,2-naphthoic acid than it is to 1,2-dihydroxynaphthalene and 9,10-phenanthrenquinone (shown in Section 2.3.1.2).

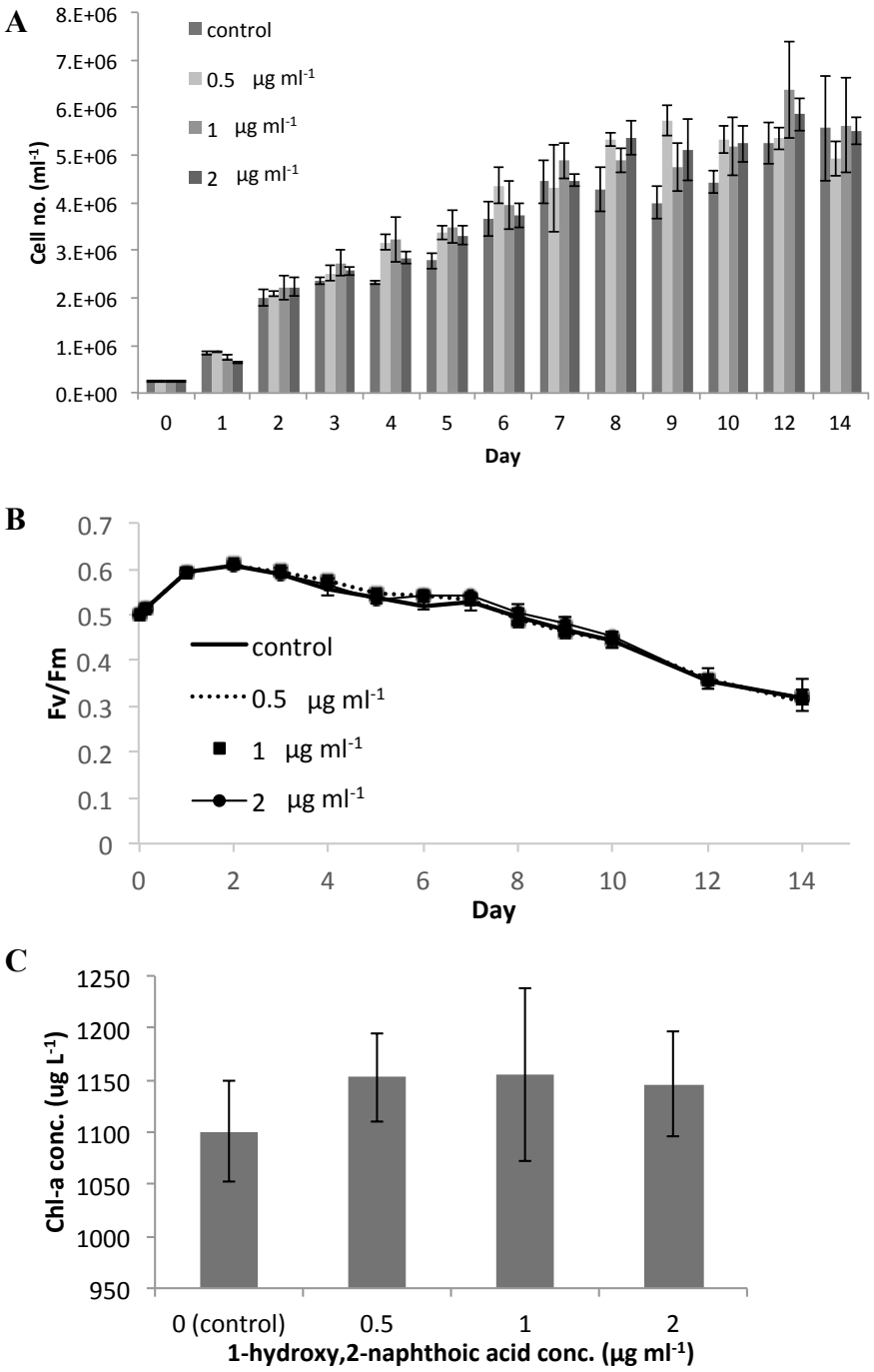

Figure 28. Variation in cell growth (A) and maximal quantum yield of PSII (F_v/F_m) (B) in *T. pseudonana* in response to enrichment with 1-hydroxy,2-naphthoic acid (concentration shown on graphs, control contains 0 µg ml^{-1}). Chlorophyll-*a* concentrations in the 4 treatments after 14 days are also shown (C). Means and standard deviation are shown for four replicates. No significant differences were found between the 4 treatments on any day.

Appendix B: Preparations for Section 2.2.1.3

Appendix B.1: Incubating P. algicola with phenanthrene and pyruvate to extract fractions while monitoring growth

In preparation for assessing the effect of *P. algicola* phenanthrene-degradation fractions on *T. pseudonana* growth and photosynthetic efficiency (Section 2.2.1.3), *P. algicola* was incubated in triplicate into ONR7a medium enriched with either sodium-pyruvate (0.1% final concentration) or phenanthrene (60 mg in 500 ml [120 μg ml^{-1})]) (as outlined in Section 2.2.1.3) so that fractions could be extracted. *P. algicola* growth in both treatments was monitored by using a spectrophotometer to determine optical density at 600 nm (OD600). In Figure 29 the results from OD600 growth monitoring show that in the pyruvate culture the OD600 rose to 0.29 ± 0.011 (and was visibly cloudy) but the phenanthrene culture remained close to zero throughout. There was a red-orange (rusty) hue noticed in the phenanthrene incubations from day 5 onwards (Figure 29), indicating that the phenanthrene was being transformed. Samples from were analysed for UV-absorbance using a spectrophotometer. A broad absorbance peak was also detected at 340 nm (320 – 360 nm, i.e. UV-A) (Figure 30). This absorbance range is indicative of 3-ring PAHs (Yu, 2002), although the higher absorbance at 310 nm compared to 370 nm may infer two ring compounds formation (i.e. naphthalenes).

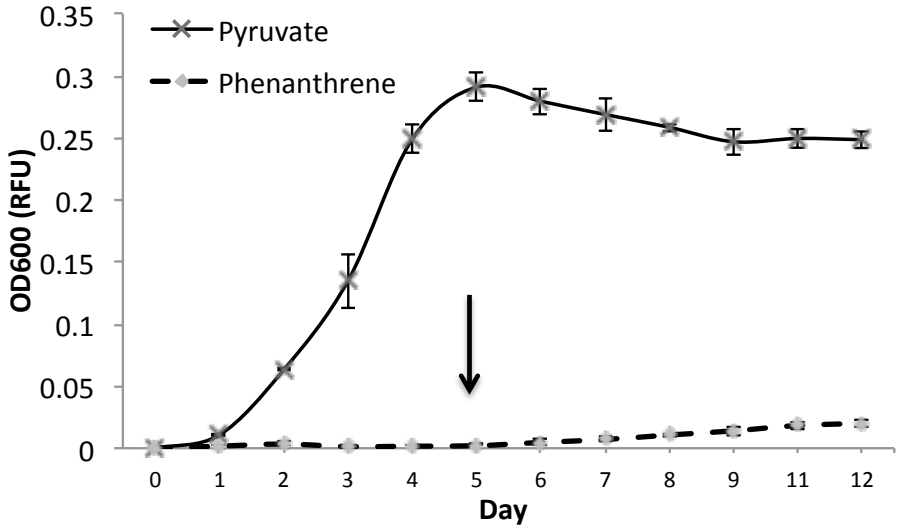

Figure 29. Variation in growth (shown by optical density at 600 nm) of *P. algicola* grown in ONR7a amended with pyruvate (solid line) or phenanthrene (dashed line). The black arrow shows where the colour of the phenanthrene incubations had changed to rusty orange. Averages and standard deviation from 3 replicates shown.

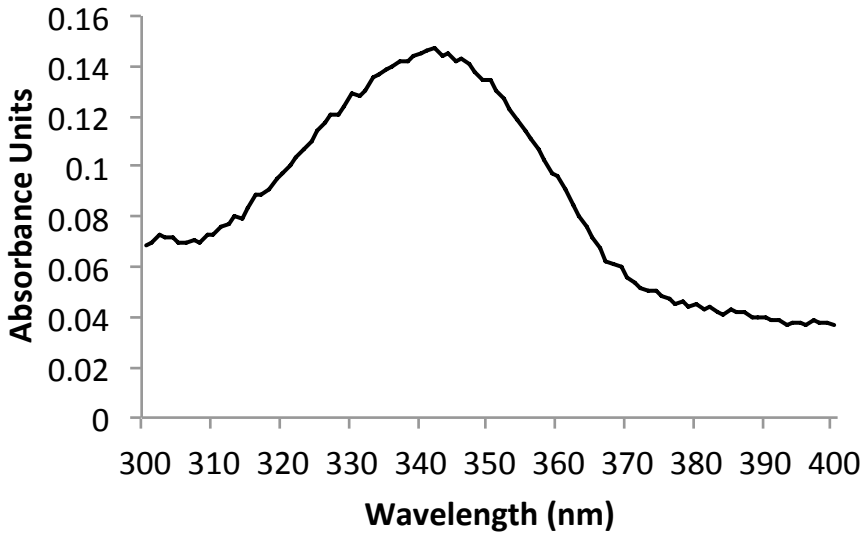

Figure 30. UV absorbance spectrum of day-5 filtrate extracted from the phenanthrene-enriched ONR7a medium inoculated with *P. algicola*.

Appendix B.2: Selecting ONR7a:F/2+Si ratio

An experiment was performed assessing the effect of ONR7a (minimal growth medium for bacteria) on *T. pseudonana* growth. This was done to determine if ONR7a alone (without phenanthrene enrichment) had an impact on *T. pseudonana*, and if this impact was ONR7a-concentration dependent, before commencement of Section 2.2.1.3 (ONR7a containing phenanthrene degradation fractions). In Section 2.2.1.3, in order to assess the effect of different phenanthrene-metabolite-enriched ONR7a fractions, the maximum ratio of ONR7a:F/2+Si media was selected so that filtrate-dependent effects would be more pronounced. ONR7a is an artificial seawater medium for growth of marine bacteria and has been used previously to grow *P. algicola* strain TG408 (Gutierrez *et al.*, 2013b). In 20 ml test tubes, sterile ONR7a was mixed with sterile F/2+Si media at concentrations of 0% (or 100% F/2+Si), 25%, 50% and 100% (or 0% F/2+Si) to make total 10 ml volumes (in triplicate). A volume of 200 µl inoculum (~300,000 cells ml^{-1}) *T. pseudonana* cells (at exponential-phase) was then added to each tube. Cell counts were taken periodically (days 4, 6 and 8) using a haemocytometer in order to monitor diatom growth and detect growth-inhibition due to ONR7a.

Significant differences ($P < 0.05$) were found on days 4, 6 and 8 (1-way ANOVA with Tukey's *post hoc* test) (Figure 31). On day 4 the 75% ONR7a treatment had significantly lower cell numbers than the control (F/2+Si only) and 25 – 50% ONR7a

treatments. However by day 8 all ONR7a containing treatments had roughly 2×10^6 diatom cells per ml of culture, whereas the control incubation had around 3.5×10^6. These results show that ONR7a inhibits *T. pseudonana* growth but that the effects of the 3 ONR7a ratios tested in this experiment were not different from each other after 8 days. Therefore the of ONR7a:F/2+Si chosen for Section 2.2.1.3 was 3:1 (i.e. 75% ONR7a and 25% F/2+Si).

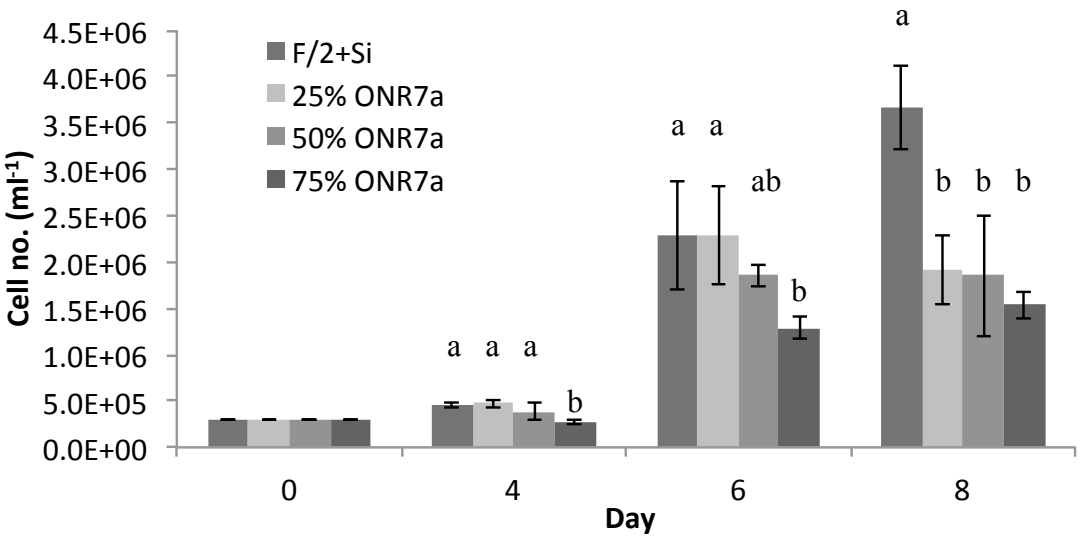

Figure 31. Variation in *T. pseudonana* cell growth (shown by cell number ml^{-1}) in response to incubation (in F/2+Si medium) with different levels of ONR7a amendment (25 – 75%). Means and standard deviation are shown for three replicates. Lower case letters show the results of Tukey's *post hoc* test: a treatment sharing the same letter with another treatment at the same time-point denotes the treatments were not significantly different from each another.

Appendix C: Raman spectra for *T. pseudonana* and *P. algicola* comparison

In Section 2.3.1.5 a stable isotope probing experiment was performed in an attempt to detect stable isotope incorporation in *P. algicola* and *T. pseudonana* using phenylalanine Raman band shift (as explained in the relevant section). The following figures are examples of Raman spectra produced by *T. pseudonana* and *P. algicola* cells after incubation with phenanthrene. There is also one example of a spectrum acquired through surface-enhanced Raman spectroscopy (SERS-Raman) using Klarite gold-coated slides produced by Renishaw to act as a comparison with a *P. algicola* cell from a late exponential/stationary phase culture. It was difficult to compare the pyruvate grown *P. algicola* cell spectrum to cells in the phenanthrene-enriched treatment (Figures

32A and B) due to different equipment being used (SERS-Raman vs. Raman). However the phenanthrene treated *P. algicola* cells displayed two distinct Raman bands: a high lipid peak at 1450 cm^{-1} and another peak (possibly protein) above 1650 cm^{-1} (see Huang *et al.*, 2007b).

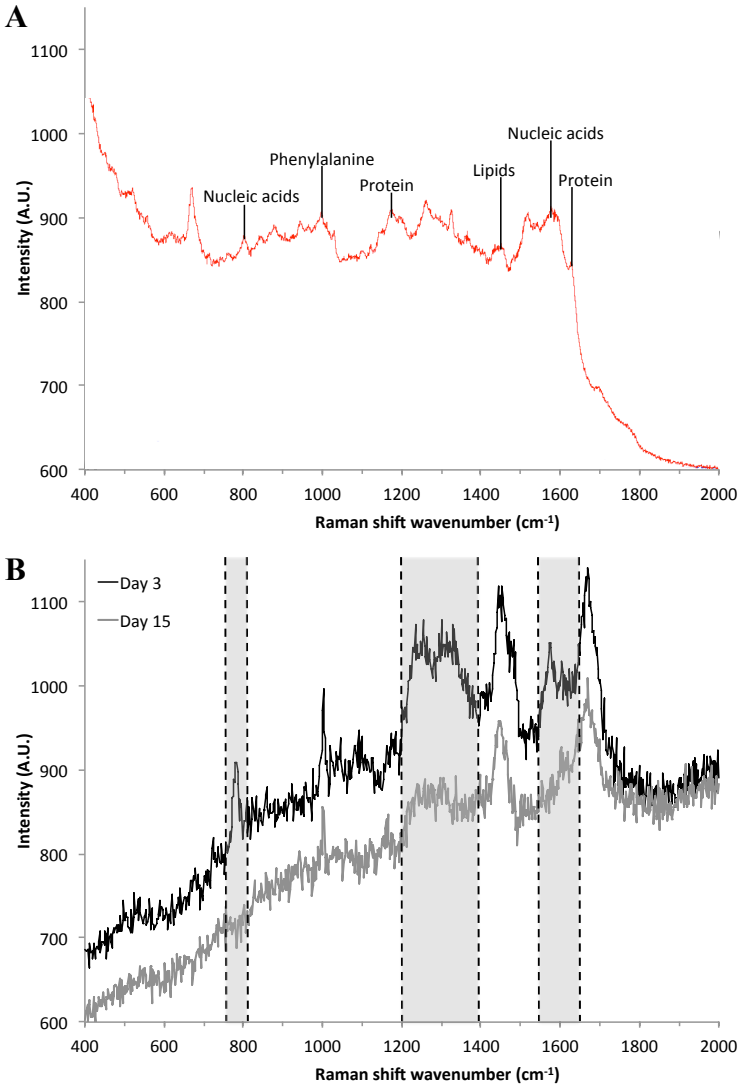

Figure 32. Raman spectra for (A) a *P. algicola* cell growing on pyruvate obtained using SERS-Raman on Klarite (Renishaw) gold-coated stage and labelled using Raman band assignments collected from Huang *et al.* (2007b) and (B) *P. algicola* cells extracted from the co-culture phenanthrene treatment on days 3 and 15 using aluminum-coated slides (EMF) (grey areas show regions exhibiting greatest band intensity differences between days 3 and 15). For spectra overlaid on the same y-axis intensity values in arbitrary units (A.U.) and are only proportional to the individual spectrum and not across other cell spectra. Raman spectra in (B) collected by Dr. Márton Palatinszky.

When comparing the *P. algicola* Raman spectra from the phenanthrene treatments (co-culture treatments, Section 2.3.1.5) on days 3 and 15 (Figure 32B) cells on day 15

displayed a complete reduction in the nucleic acid spectral peaks at wavenumber ~800 cm^{-1} and a reduction in the spectral peaks from wavenumbers 1200 – 1400 cm^{-1} (possibly lipids or proteins) and around wavenumber 1600 cm^{-1} (possibly also nucleic acids). These regions are highlighted in grey in Figure 32B, and may infer a decrease in DNA content in the cell (i.e. possible interference in DNA replication after 15 days). Similar to the *P. algicola* spectra the *T. pseudonana* cells in all phenanthrene treatments exhibited two distinct peaks at wavenumbers 1450 cm^{-1} (possibly lipid alkyl C–H_2 stretch) and 1670 cm^{-1} (either lipid alkyl C=C stretch or protein amide 1 resonance), using resonance band assignments collected from Wu *et al.* (2011) (Figure 33).

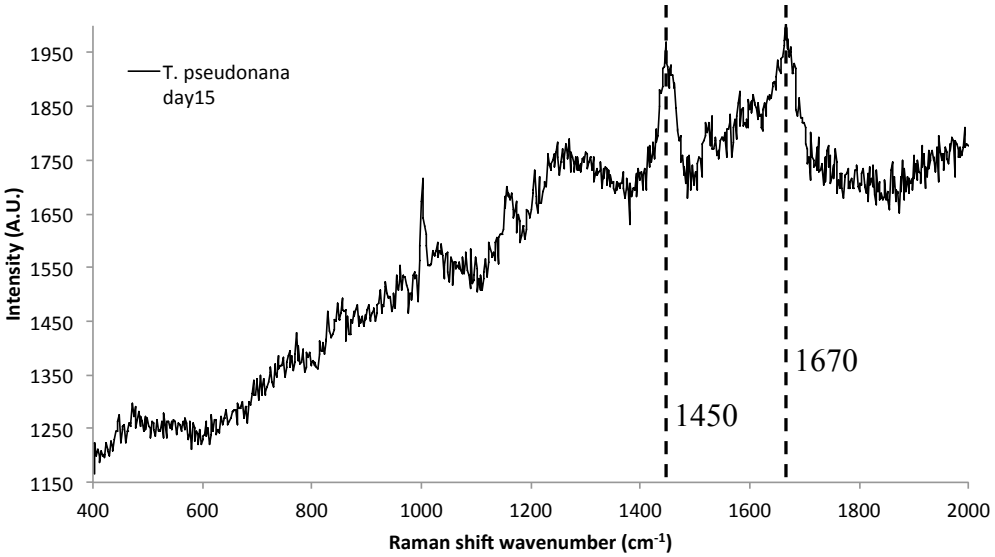

Figure 33. Raman spectra for a *T. pseudonana* cell from the phenanthrene co-culture treatment on day 15 showing prominent lipid and/or protein at wavenumbers 1450 and 1670 cm^{-1} using assignments collected from Wu *et al.* (2011). Spectra collected by Dr. Márton Palatinszky.

Appendix D: CARD-FISH probe optimization

In Chapter 2 (Section 2.2.2.1) CARD-FISH was used to locate *P. algicola* strain TG408 and *A. aromaticivorans* strain DG1253 in micro-algal cultures. In Chapter 5 (Section 5.2.2.4) CARD-FISH was used to locate the *Marinobacter* genus on *L. pertusa* polyp sections. The probes PCY223, ALGAR209 and MRB625a target the 16S rRNA of *P. algicola*, *A. aromaticivorans* and *Marinobacter* (62.5% of this genus) respectively. These probes have never been used before for CARD-FISH analysis before so hybridization conditions had to be optimized for use with their respective target organisms before the experiments in Chapters 2 and 5 could commence. This meant

performing multiple hybridizations at different stringencies (manipulated using different formamide concentrations) in order to select the most stringent conditions at which the oligonucleotide probes hybridize with their target rRNA sequences, producing maximum fluorescence intensity after CARD-FISH with minimum non-specific hybrids.

The strains *P. algicola* strain TG408 and *A. aromaticivorans* strain DG1253 were grown in 3ml volumes of liquid medium in the same way as described in Section 2.2.2.3, while *M. algicola* (positive target bacterium for MCTG625a) was grown on ZM/10 at 24°C until cloudy (4 -7 days). Once in late exponential-phase, 1 ml aliquots of bacterial cultures were washed twice (1xPBS) by centrifugation (8,000 *g*, 3 min) and fixed with 3% (v/v) paraformaldehyde (PFA) in PBS (1x) for 3 h at 4°C. After washing (×3) with PBS (1x) samples were stored in 1:1 (v/v) solution of PBS (1x) and ethanol (99%) at -20°C. In wells on Teflon-coated (10-well) glass microscopic slides a small (3 µl) volume of each bacterial cell suspension was pipetted and allowed to dry under a laminar flow hood. The bacterial cells were equilibrated with sterile PBS (1x) before permeabilization and hybridization.

The oligonucleotide probes for CARD-FISH (ALGAR209 from Biomers; PCY223 and MRB625a from Thermo Fisher Biopolymers) were purchased labelled with horseradish peroxidase (HRP) in order to catalyze deposition of the Fluorescein or Cy3 labelled tyramides (purchased from Perkin Elmer). Competitor probes for ALGAR209 (cALGAR209) and MRB625a (HAL625a) probes were purchased from Integrated DNA Technologies (IDT), these competitors were always included in hybridizations with their respective HRP-labelled probes. Fluorescent tyramides were dissolved as per manufacturers instructions; oligonucleotide probes were used at a working concentration of 50 ng μl^{-1}. Cyanine 3 (Cy3) and fluorescein tyramide conjugates (Perkin-Elmer) were dissolved according to the manufacturer's instructions. NON338 and EUB338-I, -II and -III probes (purchased from Thermo Fisher Biopolymers) were used to confirm successful CARD-FISH technique and absence of nonspecific binding. NON338 hybridizations were inspected for absence of fluorescent signals. Oligonucleotide probe sequences are listed below.

Probe sequences 5'- 3':

EUB338-I HRP-5' - GCT GCC TCC CGT AGG AGT- 3' most bacteria (Amann *et al.*, 1990)

EUB338-II HRP-5' - GCA GCC ACC CGT AGG TGT - 3' *Planctomycetales* (Daims *et al.*, 1999)

EUB338-III HRP-5' - GCT GCC ACC CGT AGG TGT - 3' *Verrucomicrobia* (Daims *et al.*, 1999)

NON338 HRP-5' - ACT CCT ACG GGA GGC AGC - 3' Negative control probe (Wallner *et al.*, 1993)

ALGAR209 HRP-5' - CCT CCA GCG TGA GGT CCG - 3' *Algiphilus aromaticivorans*

c1ALGAR209 5' - CCT CCA GCG CGA GGT CCG - 3' (competitor for probe ALGAR209)

MRB625a HRP-5' - CAG TTC GAA ATG CCG TTC CCA - 3' *Marinobacter* probe McKay *et al.* (2016)

HAL625a - 5' - CAG TTC CAA ATG CCG TTC CCA - 3' – MRB625a competitor probe (McKay *et al.*, 2016)

PCY223 HRP-5' - TCA GAC ATA GGC TCC TCC AA - 3' *Polycyclovorans algicola* (Gutierrez *et al.*, 2013b)

Protocols for lysozyme permeabilization, hybridization and signal amplification have been previously described by (Neulinger *et al.*, 2009). Cells were permeabilized by incubation in lysozyme buffer (1.355×10^6 U ml^{-1} lysozyme, 50 mM EDTA [pH 8.0], 300 mM Tris-HCl [pH 8.0]) at 37°C for 2 h. The slides were washed in H_2O for 1 min then incubated in of 0.01M HCl (10 min, RT) to bleach endogenous peroxidases, followed by another wash in H_2O (1 min, RT) and air-drying. Hybridization buffers were mixed with probe working solutions at a ratio of 1:249 and 30 µl of was placed into the wells on the Teflon coated slides (for filter sections in Chapter 2 and coral sections in Chapter 5 50 – 100 µl volumes were used). Slides were incubated at 46°C for at least 90 min, followed by 15 min in washing buffer (48°C). Optimal hybridization conditions were determined by performing multiple hybridizations using hybridization buffers containing a range of formamide (0% – 70%) concentrations. Competitor probes were always added in equimolar amounts to their respective probes. Hybridization buffers contained 900 mM NaCl, 20mM Tris-HCl (pH 8), 10% (w/v)

dextran sulfate (Sigma), 0.01% (w/v) sodium dodecyl sulphate and 10% blocking solution. The blocking solution consisted of 10% blocking reagent (Perkin Elmer) and maleic acid buffer (1.16% [w/v] maleic acid, 150 mM NaCl, pH 7.5). The washing buffer consisted of NaCl (variable concentration to maintain hybridization stringency) 20 mM Tris-HCl (pH 8), 5 mM EDTA (pH 8) and 0.01% (w/v) SDS. Excess washing buffer was removed with blotting paper. The samples were incubated with PBS (~10 ml, RT, 20 min) and once again excess liquid was removed. Samples were incubated at 46°C for 30 min with 1 part fluorescently labelled tyramide and 499 parts amplification buffer (10% [v/v] blocking solution (see above), 2 M NaCl, 10% [w/v] dextran sulfate, 0.0015% [v/v] H_2O_2, 100% [v/v] PBS [pH 7.3]). Samples were washed in PBS (pH 7.3, 20 min, RT) and H_2O three times (~10 ml, RT, 1 min) and 96% ethanol (~10 ml, RT, 3 sec) before air-drying (some were stored in freezer at -20°C). Samples were covered in mountant (80% [v/v] Citifluor, 14% [v/v] Vectashield, 1 μg ml^{-1} DAPI in 100% PBS [pH 9]) before microscopic observation.

Samples were visualized using a Zeiss (Axio Scope.A1) epifluorescence microscope fitted with Carl Zeiss Filter Sets 01, 09 and 15 (for use with DAPI, Fluorescein and Cy3 respectively) and a Zeiss digital fluorescence imaging camera (AxioCam MRm). Amplified signal intensities were quantified using Zeiss Zen-Blue (2012) imaging analysis module. Six to eight fields of view (~300 – 500 bacterial cells) were counted for fluorescence intensity maximum quantification. The melting curves for each probe are shown in Figure 34. For the PCY223 HRP-labelled probe a formamide concentration of 55 – 60% is recommended (Figure 34A), for the ALGAR209 HRP-labelled probe a formamide concentration of 35 – 40% is recommended (Figure 34B) and for the MRB625a HRP-labelled probe a formamide concentration of 55% is recommended (Figure 34C) in order to obtain maximum fluorescence and to minimize non-specific binding. These concentrations were used for probing for PAH-degraders in diatom cultures (in Chapter 2) and for probing *L. pertusa* polyps for *Marinobacter* (in Chapter 5).

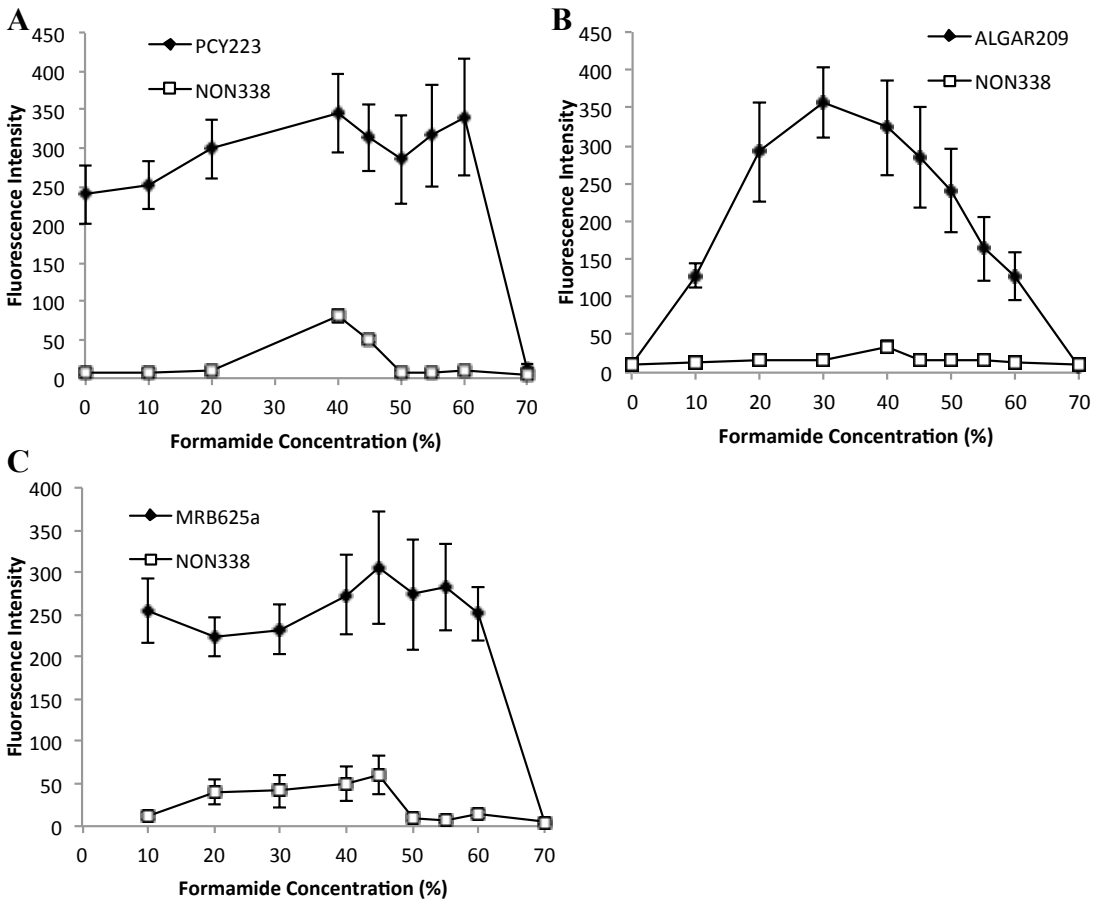

Figure 34. Maximum pixel intensity melting curves (mean intensity ± standard deviation) at different formamide concentrations (%). Target bacterial cells were measured after CARD-FISH using the following (5'-) HRP-labelled oligonucleotide probes: PCY223 (A), ALGAR209 (B) and MRB625a (C).

Appendix E: Details of micro-algal and bacterial growth media

Berges ASW was made following the recipe of Berges *et al.*, (2001) contained (per L of deionized water) 21.19 g NaCl, 9.592 g $MgCl_2 \cdot 6H_2O$, 3.55 g Na_2SO_4, 1.344 g $CaCl_2 \cdot 2H_2O$, 599 mg KCl, 174 mg $NaHCO_3$, 86.3 mg KBr, 46.7 mg $NaNO_3$, 30 mg $Na_2SiO_3 \cdot 9H_2O$, 23 mg H_3BO_3, 12.9 mg $SrCl_2$, 3.987 mg $Na_2HPO_4.2H_2O$, 3.09 mg $Na_2EDTA \cdot 2H_2O$, 2.8 mg NaF, 2.44 mg $Na_2EDTA \cdot 2H_2O$, 1.77 mg $FeCl_3 \cdot 6H_2O$, 540 µg $MnSO_4 \cdot 4H_2O$, 73 µg $ZnSO_4 \cdot 7H_2O$, 13.54 µg $CoCl_2.6H_2O$, 1.48 µg $Na_2MoO_4 \cdot 2H_2O$, 1.49 µg $NiCl_2 \cdot 6H_2O$, 0.173 µg Na_2SeO_3, 100 µg Thiamine HCl, 2 µg Biotin and 1 µg Cyanocobalamin.

F/2 medium (Guillard, 1975) contained (per L of filtered and autoclaved natural seawater) 75 mg $NaNO_3$, 5.65 mg $NaH_2PO_4 \cdot 2H_2O$, 4.16 mg Na_2 EDTA, 3.15 mg $FeCl_3 \cdot 6H2O$, 10 µg $CuSO_4 \cdot 5H2O$, 22 µg $ZnSO_4 \cdot 7H2O$, 10 µg $CoCl_2 \cdot 6H2O$, 180 µg $MnCl_2 \cdot 4H2O$, 6 µg $Na_2MoO4 \cdot 2H2O$, 100 µg Thiamine HCl, 1 µg Biotin and 1 µg Cyanocobalamin (pH adjusted to 8 using NaOH and HCl). Additionally **F/2+Si** for diatoms contained 30 mg $Na_2SiO_3 \cdot 9H_2O$ and while **F/2+Se** for dinoflagellates contained 2 mg Na_2SeO_3 (Band-Schmidt *et al.*, 2004; McQuoid *et al.*, 2002).

ONR7a was made following the recipe of Dyksterhouse *et al.*, (1995) and contained (per L of deionized water) 22.8 g NaCl, 11.18 g $MgCl_2 \cdot 6H_2O$, 3.98 g Na_2SO_4, 1.46 g $CaCl_2 \cdot 2H_2O$, 1.3 g TAPSO, 0.72 g KCl, 0.27 g NH_4Cl, 89 mg $Na_2HPO_4 \cdot 7H_2O$, 83 mg NaBr, 31 mg $NaHCO_3$, 27 mg H_3BO_3, 24 mg $SrCl_2 \cdot 6H_2O$, 2.6 mg NaF, 2.36 mg $FeCl_3 \cdot 6H_2O$ (pH adjusted to 8 using NaOH and HCl) (plus 15 g agar if solid media was required for plating).

ZM/10 contained (per L) 0.5 g bacto-peptone, 0.1 g yeast extract, 250 ml deionized water, 750 ml GF/C-filtered seawater (plus 15 g agar if solid media was required for plating). After serilization by autoclaving at 121˚C for 15 min the medium was supplemented with sterile trace elements and vitamins at the same concentrations as specified in Blackburn *et al.*, (1989).

Appendix F: Heidrun crude oil

A GC-FID chromatogram for the Heidrun crude oil at the time of inoculation is shown in Figure 35.

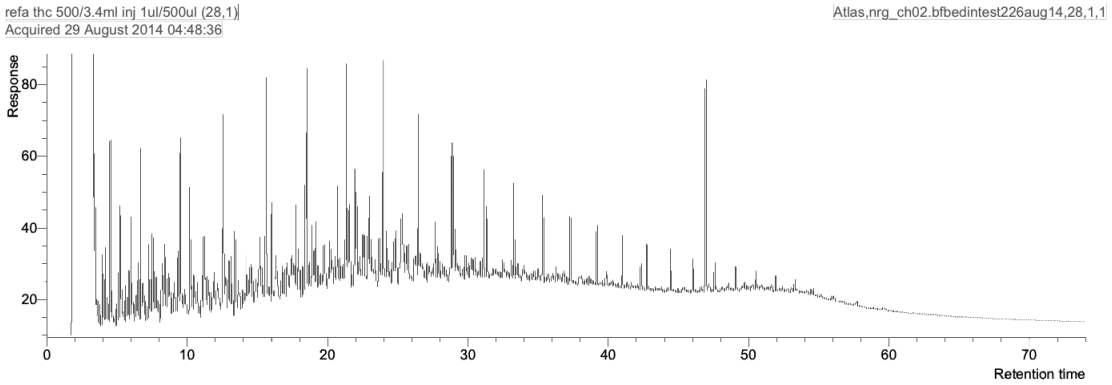

Figure 35. GC-FID chromatogram of the TPH fraction of Heidrun crude oil.

References

Abed, R.M.M. (2010) Interaction between cyanobacteria and aerobic heterotrophic bacteria in the degradation of hydrocarbons. *International Biodeterioration & Biodegradation*. **64**(1), 58–64.

Acuña Alvarez, L., Exton, D.A., Timmis, K.N., Suggett, D.J., McGenity, T.J. (2009) Characterization of marine isoprene-degrading communities. *Environmental Microbiology*. **11**(12), 3280–3291.

Adekunle, I.M., Ajijo, M.R., Adeofun, C.O., Omoniyi, I.T. (2010) Response of four phytoplankton species found in some sectors of nigerian coastal waters to crude oil in controlled ecosystem. *International Journal of Environmental Research*. **4**(1), 65–74.

Adger, W.N. (2000) Social and ecological resilience: are they related? *Progress in Human Geography*. **24**(3), 347–364.

Adiba, S., Nizak, C., van Baalen, M., Denamur, E., Depaulis, F. (2010) From grazing resistance to pathogenesis: The coincidental evolution of virulence factors. *PLoS ONE*. **5**(8), 1–10.

Akcha, F., Izuel, C., Venier, P., Budzinski, H., Burgeot, T., Narbonne, J.-F. (2000) Enzymatic biomarker measurement and study of DNA adduct formation in benzo[a]pyrene-contaminated mussels, *Mytilus galloprovincialis*. *Aquatic Toxicology*. **49**(4), 269–287.

Aksmann, A., Tukaj, Z. (2008) Intact anthracene inhibits photosynthesis in algal cells: A fluorescence induction study on *Chlamydomonas reinhardtii* cw92 strain. *Chemosphere*. **74**(1), 26–32.

Al-Bader, D., Eliyas, M., Rayan, R., Radwan, S. (2012) Air-dust-borne associations of phototrophic and hydrocarbon-utilizing microorganisms: promising consortia in volatile hydrocarbon bioremediation. *Environmental Science and Pollution Research International*. **19**(9), 3997–4005.

Alagely, A., Krediet, C.J., Ritchie, K.B., Teplitski, M. (2011) Signaling-mediated cross-talk modulates swarming and biofilm formation in a coral pathogen *Serratia marcescens*. *ISME Journal*. **5**(10), 1609–1620.

Alhassan, A., Andersson, J.T. (2013) Ketones in Fossil Materials – A mass spectrometric analysis of a crude oil and a coal tar. *Energy & Fuels*. **27**(10), 5770–5778.

Allamandola, L.J., Tielens, A.G., Barker, J.R. (1989) Interstellar polycyclic aromatic hydrocarbons: the infrared emission bands, the excitation/emission mechanism, and the astrophysical implications. *The Astrophysical Journal. Supplement Series*. **71**, 733–775.

Alldredge, A.L., Silver, M.W. (1988) Characteristics, dynamics and significance of marine snow. *Progress in Oceanography*. **20**(1), 41–82.

Almeda, R., Hyatt, C., Buskey, E.J. (2014) Toxicity of dispersant Corexit 9500A and crude oil to marine microzooplankton. *Ecotoxicology and Environmental Safety*. **106**, 76–85.

Almeda, R., Wambaugh, Z., Wang, Z., Hyatt, C., Liu, Z., Buskey, E.J. (2013) Interactions between zooplankton and crude oil: Toxic effects and bioaccumulation of polycyclic aromatic hydrocarbons. S. J. Johnson, ed. *PLoS ONE*. **8**(6), e67212.

Amann, R.I., Binder, B.J., Olson, R.J., Chisholm, S.W., Devereux, R., Stahl, D.A. (1990) Combination of 16S rRNA-targeted oligonucleotide probes with flow cytometry for analyzing mixed microbial populations. *Applied and Environmental Microbiology*. **56**(6), 1919–1925.

Amin, S.A., Green, D.H., Hart, M.C., Küpper, F.C., Sunda, W.G., Carrano, C.J. (2009) Photolysis of iron-siderophore chelates promotes bacterial-algal mutualism. *Proceedings of the National Academy of Sciences of the United States of America*. **106**(40), 17071–17076.

Amin, S.A., Hmelo, L.R., van Tol, H.M., Durham, B.P., Carlson, L.T., Heal, K.R., Morales, R.L., Berthiaume, C.T., Parker, M.S., Djunaedi, B., Ingalls, A.E., Parsek, M.R., Moran, M.A., Armbrust, E.V. (2015) Interaction and signalling between a cosmopolitan phytoplankton and associated bacteria. *Nature*. **522**(7554), 98–101.

Amin, S.A., Parker, M.S., Armbrust, E.V. (2012) Interactions between diatoms and bacteria. *Microbiology and Molecular Biology Reviews*. **76**(3), 667–684.

Andelman, J.B., Suess, M.J. (1970) Polynuclear aromatic hydrocarbons in the water environment. *Bulletin of the World Health Organization*. **43**(3), 479–508.

Anderson, O.R., Rogerson, A. (1995) Annual abundances and growth potential of *Gymnamoebae* in the Hudson estuary with comparative data from the Firth of Clyde. *European Journal of Protistology*. **31**(2), 223–233.

Andreasson, U., Perret-Liaudet, A., van Waalwijk van Doorn, L.J.C., Blennow, K., Chiasserini, D., Engelborghs, S., Fladby, T., Genc, S., Kruse, N., Kuiperij, H.B., Kulic, L., Lewczuk, P., Mollenhauer, B., Mroczko, B., Parnetti, L., Vanmechelen, E., Verbeek, M.M., Winblad, B., Zetterberg, H., Koel-Simmelink, M., Teunissen, C.E. (2015) A practical guide to immunoassay method validation. *Frontiers in Neurology*. **6**(179), 1-8.

Ankrah, N.Y.D., Lane, T., Budinoff, C.R., Hadden, M.K. (2014) Draft genome sequence of *Sulfitobacter* sp. cb2047 , a member of the Roseobacter clade of marine bacteria, isolated from an *Emiliania Huxleyi* bloom. *Genome Announcements*. **2**(6), 1–2.

Annweiler, E., Richnow, H.H., Antranikian, G., Hebenbrock, S., Garms, C., Franke, S., Francke, W., Michaelis, W. (2000) Naphthalene degradation and incorporation of naphthalene-derived carbon into

biomass by the thermophile *Bacillus thermoleovorans*. *Applied and Environmental Microbiology*. **66**(2), 518–523.

Arar, E.J., Collins, G.B. (1997) Method 445.0 *In vitro* determination of chlorophyll a and pheophytin a in marine and freshwater algae by fluorescence. *U.S. Environmental Protection Agency, Washington, DC, 1997*. pp 1-22

Arber, W. (2000) Genetic variation: molecular mechanisms and impact on microbial evolution. *FEMS Microbiology Reviews*. **24**(1) 1-7.

Archer, M.D., Barber, J. (2004) Molecular to global photosynthesis. Imperial College Press. pp 1-764.

Arias, A.H., Souissi, A., Roussin, M., Ouddane, B., Souissi, S. (2016) Bioaccumulation of PAHs in marine zooplankton: an experimental study in the copepod *Pseudodiaptomus marinus*. *Environmental Earth Sciences*. **75**(8), p 691.

Arias, L., Bauzá, J., Tobella, J., Vila, J., Grifoll, M. (2008) A microcosm system and an analytical protocol to assess PAH degradation and metabolite formation in soils. *Biodegradation*. **19**(3), 425–34.

Armbrust, E.V., Berges, J.A., Bowler, C., Green, B.R., Martinez, D., Putnam, N.H., Zhou, S., Allen, A.E., Apt, K.E., Bechner, M., Brzezinski, M.A., Chaal, B.K., Chiovitti, A., Davis, A.K., Demarest, M.S., Detter, J.C., Glavina, T., Goodstein, D., Hadi, M.Z., Hellsten, U. (2004) The genome of the diatom *Thalassiosira pseudonana*: ecology, evolution, and metabolism. *Science (New York, N.Y.)*. **306**(5693), 79–86.

Arnosti, C. (2011) Microbial extracellular enzymes and the marine carbon cycle. *Annual Review of Marine Science.* **3**,401-425

Arnosti, C., Ziervogel, K., Yang, T., Teske, A. (2015) Oil-derived marine aggregates - hot spots of polysaccharide degradation by specialized bacterial communities. *Deep-Sea Research Part II: Topical Studies in Oceanography*. **129**, 179–186.

Aslam, S.N., Underwood, G.J.C., Kaartokallio, H., Norman, L., Autio, R., Fischer, M., Kuosa, H., Dieckmann, G.S., Thomas, D.N. (2012) Dissolved extracellular polymeric substances (dEPS) dynamics and bacterial growth during sea ice formation in an ice tank study. *Polar Biology*. **35**(5), 661–676.

Atlas, R.M., Hazen, T.C. (2011) Oil biodegradation and bioremediation: A tale of the two worst spills in U.S. History. *Environmental Science and Technology*. **45**(16), 6709–6715.

Atlas, R.M.M. (1981) Microbial degradation of petroleum hydrocarbons: an environmental perspective. *Microbiological Reviews*. **45**(1), 180–209.

Aumont, O., Belviso, S., Monfray, P. (2002) Dimethylsulfoniopropionate (DMSP) and dimethylsulfide (DMS) sea surface distributions simulated from a global three-dimensional ocean carbon cycle model. *Journal of Geophysical Research*. **107**(C4), 4-1–4-19.

Bacosa, H.P., Liu, Z., Erdner, D.L. (2015) Natural sunlight shapes crude oil-degrading bacterial communities in northern Gulf of Mexico surface waters. *Frontiers in Microbiology*. **6**, 1-14.

Bælum, J., Borglin, S., Chakraborty, R., Fortney, J.L., Lamendella, R., Mason, O.U., Auer, M., Zemla, M., Bill, M., Conrad, M.E., Malfatti, S.A., Tringe, S.G., Holman, H.Y., Hazen, T.C., Jansson, J.K. (2012) Deep-sea bacteria enriched by oil and dispersant from the Deepwater Horizon spill. *Environmental Microbiology*. **14**(9), 2405–2416.

Bagi, A., Pampanin, D.M., Lanzén, A., Bilstad, T., Kommedal, R. (2014) Naphthalene biodegradation in temperate and arctic marine microcosms. *Biodegradation*. **25**(1), 111–125.

Baker, K.H., Herson, D.S. (1978) Interactions between the diatom *Thallasiosira pseudonanna* and an associated pseudomonad in a mariculture system. *Applied and Environmental Microbiology*. **35**(4), 791–796.

Baña, Z., Ayo, B., Marrasé, C., Gasol, J.M., Iriberri, J. (2014) Changes in bacterial metabolism as a response to dissolved organic matter modification during protozoan grazing in coastal Cantabrian and Mediterranean waters. *Environmental Microbiology*. **16**(2), 498–511.

Band-Schmidt, C.J., Morquecho, L., Lechuga-Devéze, C.H., Anderson, D.M. (2004) Effects of growth medium, temperature, salinity and seawater source on the growth of *Gymnodinium catenatum* (*Dinophyceae*) from Bahia Concepcion, Gulf of California, Mexico. *Journal of Plankton Research*. **26**(12), 1459–1470.

Barakat, A.O., Qian, Y., Kim, M., Kennicutt Ii, M.C. (2002) Compositional changes of aromatic steroid hydrocarbons in naturally weathered oil residues in the Egyptian Western Desert. *Environmental Forensics*. **3**, 219–225.

Barbirato, F., Verdoes, J.C., de Bont, J.A.., van der Werf, M.J. (1998) The *Rhodococcus erythropolis* DCL14 limonene-1,2-epoxide hydrolase gene encodes an enzyme belonging to a novel class of epoxide hydrolases. *FEBS Letters*. **438**(3), 293–296.

Barker, R.A., Tisnado, J., Lambert, L.A., Gärdes, A., Carrano, M.W., Carrano, P.N., Gillian, C., Carrano, C.J. (2015) Molecular characterization of a homolog of the ferric-uptake regulator, Fur, from the marine bacterium *Marinobacter algicola* DG893. *Biometals*. **28**(1), 197–206.

Beaudet, J.M., Weyers, A., Solakyildirim, K., Yang, B., Takieddin, M., Mousa, S., Zhang, F., Linhardt, R.J. (2011) Impact of autoclave sterilization on the activity and structure of formulated heparin. *Journal of Pharmaceutical Sciences*. **100**(8), 3396–404.

Becker, J.R. (1997) Crude oil waxes, emulsions, and asphaltenes. Pennwell Books.

Bell, D., Rossman, G.R. (1992) Water in Earth's mantle: The role of nominally anhydrous minerals. *Science*. **255**(5050), 1391-1397.

Bell, W., Mitchell, R. (1972) Chemotactic and growth responses of marine bacteria to algal extracellular products. *Biological Bulletin*. **143**, 265–277.

Bendich, A., Machlin, L.J., Scandurra, O., Burton, G.W., Wayner, D.D.M. (1986) The antioxidant role of vitamin C. *Advances in Free Radical Biology & Medicine*. **2**(2), 419–444.

Berges, J.A., Charlebois, D.O., Mauzerall, D.C., Falkowski, P.G. (1996) Differential effects of nitrogen limitation on photosynthetic efficiency of Photosystems I and II in microalgae. *Plant Physiology*. **110**(2), 689–696.

Berges, J.A., Franklin, D.J., Harrison, P.J. (2001) Evolution of an artificial seawater medium: Improvements in enriched seawater, artificial water over the last two decades. *Journal of Phycology*. **37**(6), 1138–1145.

Berntssen, M.H.G., Julshamn, K., Lundebye, A.K. (2010) Chemical contaminants in aquafeeds and Atlantic salmon (*Salmo salar*) following the use of traditional- versus alternative feed ingredients. *Chemosphere*. **78**(6), 637–646.

Berrojalbiz, N., Lacorte, S., Calbet, A., Saiz, E., Barata, C., Dachs, J. (2009) Accumulation and cycling of polycyclic aromatic hydrocarbons in zooplankton. *Environmental Science & Technology*. **43**(7), 2295–2301.

Biegala, I.C., Not, F., Vaulot, D., Simon, N. (2003) Quantitative assessment of picoeukaryotes in the natural environment by using taxon-specific oligonucleotide probes in association with tyramide signal amplification-fluorescence *in situ* hybridization and flow cytometry. *Applied and Environmental Microbiology*. **69**(9), 5519–5529.

Binark, N., Güven, K.C., Gezgin, T., Ünlü, S. (2000) Oil pollution of marine algae. *Bulletin of Environmental Contamination and Toxicology*. **64**(6), 866–872.

Biswas, N.N., Kutty, S.K., Barraud, N., Iskander, G.M., Griffith, R., Rice, S.A., Willcox, M., Black, D.S., Kumar, N. (2015) Indole-based novel small molecules for the modulation of bacterial signalling pathways. *Organic & Biomolecular Chemistry*. **13**(3), 925–937.

Blackburn, S.I., Hallegraef, G.M., Bolch, C.J. (1989) Vegetative reproduction and sexual life cycle of the toxic dinoflagellate *Gymnodinium catenatum* from Tasmania, Australia. *Journal of Phycology*. **25**(3), 577–590.

Bode, A., González, N., Lorenzo, J., Valencia, J., Varela, M.M., Varela, M. (2006) Enhanced bacterioplankton actvity after the 'Prestige' oil spill off Galicia, NWW Spain. *Aquatic Microbial Ecology*. **43**, 33–41.

Boden, R., Kelly, D.P., Murrell, J.C., Schäfer, H. (2010) Oxidation of dimethylsulfide to tetrathionate by *Methylophaga thiooxidans* sp. nov.: A new link in the sulfur cycle. *Environmental Microbiology*. **12**(10), 2688–2699.

Boehm, P.D., Neff, J.M., Page, D.S. (2007) Assessment of polycyclic aromatic hydrocarbon exposure in the waters of Prince William Sound after the Exxon Valdez oil spill: 1989–2005. *Marine Pollution Bulletin.* **54**, 339-356.

Boehm, P.D., Page, D.S. (2007) Exposure elements in oil spill risk and natural resource damage assessments: A review. *Human and Ecological Risk Assessment: An International Journal*. **13**(12), 418–448.

Bojes, H.K., Pope, P.G. (2007) Characterization of EPA's 16 priority pollutant polycyclic aromatic hydrocarbons (PAHs) in tank bottom solids and associated contaminated soils at oil exploration and production sites in Texas. *Regulatory Toxicology and Pharmacology*. **47**(3), 288–295.

Bolton, J.L., Trush, M.A., Penning, T.M., Dryhurst, G., Monks, T.J. (2000) Role of quinones in toxicology. *Chemical research in toxicology*. **13**(3), 135–60.

Bonin, P., Vieira, C., Grimaud, R., Militon, C., Cuny, P., Lima, O., Guasco, S., Brussaard, C.P.D., Michotey, V. (2015) Substrates specialization in lipid compounds and hydrocarbons of *Marinobacter* genus. *Environmental Science and Pollution Research*. **22**(20), 15347–15359.

Bopp, S.K., Lettieri, T. (2007) Gene regulation in the marine diatom *Thalassiosira pseudonana* upon exposure to polycyclic aromatic hydrocarbons (PAHs). *Gene*. **396**(2), 293–302.

Borde, X., Guieysse, B., Delgado, O., Muñoz, R., Hatti-Kaul, R., Nugier-Chauvin, C., Patin, H., Mattiasson, B. (2003) Synergistic relationships in algal–bacterial microcosms for the treatment of aromatic pollutants. *Bioresource Technology*. **86**(3), 293–300.

Borghoff, S.J., Parkinson, H., Leavens, T.L. (2010) Physiologically based pharmacokinetic rat model for methyl tertiary-butyl ether; comparison of selected dose metrics following various MTBE exposure scenarios used for toxicity and carcinogenicity evaluation. *Toxicology*. **275**(1–3), 79–91.

Borneff, J., Selenka, F., Kunte, H., Maximos, A. (1968) Experimental studies on the formation of polycyclic aromatic hydrocarbons in plants. *Environmental Research*. **2**(1), 22–29.

Bowman, J.P., McCammon, S.A., Brown, M. V, Nichols, D.S., McMeekin, T.A. (1997) Diversity and association of psychrophilic bacteria in Antarctic sea ice. *Applied and Environmental Microbiology*. **63**(8),

3068–3078.

Brakstad, O.G., Nonstad, I., Faksness, L.G., Brandvik, P.J. (2008) Responses of microbial communities in Arctic sea ice after contamination by crude petroleum oil. *Microbial Ecology*. **55**(3), 540–552.

Brakstad, O.G., Throne-Holst, M., Netzer, R., Stoeckel, D.M., Atlas, R.M. (2015) Microbial communities related to biodegradation of dispersed Macondo oil at low seawater temperature with Norwegian coastal seawater. *Microbial Biotechnology*. **8**(6), 989–998.

Braun, V., Hantke, K. (2011) Recent insights into iron import by bacteria. *Current Opinion in Chemical Biology*. **15**(2), 328–334.

Brimblecombe, P. (1986) *Air Composition and Chemistry*. Cambridge University Press.

Broecker, W., Clark, E. (2009) Ratio of coccolith $CaCO_3$ to foraminifera $CaCO_3$ in late Holocene deep sea sediments. *Paleoceanography*. **24**(PA3205), 1-11.

Brooke, S., Young, C.M. (2009) In situ measurement of survival and growth of *Lophelia pertusa* in the northern Gulf of Mexico. *Marine Ecology Progress Series*. **397**, 153–161.

Brookfield, K., Gray, T., Hatchard, J. (2005) The concept of fisheries-dependent communities: A comparative analysis of four UK case studies: Shetland, Peterhead, North Shields and Lowestoft. *Fisheries Research*. **72**, 55–69.

Brown, S.D., Chiavari, G., Ediger, V., Fabbri, D., Gaines, A.F., Galletti, G., Karayigit, A.I., Love, G.D., Snape, C.E., Sirkecioglu, O., Toprak, S. (2000) Black Sea sapropels: Relationship to kerogens and fossil fuel precursors. *Fuel*. **79**(14), 1725–1742.

Brück, T.B., Brück, W.M., Santiago-Vázquez, L.Z., McCarthy, P.J., Kerr, R.G. (2007) Diversity of the bacterial communities associated with the azooxanthellate deep water octocorals *Leptogorgia minimata*, *Iciligorgia schrammi*, and *Swiftia exertia*. *Marine Biotechnology*. **9**(5), 561–576.

Bruckner, C.G., Bahulikar, R., Rahalkar, M., Schink, B., Kroth, P.G. (2008) Bacteria associated with benthic diatoms from Lake Constance: Phylogeny and influences on diatom growth and secretion of extracellular polymeric substances. *Applied and Environmental Microbiology*. **74**(24), 7740–7749.

Bruckner, C.G., Rehm, C., Grossart, H.-P., Kroth, P.G. (2011) Growth and release of extracellular organic compounds by benthic diatoms depend on interactions with bacteria. *Environmental Microbiology*. **13**(4), 1052–1063.

Brunel, F., Davison, J. (1988) Cloning and sequencing of *Pseudomonas* genes encoding vanillate demethylase. *Journal Of Bacteriology*. **170**(10), 4924–4930.

Brussaard, C.P.D., Peperzak, L., Beggah, S., Wick, L.Y., Wuerz, B., Weber, J., Samuel Arey, J., van der Burg, B., Jonas, A., Huisman, J., van der Meer, J.R. (2016) Immediate ecotoxicological effects of short-lived oil spills on marine biota. *Nature Communications*. **7**, 11206.

Brzostek, A., Pawelczyk, J., Rumijowska-Galewicz, A., Dziadek, B., Dziadek, J. (2009) *Mycobacterium tuberculosis* is able to accumulate and utilize cholesterol. *Journal of Bacteriology*. **191**(21), 6584–6591.

Buchan, A., LeCleir, G.R., Gulvik, C.A., González, J.M. (2014) Master recyclers: features and functions of bacteria associated with phytoplankton blooms. *Nature Reviews Microbiology*. **12**(10), 686–698.

Cappello, S., Russo, D., Santisi, S., Calogero, R., Gertler, C., Crisafi, F., De Domenico, M., Yakimov, M.M. (2012) Presence of hydrocarbon-degrading bacteria in the gills of mussel *Mytilus galloprovincialis* in a contaminated environment: a mesoscale simulation study. *Chemistry and Ecology*. **28**(3), 239–252.

Capy, P., Gasperi, G., Biémont, C., Bazin, C. (2000) Stress and transposable elements: co-evolution or useful parasites? *Heredity*. **85**(2), 101–106.

Carlos, C., Torres, T.T., Ottoboni, L.M.M. (2013) Bacterial communities and species-specific associations with the mucus of Brazilian coral species. *Scientific Reports*. **3**, 01624.

Carls, M.G., Holland, L., Larsen, M., Collier, T.K., Scholz, N.L., Incardona, J.P. (2008) Fish embryos are damaged by dissolved PAHs, not oil particles. *Aquatic Toxicology*. **88**(2), 121–127.

Caron, D.A., Davis, P.G., Madin, L.P., Sieburth, J.M. (1982) Heterotrophic bacteria and bacterivorous protozoa in oceanic macroaggregates. *Science*. **218**(4574), 795–797.

Carvalho, R.N., Bopp, S.K., Lettieri, T. (2011) Transcriptomics responses in marine diatom *Thalassiosira pseudonana* exposed to the polycyclic aromatic hydrocarbon benzo[a]pyrene. *PLoS ONE*. **6**(11), e26985.

Chalfie, M. (2009) GFP: lighting up life (Nobel lecture). *Angewandte Chemie (International ed. in English)*. **48**(31), 5603–5611.

Chang, F.H., Zeldis, J., Gall, M., Hall, J. (2003) Seasonal and spatial variation of phytoplankton assemblages, biomass and cell size from spring to summer across the north-eastern New Zealand continental shelf. *Journal of Plankton Research*. **25**(7), 737–758.

Chang, Y.-J., Stephen, J.R., Richter, A.P., Venosa, A.D., Brüggemann, J., Macnaughton, S.J., Kowalchuk, G.A., Haines, J.R., Kline, E., White, D.C. (2000) Phylogenetic analysis of aerobic freshwater and marine enrichment cultures efficient in hydrocarbon degradation: Effect of profiling method. *Journal of Microbiological Methods*. **40**(1), 19–31.

Charrié-Duhaut, A., Lemoine, S., Adam, P., Connan, J., Albrecht, P. (2000) Abiotic oxidation of petroleum bitumens under natural conditions. *Organic Geochemistry*. **31**(10), 977–1003.

Chavez-Dozal, A., Gorman, C., Erken, M., Steinberg, P.D., McDougald, D., Nishiguchi, M.K. (2013) Predation response of *Vibrio fischeri* biofilms to bacterivorus protists. *Applied and Environmental Microbiology*. **79**(2), 553–558.

Chin, C.-S., Alexander, D.H., Marks, P., Klammer, A.A., Drake, J., Heiner, C., Clum, A., Copeland, A., Huddleston, J., Eichler, E.E., Turner, S.W., Korlach, J. (2013) Nonhybrid, finished microbial genome assemblies from long-read SMRT sequencing data. *Nature Methods*. **10**(6), 563–569.

Chisti, Y. (2006) Biodiesel from microalgae. *Biotechnology Advances*. **25**(3), 294–306.

Cho, H.J., Kim, K., Sohn, S.Y., Cho, H.Y., Kim, K.J., Kim, M.H., Kim, D., Kim, E., Kang, B.S. (2010) Substrate binding mechanism of a type I extradiol dioxygenase. *The Journal of Biological Chemistry*. **285**(45), 34643–34652.

Chrimes, A.F., Khoshmanesh, K., Tang, S.Y., Wood, B.R., Stoddart, P.R., Collins, S.S.E., Mitchell, A., Kalantar-zadeh, K. (2013) *In situ* SERS probing of nano-silver coated individual yeast cells. *Biosensors and Bioelectronics*. **49**, 536–541.

Chronopoulou, P.-M., Fahy, A., Coulon, F., Païssé, S., Goñi-Urriza, M., Peperzak, L., Acuña Alvarez, L., McKew, B.A., Lawson, T., Timmis, K.N., Duran, R., Underwood, G.J.C., McGenity, T.J. (2013) Impact of a simulated oil spill on benthic phototrophs and nitrogen-fixing bacteria in mudflat mesocosms. *Environmental Microbiology*. **15**(1), 242–252.

Clark, R.B., Frid, C., Attrill, M. (2001) *Marine pollution*. Oxford University Press.

Cnossen, I., Sanz-Forcada, J., Favata, F., Witasse, O., Zegers, T., Arnold, N.F. (2007) Habitat of early life: Solar X-ray and UV radiation at Earth's surface 4–3.5 billion years ago. *Journal of Geophysical Research.* **112**, E02008. **112**, E02008.

Coelho, F., Sousa, S., Santos, L., Santos, A., Almeida, A., Gomes, N., Cunha, Â. (2011) Exploring hydrocarbonoclastic bacterial communities in the estuarine surface microlayer. *Aquatic Microbial Ecology*. **64**(2), 185–195.

Cooper, M.B., Smith, A.G. (2015) Exploring mutualistic interactions between microalgae and bacteria in the omics age. *Current Opinion in Plant Biology*. **26**, 147–153.

Copeland, D.D., Facer, M., Newton, R., Walker, P.J., Leermakers, M., Lansens, P., Baeyens, W., Bothner, M.H., Robertson, D.E., Farey, B.J., Nelson, L.A., Rolph, M.G., Farey, B.J., Nelson, L.A., Griepink, B., Thompson, K.C., Godden, R.G. (1996) Use of poly(ethylene terephthalate) plastic bottles for the sampling, transportation and storage of potable water prior to mercury determination. *The Analyst*. **121**, 173-176.

Costello, M.J. (2014) Long live marine reserves: A review of experiences and benefits. *Biological Conservation*. **176**, 289–296.

Couillard, C.M., Lee, K. (2005) Effect of dispersant on the composition of the water-accommodated fraction of crude oil and its toxicity to larval marine fish. *Environmental Toxicology and Chemistry*. **24**(6), 1496–1504.

Coulon, F., Chronopoulou, P.-M., Fahy, A., Païssé, S., Goñi-Urriza, M., Peperzak, L., Acuña Alvarez, L., McKew, B.A., Brussaard, C.P.D., Underwood, G.J.C., Timmis, K.N., Duran, R., McGenity, T.J. (2012) Central role of dynamic tidal biofilms dominated by aerobic hydrocarbonoclastic bacteria and diatoms in the biodegradation of hydrocarbons in coastal mudflats. *Applied and Environmental Microbiology*. **78**(10), 3638–3648.

Crane, M., Watts, C., Boucard, T. (2006) Chronic aquatic environmental risks from exposure to human pharmaceuticals. *Science of the Total Environment*. **367**(1), 23–41.

Croce, R., van Amerongen, H. (2014) Natural strategies for photosynthetic light harvesting. *Nature Chemical Biology*. **10**(7), 492–501.

Croft, M.T., Lawrence, A.D., Raux-Deery, E., Warren, M.J., Smith, A.G. (2005) Algae acquire vitamin B12 through a symbiotic relationship with bacteria. *Nature*. **438**(7064), 90–3.

Croft, M.T., Warren, M.J., Smith, A.G. (2006) Algae need their vitamins. *Eukaryotic Cell*. **5**(8), 1175–1183.

Crump, B.C., Armbrust, E.V., Baross, J.A. (1999) Phylogenetic analysis of particle-attached and free-living bacterial communities in the Columbia River, it's Estuary, and the adjacent coastal ocean phylogenetic analysis of particle-attached and free-living bacterial communities in the Columbia River. *Applied and Environmental Microbiology*. **65**(7), 3192–3103.

Cruz-López, R., Maske, H. (2016) The vitamin B1 and B12 required by the marine dinoflagellate *Lingulodinium polyedrum* can be provided by its associated bacterial community in culture. *Frontiers in Microbiology*. **7**(560) 1-13.

Cui, Z., Xu, G., Gao, W., Li, Q., Yang, B., Yang, G., Zheng, L. (2014) Isolation and characterization of *Cycloclasticus* strains from Yellow Sea sediments and biodegradation of pyrene and fluoranthene by their syntrophic association with *Marinobacter* strains. *International Biodeterioration and Biodegradation*. **91**, 45–51.

Cuny, P., Acquaviva, M., Gilewicz, M., Gilewicz, M. (2004) Phenanthrene degradation, emulsification and surface tension activities of a *Pseudomonas putida* strain isolated from a coastal oil contaminated

microbial mat. *Ophelia*. **58**, 283–287.

D'souza, N.A., Subramaniam, A., Juhl, A.R., Hafez, M., Chekalyuk, A., Phan, S., Yan, B., MacDonald, I.R., Weber, S.C., Montoya, J.P. (2016) Elevated surface chlorophyll associated with natural oil seeps in the Gulf of Mexico. *Nature Geoscience*. **9**, 1–4.

da Fonseca, C.O., Simão, M., Lins, I.R., Caetano, R.O., Futuro, D., Quirico-Santos, T. (2011) Efficacy of monoterpene perillyl alcohol upon survival rate of patients with recurrent glioblastoma. *Journal of Cancer Research and Clinical Oncology*. **137**(2), 287–293.

da Silva, W.L., Lansarin, M.A., Livotto, P.R., dos Santos, J.H.Z. (2015) Photocatalytic degradation of drugs by supported titania-based catalysts produced from petrochemical plant residue. *Powder Technology*. **279**, 166–172.

Daims, H., Brühl, A., Amann, R., Schleifer, K.H., Wagner, M. (1999) The domain-specific probe EUB338 is insufficient for the detection of all Bacteria: development and evaluation of a more comprehensive probe set. *Systematic and Applied Microbiology*. **22**(3), 434–44.

Dalrymple, G.B. (2001) The age of the Earth in the twentieth century: a problem (mostly) solved. *Geological Society, London, Special Publications*. **190**(1), 205–221.

Daly, K.L., Passow, U., Chanton, J., Hollander, D. (2016) Assessing the impacts of oil-associated marine snow formation and sedimentation during and after the Deepwater Horizon oil spill. *Anthropocene*. **13**, 18-33.

Dashti, N., Ali, N., Eliyas, M., Khanafer, M., Sorkhoh, N.A., Radwan, S.S. (2015) Most hydrocarbonoclastic bacteria in the total environment are diazotrophic, which highlights their value in the bioremediation of hydrocarbon contaminants. *Microbes and Environments / Japanese Society of Microbial Ecology*. **30**(1), 70–5.

Daughtrey, W.C., Gill, M.W., Pritts, I.M., Douglas, J.F., Kneiss, J.J., Andrews, L.S. (1997) Neurotoxicological evaluation of methyl tertiary-butyl ether in rats. *Journal of Applied Toxicology*. Suppl **1**, S57-64.

Dawson, K.S., Schaperdoth, I., Freeman, K.H., Macalady, J.L. (2013) Anaerobic biodegradation of the isoprenoid biomarkers pristane and phytane. *Organic Geochemistry*. **65**, 118–126.

del Río, J.C., García-Mollá, J., González-Vila, F.J., Martín, F. (1993) Flash pyrolysis-gas chromatography of the kerogen and asphaltene fractions isolated from a sequence of oil shales. *Journal of Chromatography A*. **657**(1), 119–122.

Del Vento, S., Dachs, J. (2002) Prediction of uptake dynamics of persistent organic pollutants by bacteria and phytoplankton. *Environmental Toxicology and Chemistry*. **21**(10), 2099–2107.

Delong, E.F., Franks, D.G., Alldredge, A.L. (1993) Phylogenetic diversity of aggregate-attached vs. free-living marine bacterial assemblages. *Limnology and Oceanography*. **38**(5), 924–934.

DeSantis, T.Z., Hugenholtz, P., Larsen, N., Rojas, M., Brodie, E.L., Keller, K., Huber, T., Dalevi, D., Hu, P., Andersen, G.L. (2006) Greengenes, a chimera-checked 16S rRNA gene database and workbench compatible with ARB. *Applied and Environmental Microbiology*. **72**(7), 5069–5072.

Deveryshetty, J., Phale, P.S. (2009) Biodegradation of phenanthrene by *Pseudomonas* sp. strain PPD: purification and characterization of 1-hydroxy-2-naphthoic acid dioxygenase. *Microbiology*. **155**(9), 3083–3091.

Dewapriya, P., Kim, S. (2014) Marine microorganisms: An emerging avenue in modern nutraceuticals and functional foods. *Food Research International*. **56**, 115–125.

Didyk, B.M., Simoneit, B.R.T. (1989) Hydrothermal oil of Guaymas Basin and implications for petroleum formation mechanisms. *Nature*. **342**(6245), 65–69.

Didyk, B.M., Simoneit, B.R.T. (1990) Petroleum characteristics of the oil in a Guaymas Basin hydrothermal chimney. *Applied Geochemistry*. **5**(1–2), 29–40.

Diercks, A.-R., Highsmith, R.C., Asper, V.L., Joung, D., Zhou, Z., Guo, L., Shiller, A.M., Joye, S.B., Teske, A.P., Guinasso, N., Wade, T.L., Lohrenz, S.E. (2010) Characterization of subsurface polycyclic aromatic hydrocarbons at the Deepwater Horizon site. *Geophysical Research Letters*. **37**(20), L20602.

Díez, S., Sabatté, J., Viñas, M., Bayona, J.M., Solanas, A.M., Albaigés, J. (2005) The prestige oil spill. I. Biodegradation of a heavy fuel oil under simulated conditions. *Environmental Toxicology and Chemistry / SETAC*. **24**(9), 2203–2217.

Dodds, L., Black, K., Orr, H., Roberts, J. (2009) Lipid biomarkers reveal geographical differences in food supply to the cold-water coral *Lophelia pertusa* (*Scleractinia*). *Marine Ecology Progress Series*. **397**, 113–124.

Dodds, L.A., Roberts, J.M., Taylor, A.C., Marubini, F. (2007) Metabolic tolerance of the cold-water coral *Lophelia pertusa* (Scleractinia) to temperature and dissolved oxygen change. *Journal of Experimental Marine Biology and Ecology*. **349**(2), 205–214.

Dong, C., Bai, X., Sheng, H., Jiao, L., Zhou, H., Shao, Z. (2015) Distribution of PAHs and the PAH-degrading bacteria in the deep-sea sediments of the high-latitude Arctic Ocean. *Biogeosciences*. **12**(7), 2163–2177.

Donnenberg, V.S., Donnenberg, A.D. (2015) Coping with artifact in the analysis of flow cytometric data. *Methods*. **82**, 3–11.

Doyle, A., Saavedra, A., Tristão, M.L.B., Nele, M., Aucélio, R.Q. (2011) Direct chlorine determination in crude oils by energy dispersive X-ray fluorescence spectrometry: An improved method based on a proper strategy for sample homogenization and calibration with inorganic standards. *Spectrochimica Acta Part B: Atomic Spectroscopy*. **66**(5), 368–372.

Droop, M.R. (2007) Vitamins, phytoplankton and bacteria: Symbiosis or scavenging? *Journal of Plankton Research*. **29**(2), 107–113.

Ducklow, H.W., Steinberg, D.K., Buesseler, K.O. (2001) Upper ocean carbon export and the biological pump. *Oceanography*. **14**(4), 50–58.

Duineveld, G., Lavaleye, M., Berghuis, E. (2004) Particle flux and food supply to a seamount cold-water coral community (Galicia Bank, NW Spain). *Marine Ecology Progress Series*. **277**, 13–23.

Duran, R. (2010) In *Handbook of Hydrocarbon and Lipid Microbiology*. K.N. Timmis (ed.) Springer, Berlin. pp 1725-1736.

Duran, R., Cuny, P., Bonin, P., Cravo-Laureau, C. (2015) Microbial ecology of hydrocarbon-polluted coastal sediments. *Environmental Science and Pollution Research*. **22**(20), 15195–15199.

Dyksterhouse, S.E., Gray, J.P., Herwig, R.P., Staley, J.T. (1995) an Aromatic Hydrocarbon-Degrading Bacterium from Marine Sediments. *International Journal of Systematic Bacteriology*. **45**(1), 116–123.

Echeveste, P., Agustí, S., Dachs, J. (2010) Cell size dependent toxicity thresholds of polycyclic aromatic hydrocarbons to natural and cultured phytoplankton populations. *Environmental Pollution*. **158**(1), 299–307.

El-Dib, M., Moursy, A.S., Badawy, M.I. (1978) Role of adsorbents in the removal of soluble aromatic hydrocarbons from drinking waters. *Water Research*. **12**(12), 1131–1137.

Eneh, O.C. (2011) A Review on Petroleum: Source, Uses, Processing, Products and the Environment. *Journal of Applied Sciences*. **11**(12), 2084–2091.

Engel, U., Pertz, O., Fauser, C., Engel, J., David, C.N., Holstein, T.W. (2001) A switch in disulfide linkage during minicollagen assembly in *Hydra* nematocysts. *The EMBO Journal*. **20**(12), 3063–3073.

Erlacher, E., Loibner, A.P., Kendler, R., Scherr, K.E. (2013) Distillation fraction-specific ecotoxicological evaluation of a paraffin-rich crude oil. *Environmental Pollution*. **174**, 236–243.

Evdokimov, I.N., Eliseev, N.Y., Akhmetov, B.R. (2003) Assembly of asphaltene molecular aggregates as studied by near-UV/visible spectroscopy: I. Structure of the absorbance spectrum. *Journal of Petroleum Science and Engineering*. **37**(3), 135–143.

Exton, D.A., Suggett, D.J., McGenity, T.J., Steinke, M. (2013) Chlorophyll-normalized isoprene production in laboratory cultures of marine microalgae and implications for global models. *Limnology and Oceanography*. **58**(4), 1301–1311.

Exton, D.A., Suggett, D.J., Steinke, M., McGenity, T.J. (2012) Spatial and temporal variability of biogenic isoprene emissions from a temperate estuary. *Global Biogeochemical Cycles*. **26**, GB2012

Fabiani, R., Rosignoli, P., De Bartolomeo, A., Fuccelli, R., Morozzi, G. (2012) Genotoxicity of alkene epoxides in human peripheral blood mononuclear cells and HL60 leukaemia cells evaluated with the comet assay. *Mutation Research*. **747**(1), 1–6.

Falciatore, A., Bowler, C. (2002) Revealing the molecular secrets of marine diatoms. *Annual Review of Plant Biology*. **53**(1), 109–130.

Fall, R., Copley, S.D. (2000) Bacterial sources and sinks of isoprene, a reactive atmospheric hydrocarbon. *Environmental Microbiology*. **2**(2), 123–130.

Fan, C.-W., Reinfelder, J.R. (2003) Phenanthrene accumulation kinetics in marine diatoms. *Environmental Science & Technology*. **37**(15), 3405–3412.

Fathepure, B.Z. (2014) Recent studies in microbial degradation of petroleum hydrocarbons in hypersaline environments. *Frontiers in Microbiology*. **5**, 173.

Field, C.B., Behrenfeld, M.J., Randerson, J.T., Falkowski, P. (1998) Primary Production of the Biosphere: Integrating Terrestrial and Oceanic Components. **281**(5374), 237-240.

Foley, N.S., van Rensburg, T.M., Armstrong, C.W. (2010) The ecological and economic value of cold-water coral ecosystems. *Ocean & Coastal Management*. **53**(7), 313–326.

Formigaro, C., Henríquez-Hernandez, L.A., Zaccaroni, A., Garcia-Hartmann, M., Camacho, M., Boada, L.D., Zumbado, M., Luzardo, O.P. (2014) Assessment of current dietary intake of organochlorine contaminants and polycyclic aromatic hydrocarbons in killer whales (*Orcinus orca*) through direct determination in a group of whales in captivity. *The Science of the Total Environment*. **472**, 1044–1051.

Fosså, J.H., Mortensen, P.B., Furevik, D.M. (2002) The deep-water coral *Lophelia pertusa* in Norwegian waters: distribution and fishery impacts. *Hydrobiologia*. **471**(1), 1–12.

Freese, H.M., Dalingault, H., Petersen, J., Pradella, S., Davenport, K., Teshima, H., Chen, A., Pati, A., Ivanova, N., Goodwin, L.A., Chain, P., Detter, J.C., Rohde, M., Gronow, S., Kyrpides, N.C., Woyke, T., Brinkhoff, T., Göker, M., Overmann, J., Klenk, H.-P. (2013) Genome sequence of the phage-gene rich marine *Phaeobacter arcticus* type strain DSM 23566(T.). *Standards in Genomic Sciences*. **8**(3), 450–64.

Freiwald, A., Hühnerbach, V., Lindberg, B., Wilson, J.B., Campbell, J. (2002) The Sula Reef Complex, Norwegian shelf. *Facies*. **47**(1), 179–200.

Freiwald, A., Roberts, J.M. eds. (2005) *Cold-Water Corals and Ecosystems*. Berlin, Heidelberg:

Springer Berlin Heidelberg.

Frias, J.P.G.L., Sobral, P., Ferreira, A.M. (2010) Organic pollutants in microplastics from two beaches of the Portuguese coast. *Marine Pollution Bulletin*. **60**(11), 1988–1992.

Friedrich, U., Lenke, J. (2006) Improved enumeration of lactic acid bacteria in mesophilic dairy starter cultures by using multiplex quantitative real-time pcr and flow cytometry-fluorescence *in situ* hybridization. *Applied and Environmental Microbiology*. **72**(6), 4163–4171.

Frost, B.W. (1987) Grazing control of phytoplankton stock in the the role of mesozooplankton , particularly the. *Marine Ecology Progress Series*. **39**, 49–68.

Fu, J., Gong, Y., Zhao, X., O'Reilly, S.E., Zhao, D. (2014) Effects of oil and dispersant on formation of marine oil snow and transport of oil hydrocarbons. *Environmental Science and Technology*. **48**(24), 14392–14399.

Furusawa, Y., Nagarajan, V., Tanokura, M., Masai, E., Fukuda, M., Senda, T. (2004) Crystal structure of the terminal oxygenase component of biphenyl dioxygenase derived from *Rhodococcus* sp. Strain RHA1. *Journal of Molecular Biology*. **342**(3), 1041–1052.

Galliano, F., Dwek, E., Chanial, P. (2008) Stellar evolutionary effects on the abundances of polycyclic aromatic hydrocarbons and supernova–condensed dust in galaxies. *The Astrophysical Journal*. **672**(1), 214–243.

Gao, S., Seo, J.-S., Wang, J., Keum, Y.-S., Li, J., Li, Q.X. (2013) Multiple degradation pathways of phenanthrene by *Stenotrophomonas maltophilia* C6. *International Biodeterioration & Biodegradation*. **79**, 98–104.

Gärdes, A., Iversen, M.H., Grossart, H.-P., Passow, U., Ullrich, M.S. (2011) Diatom-associated bacteria are required for aggregation of *Thalassiosira weissflogii*. *The ISME Journal*. **5**(3), 436–445.

Gargaud, M., Lopez-Garcia, P., Martin, H. (2010) *Origins and Evolution of Life:An Astrobiological Perspective*. M. Gargaud, P. Lopez-Garcia, & H. Martin (ed.) Cambridge: Cambridge University Press.

Gass, S.E., Roberts, J.M. (2006) The occurrence of the cold-water coral *Lophelia pertusa* (*Scleractinia*) on oil and gas platforms in the North Sea: colony growth, recruitment and environmental controls on distribution. *Marine Pollution Bulletin*. **52**(5), 549–559.

Gauthier, M.J., Lafay, B., Christen, R., Fernandez, L., Acquaviva, M., Bonin, P., Bertrand, J.-C. (1992) *Marinobacter hydrocarbonoclasticus* gen. nov., sp. nov., a new, extremely halotolerant, hydrocarbon-degrading marine bacterium. *International Journal of Systematic Bacteriology*. **42**(4), 568–576.

Ge, Y., Vaillancourt, F.H., Agar, N.Y.R., Eltis, L.D. (2002) Reactivity of toluate dioxygenase with substituted benzoates and dioxygen. *Journal of Bacteriology*. **184**(15), 4096–4103.

Geiselbrecht, A.D., Hedlund, B.P., Tichi, M.A., Staley, J.T. (1998) Isolation of marine polycyclic aromatic hydrocarbon (PAH)-degrading *Cycloclasticus* strains from the Gulf of Mexico and comparison of their PAH degradation ability with that of Puget Sound *Cycloclasticus* strains. *Applied and Environmental Microbiology*. **64**(12), 4703–4710.

Geng, H., Belas, R. (2010) Molecular mechanisms underlying *Roseobacter*-phytoplankton symbioses. *Current Opinion in Biotechnology*. **21**(3), 332–338.

Gentile, G., Bonasera, V., Amico, C., Giuliano, L., Yakimov, M.M. (2003) *Shewanella* sp. GA-22, a psychrophilic hydrocarbonoclastic antarctic bacterium producing polyunsaturated fatty acids. *Journal of Applied Microbiology*. **95**(5), 1124–1133.

Gentile, G., Bonsignore, M., Santisi, S., Catalfamo, M., Giuliano, L., Genovese, L., Yakimov, M.M., Denaro, R., Genovese, M., Cappello, S. (2016) Biodegradation potentiality of psychrophilic bacterial strain *Oleispira antarctica* RB-8T. *Marine Pollution Bulletin*. **105**(1), 125–130.

Genty, B., Briantais, J.-M., Baker, N.R. (1989) The relationship between the quantum yield of photosynthetic electron transport and quenching of chlorophyll fluorescence. *Biochimica et Biophysica Acta - General Subjects*. **990**(1), 87–92.

Gerdes, B., Brinkmeyer, R., Dieckmann, G., Helmke, E. (2005) Influence of crude oil on changes of bacterial communities in Arctic sea-ice. *FEMS Microbiology Ecology*. **53**(1), 129–139.

Gertler, C., Näther, D.J., Cappello, S., Gerdts, G., Quilliam, R.S., Yakimov, M.M., Golyshin, P.N. (2012) Composition and dynamics of biostimulated indigenous oil-degrading microbial consortia from the Irish, North and Mediterranean Seas: A mesocosm study. *FEMS Microbiology Ecology*. **81**(3), 520–536.

Ghori, K.A.R., Craig, J., Thusu, B., Luning, S., Geiger, M. (2009) Global infracambrian petroleum systems: A review. *Geological Society, London, Special Publications*. **326**(1), 109–136.

Gilde, K., Pinckney, J.L. (2012) Sublethal effects of crude oil on the community structure of estuarine phytoplankton. *Estuaries and Coasts*. **35**(3), 853–861.

Goecke, F., Thiel, V., Wiese, J., Labes, A., Imhoff, J.F. (2013) Algae as an important environment for bacteria – phylogenetic relationships among new bacterial species isolated from algae. *Phycologia*. **52**(1), 14–24.

Gold, G., Rodriguez, S. (1989) The effect of temperature and salinity on the Setschenow parameters of naphthalene in seawater. *Canadian Journal of Chemistry*. **67**(5), 822–826.

Gomes, R., Levison, H.F., Tsiganis, K., Morbidelli, A. (2005) Origin of the cataclysmic Late Heavy Bombardment period of the terrestrial planets. *Nature*. **435**(7041), 466–469.

Gong, J., Qing, Y., Zou, S., Fu, R., Su, L., Zhang, X., Zhang, Q. (2016) Protist-bacteria associations: *Gammaproteobacteria* and *Alphaproteobacteria* are prevalent as digestion-resistant bacteria in ciliated protozoa. *Frontiers in Microbiology*. **7**, 498.

González, J., Figueiras, F.G., Aranguren-Gassis, M., Crespo, B.G., Fernández, E., Morán, X.A.G., Nieto-Cid, M. (2009) Effect of a simulated oil spill on natural assemblages of marine phytoplankton enclosed in microcosms. *Estuarine, Coastal and Shelf Science*. **83**(3), 265–276.

Goodlad, J. (1996) Effects of the Braer oil spill on the Shetland seafood industry. *Science of the Total Environment*. **186**(1–2), 127–133.

Goutx, M., Saliot, A. (1980) Relationship between dissolved and particulate fatty acids and hydrocarbons, chlorophyll a and zooplankton biomass in Villefranche Bay, Mediterranean Sea. *Marine Chemistry*. **8**(4), 299–318.

Graham, W.M., Condon, R.H., Carmichael, R.H., D'Ambra, I., Patterson, H.K., Linn, L.J., Hernandez Jr, F.J. (2010) Oil carbon entered the coastal planktonic food web during the Deepwater Horizon oil spill. *Environmental Research Letters*. **5**(4), 45301.

Gram, L., Grossart, H.-P., Schlingloff, A., Kiorboe, T. (2002) Possible quorum sensing in marine snow bacteria: production of acylated homoserine lactones by *Roseobacter* strains isolated from marine snow. *Applied and Environmental Microbiology*. **68**(8), 4111–4116.

Green, D.H., Bowman, J.P., Smith, E.A., Gutierrez, T., Bolch, C.J.S. (2006) *Marinobacter algicola* sp. nov., isolated from laboratory cultures of paralytic shellfish toxin-producing dinoflagellates. *International Journal of Systematic and Evolutionary Microbiology*. **56**(Pt 3), 523–527.

Green, D.H., Echavarri-Bravo, V., Brennan, D., Hart, M.C., Green, D.H., Echavarri-Bravo, V., Brennan, D., Hart, M.C. (2015) Bacterial diversity associated with the coccolithophorid algae emiliania huxleyi and coccolithus pelagicus f. braarudii. *BioMed Research International*. **2015**, 1–15.

Green, D.H., Llewellyn, L.E., Negri, A.P., Blackburn, S.I., Bolch, C.J.S. (2004) Phylogenetic and functional diversity of the cultivable bacterial community associated with the paralytic shellfish poisoning dinoflagellate *Gymnodinium catenatum. FEMS Microbiology Ecology*. **47**(3), 345–357.

Grenfell, J.L., Rauer, H., Selsis, F., Kaltenegger, L., Beichman, C., Danchi, W., Eiroa, C., Fridlund, M., Henning, T., Herbst, T., Lammer, H., Léger, A., Liseau, R., Lunine, J., Paresce, F., Penny, A., Quirrenbach, A., Röttgering, H., Schneider, J., Stam, D., Tinetti, G., White, G.J. (2010) Co-evolution of atmospheres, life, and climate. *Astrobiology*. **10**(1), 77–88.

Grigson, S., Cheong, C., Way, E. (2006) Studies of produced water toxicity using luminescent marine bacteria. *WIT Transactions on Biomedicine and Health*. **10**, 111–121.

Grossart, H.P. (1999) Interactions between marine bacteria and axenic diatoms (*Cylindrotheca fusiformis*, *Nitzschia laevis*, and *Thalassiosira weissflogii*) incubated under various conditions in the lab. *Aquatic Microbial Ecology*. **19**(1), 1–11.

Gründger, F., Jiménez, N., Thielemann, T., Straaten, N., Lüders, T., Richnow, H.-H., Krüger, M. (2015) Microbial methane formation in deep aquifers of a coal-bearing sedimentary basin, Germany. *Frontiers in Microbiology*. **6**, 200.

Guéguen, C., Clarisse, O., Perroud, A., McDonald, A. (2011) Chemical speciation and partitioning of trace metals (Cd, Co, Cu, Ni, Pb) in the lower Athabasca river and its tributaries (Alberta, Canada). *Journal of Environmental Monitoring*. **13**(10), 2865–2872.

Guha, S., Jaffé, P.R. (1996) Biodegradation kinetics of phenanthrene partitioned into the micellar phase of nonionic surfactants. *Environmental Science & Technology*. **30**(2), 605–611.

Guillard, R. R. L. (1973) Methods for microflagellates and nannoplankton. In *Handbook of Phycological Methods: Culture Methods and Growth Measurements.* Stein, J. R. (ed.) Cambridge University Press, Cambridge, UK, pp. 69–85.

Guillard, R.R.L. (1975) Culture of phytoplankton for feeding marine invertebrates. In *Culture of Marine Invertebrate Animals*. W. L. Smith & M. H. Chanley, (ed.) Boston, MA: Springer US, pp. 29–60.

Guo, B., Li, Y. (2012) Analysis and simulation of reactive distillation for gasoline alkylation desulfurization. *Chemical Engineering Science*. **72**, 115–125.

Gutiérrez, T., Mulloy, B., Black, K., Green, D.H. (2007) Glycoprotein emulsifiers from two marine *Halomonas* species: chemical and physical characterization. *Journal of Applied Microbiology*. **103**(5), 1716–1727.

Gutierrez, T., Shimmield, T., Haidon, C., Black, K., Green, D.H. (2008) Emulsifying and metal ion binding activity of a glycoprotein exopolymer produced by *Pseudoalteromonas* sp. strain TG12. *Applied and Environmental Microbiology*. **74**(15), 4867–4876.

Gutierrez, T., Biller, D. V., Shimmield, T., Green, D.H. (2012a) Metal binding properties of the EPS produced by *Halomonas* sp. TG39 and its potential in enhancing trace element bioavailability to eukaryotic phytoplankton. *BioMetals*. **25**(6), 1185–1194.

Gutierrez, T., Green, D.H., Whitman, W.B., Nichols, P.D., Semple, K.T., Aitken, M.D. (2012b) *Algiphilus aromaticivorans* gen. nov., sp. nov., an aromatic hydrocarbon-degrading bacterium isolated from a culture of the marine dinoflagellate *Lingulodinium polyedrum*, and proposal of *Algiphilaceae* fam. nov. *International Journal of Systematic and Evolutionary Microbiology*. **62**(Pt 11), 2743–2749.

Gutierrez, T., Nichols, P.D., Whitman, W.B., Aitken, M.D. (2012c) *Porticoccus hydrocarbonoclasticus* sp. nov., an aromatic hydrocarbon-degrading bacterium identified in laboratory cultures of marine phytoplankton. *Applied and Environmental Microbiology*. **78**(3), 628–637.

Gutierrez, T., Berry, D., Yang, T., Mishamandani, S., McKay, L., Teske, A., Aitken, M.D. (2013a) Role of bacterial exopolysaccharides (EPS) in the fate of the oil released during the Deepwater Horizon oil spill. *PLoS ONE*. **8**(6), 1–18.

Gutierrez, T., Green, D.H., Nichols, P.D., Whitman, W.B., Semple, K.T., Aitken, M.D. (2013b) *Polycyclovorans algicola* gen. nov., sp. nov., an aromatic-hydrocarbon-degrading marine bacterium found associated with laboratory cultures of marine phytoplankton. *Applied and Environmental Microbiology*. **79**(1), 205–214.

Gutierrez, T., Rhodes, G., Mishamandani, S., Berry, D., Whitman, W.B., Nichols, P.D., Semple, K.T., Aitken, M.D. (2014) Polycyclic aromatic hydrocarbon degradation of phytoplankton-associated *Arenibacter* spp. and description of *Arenibacter algicola* sp. nov., an aromatic hydrocarbon-degrading bacterium. *Applied and Environmental Microbiology*. **80**(2), 618–628.

Gutierrez, T., Thompson, H.F., Angelova, A., Whitman, W.B., Huntemann, M., Copeland, A., Chen, A., Kyrpides, N., Markowitz, V., Palaniappan, K., Ivanova, N., Mikhailova, N., Ovchinnikova, G. (2015) Genome sequence of *Polycyclovorans algicola* strain TG408 , an obligate polycyclic aromatic hydrocarbon-degrading bacterium associated with marine eukaryotic phytoplankton. *Genome Announcements*. **3**(2), e00207-15.

Gutierrez, T., Whitman, W.B., Huntemann, M., Copeland, A., Chen, A., Kyrpides, N., Markowitz, V., Pillay, M., Ivanova, N., Mikhailova, N., Ovchinnikova, G., Andersen, E., Pati, A., Stamatis, D., Reddy, T.B.K., Ngan, C.Y., Chovatia, M., Daum, C., Shapiro, N., Cantor, M.N., Woyke, T. (2016) Genome sequence of *Marinobacter* sp. strain MCTG268 isolated from the cosmopolitan marine diatom *Skeletonema costatum*. *Genome announcements*. **4**(5), e00937–16.

Habe, H., Omori, T. (2003) Genetics of polycyclic aromatic hydrocarbon metabolism in diverse aerobic bacteria. *Bioscience, Biotechnology, and Biochemistry*. **67**(2), 225–243.

Hadibarata, T., Tachibana, S., Askari, M. (2011) Identification of metabolites from phenanthrene oxidation by phenoloxidases and dioxygenases of *Polyporus* sp. S133. *Journal of Microbiology and Biotechnology*. **21**(3), 299–304.

Hagen, E.M., McCluney, K.E., Wyant, K.A., Soykan, C.U., Keller, A.C., Luttermoser, K.C., Holmes, E.J., Moore, J.C., Sabo, J.L. (2012) A meta-analysis of the effects of detritus on primary producers and consumers in marine, freshwater, and terrestrial ecosystems. *Oikos*. **121**(10), 1507–1515.

Hambrick, G.A., Delaune, R.D., Patrick, W.H., Patrick, W.H., Jr. (1980) Effect of estuarine sediment pH and oxidation-reduction potential on microbial hydrocarbon degradation. *Applied and Environmental Microbiology*. **40**(2), 365–369.

Handley, K.M., Lloyd, J.R. (2013) Biogeochemical implications of the ubiquitous colonization of marine habitats and redox gradients by *Marinobacter* species. *Frontiers in Microbiology*. **4**, 136.

Harayama, S., Rekik, M. (1990) The meta cleavage operon of TOL degradative plasmid pWW0 comprises 13 genes. *Molecular & General Genetics : MGG*. **221**(1), 113–120.

Harayama, S., Kishira, H., Kasai, Y., Shutsubo, K. (1999) Petroleum biodegradation in marine environments. *Journal of Molecular Microbiology and Biotechnology*. **1**(1), 63–70.

Harayama, S., Kasai, Y., Hara, A. (2004) Microbial communities in oil-contaminated seawater. *Current Opinion in Biotechnology*. **15**(3), 205–214.

Haritash, A.K., Kaushik, C.P. (2009) Biodegradation aspects of polycyclic aromatic hydrocarbons (PAHs): A review. *Journal of Hazardous Materials*. **169**(1–3), 1–15.

Hartung, R. (1995) Assessment of the potential for long-term toxicological effects of the Exxon Valdez oil spill on birds and animals. In *Exxon Valdez Oil Spill: Fate And Effects In Alaskan Waters.* ASTM, Philadelphia, PA (USA) pp. 693-725.

Hatcher, P.G. (1988) Dipolar-dephasing 13C NMR studies of decomposed wood and coalified xylem tissue: evidence for chemical structural changes associated with defunctionalization of lignin structural units during coalification. *Energy & Fuels*. **2**(1), 48–58.

Hayes, J.M., Waldbauer, J.R. (2006) The carbon cycle and associated redox processes through time. *Philosophical transactions of the Royal Society of London. Series B, Biological sciences*. **361**(1470), 931–50.

Hazen, T.C., Dubinsky, E.A., DeSantis, T.Z., Andersen, G.L., Piceno, Y.M., Singh, N., Jansson, J.K., Probst, A., Borglin, S.E., Fortney, J.L., Stringfellow, W.T., Bill, M., Conrad, M.E., Tom, L.M., Chavarria, K.L., Alusi, T.R., Lamendella, R., Joyner, D.C., Spier, C., Baelum, J., Auer, M., Zemla, M.L., Chakraborty, R., Sonnenthal, E.L., D'haeseleer, P., Holman, H.-Y.N., Osman, S., Lu, Z., Van Nostrand, J.D., Deng, Y., Zhou, J., Mason, O.U. (2010) Deep-sea oil plume enriches indigenous oil-degrading bacteria. *Science*. **330**, 204–208.

Head, I.M., Jones, D.M., Röling, W.F.M. (2006) Marine microorganisms make a meal of oil. *Nature reviews. Microbiology*. **4**(3), 173–182.

Hedlund, B.P., Geiselbrecht, A.D., Bair, T.J., Staley, J.T. (1999) Polycyclic aromatic hydrocarbon

degradation by a new marine bacterium, *Neptunomonas naphthovorans* gen. nov., sp. nov. *Applied and Environmental Microbiology*. **65**(1), 251–9.

Hefnawy, T.H. (2011) Effect of processing methods on nutritional composition and anti-nutritional factors in lentils (*Lens culinaris*). *Annals of Agricultural Sciences*. **56**(2), 57–61.

Henry, N.D., Robinson, L., Johnson, E., Cherrier, J., Abazinge, M. (2011) Phenanthrene emulsification and biodegradation using rhamnolipid biosurfactants and *Acinetobacter calcoaceticus in vitro*. *Bioremediation Journal*. **15**(2), 109–120.

Hignite, C., Azarnoff, D.L. (1977) Drugs and drug metabolites as environmental contaminants: Chlorophenoxyisobutyrate and salicylic acid in sewage water effluent. *Life Sciences*. **20**(2), 337–341.

Hino, S., Watanabe, K., Takahashi, N. (1997) Isolation and characterization of slime-producing bacteria capable of utilizing petroleum hydrocarbons as a sole carbon source. *Journal of Fermentation and Bioengineering*. **84**(6), 528–531.

Hoffman, T., Hanlon, A., Taylor, J., Ball, A., Osborn, A., Underwood, G. (2009) Dynamics and compositional changes in extracellular carbohydrates in estuarine sediments during degradation. *Marine Ecology - Progress Series*. **379**, 45–58.

Holmström, C., Kjelleberg, S. (1999) Marine *Pseudoalteromonas* species are associated with higher organisms and produce biologically active extracellular agents. *FEMS Microbiology Ecology*. **30**(4), 285–293.

Holzapfel, W.B. (1969) Effect of Pressure and Temperature on the Conductivity and Ionic Dissociation of Water up to 100 kbar and 1000°C. *The Journal of Chemical Physics*. **50**(10), 4424.

Hoppe, H.-G. (1983) Significance of exoenzymatic activities in the ecology of brackish water: measurements by means of methylumbelliferyl-substrates. *Marine Ecology Progress Series*. **11**, 299–308.

Horel, A., Mortazavi, B., Sobecky, P.A. (2012) Seasonal monitoring of hydrocarbon degraders in Alabama marine ecosystems following the Deepwater Horizon oil spill. *Water, Air, and Soil Pollution*. **223**(6), 3145–3154.

Horváth, E., Szalai, G., Janda, T. (2007) Induction of abiotic stress tolerance by salicylic acid signaling. *Journal of Plant Growth Regulation*. **26**(3), 290–300.

Howard, E.C., Sun, S., Biers, E.J., Moran, M.A. (2008) Abundant and diverse bacteria involved in DMSP degradation in marine surface waters. *Environmental Microbiology*. **10**(9), 2397–2410.

Howell, K.L., Holt, R., Endrino, I.P., Stewart, H. (2011) When the species is also a habitat: Comparing the predictively modelled distributions of Lophelia pertusa and the reef habitat it forms. *Biological Conservation*. **144**(11), 2656–2665.

Hryniuk, A., Ross, B.M. (2009) Detection of acetone and isoprene in human breath using a combination of thermal desorption and selected ion flow tube mass spectrometry. *International Journal of Mass Spectrometry*. **285**(1), 26–30.

Hu, J., Nakamura, J., Richardson, S.D., Aitken, M.D. (2012) Evaluating the Effects of Bioremediation on Genotoxicity of Polycyclic Aromatic Hydrocarbon-Contaminated Soil Using Genetically Engineered, Higher Eukaryotic Cell Lines. **46**(8), 4607-4613

Huang, M., Zhang, L., Mesaros, C., Zhang, S., Blaha, M.A., Blair, I.A., Penning, T.M. (2014) Metabolism of a representative oxygenated polycyclic aromatic hydrocarbon (PAH) phenanthrene-9,10-quinone in human hepatoma (HepG2) cells. *Chemical Research in Toxicology*. **27**(5), 852–863.

Huang, R., McPhedran, K.N., Yang, L., Gamal El-Din, M. (2016) Characterization and distribution of metal and nonmetal elements in the Alberta oil sands region of Canada. *Chemosphere*. **147**, 218–229.

Huang, S.C., Yen, G.-C., Chang, L.-W., Yen, W.-J., Duh, P.-D. (2003) Identification of an antioxidant, ethyl protocatechuate, in peanut seed testa. *Journal of Agricultural and Food Chemistry*. **51**(8), 2380–2383.

Huang, W.E., Bailey, M.J., Thompson, I.P., Whiteley, A.S., Spiers, A.J. (2007a) Single-cell Raman spectral profiles of *Pseudomonas fluorescens* SBW25 reflects in vitro and in planta metabolic history. *Microbial Ecology*. **53**(3), 414–425.

Huang, W.E., Stoecker, K., Griffiths, R., Newbold, L., Daims, H., Whiteley, A.S., Wagner, M. (2007b) Raman-FISH: Combining stable-isotope Raman spectroscopy and fluorescence in situ hybridization for the single cell analysis of identity and function. *Environmental Microbiology*. **9**(8), 1878–1889.

Huba, A.K., Huba, K., Gardinali, P.R. (2016) Understanding the atmospheric pressure ionization of petroleum components: The effects of size, structure, and presence of heteroatoms. *Science of The Total Environment*. **568**, 1018–1025.

Hughes, P. (2001) Animals, values and tourism — structural shifts in UK dolphin tourism provision. *Tourism Management*. **22**(4), 321–329.

Hyndman, R.D., Hyndman, D.W. (1968) Water saturation and high electrical conductivity in the lower continental crust. *Earth and Planetary Science Letters*. **4**(6), 427–432.

Ingleby, B., Huddleston, M. (2007) Quality control of ocean temperature and salinity profiles - historical and real-time data. *Journal of Marine Systems*. **65**(1), 158–175.

Isaac, P., Sánchez, L.A., Bourguignon, N., Cabral, M.E., Ferrero, M.A. (2013) Indigenous PAH-degrading bacteria from oil-polluted sediments in Caleta Cordova, Patagonia Argentina. *International*

Biodeterioration and Biodegradation. **82,** 207–214.

ITOPF (2010) Oil Tanker Spill Statistics : 2009. *ITOPF*, 1–8.

Iwabuchi, N., Sunairi, M., Urai, M., Itoh, C., Anzai, H., Nakajima, M., Harayama, S. (2002) Extracellular polysaccharides of *Rhodococcus rhodochrous* S-2 stimulate the degradation of aromatic components in crude oil by indigenous marine bacteria. *Applied and Environmental Microbiology*. **68**(5), 2337–43.

Jaekel, U., Zedelius, J., Wilkes, H., Musat, F. (2015) Anaerobic degradation of cyclohexane by sulfate-reducing bacteria from hydrocarbon-contaminated marine sediments. *Frontiers in Microbiology*. **6**, 116.

Janvier, M., Grimont, P.A.. (1995) The genus *Methylophaga*, a new line of descent within phylogenetic branch γ of proteobacteria. *Research in Microbiology*. **146**(7), 543–550.

Jennifer B. Galvin, Marashi, F. (1999) n-PENTANE. *Journal of Toxicology and Environmental Health, Part A*. **58**(1–2), 35–56.

Jermy, A. (2009) Symbiosis: A partnership cast in iron. *Nature Reviews Microbiology*. **7**(11), 760–760.

Johansson, S., Larsson, U., Boehm, P. (1980) The Tsesis oil spill. *Marine Pollution Bulletin*. **11**, 284–293.

Kalmykova, Y., Björklund, K., Strömvall, A.-M., Blom, L. (2013) Partitioning of polycyclic aromatic hydrocarbons, alkylphenols, bisphenol A and phthalates in landfill leachates and stormwater. *Water Research*. **47**(3), 1317–1328.

Kalyuzhnaya, M.G., Bowerman, S., Lara, J.C., Lidstrom, M.E., Chistoserdova, L. (2006) *Methylotenera mobilis* gen. nov., sp. nov., an obligately methelamine-utilizing bacterium within the family *Methylophilaceae*. *International Journal of Systematic and Evolutionary Microbiology*. **56**(12), 2819–2823.

Kamer, M., Rassoulzadegan, F. (1995) Extracellular enzyme activity: Indications for high short-term variability in a coastal marine ecosystem. *Microbial Ecology*. **30**(2), 143–156.

Kanaly, R. a, Harayama, S. (2000) Minireview Biodegradation of high-molecular-weight polycyclic aromatic hydrocarbons by bacteria. *Journal of Bacteriology*. **182**(8), 2059–2067.

Karner, M., Herndl, G.J. (1992) Extracellular enzymatic activity and secondary production in free-living and marine-snow-associated bacteria. *Marine Biology*. **113**(2), 341–347.

Kasai, Y., Shindo, K., Harayama, S., Misawa, N. (2003) Molecular characterization and substrate preference of a polycyclic aromatic hydrocarbon dioxygenase from *Cycloclasticus* sp. strain A5. *Applied and Environmental Microbiology*. **69**(11), 6688–6697.

Kästner, M., Streibich, S., Beyrer, M., Richnow, H.H., Fritsche, W. (1999) Formation of bound residues during microbial degradation of [14 C]anthracene in soil. *Applied and Environmental Microbiology*. **65**(5), 1834–1842.

Kazamia, E., Czesnick, H., Nguyen, T.T. Van, Croft, M.T., Sherwood, E., Sasso, S., Hodson, S.J., Warren, M.J., Smith, A.G. (2012) Mutualistic interactions between vitamin B12-dependent algae and heterotrophic bacteria exhibit regulation. *Environmental Microbiology*. **14**(6), 1466–1476.

Kazemi, N., Khavari-Nejad, R.A., Fahimi, H., Saadatmand, S., Nejad-Sattari, T. (2010) Effects of exogenous salicylic acid and nitric oxide on lipid peroxidation and antioxidant enzyme activities in leaves of *Brassica napus* L. under nickel stress. *Scientia Horticulturae*. **126**(3), 402–407.

Kazunga, C., Aitken, M.D. (2000) Products from the incomplete metabolism of pyrene by polycyclic aromatic hydrocarbon-degrading bacteria. *Applied and Environmental Microbiology*. **66**(5), 1917–1922.

Keeling, P.J., Archibald, J.M. (2008) Organelle evolution: What's in a name? *Current Biology*. **18**(8), R345–R347.

Kellogg, C.A., Lisle, J.T., Galkiewicz, J.P. (2009) Culture-independent characterization of bacterial communities associated with the cold-water coral Lophelia pertusa in the northeastern Gulf of Mexico. *Applied and Environmental Microbiology*. **75**(8), 2294–2303.

Kellogg, C.T.E., Deming, J.W. (2009) Comparison of free-living, suspended particle, and aggregate-associated bacterial and archaeal communities in the Laptev Sea. *Aquatic Microbial Ecology*. **57**(1), 1–18.

Kiene, R.P. (1990) Dimethyl sulfide production from dimethylsulfoniopropionate in coastal seawater samples and bacterial cultures. *Applied and Environmental Microbiology*. **56**(11), 3292–3297.

Kikuchi, Y., Yasukochi, Y., Nagata, Y., Fukuda, M., Takagi, M. (1994) Nucleotide sequence and functional analysis of the meta-cleavage pathway involved in biphenyl and polychlorinated biphenyl degradation in *Pseudomonas* sp. strain KKS102. *Journal of Bacteriology*. **176**(14), 4269–4276.

Kim, S.-J., Kweon, O., Jones, R.C., Edmondson, R.D., Cerniglia, C.E. (2008) Genomic analysis of polycyclic aromatic hydrocarbon degradation in *Mycobacterium vanbaalenii* PYR-1. *Biodegradation*. **19**(6), 859–81.

Kirso, U., Irha, N. (1998) Role of algae in fate of carcinogenic polycyclic aromatic hydrocarbons in the aquatic environment. *Ecotoxicology and Environmental Safety*. **41**(1), 83–89.

Klein, B., Grossi, V., Bouriat, P., Goulas, P., Grimaud, R. (2008) Cytoplasmic wax ester accumulation during biofilm-driven substrate assimilation at the alkane–water interface by Marinobacter hydrocarbonoclasticus SP17. *Research in Microbiology*. **159**(2), 137–144.

Kneip, C., Lockhart, P., Voß, C., Maier, U.-G. (2007) Nitrogen fixation in eukaryotes – New models for symbiosis. *BMC Evolutionary Biology*. **7**, 55.

Kodama, Y., Stiknowati, L.I., Ueki, A., Ueki, K., Watanabe, K. (2008) *Thalassospira tepidiphila* sp. nov., a polycyclic aromatic hydrocarbon-degrading bacterium isolated from seawater. *International Journal of Systematic and Evolutionary Microbiology*. **58**(3), 711–715.

Kostka, J.E., Prakash, O., Overholt, W.A., Green, S.J., Freyer, G., Canion, A., Delgardio, J., Norton, N., Hazen, T.C., Huettel, M. (2011) Hydrocarbon-degrading bacteria and the bacterial community response in Gulf of Mexico beach sands impacted by the Deepwater Horizon oil spill. *Applied and Environmental Microbiology*. **77**(22), 7962–7974.

Kowalewska, G. (1999) Phytoplankton - the main factor responsible for transport of polynuclear aromatic hydrocarbons from water to sediments in the Southern Baltic ecosystem. *ICES Journal of Marine Science*. **56**, 219–222.

Kromkamp, J.C., Forster, R.M. (2003) The use of variable fluorescence measurements in aquatic ecosystems: differences between multiple and single turnover measuring protocols and suggested terminology. *European Journal of Phycology*. **38**(2), 103–112.

Kuhn, W.R., Atreya, S.K. (1979) Ammonia photolysis and the greenhouse effect in the primordial atmosphere of the earth. *Icarus*. **37**(1), 207–213.

Kujawinski, E.B. (2011) The impact of microbial metabolism on marine dissolved organic matter. *Annual Review of Marine Science*. **3**(1), 567–599.

Kuo, R.C., Lin, S. (2013) Ectobiotic and endobiotic bacteria associated with *Eutreptiella* sp. isolated from Long Island Sound. *Protist*. **164**(1), 60–74.

Kurz, E.M., Holstein, T.W., Petri, B.M., Engel, J., David, C.N. (1991) Mini-collagens in *hydra* nematocytes. *The Journal of Cell Biology*. **115**(4), 1159–1169.

Kuzma, J., Nemecek-Marshall, M., Pollock, W.H., Fall, R. (1995) Bacteria produce the volatile hydrocarbon isoprene. *Current Microbiology*. **30**(2), 97–103.

Kvenvolden, K., Lawless, J., Pering, K., Peterson, E., Flores, J., Ponnamperuma, C., Kaplan, I.R., Moore, C. (1970) Evidence for extraterrestrial amino-acids and hydrocarbons in the murchison meteorite. *Nature*. **228**(5275), 923–926.

Kvenvolden, K.A., Cooper, C.K. (2003) Natural seepage of crude oil into the marine environment. *Geo-Marine Letters*. **23**(3–4), 140–146.

Kwak, M.J., Lee, J.S., Lee, K.C., Kim, K.K., Eom, M.K., Kim, B.K., Kim, J.F. (2014) *Sulfitobacter geojensis* sp. nov., *Sulfitobacter noctilucae* sp. nov., and *Sulfitobacter noctilucicola* sp. nov., isolated from coastal seawater. *International Journal of Systematic and Evolutionary Microbiology*. **64**(May 2012), 3760–3767.

Kwok, S., Zhang, Y. (2011) Mixed aromatic-aliphatic organic nanoparticles as carriers of unidentified infrared emission features. *Nature*. **479**(7371), 80–3.

La Rocca, C., Conti, L., Crebelli, R., Crochi, B., Iacovella, N., Rodriguez, F., Turrio-Baldassarri, L., di Domenico, A. (1996) PAH content and mutagenicity of marine sediments from the Venice lagoon. *Ecotoxicology and Environmental Safety*. **33**(3), 236–45.

Lachnit, T., Meske, D., Wahl, M., Harder, T., Schmitz, R. (2011) Epibacterial community patterns on marine macroalgae are host-specific but temporally variable. *Environmental Microbiology*. **13**(3), 655–665.

Lai, Q., Li, W., Shao, Z. (2012) Complete genome sequence of *Alcanivorax dieselolei* type strain B5. *Journal of Bacteriology*. **194**(23), 6674–6674.

Landry, M., Constantinou, J., Latasa, M., Brown, S., Bidigare, R., Ondrusek, M. (2000a) Biological response to iron fertilization in the eastern equatorial Pacific (IronEx II). III. Dynamics of phytoplankton growth and microzooplankton grazing. *Marine Ecology Progress Series*. **201**, 57–72.

Landry, M.R., Ondrusek, M.E., Tanner, S.J., Brown, S.L., Constantinou, J., Bidigare, R.R., Coale, K.H., Fitzwater, S. (2000b) Biological response to iron fertilization in the eastern equatorial Pacific (IronEx II). I. Microplankton community abundances and biomass. *Marine Ecology Progress Series*. **201**, 27–42.

Lappalainen, M., Tett, P. (2014) Creran microplankton 1979-81 and 2010-12. *SAMS Internal Report*. pp. 1-55.

Laskin, S., Goldstein, B.D. (1977) *Benzene toxicity: a critical evaluation*. 1st ed. Sidney Laskin & Bernard D. Goldstein (eds.) Washington, U.S.A.: American Petroleum Institute.

Lauro, F., Stratton, T., Chastain, R., Ferriera, S., Johnson, J., S, G., Yayanos, A., Bartlett, D. (2013) Complete genome sequence of the deep-sea bacterium *Psychromonas* strain CNPT3. *Genome Announcements*. **1**(3), e00304-13.

Law, R.J. (1981) Hydrocarbon concentrations in water and sediments from UK marine waters, determined by fluorescence spectroscopy. *Marine Pollution Bulletin*. **12**(5), 153–157.

Lea-Smith, D.J., Biller, S.J., Davey, M.P., Cotton, C.A.R., Perez Sepulveda, B.M., Turchyn, A. V, Scanlan, D.J., Smith, A.G., Chisholm, S.W., Howe, C.J. (2015) Contribution of cyanobacterial alkane production to the ocean hydrocarbon cycle. *Proceedings of the National Academy of Sciences of the United States of America*. **112**(44), 13591–13596.

Leahy, J.G., Colwell, R.R. (1990) Microbial degradation of hydrocarbons in the environment. *Microbiological Reviews*. **54**(3), 305–315.

Lebaron, P., Catala, P., Fajon, C., Joux, F., Baudart, J., Bernard, L. (1997) A new sensitive, whole-cell hybridization technique for detection of bacteria involving a biotinylated oligonucleotide probe targeting rRNA and tyramide signal amplification. *Applied and Environmental Microbiology*. **63**(8), 3274–3278.

Leblanc, K., Arístegui, J., Armand, L., Assmy, P., Beker, B., Bode, A., Breton, E., Cornet, V., Gibson, J., Gosselin, M.-P., Kopczynska, E., Marshall, H., Peloquin, J., Piontkovski, S., Poulton, A.J., Quéguiner, B., Schiebel, R., Shipe, R., Stefels, J., Van Leeuwe, M.A., Varela, M., Widdicombe, C., Yallop, M. (2012) A global diatom database – abundance, biovolume and biomass in the world ocean. *Earth System Science Data* **4**, 149–165.

Lee, O.O., Yang, J., Bougouffa, S., Wang, Y., Batang, Z., Tian, R., Al-Suwailem, A., Qian, P.-Y. (2012) Spatial and species variations in bacterial communities associated with corals from the Red Sea as revealed by pyrosequencing. *Applied and Environmental Microbiology*. **78**(20), 7173–7184.

Lemos, M.F.L., Gomes, I., Rodrigues, D., Leston, S., Miguel, P.A., Ramos, F., Mendão, A.R., Soares, A.M.V.M., Pestana, J.L.T. (2011) Xenobiotic phytoremediation in marine environments: Potential impact of climate changes. *Current Opinion in Biotechnology*. **22**, S67.

Li, D., Yuan, C., Gong, Y., Huang, Y., Han, X. (2008) The effects of methyl tert-butyl ether (MTBE) on the male rat reproductive system. *Food and Chemical Toxicology*. **46**(7), 2402–2408.

Liang, Y., Tse, M.F., Young, L., Wong, M.H. (2007) Distribution patterns of polycyclic aromatic hydrocarbons (PAHs) in the sediments and fish at Mai Po Marshes Nature Reserve, Hong Kong. *Water Research*. **41**(6), 1303–1311.

Liu, C., Wu, Y., Li, L., Yingfei, M., Shao, Z. (2007) *Thalassospira xiamenensis* sp. nov. and *Thalassospira profundimaris* sp. nov. *International Journal of Systematic and Evolutionary Microbiology*. **57**(2), 316–320.

Lobo, V., Patil, A., Phatak, A., Chandra, N. (2010) Free radicals, antioxidants and functional foods: Impact on human health. *Pharmacognosy Reviews*. **4**(8), 118–126.

Loh, P.S., Reeves, A.D., Miller, A.E.J., Harvey, S.M., Overnell, J. (2014) Sediment fluxes and carbon budgets in Loch Creran, western Scotland. *Geological Society, London, Special Publications*. **344**(1), 103–124.

Longhurst, A.R., Glen Harrison, W. (1989) The biological pump: Profiles of plankton production and consumption in the upper ocean. *Progress in Oceanography*. **22**(1), 47–123.

Louvado, A., Gomes, N.C.M., Simões, M.M.Q., Almeida, A., Cleary, D.F.R., Cunha, A. (2015) Polycyclic aromatic hydrocarbons in deep sea sediments: Microbe–pollutant interactions in a remote environment. *Science of The Total Environment*. **526**, 312–328.

Lü, F., Ji, J., Shao, L., He, P. (2013) Bacterial bioaugmentation for improving methane and hydrogen production from microalgae. *Biotechnology for Biofuels*. **6**(1), 92.

Lupette, J., Lami, R., Krasovec, M., Grimsley, N., Moreau, H., Piganeau, G., Sanchez-Ferandin, S. (2016) *Marinobacter* dominates the bacterial community of the *Ostreococcus tauri* phycosphere in culture. *Frontiers in Microbiology*. **7**(September), 1–14.

Lyu, Y., Zheng, W., Zheng, T., Tian, Y., Johnson, S.J. (2014) Biodegradation of polycyclic aromatic hydrocarbons by *Novosphingobium pentaromativorans* US6-1. *PLoS ONE*. **9**(7), e101438.

Mahajan, T.B., Elsila, J.E., Deamer, D.W., Zare, R.N. (2003) Formation of carbon-carbon bonds in the photochemical alkylation of polycyclic aromatic hydrocarbons. *Origins of Life and Evolution of the Biosphere*. **33**(1), 17–35.

Mahan, K.M., Odom, O.W., Herrin, D.L. (2005) Controlling fungal contamination in *Chlamydomonas reinhardtii* cultures. *BioTechniques*. **39**(39), 457–458.

Martin, W. (1999) A briefly argued case that mitochondria and plastids are descendants of endosymbionts, but that the nuclear compartment is not. *Proceedings of the Royal Society B: Biological Sciences*. **266**(1426), 1387–1395.

Martinez, J., Smith, D., Steward, G., Azam, F. (1996) Variability in ectohydrolytic enzyme activities of pelagic marine bacteria and its significance for substrate processing in the sea. *Aquatic Microbial Ecology*. **10**(3), 223–230.

Martins, Z., Botta, O., Fogel, M.L., Sephton, M.A., Glavin, D.P., Watson, J.S., Dworkin, J.P., Schwartz, A.W., Ehrenfreund, P. (2008) Extraterrestrial nucleobases in the Murchison meteorite. *Earth and Planetary Science Letters* **270**(1-2),130-136.

Martonová, M., Škárka, B., Raděj, Z. (1972) Degradation of naphthalene to salicylic acid by cultures of *Pseudomonas denitrificans* and *Achromobacter* sp. from the effluents of petroleum refinery. *Folia Microbiologica*. **17**(1), 63–65.

Mas-Lladó, M., Piña-Villalonga, J.M., Brunet-Galmés, I., Nogales, B., Bosch, R. (2014) Draft genome sequences of two isolates of the Roseobacter group, *Sulfitobacter* sp. strains 3SOLIMAR09 and 1FIGIMAR09, from harbors of Mallorca Island (Mediterranean Sea). *Genome Announcements*. **2**(3), e00350-14.

Master, E.R., Mohn, W.W. (2001) Induction of bphA, encoding biphenyl dioxygenase, in two

polychlorinated biphenyl-degrading bacteria, psychrotolerant *Pseudomonas* strain Cam-1 and mesophilic *Burkholderia* strain LB400. *Applied and Environmental Microbiology*. **67**(6), 2669–2676.

Mato, Y., Isobe, T. (2001) Plastic resin pellets as a transport medium for toxic chemicals in the marine environment. *Environmental Science & Technology*. **35**(2), 318-324.

Matthäus, C., Bird, B., Miljković, M., Chernenko, T., Romeo, M., Diem, M. (2008) Chapter 10: Infrared and Raman microscopy in cell biology. *Methods in Cell Biology*. **89**, 275–308.

Mayali, X., Franks, P.J.S., Burton, R.S. (2011) Temporal attachment dynamics by distinct bacterial taxa during a dinoflagellate bloom. *Aquatic Microbial Ecology*. **63**(2), 111–122.

Mayes, D.F., Rogerson, A., Marchant, H.J., Laybourn-Parry, J. (1998) Temporal abundance of naked bacterivore amoebae in coastal East Antarctica. *Estuarine, Coastal and Shelf Science*. **46**, 565–572.

Mazzini, A., Duranti, D., Jonk, R., Parnell, J., Cronin, B.T., Hurst, A., Quine, M. (2003) Palaeo-carbonate seep structures above an oil reservoir, Gryphon Field, Tertiary, North Sea. *Geo-Marine Letters*. **23**(3–4), 323–339.

McClay, K., Fox, B.G., Steffan, R.J. (2000) Toluene monooxygenase-catalyzed epoxidation of alkenes. *Applied and Environmental Microbiology*. **66**(5), 1877–1882.

McGenity, T.J., Folwell, B.D., McKew, B.A., Sanni, G.O. (2012) Marine crude-oil biodegradation: a central role for interspecies interactions. *Aquatic Biosystems*. **8**(1), 10.

McKay, L.J., Gutierrez, T., Teske, A.P. (2016) Development of a group-specific 16S rRNA-targeted probe set for the identification of *Marinobacter* by fluorescence in situ hybridization. *Deep Sea Research Part II: Topical Studies in Oceanography*. **129**, 360–367.

McKew, B.A., Coulon, F., Yakimov, M.M., Denaro, R., Genovese, M., Smith, C.J., Osborn, A.M., Timmis, K.N., McGenity, T.J. (2007) Efficacy of intervention strategies for bioremediation of crude oil in marine systems and effects on indigenous hydrocarbonoclastic bacteria. *Environmental Microbiology*. **9**(6), 1562–1571.

McKew, B.A., Taylor, J.D., McGenity, T.J., Underwood, G.J.C. (2011) Resistance and resilience of benthic biofilm communities from a temperate saltmarsh to desiccation and rewetting. *The ISME Journal*. **5**(1), 30–41.

McQuoid, M., Godhe, A., Nordberg, K., Mcquoid, M.R. (2002) Viability of phytoplankton resting stages in the sediments of a coastal Swedish fjord. *European Journal of Phycology*. **37**(2), 191–201.

Meckenstock, R.U., Safinowski, M., Griebler, C. (2004) Anaerobic degradation of polycyclic aromatic hydrocarbons. *FEMS Microbiology Ecology*. **49**(1), 27–36.

Melander, R.J., Minvielle, M.J., Melander, C. (2014) Controlling bacterial behavior with indole-containing natural products and derivatives. *Tetrahedron*. **70**(37), 6363–6372.

Melcher, R.J., Apitz, S.E., Barbara, B., Hemmingsen, B.B. (2002) Impact of Irradiation and Polycyclic Aromatic Hydrocarbon Spiking on Microbial Populations in Marine Sediment for Future Aging and Biodegradability Studies. *Applied and Environmental Microbiology*. **68**(6), 2858–2868.

Miki, T., Jacquet, S. (2008) Complex interactions in the microbial world: Underexplored key links between viruses, bacteria and protozoan grazers in aquatic environments. *Aquatic Microbial Ecology*. **51**(2), 195–208.

Mishamandani, S., Gutierrez, T., Aitken, M.D. (2014) DNA-based stable isotope probing coupled with cultivation methods implicates *Methylophaga* in hydrocarbon degradation. *Frontiers in Microbiology*. **5**, 76.

Mishamandani, S., Gutierrez, T., Berry, D., Aitken, M.D. (2016) Response of the bacterial community associated with a cosmopolitan marine diatom to crude oil shows a preference for the biodegradation of aromatic hydrocarbons. *Environmental Microbiology*. **18**(6), 1817–1833.

Moisander, P.H., Paerl, H.W., Zehr, J.P. (2008) Effects of inorganic nitrogen on taxa-specific cyanobacterial growth and nifH expression in a subtropical estuary. *Limnology and Oceanography*. **53**(6), 2519–2532.

Moran, M.A., Belas, R., Schell, M.A., González, J.M., Sun, F., Sun, S., Binder, B.J., Edmonds, J., Ye, W., Orcutt, B., Howard, E.C., Meile, C., Palefsky, W., Goesmann, A., Ren, Q., Paulsen, I., Ulrich, L.E., Thompson, L.S., Saunders, E., Buchan, A. (2007) Ecological genomics of marine Roseobacters. *Applied and Environmental Microbiology*. **73**(14), 4559–4569.

Mounier, J., Camus, A., Mitteau, I., Vaysse, P.-J., Goulas, P., Grimaud, R., Sivadon, P. (2014) The marine bacterium *Marinobacter hydrocarbonoclasticus* SP17 degrades a wide range of lipids and hydrocarbons through the formation of oleolytic biofilms with distinct gene expression profiles. *FEMS Microbiology Ecology*. **90**(3), 816–831.

Muñoz, R., Guieysse, B., Mattiasson, B. (2003) Phenanthrene biodegradation by an algal-bacterial consortium in two-phase partitioning bioreactors. *Applied Microbiology and Biotechnology*. **61**(3), 261–267.

Muyzer, G., De Waal, E.C., Uitterlinden, A.G. (1993) Profiling of complex microbial populations by denaturing gradient gel electrophoresis analysis of polymerase chain reaction-amplified genes coding for 16S rRNA. *Applied and Environmental Microbiology*, **59**, 695–700.

Myklestad, S.M. (1995) Release of extracellular products by phytoplankton with special emphasis on

polysaccharides. *Science of the Total Environment*. **165**(1–3), 155–164.

Nagata, T. (1986) Carbon and nitrogen content of natural planktonic bacteria. *Applied and Environmental Microbiology*. **52**(1), 28–32.

Nakata, H., Sakai, Y., Miyawaki, T., Takemura, A. (2003) Bioaccumulation and toxic potencies of polychlorinated biphenyls and polycyclic aromatic hydrocarbons in tidal flat and coastal ecosystems of the Ariake Sea, Japan. *Environmental Science & Technology*. **37**(16), 3513–3521.

Nanninga, H., Tyrrell, T. (1996) Importance of light for the formation of algal blooms by *Emiliania huxleyi*. *Marine Ecology Progress Series*. **136**, 195–203.

Napolitano, G.E., Ackman, R.G., Ratnayake, W.M.N. (1990) Fatty acid composition of three cultured algal species (*Isochvysis galbana*, *Chaetoceros gracilis* and *Chaetoceros calcitrans*) used as food for bivalve larvae. *Journal of the World Aquaculture Society*. **21**(2), 122–130.

Nettmann, E., Fröhling, A., Heeg, K., Klocke, M., Schlüter, O., Mumme, J. (2013) Development of a flow-fluorescence in situ hybridization protocol for the analysis of microbial communities in anaerobic fermentation liquor. *BMC Microbiology*. **13**(1), 278.

Netzeva, T.I., Schultz, T.W. (2005) QSARs for the aquatic toxicity of aromatic aldehydes from Tetrahymena data. *Chemosphere*. **61**(11), 1632–1643.

Neulinger, S.C., Gärtner, A., Järnegren, J., Ludvigsen, M., Lochte, K., Dullo, W.C. (2009) Tissue-associated '*Candidatus Mycoplasma corallicola*' and filamentous bacteria on the cold-water coral *Lophelia pertusa* (*Scleractinia*). *Applied and Environmental Microbiology*. **75**(5), 1437–1444.

Neulinger, S.C., Järnegren, J., Ludvigsen, M., Lochte, K., Dullo, W.C. (2008) Phenotype-specific bacterial communities in the cold-water coral *Lophelia pertusa* (*Scleractinia*) and their implications for the coral's nutrition, health, and distribution. *Applied and Environmental Microbiology*. **74**(23), 7272–7285.

Newman, D.K., Kolter, R. (2000) A role for excreted quinones in extracellular electron transfer. *Nature*. **405**(6782), 94–97.

Niemann, H., Elvert, M., Hovland, M., Orcutt, B., Judd, A., Suck, I., Gutt, J., Joye, S., Damm, E., Finster, K., Boetius, A. (2005) Methane emission and consumption at a North Sea gas seep (Tommeliten area). *Biogeosciences*. **2**(4), 335–351.

Niemz, P., Hofmann, T., Rétfalv, T. (2010) Investigation of chemical changes in the structure of thermally modified wood. *Maderas. Ciencia y Tecnología*. **12**(2), 69–78.

Noffke, N., Christian, D., Wacey, D., Hazen, R.M. (2013) Microbially induced sedimentary structures recording an ancient ecosystem in the ca. 3.48 billion-year-old Dresser Formation, Pilbara, Western Australia. *Astrobiology*. **13**(12), 1103–1124.

Notingher, I., Verrier, S., Romanska, H., Bishop, A.E., Polak, J.M., Hench, L.L. (2002) *In situ* characterisation of living cells by Raman spectroscopy. *Spectroscopy*. **16**(2), 43–51.

Novakova, M., Mackova, M., Antosova, Z., Viktorova, J., Szekeres, M., Demnerova, K., Macek, T. (2010) Cloning the bacterial bphC gene into *Nicotiana tabacum* to improve the efficiency of phytoremediation of polychlorinated biphenyls. *Bioengineered Bugs*. **1**(6), 419–423.

Nowicka, B., Kruk, J. (2010) Occurrence, biosynthesis and function of isoprenoid quinones. *Biochimica et Biophysica Acta (BBA) - Bioenergetics*. **1797**(9), 1587–1605.

Nowitzki, U., Flechner, A., Kellermann, J., Hasegawa, M., Schnarrenberger, C., Martin, W. (1998) Eubacterial origin of nuclear genes for chloroplast and cytosolic glucose-6-phosphate isomerase from spinach: sampling eubacterial gene diversity in eukaryotic chromosomes through symbiosis. *Gene*. **214**(1), 205–213.

Okai, M., Watanabe, A., Ishida, M., Urano, N. (2015) Draft genome sequence of a benzo[a]pyrene-degrading bacterium, *Olleya* sp. strain ITB9. *Genome Announcements*. **3**(6), e01328-15.

Olahová, N., Bajus, M., Hájeková, E., Šugár, L., Markoš, J. (2014) Kinetics and modelling of heptane steam-cracking. *Chemical Papers*. **68**(12), 1678–1689.

OSPAR Commission (2013) Levels and trends in marine contaminants and their biological effects – CEMP Assessment report 2012. *Monitoring and Assessment Series, OSPAR Commission*. **596**, 28pp.

Oudot, J., Chaillan, F. (2010) Pyrolysis of asphaltenes and biomarkers for the fingerprinting of the Amoco-Cadiz oil spill after 23 years. *Comptes Rendus Chimie*. **13**(5), 548–552.

Özhan, K., Bargu, S. (2014a) Can crude oil toxicity on phytoplankton be predicted based on toxicity data on benzo(a)pyrene and naphthalene? *Bulletin of Environmental Contamination and Toxicology*. **92**(2), 225–230.

Özhan, K., Bargu, S. (2014b) Distinct responses of Gulf of Mexico phytoplankton communities to crude oil and the dispersant corexit® Ec9500A under different nutrient regimes. *Ecotoxicology*. **23**(3), 370–384.

Özhan, K., Bargu, S. (2014c) Responses of sympatric *Karenia brevis*, *Prorocentrum minimum*, and *Heterosigma akashiwo* to the exposure of crude oil. *Ecotoxicology*. **23**(8), 1387–1398.

Özhan, K., Parsons, M.L., Bargu, S. (2014) How were phytoplankton affected by the Deepwater Horizon oil spill? *BioScience*. **64**(9), 829–836.

Page, R.D. (1996) TreeView: an application to display phylogenetic trees on personal computers. *Computer Applications in the Biosciences : CABIOS*. **12**(4), 357–358.

Palackal, N.T., Lee, S.H., Harvey, R.G., Blair, I.A., Penning, T.M. (2002) Activation of polycyclic aromatic hydrocarbontrans-dihydrodiol proximate carcinogens by human aldo-keto reductase (AKR1C) enzymes and their functional overexpression in human lung carcinoma (A549) cells. *Journal of Biological Chemistry*. **277**(27), 24799–24808.

Palleroni, N.J., Port, A.M., Chang, H.-K., Zylstra, G.J. (2004) *Hydrocarboniphaga effusa* gen. nov., sp. nov., a novel member of the *gamma-Proteobacteria* active in alkane and aromatic hydrocarbon degradation. *International Journal Of Systematic and Evolutionary Microbiology*. **54**(Pt 4), 1203–1207.

Papazova, D., Pavlova, a (1999) Development of a simple gas chromatographic method for differentiation of spilled oils. *Journal of Chromatographic Science*. **37**(January), 6–9.

Parsons, M.L., Morrison, W., Rabalais, N.N., Turner, R.E., Tyre, K.N. (2015) Phytoplankton and the Macondo oil spill: A comparison of the 2010 phytoplankton assemblage to baseline conditions on the Louisiana shelf. *Environmental Pollution*. **207**, 152–160.

Parsons, M.L., Turner, R.E., Overton, E.B. (2014) Sediment-preserved diatom assemblages can distinguish a petroleum activity signal separately from the nutrient signal of the Mississippi River in coastal Louisiana. *Marine Pollution Bulletin*. **85**(1), 164–171.

Passow, U. (2016) Formation of rapidly-sinking, oil-associated marine snow. *Deep Sea Research Part II: Topical Studies in Oceanography*. **129**, 232–240.

Passow, U., Alldredge, A.L. (1994) Distribution, size and bacterial colonization of transparent exopolymer particles (TEP) in the ocean. *Marine Ecology Progress Series*. **113**(1–2), 185–198.

Passow, U., Alldredge, A.L., Logan, B.E. (1994) The role of particulate carbohydrate exudates in the flocculation of diatom blooms. *Deep Sea Research Part I: Oceanographic Research Papers*. **41**(2), 335–357.

Passow, U., Ziervogel, K., Asper, V., Diercks, A. (2012) Marine snow formation in the aftermath of the Deepwater Horizon oil spill in the Gulf of Mexico. *Environmental Research Letters*. **7**(3), 1–11.

Patton, J.S., Rigler, M.W., Boehm, P.D., Fiest, D.L. (1981) Ixtoc 1 oil spill: flaking of surface mousse in the Gulf of Mexico. *Nature*. **290**(5803), 235–238.

Paul, C., Mausz, M.A., Pohnert, G. (2013a) A co-culturing/metabolomics approach to investigate chemically mediated interactions of planktonic organisms reveals influence of bacteria on diatom metabolism. *Metabolomics*. **9**(2), 349–359.

Paul, J.H., Hollander, D., Coble, P., Daly, K.L., Murasko, S., English, D., Basso, J., Delaney, J., McDaniel, L., Kovach, C.W. (2013b) Toxicity and mutagenicity of Gulf of Mexico waters during and after the Deepwater Horizon oil spill. *Environmental Science & Technology*. **47**(17), 9651–9659.

Pearlman, R.S., Yalkowsky, S.H., Banerjee, S. (1984) Water solubilities of polynuclear aromatic and heteroaromatic compounds. *Journal of Physical and Chemical Reference Data*. **13**(2), 555–562.

Pearson, W.R. (2013) An introduction to sequence similarity ('homology') searching. In *Current Protocols in Bioinformatics*. Chapter **3**, 1–9.

Pelz, O., Tesar, M., Wittich, R.M., Moore, E.R., Timmis, K.N., Abraham, W.R. (1999) Towards elucidation of microbial community metabolic pathways: unravelling the network of carbon sharing in a pollutant-degrading bacterial consortium by immunocapture and isotopic ratio mass spectrometry. *Environmental Microbiology*. **1**, 167–174.

Peng, R.-H., Xiong, A.-S., Xue, Y., Fu, X.-Y., Gao, F., Zhao, W., Tian, Y.-S., Yao, Q.-H. (2008) Microbial biodegradation of polyaromatic hydrocarbons. *FEMS Microbiology Reviews*. **32**(6), 927–955.

Penn, K., Wu, D., Eisen, J. a, Ward, N. (2006) Characterization of bacterial communities associated with deep-sea corals on gulf of alaska seamounts characterization of bacterial communities associated with deep-sea corals on gulf of Alaska seamounts. *Applied and Environmental Microbiology*. **72**(2), 1680–1683.

Pérez, P., Fernández, E., Beiras, R. (2010) Use of fast repetition rate fluorometry on detection and assessment of PAH toxicity on microalgae. *Water, Air, & Soil Pollution*. **209**(1–4), 345–356.

Pernthaler, A., Pernthaler, J., Amann, R. (2002) Fluorescence *in situ* hybridization and catalyzed reporter deposition for the identification of marine bacteria. *Applied and Environmental Microbiology*. **68**(6), 3094–3101.

Petrov, A.A. (1987) *Petroleum Hydrocarbons*. Berlin, Heidelberg: Springer Berlin Heidelberg.

Phale, P.S., Basu, A., Majhi, P.D., Deveryshetty, J., Vamsee-Krishna, C., Shrivastava, R. (2007) Metabolic diversity in bacterial degradation of aromatic compounds. *Omics*. **11**(3), 252–279.

Pinhassi, J., Sala, M.M., Havskum, H., Peters, F., Guadayol, Ò., Malits, A., Marrasé, C. (2004) Changes in bacterioplankton composition under different phytoplankton regimens. *Applied and Environmental Microbiology*. **70**(11), 6753–6766.

Pinyakong, O., Habe, H., Omori, T. (2003) The unique aromatic catabolic genes in sphingomonads degrading polycyclic aromatic hydrocarbons(PAHs). *The Journal of General and Applied Microbiology*. **49**(1), 1–19.

Pistocchi, R., Trigari, G., Serrazanetti, G.P., Taddei, P., Monti, G., Palamidesi, S., Guerrini, F., Bottura, G., Serratore, P., Fabbri, M., Pirini, M., Ventrella, V., Pagliarani, A., Boni, L., Borgatti, A.R. (2005) Chemical and biochemical parameters of cultured diatoms and bacteria from the Adriatic Sea as possible biomarkers of mucilage production. *Science of The Total Environment*. **353**(1), 287–299.

Pohjola, S.K., Lappi, M., Honkanen, M., Rantanen, L., Savela, K. (2003) DNA binding of polycyclic aromatic hydrocarbons in a human bronchial epithelial cell line treated with diesel and gasoline particulate extracts and benzo[a]pyrene. *Mutagenesis*. **18**(5), 429–438.

Ponomarenko, L.P., Stonik, I.V., Aizdaicher, N.A., Orlova, T.Y., Popovskaya, G.I., Pomazkina, G.V., Stonik, V.A. (2004) Sterols of marine microalgae *Pyramimonas* cf. *cordata* (*Prasinophyta*), *Attheya ussurensis* sp. nov. (*Bacillariophyta*) and a spring diatom bloom from Lake Baikal. *Comparative Biochemistry and Physiology Part B: Biochemistry and Molecular Biology*. **138**(1), 65–70.

Powell, T.G., McKirdy, D.M. (1973) Relationship between ratio of pristane to phytane, crude oil composition and geological environment in Australia. *Nature,* **243**(124), 37-39.

Prabagaran, S.R., Manorama, R., Delille, D., Shivaji, S. (2007) Predominance of *Roseobacter*, *Sulfitobacter*, *Glaciecola* and *Psychrobacter* in seawater collected off Ushuaia, Argentina, Sub-Antarctica. *FEMS Microbiology Ecology*. **59**(2), 342–355.

Priefert, H., Rabenhorst, J., Steinbüchel, A. (1997) Molecular characterization of genes of *Pseudomonas* sp. strain HR199 involved in bioconversion of vanillin to protocatechuate. *Journal of Bacteriology*. **179**(8), 2595–2607.

Prince, R.C., Gramain, A., McGenity, T.J. (2010) In *Handbook of Hydrocarbon and Lipid Microbiology*. K.N. Timmis (ed.) Springer, Berlin. pp 1672-1692.

Proemse, B.C., Mayer, B., Chow, J.C., Watson, J.G. (2012a) Isotopic characterization of nitrate, ammonium and sulfate in stack PM 2.5 emissions in the Athabasca oil sands region, Alberta, Canada. *Atmospheric Environment*. **60**(2), 555–563.

Proemse, B.C., Mayer, B., Fenn, M.E. (2012b) Tracing industrial sulfur contributions to atmospheric sulfate deposition in the Athabasca oil sands region, Alberta, Canada. *Applied Geochemistry*. **27**(12), 2425–2434.

Prouse, N.J., Gordon Jr., D.C., Keizer, P.D. (1976) Effects of low concentrations of oil accommodated in sea water on the growth of unialgal marine phytoplankton cultures. *Journal of the Fisheries Research Board of Canada*. **33**(4), 810–818.

Puttaswamy, N., Liber, K. (2012) Influence of inorganic anions on metals release from oil sands coke and on toxicity of nickel and vanadium to *Ceriodaphnia dubia*. *Chemosphere*. **86**(5), 521–529.

Rabus, R., Jarling, R., Lahme, S., Kühner, S., Heider, J., Widdel, F., Wilkes, H. (2011) Co-metabolic conversion of toluene in anaerobic n-alkane-degrading bacteria. *Environmental Microbiology*. **13**(9), 2576–2586.

Rabus, R., Trautwein, K., Wöhlbrand, L. (2014) Towards habitat-oriented systems biology of '*Aromatoleum aromaticum*' EbN1. *Applied Microbiology and Biotechnology*. **98**(8), 3371–3388.

Radi, S., Tighadouini, S., El Massaoudi, M., Bacquet, M., Degoutin, S., Revel, B., Mabkhot, Y.N. (2015) Thermodynamics and kinetics of heavy metals adsorption on silica particles chemically modified by conjugated β-ketoenol furan. *Journal of Chemical & Engineering Data*. **60**(10), 2915–2925.

Radović, J.R., Aeppli, C., Nelson, R.K., Jimenez, N., Reddy, C.M., Bayona, J.M., Albaigés, J. (2014) Assessment of photochemical processes in marine oil spill fingerprinting. *Marine Pollution Bulletin*. **79**(1), 268–277.

Raines, D.E., Claycomb, R.J., Scheller, M., Forman, S.A. (2001) Nonhalogenated alkane anesthetics fail to potentiate agonist actions on two ligand-gated ion channels. *Anesthesiology*. **95**(2), 470–477.

Raven, J.A., Allen, J.F. (2003) Genomics and chloroplast evolution: what did cyanobacteria do for plants? *Genome Biology*. **4**(3), 209.

Ravin, N. V, Mardanova, A. V, Skryabin, K.G. (2015) Metagenomics as a tool for the investigation of uncultured microorganisms. *Genetika*. **51**(5), 519–528.

Redman, A.D., McGrath, J.A., Stubblefield, W.A., Maki, A.W., Di Toro, D.M. (2012) Quantifying the concentration of crude oil microdroplets in oil-water preparations. *Environmental Toxicology and Chemistry / SETAC*. **31**(8), 1814–1822.

Redmond, M., Valentine, D. (2012) Natural gas and temperature structured a microbial community response to the Deepwater Horizon oil spill. *PNAS*. **109**, 20292–20297.

Riemann, L., Steward, G.F., Azam, F. (2000) Dynamics of bacterial community composition and activity during a mesocosm diatom bloom. *Applied and Environmantal Microbiology*. **66**(2), 578–587.

Rios, L.M., Moore, C., Jones, P.R. (2007) Persistent organic pollutants carried by synthetic polymers in the ocean environment. *Marine Pollution Bulletin*. **54**(8), 1230–1237.

Rischer, M., Klassen, J.L., Wolf, T., Guo, H., Shelest, E., Clardy, J., Beemelmanns, C. (2016) Draft genome sequence of *Shewanella* sp. strain P1-14-1, a Bacterial inducer of settlement and morphogenesis in larvae of the marine hydroid *Hydractinia echinata*. *Genome Announcements*. **4**(1) e00003-16.

Ritchie, G.D., Still, K.R., Alexander, W.K., Nordholm, A.F., Wilson, C.L., III, J.R., Mattie, D.R. (2001) A review of the neurotoxicity risk of selected hydrocarbon fuels. *Journal of Toxicology and Environmental Health, Part B*. **4**(3), 223–312.

Roberts, J.M., Long, D., Wilson, J.B., Mortensen, P.B., Gage, J.D. (2003) The cold-water coral *Lophelia pertusa* (*Scleractinia*) and enigmatic seabed mounds along the north-east Atlantic margin: Are they related? *Marine Pollution Bulletin*. **46**(1), 7–20.

Rogers, C.S. (1990) Responses of coral reefs and reef organisms to sedimentation. *Marine Ecology Progress Series*. **62**, 185–202.

Rogerson, A., Berger, J. (1981) The toxicity of the dispersant Corexit 9527 and oil-dispersant mixtures to ciliate protozoa. *Chemosphere*. **10**(1), 33–39.

Rogerson, A., Berger, J. (1982) Ultrastructural Modification of the Ciliate Protozoan, *Colpidium colpoda*, following chronic exposure to partially degraded crude oil. *BioScience*. **32**(6), 534–535.

Rontani, J.-F., Mouzdahir, A., Michotey, V., Caumette, P., Bonin, P. (2003) Production of a polyunsaturated isoprenoid wax ester during aerobic metabolism of squalene by *Marinobacter squalenivorans* sp. nov. *Applied and Environmental Microbiology*. **69**(7), 4167–4176.

Rontani, J., Bonin, P.C., John, K. (1999) Biodegradation of free phytol by bacterial communities isolated from marine sediments under aerobic and denitrifying conditions. **65**(12), 5484–5492.

Ropp, J.D., Donahue, C.J., Wolfgang-Kimball, D., Hooley, J.J., Chin, J.Y., Hoffman, R.A., Cuthbertson, R.A., Bauer, K.D. (1995) *Aequorea* green fluorescent protein analysis by flow cytometry. *Cytometry*. **21**(4), 309–317.

Ruban, A. V., Johnson, M.P., Duffy, C.D.P. (2011) Natural light harvesting: principles and environmental trends. *Energy & Environmental Science*. **4**(5), 1643.

Ruberto, L., Vazquez, S.C., Mac Cormack, W.P. (2003) Effectiveness of the natural bacterial flora, biostimulation and bioaugmentation on the bioremediation of a hydrocarbon contaminated Antarctic soil. *International Biodeterioration & Biodegradation*. **52**(2), 115–125.

Safonova, E.T., Dmitrieva, I.., Kvitko, K.. (1999) The interaction of algae with alcanotrophic bacteria in black oil decomposition. *Resources, Conservation and Recycling*. **27**(1), 193–201.

Salgado, H., Moreno-Hagelsieb, G., Smith, T.F., Collado-Vides, J. (2000) Operons in *Escherichia coli*: genomic analyses and predictions. *Proceedings of the National Academy of Sciences of the United States of America*. **97**(12), 6652–6657.

Saliot, A. (1981) Chapter 11 Natural Hydrocarbons in Sea Water Alain Saliot. *Elsevier Oceanography Series*. **31**, 327–374.

Santella, R.M., Perera, F.P., Young, T.L., Zhang, Y.J., Chiamprasert, S., Tang, D., Wang, L.W., Beachman, A., Lin, J.H., DeLeo, V.A. (1995) Polycyclic aromatic hydrocarbon-DNA and protein adducts in coal tar treated patients and controls and their relationship to glutathione S-transferase genotype. *Mutation Research*. **334**(2), 117–124.

Sañudo-Wilhelmy, S.A., Gobler, C.J., Okbamichael, M., Taylor, G.T. (2006) Regulation of phytoplankton dynamics by vitamin B_{12}. *Geophysical Research Letters*. **33**(4), L04604.

Sargian, P., Mostajir, B., Chatila, K., Ferreyra, G., Pelletier, E., Demers, S. (2005) Non-synergistic effects of water-soluble crude oil and enhanced ultraviolet-B radiation on a natural plankton assemblage. *Marine Ecology Progress Series*. **294**, 63–77.

Sauer, T., Boehm, P. (1991) The use of defensible analytical chemical measurements for oil spill natural resource damage assessment. *International Oil Spill Conference Proceedings*. **1**, 363–369.

Savjani, K.T., Gajjar, A.K., Savjani, J.K. (2012) Drug solubility: Importance and enhancement techniques. *ISRN Pharmaceutics*. **2012**, 1–10.

Sawamura, S., Tsuchiya, M., Ishigami, T., Taniguchi, Y., Suzuki, K. (1993) Effect of pressure on the solubility of naphthalene in water at 25°C. *Journal of Solution Chemistry*. **22**(8), 727–732.

Schimmelmann, A., Boudou, J.-P., Lewan, M.D., Wintsch, R.P. (2001) Experimental controls on D/H and 13C/12C ratios of kerogen, bitumen and oil during hydrous pyrolysis. *Organic Geochemistry*. **32**(8), 1009–1018.

Schipper, J., Tilders, F.J.H. (1982) Quantification of formaldehyde induced fluorescence and its application in neurobiology. *Brain Research Bulletin*. **9**(1–6), 69–80.

Schirmer, A., Rude, M.A., Li, X., Popova, E., del Cardayre, S.B. (2010) Microbial biosynthesis of alkanes. *Science (New York, N.Y.)*. **329**(5991), 559–562.

Schleheck, D., Tindall, B.J., Rosselló-Mora, R., Cook, A.M. (2004) *Parvibaculum lavamentivorans* gen. nov., sp. nov., a novel heterotroph that initiates catabolism of linear alkylbenzenesulfonate. *International Journal of Systematic and Evolutionary Microbiology*. **54**(Pt 5), 1489–1497.

Schmid, A.-M.M. (2003a) Endobacteria in the diatom *Pinnularia* (*Bacillariophyceae*). I. Scattered ct-nucleoids explained: DAPI-DNA complexes stem from exoplastidial bacteria boring into the chloroplasts. *Journal of Phycology*. **39**(1), 122–138.

Schmid, A.-M.M. (2003b) Endobacteria in the diatom *Pinnularia* (*Bacillariophyceae*). II. Host cell cycle-dependent translocation and transient chloroplast scars. *Journal of Phycology*. **39**(1), 139–153.

Schmidt, H., Bich Ha, N., Pfannkuche, J., Amann, H., Kronfeldt, H.-D., Kowalewska, G. (2004) Detection of PAHs in seawater using surface-enhanced Raman scattering (SERS). *Marine Pollution Bulletin*. **49**(3), 229–234.

Schoell, M., McCaffrey, M.A., Fago, F.J., Moldowan, J.M. (1992) Carbon isotopic compositions of 28,30-bisnorhopanes and other biological markers in a Monterey crude oil. *Geochimica et Cosmochimica Acta*. **56**(3), 1391–1399.

Schönhuber, W., Fuchs, B., Juretschko, S., Amann, R. (1997) Improved sensitivity of whole-cell

hybridization by the combination of horseradish peroxidase-labeled oligonucleotides and tyramide signal amplification. *Applied and Environmental Microbiology*. **63**(8), 3268–3273.

Schönhuber, W., Zarda, B., Eix, S., Rippka, R., Herdman, M., Ludwig, W., Amann, R. (1999) In situ identification of cyanobacteria with horseradish peroxidase-labeled, rRNA-targeted oligonucleotide probes. *Applied and Environmental Microbiology*. **65**(3), 1259–1267.

Schreiber, U., Bilger, W., Neubauer, C. (1995) Chlorophyll fluorescence as a nonintrusive indicator for rapid assessment of in vivo photosynthesis. In *Ecophysiology of Photosynthesis*. Berlin, Heidelberg: Springer Berlin Heidelberg, pp. 49–70.

Schreiber, U., Klughammer, C., Kolbowski, J. (2011) High-end chlorophyll fluorescence analysis with the MULTI-COLOR-PAM. I. Various light qualities and their applications. *PAM Application Notes*. **1**, 1–21.

Schuler, L., Jouanneau, Y., Ní Chadhain, S.M., Meyer, C., Pouli, M., Zylstra, G.J., Hols, P., Agathos, S.N. (2009) Characterization of a ring-hydroxylating dioxygenase from phenanthrene-degrading *Sphingomonas* sp. strain LH128 able to oxidize benz[a]anthracene. *Applied Microbiology and Biotechnology*. **83**(3), 465–475.

Schweigert, N., Zehnder, A.J., Eggen, R.I. (2001) Chemical properties of catechols and their molecular modes of toxic action in cells, from microorganisms to mammals. *Environmental microbiology*. **3**(2), 81–91.

Sekar, R., Fuchs, B.M., Amann, R., Pernthaler, J. (2004) Flow sorting of marine bacterioplankton after fluorescence *in situ* hybridization. *Applied and Environmental Microbiology*. **70**(10), 6210–6219.

Sharabi, M., Mandelberg, Y., Benayahu, D., Benayahu, Y., Azem, A., Haj-Ali, R. (2014) A new class of bio-composite materials of unique collagen fibers. *Journal of the Mechanical Behavior of Biomedical Materials*. **36**, 71–81.

Sharma, P. (2011) Cinnamic acid derivatives: A new chapter of various pharmacological activities. *Journal of Chemical and Pharmaceutical Research*. **3**(2), 403–423.

Sharp, K.H., Distel, D., Paul, V.J. (2012) Diversity and dynamics of bacterial communities in early life stages of the Caribbean coral *Porites astreoides*. *ISME Journal*. **6**(4), 790–801.

Shaw, S.L., Gantt, B., Meskhidze, N., Shaw, S.L., Gantt, B., Meskhidze, N. (2010) Production and Emissions of Marine Isoprene and Monoterpenes: A Review. *Advances in Meteorology*. **2010**, 1–24.

Sherr, E., Sherr, B. (1988) Role of microbes in pelagic food webs: A revised concept. *Limnology and Oceanography*. **33**(5), 1225–1227.

Shingler, V., Powlowski, J., Marklund, U. (1992) Nucleotide sequence and functional analysis of the complete phenol/3,4-dimethylphenol catabolic pathway of *Pseudomonas* sp. strain CF600. *Journal of Bacteriology*. **174**(3), 711–724.

Shoulders, M.D., Raines, R.T. (2009) Collagen structure and stability. *Annual Review of Biochemistry*. **78**, 929–958.

Sikkema, J., de Bont, J.A., Poolman, B. (1995) Mechanisms of membrane toxicity of hydrocarbons. *Microbiological Reviews*. **59**(2), 201–222.

Simon, M.J., Osslund, T.D., Saunders, R., Ensley, B.D., Suggs, S., Harcourt, A., Suen, W.C., Cruden, D.L., Gibson, D.T., Zylstra, G.J. (1993) Sequences of genes encoding naphthalene dioxygenase in *Pseudomonas putida* strains G7 and NCIB 9816-4. *Gene*. **127**(1), 31–37.

Simon, M., Grossart, H.P., Schweitzer, B., Ploug, H. (2002a) Microbial ecology of organic aggregates in aquatic ecosystems. *Aquatic Microbial Ecology*. **28**(2), 175–211.

Simon, N., Biegala, I.C., Smith, E.A., Vaulot, D. (2002b) Kinetics of attachment of potentially toxic bacteria to *Alexandrium tamarense*. *Aquatic Microbial Ecology*. **28**(3), 249–256.

Singer, A.C., Crowley, D.E., Thompson, I.P. (2003) Secondary plant metabolites in phytoremediation and biotransformation. *Trends in Biotechnology*. **21**(3), 123–130.

Singer, E., Webb, E.A., Nelson, W.C., Heidelberg, J.F., Ivanova, N., Pati, A., Edwards, K.J. (2011) Genomic potential of *Marinobacter aquaeolei,* a biogeochemical "opportunitroph". *Applied and Environmental Microbiology*. **77**(8), 2763–2771.

Singleton, D.R., Dickey, A.N., Scholl, E.H., Wright, F.A., Aitken, M.D. (2015) Complete genome sequence of a novel bacterium within the family *Rhodocyclaceae* that degrades polycyclic aromatic hydrocarbons. *Genome Announcements*. **3**(2) e00251-15.

Siron, R., Pelletier, É., Brochu, C. (1995) Environmental factors influencing the biodegradation of petroleum hydrocarbons in cold seawater. *Archives of Environmental Contamination and Toxicology*. **28**(4), 406–416.

Snyder, M.J. (2000) Cytochrome P450 enzymes in aquatic invertebrates: recent advances and future directions. *Aquatic Toxicology*. **48**(4), 529–547.

Sohlenkamp, C., Geiger, O. (2016) Bacterial membrane lipids: diversity in structures and pathways. *FEMS Microbiology Reviews*. **40**(1), 133–159.

Solash, J., Hazlett, R.N., Hall, J.M., Nowack, C.J. (1978) Relation between fuel properties and chemical composition. 1. Jet fuels from coal, oil shale and tar sands. *Fuel*. **57**(9), 521–528.

Sonnenschein, E.C., Gärdes, A., Seebah, S., Torres-Monroy, I., Grossart, H.-P., Ullrich, M.S. (2011)

Development of a genetic system for *Marinobacter adhaerens* HP15 involved in marine aggregate formation by interacting with diatom cells. *Journal of Microbiological Methods*. **87**(2), 176–183.

Sonnenschein, E.C., Syit, D.A., Grossart, H.-P., Ullrich, M.S. (2012) Chemotaxis of *Marinobacter adhaerens* and its impact on attachment to the diatom *Thalassiosira weissflogii*. *Applied and Environmental Microbiology*. **78**(19), 6900–6907.

Stagg, R.M., McIntosh, A. (1996) Hydrocarbon concentrations in the northern North Sea and effects on fish larvae. *Science of The Total Environment*. **186**(3), 189–201.

Steen, H.B. (2004) Flow cytometer for measurement of the light scattering of viral and other submicroscopic particles. *Cytometry A*. **57**(2), 94–99.

Stefanova, M., Maman, O., Guillet, B., Disnar, J.-R. (2004) Preserved lignin structures in Miocene-aged lignite lithotypes, Bulgaria. *Fuel*. **83**(1), 123–128.

Stefels, J., Boekel, W.H.M. Van (1993) Production of DMS from dissolved DMSP in axenic cultures of the marine phytoplankton species *Phaeocystis* sp. *Marine Ecology Progress Series*. **97**, 11–18.

Stel'makh, L. V., Babich, I.I., Tugrul, S., Moncheva, S., Stefanova, K. (2009) Phytoplankton growth rate and zooplankton grazing in the western part of the Black Sea in the autumn period. *Oceanology*. **49**(1), 83–92.

Suárez-Suárez, A., López-López, A., Tovar-Sánchez, A., Yarza, P., Orfila, A., Terrados, J., Arnds, J., Marqués, S., Niemann, H., Schmitt-Kopplin, P., Amann, R., Rosselló-Móra, R. (2011) Response of sulfate-reducing bacteria to an artificial oil-spill in a coastal marine sediment. *Environmental Microbiology*. **13**(6), 1488–1499.

Suchanek, T.H. (1993) Oil impacts on marine invertebrate populations and communities. *American Zoologist*. **33**(6), 510–523.

Suggett, D.J., Oxborough, K., Baker, N.R., MacIntyre, H.L., Kana, T.M., Geider, R.J. (2003) Fast repetition rate and pulse amplitude modulation chlorophyll a fluorescence measurements for assessment of photosynthetic electron transport in marine phytoplankton. *European Journal of Phycology*. **38**(4), 371–384.

Suh, H.S., Ha, J.Y., Yoon, J.H., Ha, C.S., Suh, H., Kim, I. (2010) Polyester polyol synthesis by alternating copolymerization of propylene oxide with cyclic acid anhydrides by using double metal cyanide catalyst. *Reactive and Functional Polymers*. **70**(5), 288–293.

Summons, R.E., Jahnke, L.L., Hope, J.M., Logan, G.A. (1999) 2-Methylhopanoids as biomarkers for cyanobacterial oxygenic photosynthesis. *Nature*. **400**(6744), 554–557.

Sureshkumar, S., Jasmin, B., Mujeeb Rahiman, K.M., Hatha Mohammed, A.A. (2014) Growth enhancement of micro algae, *Chaetoceros calcitrans* and *Nannochloropsis oculata*, using selected bacterial strains. *International Journal of Current Microbiology and Applied Sciences*. **3**(4), 352–359.

Suzuki, M., Hayakawa, T., Shaw, J.P., Rekik, M., Harayama, S. (1991) Primary structure of xylene monooxygenase: Similarities to and differences from the alkane hydroxylation system. *Journal of Bacteriology*. **173**(5), 1690–1695.

Sverdrup, L.E., Nielsen, T., Krogh‖, P.H. (2002) Soil ecotoxicity of polycyclic aromatic hydrocarbons in relation to soil sorption, lipophilicity, and water solubility. *Environmental Science & Technology*. **36**(11), 2429–2435.

Sweeney, R.E. (1988) Petroleum-related hydrocarbon seep age in a recent North Sea sediment. *Chemical Geology*. **71**(1–3), 53–64.

Swift, D.G., Guillard, R.R.L. (1978) Unexpected response to vitamin B_{12} of dominant centric diatoms from the spring bloom in the Gulf of Maine (Northeast Atlantic Ocean). *Journal of Phycology*. **14**(4), 377–386.

Swigert, J.P., Lee, C., Wong, D.C.L., Podhasky, P. (2014) Aquatic hazard and biodegradability of light and middle atmospheric distillate petroleum streams. *Chemosphere*. **108**, 1–9.

Tadros, M.G., Hughes, J.B. (1997) Degradation of polycyclic aromatic hydrocarbons (PAHs) by indigenous mixed and pure cultures isolated from coastal sediments. *Applied Biochemistry and Biotechnology*. **63–65**, 865–870.

Tam, N.F.Y., Guo, C.L., Yau, W.Y., Wong, Y.S. (2002) Preliminary study on biodegradation of phenanthrene by bacteria isolated from mangrove sediments in Hong Kong. *Marine Pollution Bulletin*. **45**(1–12), 316–324.

Tandlich, R., Brežná, B., Dercová, K. (2001) The effect of terpenes on the biodegradation of polychlorinated biphenyls by *Pseudomonas stutzeri*. *Chemosphere*. **44**(7), 1547–1555.

Tang, Y.Z., Koch, F., Gobler, C.J. (2010) Most harmful algal bloom species are vitamin B1 and B12 auxotrophs. *Proceedings of the National Academy of Sciences of the United States of America*. **107**(48), 20756–61.

Tett, P., Edwards, V. (2002) Review of harmful algal blooms in Scottish coastal waters. *Report to SEPA*. (June), 125pp.

Thompson, A.W., Foster, R.A., Krupke, A., Carter, B.J., Musat, N., Vaulot, D., Kuypers, M.M.M., Zehr, J.P. (2012) Unicellular cyanobacterium symbiotic with a single-celled eukaryotic alga. *Science*. **337**(6101), 1546–1550.

Thompson, J.D., Gibson, T.J., Plewniak, F., Jeanmougin, F., Higgins, D.G. (1997) The CLUSTAL X windows interface: Flexible strategies for multiple sequence alignment aided by quality analysis tools. *Nucleic Acids Research*. **25**(24), 4876–4882.

Thornton, D.C.O. (2002) Diatom aggregation in the sea: mechanisms and ecological implications. *European Journal of Phycology*. **37**(2), 149–161.

Tielens, A.G.G.M. (2008) Interstellar polycyclic aromatic hydrocarbon molecules. *Annual Review of Astronomy and Astrophysics*. **46**(1), 289–337.

Toren, A., Orr, E., Paitan, Y., Ron, E.Z., Rosenberg, E. (2002) The active component of the bioemulsifier alasan from *Acinetobacter radioresistens* KA53 is an OmpA-like protein. *Journal of Bacteriology*. **184**(1), 165–170.

Touhara, K., Prestwich, G.D. (1993) Juvenile hormone epoxide hydrolase. Photoaffinity labeling, purification, and characterization from tobacco hornworm eggs. *Journal of Biological Chemistry*. **268**(26), 19604–19609.

Tourney, J., Ngwenya, B.T. (2014) The role of bacterial extracellular polymeric substances in geomicrobiology. *Chemical Geology*. **386**, 115–132.

Tourney, J., Ngwenya, B.T., Fred Mosselmans, J.W., Magennis, M. (2009) Physical and chemical effects of extracellular polymers (EPS) on Zn adsorption to *Bacillus licheniformis* S-86. *Journal of Colloid and Interface Science*. **337**(2), 381–389.

Treibs, A. (1936) Chlorophyll- und häminderivate in organischen mineralstoffen. *Angewandte Chemie*. **49**(38), 682–686.

Tujula, N.A., Holmström, C., Mußmann, M., Amann, R., Kjelleberg, S., Crocetti, G.R. (2005) A CARD–FISH protocol for the identification and enumeration of epiphytic bacteria on marine algae. **5**(3), 604-607.

Tully, B.J., Sachdeva, R., Heidelberg, K.B., Heidelberg, J.F. (2014) Comparative genomics of planktonic *Flavobacteriaceae* from the Gulf of Maine using metagenomic data. *Microbiome*. **2**, 34.

Turley, C.M., Bianchi, M., Christaki, U., Conan, P., Harris, J.R.W., Psarra, S., Ruddy, G., Stutt, E.D., Tselepides, A., Van Wambeke, F. (2000) Relationship between primary producers and bacteria in an oligotrophic sea - the Mediterranean and biogeochemical implications. *Marine Ecology Progress Series*. **193**, 11–18.

Turner, R.E., Overton, E.B., Meyer, B.M., Miles, M.S., Hooper-Bui, L. (2014) Changes in the concentration and relative abundance of alkanes and PAHs from the Deepwater Horizon oiling of coastal marshes. *Marine Pollution Bulletin*. **86**(1), 291–297.

Valentine, D.L., Kessler, J.D., Redmond, M.C., Mendes, S.D., Heintz, M.B., Farwell, C., Hu, L., Kinnaman, F.S., Yvon-Lewis, S., Du, M., Chan, E.W., Garcia Tigreros, F., Villanueva, C.J. (2010) Propane respiration jump-starts microbial response to a deep oil spill. *Science (New York, N.Y.)*. **330**(6001), 208–211.

van der Werf, M.J., Overkamp, K.M., de Bont, J.A. (1998) Limonene-1,2-epoxide hydrolase from *Rhodococcus erythropolis* DCL14 belongs to a novel class of epoxide hydrolases. *Journal of Bacteriology*. **180**(19), 5052–5057.

Van Domselaar, G.H., Stothard, P., Shrivastava, S., Cruz, J.A., Guo, A., Dong, X., Lu, P., Szafron, D., Greiner, R., Wishart, D.S. (2005) BASys: a web server for automated bacterial genome annotation. *Nucleic Acids Research*. **33**(Web Server issue), W455-9.

van Eenennaam, J.S., Wei, Y., Grolle, K.C.F., Foekema, E.M., Murk, A.J. (2016) Oil spill dispersants induce formation of marine snow by phytoplankton-associated bacteria. *Marine Pollution Bulletin*. **104**(1–2), 294–302.

Vandermeer, K.D., Daugulis, A.J. (2007) Enhanced degradation of a mixture of polycyclic aromatic hydrocarbons by a defined microbial consortium in a two-phase partitioning bioreactor. *Biodegradation*. **18**, 211–221.

Vaysse, P.-J., Prat, L., Mangenot, S., Cruveiller, S., Goulas, P., Grimaud, R. (2009) Proteomic analysis of *Marinobacter hydrocarbonoclasticus* SP17 biofilm formation at the alkane-water interface reveals novel proteins and cellular processes involved in hexadecane assimilation. *Research in Microbiology*. **160**(10), 829–837.

Venosa, A.D., Zhu, X. (2003) Biodegradation of crude oil contaminating marine shorelines and freshwater wetlands. *Spill Science & Technology Bulletin*. **8**(2), 163–178.

Verschueren, K. (2001) Handbook of environmental data on organic chemicals. 4th ed. New York: John Wiley & Sons.

Vetter, Y.A., Deming, J.W., Jumars, P.A., Krieger-Brockett, B.B. (1997) A predictive model of bacterial foraging by means of freely released extracellular enzymes. *Microbial Ecology*. **36**(1), 75–92.

Villareal, T.A. (1990) Laboratory culture and preliminary characterization of the nitrogen-fixing *Rhizosolenia-Richelia* symbiosis. *Marine Ecology*. **11**(2), 117–132.

Wagner, M. (2009) Single-cell ecophysiology of microbes as revealed by Raman microspectroscopy or secondary ion mass spectrometry imaging. *Annual Review of Microbiology*. **63**, 411–429.

Wallner, G., Amann, R., Beisker, W. (1993) Optimizing fluorescent in sit hybridization with rRNA-

targeted oligonucleotide probes for flow cytometric identification of microorganisms. *Cytometry*. **14**(2), 136–143.

Wang, W., Omori, M., Hayashibara, T., Shimoike, K., Hatta, M., Sugiyama, T., Fujisawa, T. (1995) Isolation and characterization of a mini-collagen gene encoding a nematocyst capsule protein from a reef-building coral, *Acropora donei*. *Gene*. **152**(2), 195–200.

Wang, X., Wang, W. (2006) Bioaccumulation and transfer of benzo(a)pyrene in a simplified marine food chain. *Marine Ecology Progress Series*. **312**, 101–111.

Wang, W., Nykamp, J., Huang, X.-D., Gerhardt, K., Dixon, D.G., Greenberg, B.M. (2009) Examination of the mechanism of phenanthrenequinone toxicity to *Vibrio fischeri*: evidence for a reactive oxygen species-mediated toxicity mechanism. *Environmental Toxicology and Chemistry / SETAC*. **28**(8), 1655–1662.

Wang, W., Zhang, R., Zhong, R., Shan, D., Shao, Z. (2014) Indigenous oil-degrading bacteria in crude oil-contaminated seawater of the Yellow sea, China. *Applied Microbiology and Biotechnology*. **98**(16), 7253–7269.

Wang, S., Bai, N., Wang, B., Feng, Z., Hutchins, W.C., Yang, C.-H., Zhao, Y. (2015) Characterization of the molecular degradation mechanism of diphenyl ethers by *Cupriavidus* sp. WS. *Environmental Science and Pollution Research International*. **22**(21), 16914–16926.

Wang, J., Sandoval, K., Ding, Y., Stoeckel, D., Minard-Smith, A., Andersen, G., Dubinsky, E.A., Atlas, R., Gardinali, P. (2016a) Biodegradation of dispersed Macondo crude oil by indigenous Gulf of Mexico microbial communities. *Science of The Total Environment*. **557**–**558**, 453–468.

Wang, R., Gallant, É., Seyedsayamdost, M.R. (2016b) Investigation of the genetics and biochemistry of roseobacticide production in the Roseobacter clade bacterium *Phaeobacter inhibens*. *mBio*. **7**(2), e02118.

Warshawsky, D., LaDow, K., Schneider, J. (2007) Enhanced degradation of benzo[a]pyrene by *Mycobacterium* sp. in conjunction with green alga. *Chemosphere*. **69**(3), 500–506.

Webb, J.S., Givskov, M., Kjelleberg, S. (2003) Bacterial biofilms: Prokaryotic adventures in multicellularity. *Current Opinion in Microbiology*. **6**(6), 578–585.

Weiner, R.M., Melick, M., O'Neill, K., Quintero, E. (2000) *Hyphomonas adhaerens* sp. nov., *Hyphomonas johnsonii* sp. nov. and *Hyphomonas rosenbergii* sp. nov., marine budding and prosthecate bacteria. *International Journal of Systematic and Evolutionary Microbiology*. **50**(2), 459–469.

Weisburg, W.G., Barns, S.M., Pelletier, D.A., Lane, D.J. (1991) 16S ribosomal DNA amplification for phylogenetic study. *Journal of Bacteriology*. **173**(2), 697–703.

Welschmeyer, N.A. (1994) Fluorometric analysis of chlorophyll a in the presence of chlorophyll b and pheopigments. *Limnology and Oceanography*. **39**(8), 1985–1992.

Wentzel, A., Ellingsen, T.E., Kotlar, H.-K., Zotchev, S.B., Throne-Holst, M. (2007) Bacterial metabolism of long-chain *n*-alkanes. *Applied Microbiology and Biotechnology*. **76**(6), 1209–1221.

White, H.K., Hsing, P.-Y., Cho, W., Shank, T.M., Cordes, E.E., Quattrini, A.M., Nelson, R.K., Camilli, R., Demopoulos, A.W.J., German, C.R., Brooks, J.M., Roberts, H.H., Shedd, W., Reddy, C.M., Fisher, C.R. (2012) Impact of the Deepwater Horizon oil spill on a deep-water coral community in the Gulf of Mexico. *Proceedings of the National Academy of Sciences of the United States of America*. **109**(50), 20303–20308.

Whiticar, M.J. (1996) Stable isotope geochemistry of coals, humic kerogens and related natural gases. *International Journal of Coal Geology*. **32**(1–4), 191–215.

Wild, C., Huettel, M., Klueter, A., Kremb, S.G., Rasheed, M.Y.M., Jørgensen, B.B. (2004) Coral mucus functions as an energy carrier and particle trap in the reef ecosystem. *Nature*. **428**(6978), 66–70.

Wild, C., Naumann, M., Niggl, W., Haas, A. (2010) Carbohydrate composition of mucus released by scleractinian warm- and cold-water reef corals. *Aquatic Biology*. **10**(1), 41–45.

Wilkes. H., Schwarzbauer, J. (2010) In *Handbook of Hydrocarbon and Lipid Microbiology*. K.N. Timmis (ed.) Springer, Berlin. pp 5-48.

William, S., Feil, H., Copeland, A. (2004) Bacterial genomic DNA isolation using CTAB. *DOE Joint Genome Institute*. Version **4,** pp 4.

Williams, M.L., Vogel, J.S., Ghadially, R., Brown, B.E., Elias, P.M. (1992) Exogenous origin of *n*-alkanes in pathologic scale. *Archives of Dermatology*. **128**(8), 1065–1071.

Wong, C.S., Crawford, D.W. (2002) Flux of particulate inorganic carbon to the deep subarctic Pacific correlates with El Niño. *Deep-Sea Research Part II: Topical Studies in Oceanography*. **49**(24–25), 5705–5715.

Wood, B.J., Walter, M.J., Wade, J. (2006) Accretion of the Earth and segregation of its core. *Nature*. **441**(7095), 825–833.

Wotton, R. (2005) The essential role of exopolymers (EPS) in aquatic systems. *Oceanography and Marine Biology*. **42**, 57–94.

Wu, H., Volponi, J. V, Oliver, A.E., Parikh, A.N., Simmons, B.A., Singh, S. (2011) *In vivo* lipidomics using single-cell Raman spectroscopy. *Proceedings of the National Academy of Sciences of the United States of America*. **108**(9), 3809–3814.

Xie, F., Koziar, S.A., Lampi, M.A., Dixon, D.G., Warren, N.P., Borgmann, U., Huang, X.-D.,

Greenberg, B.M. (2006) Assessment of the toxicity of mixtures of copper, 9,10-phenanthrenequinone, and phenanthrene to *Daphnia magna*: Evidence for a reactive oxygen mechanism. *Environmental Toxicology and Chemistry / SETAC*. **25**(2), 613–622.

Xiu, M., Pan, L., Jin, Q. (2014) Bioaccumulation and oxidative damage in juvenile scallop *Chlamys farreri* exposed to benzo[a]pyrene, benzo[b]fluoranthene and chrysene. *Ecotoxicology and Environmental Safety*. **107**, 103–110.

Xue, J., Yu, Y., Bai, Y., Wang, L., Wu, Y. (2015) Marine oil-degrading microorganisms and biodegradation process of petroleum hydrocarbon in marine environments: A review. *Current Microbiology*. **71**(2), 220–228.

Yakimov, M.M., Golyshin, P.N., Lang, S., Moore, E.R., Abraham, W.R., Lünsdorf, H., Timmis, K.N. (1998) *Alcanivorax borkumensis* gen. nov., sp. nov., a new, hydrocarbon-degrading and surfactant-producing marine bacterium. *International Journal of Systematic Bacteriology*. **48 Pt 2**, 339–348.

Yakimov, M.M., Giuliano, L., Bruni, V., Scarfì, S., Golyshin, P.N. (1999) Characterization of antarctic hydrocarbon-degrading bacteria capable of producing bioemulsifiers. *The New Microbiologica*. **22**(3), 249–256.

Yakimov, M.M., Giuliano, L., Gentile, G., Crisafi, E., Chernikova, T.N., Abraham, W.R., Lünsdorf, H., Timmis, K.N., Golyshin, P.N. (2003) *Oleispira antarctica* gen. nov., sp. nov., a novel hydrocarbonoclastic marine bacterium isolated from Antarctic coastal sea water. *International Journal of Systematic and Evolutionary Microbiology*. **53**(3), 779–785.

Yakimov, M.M., Gentile, G., Bruni, V., Cappello, S., D'Auria, G., Golyshin, P.N., Giuliano, L. (2004a) Crude oil-induced structural shift of coastal bacterial communities of rod bay (Terra Nova Bay, Ross Sea, Antarctica) and characterization of cultured cold-adapted hydrocarbonoclastic bacteria. *FEMS Microbiology Ecology*. **49**(3), 419–432.

Yakimov, M.M., Giuliano, L., Denaro, R., Crisafi, E., Chernikova, T.N., Abraham, W.-R., Luensdorf, H., Timmis, K.N., Golyshin, P.N. (2004b) *Thalassolituus oleivorans* gen. nov., sp. nov., a novel marine bacterium that obligately utilizes hydrocarbons. *International Journal of Systematic and Evolutionary Microbiology*. **54**(Pt 1), 141–148.

Yakimov, M.M., Cappello, S., Crisafi, E., Tursi, A., Savini, A., Corselli, C., Scarfì, S., Giuliano, L. (2006) Phylogenetic survey of metabolically active microbial communities associated with the deep-sea coral Lophelia pertusa from the Apulian plateau, Central Mediterranean Sea. *Deep-Sea Research Part I: Oceanographic Research Papers*. **53**(1), 62–75.

Yakimov, M.M., Timmis, K.N., Golyshin, P.N. (2007) Obligate oil-degrading marine bacteria. *Current Opinion in Biotechnology*. **18**(3), 257–266.

Yamada, M., Takada, H., Toyoda, K., Yoshida, A., Shibata, A., Nomura, H., Wada, M., Nishimura, M., Okamoto, K., Ohwada, K. (2003) Study on the fate of petroleum-derived polycyclic aromatic hydrocarbons (PAHs) and the effect of chemical dispersant using an enclosed ecosystem, mesocosm. *Marine Pollution Bulletin*. **47**(1–6), 105–13.

Yang, C., Wang, Z., Liu, Y., Yang, Z., Li, Y., Shah, K., Zhang, G., Landriault, M., Hollebone, B., Brown, C., Lambert, P., Liu, Z., Tian, S. (2013) Aromatic steroids in crude oils and petroleum products and their applications in forensic oil spill identification. *Environmental Forensics*. **14**(4), 278–293.

Yang, H.-Y., Jia, R.-B., Chen, B., Li, L. (2014) Degradation of recalcitrant aliphatic and aromatic hydrocarbons by a dioxin-degrader *Rhodococcus* sp. strain p52. *Environmental Science and Pollution Research*. **21**(18), 11086–11093.

Yang, T., Nigro, L.M., Gutierrez, T., D'Ambrosio, L., Joye, S.B., Highsmith, R., Teske, A. (2016) Pulsed blooms and persistent oil-degrading bacterial populations in the water column during and after the Deepwater Horizon blowout. *Deep Sea Research Part II: Topical Studies in Oceanography*. **129**, 282–291.

Yavari, S., Malakahmad, A., Sapari, N.B. (2015) A review on phytoremediation of crude oil spills. *Water, Air, & Soil Pollution*. **226**(8), 226-279.

Young, S.D. (1973) Collagen and other mesoglea protein from the coral *lbophyllia crymbosa* (*Anthozoa, Scleractinla*). *International Journal of Biochemistry*. **4**(22), 339–344.

Yu, H. (2002) Environmental carcinogenic polycyclic aromatic hydrocarbons: photochemistry and phototoxicity. *Journal of Environmental Science And Health. Part C, Environmental Carcinogenesis & Ecotoxicology Reviews*. **20**(2), 149–183.

Yu, P., Damiran, D. (2011) Heat-induced changes to lipid molecular structure in Vimy flaxseed: spectral intensity and molecular clustering. *Spectrochimica Acta. Part A, Molecular and Biomolecular Spectroscopy*. **79**(1), 51–59.

Zelibor, J.L., Romankiw, L., Hatcher, P.G., Colwell, R.R. (1988) Comparative analysis of the chemical composition of mixed and pure cultures of green algae and their decomposed residues by C nuclear magnetic resonance spectroscopy. *Applied and Environmental Microbiology*. **54**(4), 1051–1060.

Zetsche, E.-M., Baussant, T., Meysman, F.J.R., van Oevelen, D. (2016) Direct visualization of mucus production by the cold-water coral *Lophelia pertusa* with digital holographic microscopy. *PloS ONE*. **11**(2), e0146766.

Zhang, Z., Hou, Z., Yang, C., Ma, C., Tao, F., Xu, P. (2011a) Degradation of *n*-alkanes and polycyclic

aromatic hydrocarbons in petroleum by a newly isolated *Pseudomonas aeruginosa* DQ8. *Bioresource Technology*. **102**(5), 4111–4116.

Zhang, Z., Sangaiah, R., Gold, A., Ball, L.M., Holba-Schulz, P., Ernst, L., Tian, Y.S., Yao, Q.H. (2011b) Synthesis of uniformly 13C-labeled polycyclic aromatic hydrocarbons. *Organic & Biomolecular Chemistry*. **9**(15), 5431.

Zhang, L., Jin, Y., Huang, M., Penning, T.M. (2012) The role of human aldo-keto reductases in the metabolic activation and detoxication of polycyclic aromatic hydrocarbons: Interconversion of PAH catechols and PAH o-quinones. *Frontiers in Pharmacology*. **3**, 193.

Zhang, Q.-C., Song, J.-J., Yu, R.-C., Yan, T., Wang, Y.-F., Kong, F.-Z., Zhou, M.-J. (2013) Roles of mixotrophy in blooms of different dinoflagellates: Implications from the growth experiment. *Harmful Algae*. **30**, 10–26.

Zhang, P., Liu, H., Yue, Z., Chen, B., Yao, M. (2015) [Laser Induced Fluorescence Spectroscopic Analysis of Aromatics from One Ring to Four Rings]. *Guang Pu Xue Yu Guang Pu Fen Xi = Guang Pu*. **35**(6), 1592–1596.

Zhang, W., Tian, R., Bo, Y., Cao, H., Cai, L., Chen, L., Zhou, G., Sun, J., Zhang, X., Al-Suwailem, A., Qian, P.-Y. (2016) Environmental switching during biofilm development in a cold seep system and functional determinants of species sorting. *Molecular Ecology*. **25**(9), 1958–1971.

Zhao, B., Wang, H., Mao, X., Li, R. (2009) Biodegradation of phenanthrene by a halophilic bacterial consortium under aerobic conditions. *Current Microbiology*. **58**(3), 205–210.

Zhao, B., Wang, H., Li, R., Mao, X. (2010) *Thalassospira xianhensis* sp. nov., a polycyclic aromatic hydrocarbon-degrading marine bacterium. *International Journal of Systematic and Evolutionary Microbiology*. **60**(5), 1125–1129.

Zhao, X., Shi, Q., Gray, M.R., Xu, C. (2014) New vanadium compounds in Venezuela heavy crude oil detected by positive-ion electrospray ionization fourier transform ion cyclotron resonance mass spectrometry. *Scientific Reports*. **4**, 30–33.

Zhao, W., Yang, S., Huang, Q., Cai, P. (2015) Bacterial cell surface properties: Role of loosely bound extracellular polymeric substances (LB-EPS). *Colloids and Surfaces B: Biointerfaces*. **128**, 600–607.

Zielinska-Park, J., Nakamura, J., Swenberg, J.A., Aitken, M.D. (2004) Aldehydic DNA lesions in calf thymus DNA and HeLa S3 cells produced by bacterial quinone metabolites of fluoranthene and pyrene. *Carcinogenesis*. **25**(9), 1727–1733.

Ziervogel, K., McKay, L., Rhodes, B., Osburn, C.L., Dickson-Brown, J., Arnosti, C., Teske, A. (2012) Microbial activities and dissolved organic matter dynamics in oil-contaminated surface seawater from the Deepwater Horizon oil spill site. *PLoS ONE*. **7**(4), e34816.

Zook, H.A. (2001) Spacecraft measurements of the cosmic dust flux. In *Accretion of Extraterrestrial Matter Throughout Earth's History*. Boston, MA: Springer US, pp. 75–92.

Zoppini, A., Puddu, A., Fazi, S., Rosati, M., Sist, P. (2005) Extracellular enzyme activity and dynamics of bacterial community in mucilaginous aggregates of the northern Adriatic Sea. *Science of the Total Environment*. **353**(1), 270–286.

Zou, C., Zhai, G., Zhang, G., Wang, H., Zhang, G., Li, J., Wang, Z., Wen, Z., Ma, F., Liang, Y., Yang, Z., Li, X., Liang, K. (2015) Formation, distribution, potential and prediction of global conventional and unconventional hydrocarbon resources. *Petroleum Exploration and Development*. **42**(1), 14–28.

Zsolnay, A. (1973) Hydrocarbon and chlorophyll: a correlation in the upwelling region off West Africa. *Deep Sea Research and Oceanographic Abstracts*. **20**(10), 923–925.

Zuccato, E., Castiglioni, S., Fanelli, R., Reitano, G., Bagnati, R., Chiabrando, C., Pomati, F., Rossetti, C., Calamari, D. (2006) Pharmaceuticals in the environment in Italy: Causes, occurrence, effects and control. *Environmental Science and Pollution Research International*. **13**(1), 15–21.